RESEARCH

Utah Department of Transportation - Research Division
4501 South 2700 West - P.O. Box 148410 - SLC,UT 84114-8410
udot.utah.gov

SIMPLIFIED SPT PERFORMANCE-BASED ASSESSMENT OF LIQUEFACTION AND EFFECTS: *YEAR 1 (TASKS 1, 2, 5, 6, 7 AND 8)*

Prepared For:

Utah Department of Transportation
Research Division

Submitted By:

Brigham Young University
Department of Civil and Environmental Engineering

Authored By:

Kevin W. Franke
Levi T. Ekstrom
Kristin J. Ulmer

Year 1 Update Report for the TPF-5(296) Technical Advisory Committee
March 2015

DISCLAIMER

The authors alone are responsible for the preparation and accuracy of the information, data, analysis, discussions, recommendations, and conclusions presented herein. The contents do not necessarily reflect the views, opinions, endorsements, or policies of the Utah Department of Transportation or the U.S. Department of Transportation. The Utah Department of Transportation makes no representation or warranty of any kind, and assumes no liability therefore.

ACKNOWLEDGMENTS

The authors acknowledge the Utah, Idaho, Montana, Alaska, South Carolina, and Connecticut Departments of Transportation for funding this research for pooled fund study TPF-5(296). The views and opinions presented in this report represent those of its authors, and may not represent those of the state agencies funding this research.

TECHNICAL REPORT ABSTRACT

1. Report No. NA	2. Government Accession No. NA	3. Recipient's Catalog No. NA
4. Title and Subtitle SIMPLIFIED SPT PERFORMANCE-BASED ASSESSMENT OF LIQUEFACTION AND EFFECTS: *TASKS 1, 2, 5, 6, 7, AND 8*		5. Report Date March 2015 6. Performing Organization Code NA
7. Author(s) Kevin W. Franke, Levi T. Ekstrom, Kristin J. Ulmer		8. Performing Organization Report No. NA
9. Performing Organization Name and Address Brigham Young University Department of Civil and Environmental Engineering 368 Clyde Building Provo-UT 84602-4009		10. Work Unit No. 4206515D 11. Contract or Grant No. 148753
12. Sponsoring Agency Name and Address Utah Department of Transportation 4501 South 2700 West P.O. Box 148410 Salt Lake City, UT 84114-8410		13. Type of Report & Period Covered Year 1 TAC Report March 2014 - March 2015 14. Sponsoring Agency Code PIC No. UT13.407

15. Supplementary Notes

Prepared in cooperation with the Utah Department of Transportation and the U.S. Department of Transportation, Federal Highway Administration

16. Abstract

The purpose of the research being performed is to provide the benefit of the full performance-based probabilistic earthquake hazard analysis, without requiring special software, training, and experience. To do this, simplified models of liquefaction triggering and lateral spread displacements that approximate the results of the full probabilistic analysis were developed. These simplified methods are designed to require only a few calculations programmed into a spreadsheet and a provided liquefaction parameter map. The simplified procedures are based on the Boulanger and Idriss (2012) probabilistic liquefaction triggering and Youd et al. (2002) empirical models. The new simplified procedures are based on retrieving a reference parameter value (i.e. CSRref (%), log DH ref, etc.) from a hazard-targeted liquefaction parameter map, and calculating site-specific correction factors to adjust the reference value to represent the site-specific conditions. The simplified procedures were validated by comparing the results of the simplified analysis with a full performance-based analysis for 10 cities of varying seismicity. The results show that the simplified procedure is, on average, within 5% error of the full performance-based procedure. These maps were created for Alaska, Connecticut, Idaho, Montana, South Carolina, and Utah at the 475, 1033, and 2475 year return periods. The simplified procedures were compared with the deterministic and pseudo-probabilistic procedures. The deterministic procedure significantly over predicts hazard at in regions of low seismicity, slightly over predicts hazard in regions of medium seismicity, and slightly under predicts hazard in areas of high seismicity when compared to the simplified procedure at the 475 and 2475 year return periods.

17. Key Words Lateral Spread Displacements, Liquefaction Triggering, Performance-based Engineering Reference Maps, Simplified Models, Seismic Hazards		18. Distribution Statement Not restricted. Available through: UDOT Research Division 4501 South 2700 West P.O. Box 148410 Salt Lake City, UT 84114-8410 www.udot.utah.gov/go/research		23. Registrant's Seal NA
19. Security Classification (of this report) Unclassified	20. Security Classification (of this page) Unclassified	21. No. of Pages 171	22. Price NA	

TABLE OF CONTENTS

LIST OF TABLES

LIST OF FIGURES

UNIT CONVERSION FACTORS

Units used in this report and not conforming to the UDOT standard unit of measurement (U.S. Customary system) are given below with their U.S. Customary equivalents:

SI* (MODERN METRIC) CONVERSION FACTORS

APPROXIMATE CONVERSIONS TO SI UNITS

Symbol	When You Know	Multiply By	To Find	Symbol
		LENGTH		
in	inches	25.4	millimeters	mm
ft	feet	0.305	meters	m
yd	yards	0.914	meters	m
mi	miles	1.61	kilometers	km
		AREA		
in^2	square inches	645.2	square millimeters	mm^2
ft^2	square feet	0.093	square meters	m^2
yd^2	square yard	0.836	square meters	m^2
ac	acres	0.405	hectares	ha
mi^2	square miles	2.59	square kilometers	km^2
		VOLUME		
fl oz	fluid ounces	29.57	milliliters	mL
gal	gallons	3.785	liters	L
ft^3	cubic feet	0.028	cubic meters	m^3
yd^3	cubic yards	0.765	cubic meters	m^3
	NOTE: volumes greater than 1000 L shall be shown in m^3			
		MASS		
oz	ounces	28.35	grams	g
lb	pounds	0.454	kilograms	kg
T	short tons (2000 lb)	0.907	megagrams (or "metric ton")	Mg (or "t")
		TEMPERATURE (exact degrees)		
°F	Fahrenheit	5 (F-32)/9 or (F-32)/1.8	Celsius	°C
		ILLUMINATION		
fc	foot-candles	10.76	lux	lx
fl	foot-Lamberts	3.426	$candela/m^2$	cd/m^2
		FORCE and PRESSURE or STRESS		
lbf	poundforce	4.45	newtons	N
lbf/in^2	poundforce per square inch	6.89	kilopascals	kPa

APPROXIMATE CONVERSIONS FROM SI UNITS

Symbol	When You Know	Multiply By	To Find	Symbol
		LENGTH		
mm	millimeters	0.039	inches	in
m	meters	3.28	feet	ft
m	meters	1.09	yards	yd
km	kilometers	0.621	miles	mi
		AREA		
mm^2	square millimeters	0.0016	square inches	in^2
m^2	square meters	10.764	square feet	ft^2
m^2	square meters	1.195	square yards	yd^2
ha	hectares	2.47	acres	ac
km^2	square kilometers	0.386	square miles	mi^2
		VOLUME		
mL	milliliters	0.034	fluid ounces	fl oz
L	liters	0.264	gallons	gal
m^3	cubic meters	35.314	cubic feet	ft^3
m^3	cubic meters	1.307	cubic yards	yd^3
		MASS		
g	grams	0.035	ounces	oz
kg	kilograms	2.202	pounds	lb
Mg (or "t")	megagrams (or "metric ton")	1.103	short tons (2000 lb)	T
		TEMPERATURE (exact degrees)		
°C	Celsius	1.8C+32	Fahrenheit	°F
		ILLUMINATION		
lx	lux	0.0929	foot-candles	fc
cd/m^2	$candela/m^2$	0.2919	foot-Lamberts	fl
		FORCE and PRESSURE or STRESS		
N	newtons	0.225	poundforce	lbf
kPa	kilopascals	0.145	poundforce per square inch	lbf/in^2

*SI is the symbol for the International System of Units. (Adapted from FHWA report template, Revised March 2003)

LIST OF ACRONYMS

EDP	Engineering Demand Parameter
FHWA	Federal Highway Administration
GMPE	Ground Motion Predictive Equation
IM	Intensity Measure
PBEE	Performance-Based Earthquake Engineering
PSHA	Probabilistic Seismic Hazard Analysis
UDOT	Utah Department of Transportation

LIST OF TERMS

Liquefaction Triggering Terms

a_{max}	peak ground surface acceleration
CRR	cyclic resistance ratio
$CRR_{PL=50\%}$	median CRR (CRR corresponding to a probability of liquefaction of 50%)
CSR	cyclic stress ratio
CSR^{ref}	uniform hazard estimate of CSR associated with the reference soil profile
CSR^{site}	site-specific uniform hazard estimate of CSR
ΔCSR_{σ}	correction factor for vertical stress
ΔCSR_{Fpga}	correction factor for soil amplification
ΔCSR_{rd}	correction factor for shear stress reduction
ΔCSR_{MSF}	correction factor for magnitude scaling factor
$\Delta CSR_{K\sigma}$	correction factor for overburden pressure
ΔCSR	difference between CSR^{site} and CSR^{ref} values
FC	fines content (%)
FS_L	factor of safety against liquefaction triggering
$FS_L{}^{site}$	site-specific uniform hazard estimate of FS_L
F_{PGA}	soil amplification factor
K_{σ}	overburden correction factor (Idriss and Boulanger model)
MSF	magnitude scaling factor
M_w	mean moment magnitude
N	SPT blow count (uncorrected)
$(N_1)_{60}$	SPT resistance corrected to 60% efficiency and 1 atm pressure
$(N_1)_{60,cs}$	clean sand-equivalent SPT corrected to 60% efficiency and 1 atm pressure
N_{req}	SPT resistance required to resist or prevent liquefaction
$N_{req}{}^{ref}$	uniform hazard estimate of N_{req} associated with the reference soil profile
$N_{req}{}^{site}$	site-specific uniform hazard estimate of N_{req}
ΔN_L	difference between N_{site} and N_{req} values
P_a	atmospheric pressure (1 atm, 101.3 kPa, 0.2116 psf)
PGA	peak ground acceleration
P_L	probability of liquefaction
r_d	shear stress reduction coefficient
SPT	Standard Penetration Test
$V_{s,12}$	average shear wave velocity in upper 12 m (39.37 ft) of soil profile
z	depth to middle of soil profile layer
γ	unit weight of soil (i.e. pcf, kN/m^3, etc.)
σ_{ε}	error term for either model + parametric uncertainty or parametric uncertainty
σ_T	error term for both model and parametric uncertainty

σ_v	total vertical stress in the soil
σ'_v	effective vertical stress in the soil
Λ_{FSL^*}	mean annual rate of not exceeding some given value of FS_L
λ_{Nreq^*}	mean annual rate of not exceeding some given value of N_{req}
τ_{cyc}	equivalent uniform cyclic shear stress
Φ	standard normal cumulative distribution function

Lateral Spread Displacement Terms

D_H	median computed permanent lateral spread displacement (m)
R	closest horizontal distance from the site to the source (km)
M	earthquake moment magnitude
W	free-face ratio (%)
S	ground slope (%)
T_{15}	cumulative thickness (in upper 20 m) of all saturated soil layers with corrected SPT blowcounts (i.e., $(N_1)_{60}$) less than 15 blows/foot (m)
F_{15}	average fines content of the soil comprising T_{15} (%)
$D50_{15}$	average mean grain size of the soil comprising T_{15} (mm)
$\mathscr{L}$	Loading Parameter
$\mathscr{S}$	Site Parameter
$\mathscr{D}$	transformed (e.g. log, ln, square root) lateral spread displacement
ε	uncertainty term (used in lateral spread displacement model)
$[\log D_H]^{site}$	logarithm of the lateral spread displacement adjusted for site-specific conditions
$[\log D_H]^{ref}$	logarithm of the lateral spread displacement corresponding to the reference site
ΔD_H	adjustment factor for lateral spread displacement
$D_H{}^{site}$	site-specific hazard-targeted lateral spread displacement

EXECUTIVE SUMMARY

The purpose of the research being performed is to provide the benefit of the full performance-based probabilistic earthquake hazard analysis, without requiring special software, training, and experience. To do this, simplified models of liquefaction triggering and lateral spread displacements that approximate the results of the full probabilistic analysis were developed. These simplified methods are designed to require only a few calculations programmed into a spreadsheet and a provided liquefaction parameter map. This report provides the derivation and validation of these simplified models, addressing Tasks 1, 2, 5, 6, 7, and 8 of the TPF-5(296) research contract.

The simplified procedure using the Boulanger and Idriss (2012) probabilistic liquefaction triggering model is derived based on principles from the Mayfield et al. (2010) derivation of the simplified procedure for the Cetin et al. (2004) probabilistic liquefaction triggering model. The simplified procedure for predicting lateral spread displacements is derived based on the Youd et al. (2002) empirical model. The new simplified procedures are based on retrieving a reference parameter value (i.e. CSR^{ref} (%), log $D_H{}^{ref}$, etc.) from a hazard-targeted liquefaction parameter map, and calculating site-specific correction factors to adjust the reference value to represent the site-specific conditions. The simplified procedures were validated by comparing the results of the simplified analysis with a full performance-based analysis for 10 cities of varying seismicity. The results show that the simplified procedure is within 5% error of the full performance-based procedure.

To ensure that spatial bias is not introduced into the liquefaction parameter maps, a grid spacing evaluation was performed. The grid spacings determined in the evaluation were used in the development of the liquefaction parameter maps. These maps were created for Alaska, Connecticut, Idaho, Montana, South Carolina, and Utah at the 475, 1033, and 2475 year return periods.

The simplified procedures were compared with the deterministic and pseudo-probabilistic procedures. The deterministic procedure significantly over predicts hazard in regions of low seismicity, slightly over predicts hazard in regions of medium seismicity, and slightly under predicts hazard in areas of high seismicity when compared to the simplified procedure at the 475

and 2475 year return periods. The pseudo-probabilistic procedure return results very similar to the simplified method at the 1033 year return period.

To assist in implementing the simplified procedures, a tool was created to perform the simplified calculations. This tool is available in spreadsheet form and provides an easily implemented procedure. A step-by-step process is included in this report and will assist in the use of the simplified spreadsheet tool.

1.0 INTRODUCTION

1.1 Problem Statement

The purpose of the research being performed is to develop a procedure that provides the benefit of the full performance-based probabilistic earthquake hazard analysis, without requiring special software, training, and experience. To do this, simplified models of liquefaction triggering and lateral spread displacements were developed that approximate the results of the full probabilistic analysis.

1.2 Objectives

The objective of this report is to provide simplified performance-based procedures to the members of the TAC which closely approximates the results of full probabilistic analyses for liquefaction initiation and lateral spread displacement. This was done by performing the following steps:

- Introduce the original models used to determine liquefaction hazards (i.e. liquefaction triggering and lateral spread displacement) and provide in-depth derivations that demonstrate the development of the simplified methods
- Validate the simplified models by performing a site-specific analysis for several different sites using the simplified and full models
- Assess proper grid spacing for map development
- Create the hazard-targeted liquefaction and lateral spread parameter maps
- Compare the simplified procedure with deterministic methods
- Develop a tool to streamline the simplified procedure

These objectives specifically address Tasks 1, 2, 5, 6, 7 and 8 of the TPF-5(296) research contract.

1.3 Scope

The states included in this research were: Alaska, Connecticut, Idaho, Montana, South Carolina, and Utah. Hazard-targeted liquefaction parameter maps were developed for these states only. However, the same principles used in the simplified procedure provided in this report should apply similarly to other states. The final products of this research are: 1) a final report describing the findings of the research, 2) liquefaction parameter maps for the states mentioned at the 475, 1033, and 2475 year return periods, and 3) a spreadsheet that performs the simplified procedures outlined in the report.

1.4 Outline of Report

The research conducted for this report will contain the following:

- Derivation of the Simplified Models
- Validation of the Simplified Models
- Grid Spacing Study
- Development of the Parameter Maps
- Comparison with Deterministic Analyses
- Guide to the Simplified Procedure
- Conclusions
- Appendices

2.0 DERIVATION OF THE SIMPLIFIED MODELS

2.1 Overview

This section describes the derivation of the simplified liquefaction triggering and lateral spread displacement models. The original models will be introduced and the derivation process for the simplified models will be described in detail.

2.2 Performance-based Liquefaction Triggering Evaluation

This section will provide the necessary background to understand the simplified performance-based liquefaction triggering procedure. A brief discussion regarding empirical liquefaction triggering models will be provided, followed by a discussion of performance-based implementation of those models.

2.2.1 Empirical Liquefaction Triggering Models

While the use of liquefaction hazard maps can provide a useful preliminary assessment of liquefaction hazard for a site, most professionals rely upon site-specific liquefaction triggering assessment for use in design. One of the most widely used methods of assessment in engineering practice today is the simplified empirical procedure (Seed and Idriss 1971; Seed 1979; Seed and Idriss 1982; and Seed et al. 1985). According to this simplified procedure, liquefaction triggering is evaluated by comparing the seismic loading of the soil to the soil's resistance to liquefaction triggering. Seismic loading is typically characterized using a cyclic stress ratio, *CSR*, which is computed as:

$$CSR = \frac{\tau_{cyc}}{\sigma_v'} = 0.65 \frac{a_{\max}}{g} \frac{\sigma_v}{\sigma_v'} r_d \qquad (1)$$

where τ_{cyc} is the equivalent uniform cyclic shear stress, σ_v' is the effective vertical stress in the soil, $a_{\max}/g$ is the peak ground surface acceleration as a fraction of gravity, σ_v is the total vertical stress in the soil, and r_d is a shear stress reduction coefficient.

Soil resistance to liquefaction triggering is characterized by performing some in-situ soil test (e.g., standard penetration resistance, cone penetration resistance, shear wave velocity, etc.) and comparing its results to those from documented case histories of liquefaction triggering. Based on observation and/or statistical regression, a function for the in-situ test can be delineated that separates the "liquefaction" case histories from the "non-liquefaction" case histories. This delineated boundary is referred to as the cyclic resistance ratio, *CRR*, and represents the unique combinations of *CSR* and in-situ soil test values at which liquefaction triggers.

Engineers and geologists commonly quantify liquefaction triggering using a factor of safety against liquefaction triggering, FS_L. This parameter is calculated as:

$$FS_L = \frac{\text{Resistance}}{\text{Loading}} = \frac{CRR}{CSR} \tag{2}$$

Kramer and Mayfield (2007) and Mayfield et al. (2010) introduced an alternative method to quantifying liquefaction triggering. If using the standard penetration test (SPT), then *CRR* is a function of $(N_1)_{60-cs}$, which is the clean sand-equivalent, corrected SPT resistance for the soil layer. However, for a given level of seismic loading (i.e., *CSR*), the SPT resistance required to resist or prevent liquefaction, N_{req}, can be back-calculated from the *CRR* function. This term N_{req} can be used to compute FS_L using a modified form of Equation (2) as:

$$FS_L = \frac{CRR}{CSR} = \frac{CRR\left((N_1)_{60-cs}\right)}{CRR\left(N_{req}\right)} \tag{3}$$

where $CRR(N)$ denotes that *CRR* is a function of given value of SPT resistance, *N*.

Mayfield et al. (2010) defined the relationship between the actual SPT resistance for the given layer, N_{site}, and N_{req} as:

$$\Delta N_L = N_{site} - N_{req} \tag{4}$$

The relationship between *CSR*, *CRR*, N_{site}, and N_{req} is shown graphically in Figure 2-1, after Mayfield et al. (2010).

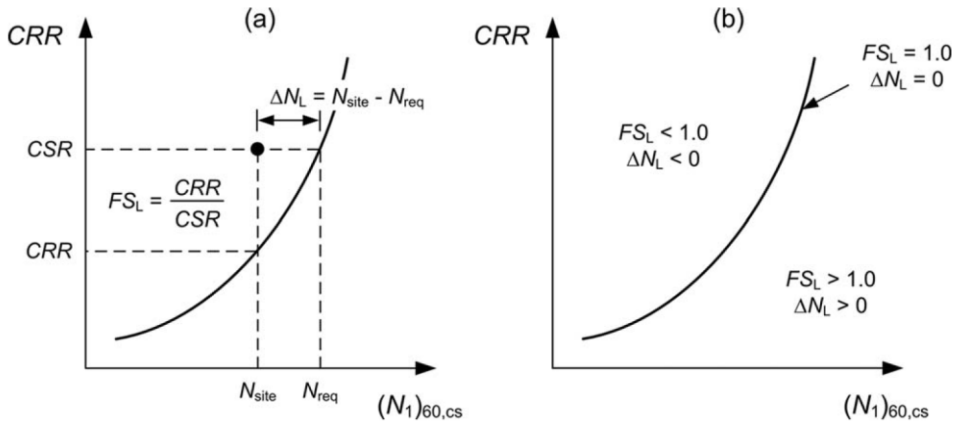

Figure 2-1 Schematic illustration of: (a) definitions of FS_L and ΔN_L; (b) relationship between FS_L and ΔN_L (after Mayfield et al. 2010)

2.2.2 Performance-based Liquefaction Triggering Assessment

Simplified empirical liquefaction triggering procedures require the selection of seismic loading parameters (i.e., peak ground surface acceleration $a_{\max}$ and moment magnitude M_w) to characterize a representative or design earthquake. When analyzing the liquefaction hazard from a single seismic source, the process of selecting seismic loading parameters is relatively straight-forward and simple. However, few seismic environments exist where only a single seismic source can contribute to liquefaction hazard. In more complex seismic environments, seismic hazard is usually calculated with a probabilistic seismic hazard analysis (PSHA), which often produces a wide range of seismic loading parameter combinations, each associated with a different likelihood of occurrence. Despite the wide variety of possible seismic loading parameter combinations produced by a PSHA, engineers must select a single set of seismic loading parameters that

adequately characterize the complex seismicity of the site. Conventional approaches to liquefaction triggering assessment typically utilize the deaggregation results associated with the PSHA for $a_{\max}$ at a targeted hazard level or return period to obtain that single set of seismic loading parameters. Engineers select either the median or mean moment magnitude from the deaggregation results, and subsequently couple this selected magnitude with the $a_{\max}$ value associated with the targeted return period. Unfortunately, these conventional approaches were shown by Kramer and Mayfield (2007) to introduce bias into the computed liquefaction triggering hazard.

Potential biases introduced into the liquefaction triggering assessment through the improper and/or incomplete utilization of probabilistic ground motions and liquefaction triggering models could be reduced through the implementation of a performance-based approach (Franke et al. 2014a). Kramer and Mayfield (2007) presented such an approach, which utilized the probabilistic framework for performance-based earthquake engineering (PBEE) developed by the Pacific Earthquake Engineering Research Center (Cornell and Krawinkler 2000; Krawinkler 2002; Deierlein et al. 2003). This implementation of the PEER PBEE framework assigned the joint occurrence of M_w and $a_{\max}$ as an intensity measure, and either FS_L or N_{req} as the engineering demand parameter.

Kramer and Mayfield (2007) demonstrated that a hazard curve for FS_L could be developed using the following relationship:

$$\Lambda_{FS_L^*} = \sum_{j=1}^{N_M} \sum_{i=1}^{N_{a_{\max}}} P\left[FS_L < FS_L^* \mid a_{\max_i}, m_j \right] \Delta\lambda_{a_{\max_i}, m_j} \tag{5}$$

where $\Lambda_{FS_L^*}$ is the mean annual rate of *not* exceeding some given value of factor of safety, FS_L^*; $P\left[FS_L < FS_L^* \mid a_{\max_i}, \mathrm{m}_j \right]$ is the conditional probability that the actual factor of safety is less than FS_L^* given peak ground surface acceleration $a_{\max_i}$ and moment magnitude m_j; $\Delta\lambda_{a_{\max_i}, m_j}$ is the incremental joint mean annual rate of exceedance for $a_{\max_i}$ and m_j; and N_M and $N_{a_{\max}}$ are the

number of magnitude and peak ground acceleration increments into which the intensity measure "hazard space" is subdivided.

The conditional probability component of Equation (5) can be solved with any selected probabilistic liquefaction triggering relationship, but that relationship must be manipulated to compute the desired probability. Assuming the inclusion of parametric uncertainty (i.e., uncertainty in SPT resistance and seismic loading), Kramer and Mayfield (2007) solved the conditional probability term using the Cetin et al. (2004) liquefaction triggering relationship as:

$$P\left[FS_L < FS_L^* \mid a_{\max_i}, m_j\right] = \Phi\left[-\frac{(N_1)_{60}(1+0.004FC) - 13.79\left(FS_L^* \cdot CSR_i\right) - 29.06\ln\left(m_j\right) - 3.82\ln\left(\frac{\sigma_v'}{p_a}\right) + 0.06FC + 15.25}{4.21}\right] \quad (6)$$

where Φ represents the standard normal cumulative distribution function, $(N_1)_{60}$ is the SPT resistance corrected for atmospheric pressure and hammer energy as computed using Cetin et al. (2004); FC is the fines content (in percent); CSR_i is equal to Equation (1) using $a_{\max_i}$ as in input; and p_a is atmospheric pressure (in the same units as σ_v').

Franke et al. (2014b) solved the conditional probability component of Equation (5) using the Boulanger and Idriss (2012) probabilistic liquefaction triggering relationship as:

$$P\left[FS_L < FS_L^* \mid a_{\max,i}, m_j\right] = \Phi\left[-\frac{\frac{(N_1)_{60,cs}}{14.1} + \left(\frac{(N_1)_{60,cs}}{126}\right)^2 - \left(\frac{(N_1)_{60,cs}}{23.6}\right)^3 + \left(\frac{(N_1)_{60,cs}}{25.4}\right)^4 - 2.67 - \ln\left(CSR_{i,j} \cdot FS_L^*\right)}{\sigma_\varepsilon}\right] \quad (7)$$

$$CSR_{i,j} = 0.65\frac{a_{\max,i}}{g}\frac{\sigma_v}{\sigma_v'}\left(r_d\right)_j\frac{1}{\left(MSF\right)_j}\frac{1}{K_\sigma} \quad (8)$$

where $(N_1)_{60}$ is the SPT resistance corrected for atmospheric pressure and hammer energy as computed using Idriss and Boulanger (2008, 2010); $(MSF)_j$ is the magnitude scaling factor for magnitude m_j and is computed according to Idriss and Boulanger (2008); $(r_d)_j$ is the depth

reduction factor for magnitude m_j and is computed according to Idriss and Boulanger (2008); K_σ the depth correction factor and is computed according to Idriss and Boulanger (2008), and σ_ε is equal to either 0.13 for model uncertainty alone or 0.277 for total (i.e., model + parametric) uncertainty.

Similar to the relationship for computing a hazard curve for FS_L, Kramer and Mayfield (2007) derived a relationship for computing a hazard curve for N_{req} as:

$$\lambda_{N^*_{req}} = \sum_{j=1}^{N_M} \sum_{i=1}^{N_{a_{\max}}} P\left[N_{req} > N^*_{req} \mid a_{\max_i}, m_j \right] \Delta\lambda_{a_{\max_i}, m_j} \tag{9}$$

where $\lambda_{N^*_{req}}$ is the mean annual rate of exceeding some given clean sand-equivalent required SPT resistance, N^*_{req}, and $P\left[N_{req} > N^*_{req} \mid a_{\max_i}, \mathrm{m}_j \right]$ is the conditional probability that the actual N_{req} is greater than N^*_{req} given peak ground surface acceleration $a_{\max_i}$ and moment magnitude m_j. Kramer and Mayfield (2007) and Mayfield et al. (2010) used the Cetin et al. (2004) probabilistic liquefaction triggering relationship (assuming the inclusion of parametric uncertainty) to solve the conditional probability component of Equation (9) as:

$$P\left[N_{req} > N^*_{req} \mid a_{\max_i}, m_j \right] = \Phi\left[-\frac{N^*_{req} - 13.79\left(CSR_i\right) - 29.06\ln\left(m_j\right) - 3.82\ln\left(\frac{\sigma'_v}{p_a}\right) + 15.25}{4.21} \right] \tag{10}$$

Franke and Wright (2013) substituted the Boulanger and Idriss (2012) model for the Cetin et al. (2004) model to develop an alternative conditional probability term for Equation (9) as:

$$P\left[N_{req} > N^*_{req} \mid a_{\max,i}, m_j \right] = \Phi\left[-\frac{\frac{N^*_{req}}{14.1} + \left(\frac{N^*_{req}}{126}\right)^2 - \left(\frac{N^*_{req}}{23.6}\right)^3 + \left(\frac{N^*_{req}}{25.4}\right)^4 - 2.67 - \ln CSR_{i,j}}{\sigma_\varepsilon} \right] \tag{11}$$

where $CSR_{i,j}$ is computed with Equation (8), and σ_{ε} is equal to either 0.13 for model uncertainty alone or 0.277 for total (i.e., model + parametric) uncertainty.

2.3 Simplified Liquefaction Triggering Model

The Kramer and Mayfield (2007) performance-based liquefaction triggering procedure summarized in Section 2.2.2 is an effective solution to mitigating the deficiencies introduced by the conventional liquefaction triggering approach, which utilizes probabilistic ground motions and a liquefaction triggering relationship in a deterministic manner. Unfortunately, the Kramer and Mayfield procedure is relatively sophisticated and difficult for many engineers and geologists to apply in a practical manner. Specialized computational tools such as *WSliq* (Kramer 2008) and *PBliquefY* (Franke et al. 2014c) have been developed to assist these professionals in implementing the performance-based procedure. However, even the availability of computational tools is not sufficient for many professionals, who routinely need to perform and/or validate liquefaction triggering hazard calculations in a rapid and efficient manner.

An ideal solution to this dilemma would be the introduction of a new liquefaction analysis procedure that combined the simplicity and user-friendliness of traditional liquefaction hazard maps with the flexibility and power of a site-specific performance-based liquefaction triggering analysis. Mayfield et al. (2010) introduced such a procedure, which was patterned after the map-based procedure used in most seismic codes and provisions for developing probabilistic ground motions for engineering design. Franke et al. (2014d) later refined the Mayfield et al. simplified procedure for easier implementation in seismic codes and provisions.

Mayfield et al. (2010) demonstrated with the Cetin et al. (2004) liquefaction model that probabilistic estimates of liquefaction resistance (i.e. N_{req}) can be computed for a reference soil profile across a grid of locations to develop contour plots called liquefaction parameter maps. A liquefaction parameter map incorporating N_{req} can be a useful tool to evaluate the seismic demand for liquefaction at a given return period because N_{req} is directly related to *CSR* (i.e. Figure 2-1). Mayfield et al. demonstrated how these mapped "reference" values of N_{req} could be adjusted for

site-specific conditions and used to develop site-specific uniform hazard estimates of N_{req} (i.e., N_{req}^{site}) and/or FS_L (i.e., FS_L^{site}) at the targeted return period or hazard level. The derivation of the simplified method for the Cetin et al. (2004) liquefaction triggering model will not be included in this report, but is presented in detail in Mayfield et al. (2010) and Franke et al. (2014d).

Because many engineers desire to evaluate liquefaction initiation hazard using either the Youd et al. (2001) or the Idriss and Boulanger (2006, 2008) (which is very similar to Youd et al. 2001) liquefaction triggering curves for the SPT, a simplified uniform hazard liquefaction procedure that incorporates the Boulanger and Idriss (2012) probabilistic liquefaction model can be developed through an approach similar to that used by Mayfield et al. (2010).

2.3.1 Simplified Procedure Using the Boulanger and Idriss (2012) Probabilistic Liquefaction Triggering Model

According to the probabilistic liquefaction triggering relationship developed by Boulanger and Idriss (2012), the probability of liquefaction P_L is given as:

$$P_L = \Phi\left[-\frac{\ln\left(CRR_{P_L=50\%}\right)-\ln\left(CSR\right)}{\sigma_T}\right] \tag{12}$$

where σ_T is the total uncertainty of the liquefaction model, and $CRR_{P_L=50\%}$ is the cyclic resistance ratio corresponding to a probability of liquefaction of 50% (i.e. median *CRR*), which is computed as:

$$CRR_{P_L=50\%} = \exp\left[\left(\frac{(N_1)_{60,cs}}{14.1}\right)+\left(\frac{(N_1)_{60,cs}}{126}\right)^2-\left(\frac{(N_1)_{60,cs}}{23.6}\right)^3+\left(\frac{(N_1)_{60,cs}}{25.4}\right)^4-2.67\right] \tag{13}$$

Unlike the Mayfield et al. (2010) simplified liquefaction procedure, which incorporates the Cetin et al. (2004) liquefaction model, the simplified uniform hazard liquefaction procedure for the Boulanger and Idriss (2012) liquefaction model cannot be derived to solve for N_{req}^{site} in a convenient manner because of the 4th-order polynomial equation in *CRR* (i.e. Equation (13)). Fortunately, this simplified procedure can be modified to incorporate *CRR* and *CSR* instead of N_{req},

which greatly simplifies the derivation of the new procedure, and also makes it somewhat more intuitive.

Figure 2-2 presents a generic soil profile representing a reference site originally introduced by Mayfield et al. (2010) and used for the simplified Cetin et al. (2004) procedure. This reference soil profile can be used with a full performance-based liquefaction analysis incorporating the Boulanger and Idriss (2012) probabilistic liquefaction model (Franke and Wright 2013) to find N_{req} at a depth of 6 meters for the targeted return period (T_R) or hazard level. Because the value of N_{req} associated with the reference soil profile does not represent any actual soil profile, Mayfield et al. (2010) distinguished it using the term N_{req}^{ref}. By substituting N_{req}^{ref} into Equation (13), the median *CSR* associated with the reference site (i.e. CSR^{ref}) at the targeted return period can be computed. In other words, CSR^{ref} represents a uniform hazard estimate of the seismic loading that must be overcome to prevent liquefaction triggering if the reference soil profile existed at the site of interest. By computing similar hazard-targeted values of CSR^{ref} at different locations across a geographic area, contoured liquefaction parameter maps for CSR^{ref} can be constructed. These maps will be called *liquefaction loading maps* because they convey information regarding the seismic loading affecting liquefaction triggering, and to distinguish them from liquefaction parameter maps, which convey information regarding N_{req}^{ref}. Because *CSR* is often a decimal value less than unity, mapping the percent of *CSR*, $CSR^{ref}\,(\%)$ allows for more precise contour mapping, as well as easier interpretation and interpolation for design engineers. Figure 2-3 presents a liquefaction loading map of $CSR^{ref}\,(\%)$ at a return period of 1,033 years for a portion of the Salt Lake Valley in Utah.

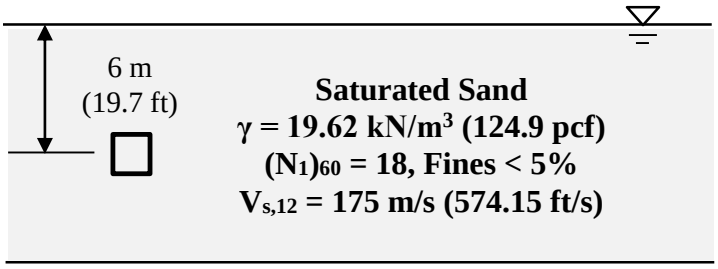

Figure 2-2. Reference soil profile used to develop liquefaction loading maps in the proposed simplified uniform hazard liquefaction procedure

Figure 2-3. Liquefaction loading map (T_R = 1,033 years) showing contours of CSR^{ref} (%) for a portion of the Salt Lake Valley in Utah.

In interpreting a liquefaction loading map such as the one presented in Figure 2.3, a qualitative assessment of relative liquefaction hazard across a geographic area at the targeted return period can be made. Higher values of $CSR^{ref}(\%)$ imply higher levels of seismic loading for liquefaction triggering. Soils located in areas of higher $CSR^{ref}(\%)$ will need greater SPT resistance to prevent liquefaction triggering than soils located in areas of lower $CSR^{ref}(\%)$. However, a liquefaction loading map by itself tells the engineer nothing regarding the actual liquefaction hazard at a site because the map does not account for site-specific soil conditions. A procedure will subsequently be derived and presented to correct the mapped liquefaction loading values to site-specific liquefaction loading values, which can be used to compute site-specific performance-based estimates of liquefaction triggering hazard at a targeted return period.

A liquefaction loading map should not be confused with a liquefaction hazard map, which attempts to account for actual soil conditions at each mapped location. The difficulty in obtaining site-specific subsurface data for all locations across a geologic region is significant, indeed. Furthermore, liquefaction hazard maps tell the engineer nothing regarding the liquefaction triggering hazard with depth in the actual soils at the site. Thus, liquefaction hazard maps constitute a preliminary hazard assessment and planning tool, and can be very helpful to engineers if used properly. However, liquefaction hazard map results should be interpreted with caution and an understanding that local site conditions and actual liquefaction hazard may deviate significantly from what is mapped.

2.3.1.1 Site-Specific Correction for CSR^{ref}

Because CSR^{ref} was developed using the reference soil profile, it must be corrected for site-specific soil conditions and depths to be used in computing site-specific uniform hazard values of FS_L, P_L, and N_{req}. If CSR^{site} represents the site-specific uniform hazard value of CSR, then CSR^{ref} and CSR^{site} can be related as:

$$\ln\left(CSR^{site}\right) = \ln\left(CSR^{ref}\right) + \Delta CSR \tag{14}$$

where ΔCSR is a site-specific correction factor. Rearranging Equation (14), we can solve for ΔCSR as:

$$\Delta CSR = \ln\left(CSR^{site}\right) - \ln\left(CSR^{ref}\right) = \ln\left(\frac{CSR^{site}}{CSR^{ref}}\right) \tag{15}$$

Similar to Equation (8), the magnitude- and stress-corrected *CSR* for level or near-level ground according to Boulanger and Idriss (2012) is computed as:

$$CSR_{M=7.5,\sigma_v'=1atm} = 0.65\frac{\sigma_v}{\sigma_v'}\frac{a_{\max}}{g} r_d \frac{1}{MSF}\frac{1}{K_\sigma} = 0.65\frac{\sigma_v}{\sigma_v'}\frac{\left(F_{pga}\cdot PGA_{rock}\right)}{g} r_d \frac{1}{MSF}\frac{1}{K_\sigma} \tag{16}$$

where F_{pga} is the soil amplification factor corresponding to the peak ground acceleration (*PGA*), and PGA_{rock} is the *PGA* corresponding to bedrock (i.e. V_S=760 m/s). Equations for r_d, *MSF*, and K_σ as defined in Idriss and Boulanger (2008, 2010) are provided in later sections of this report. If Equation (16) is substituted into Equation (15), then Equation (15) can be rewritten as:

$$\Delta CSR = \ln\left[\frac{0.65\left(\frac{\sigma_v}{\sigma_v'}\right)^{site}\left(\frac{F_{pga}^{site}\cdot PGA_{rock}^{site}}{g}\right)\cdot r_d^{site}\cdot\left(\frac{1}{MSF^{site}}\right)\cdot\left(\frac{1}{K_\sigma^{site}}\right)}{0.65\left(\frac{\sigma_v}{\sigma_v'}\right)^{ref}\left(\frac{F_{pga}^{ref}\cdot PGA_{rock}^{ref}}{g}\right)\cdot r_d^{ref}\cdot\left(\frac{1}{MSF^{ref}}\right)\cdot\left(\frac{1}{K_\sigma^{ref}}\right)}\right] \tag{17}$$

Because there should be no difference in the ground motions between the reference soil profile and the actual soil profile, $PGA_{rock}^{site} = PGA_{rock}^{ref}$. Therefore, Equation (17) can be simplified as:

$$\begin{aligned}\Delta CSR &= \ln\left(\frac{\left(\sigma_v/\sigma_v'\right)^{site}}{\left(\sigma_v/\sigma_v'\right)^{ref}}\right) + \ln\left(\frac{F_{pga}^{site}}{F_{pga}^{ref}}\right) + \ln\left(\frac{r_d^{site}}{r_d^{ref}}\right) - \ln\left(\frac{MSF^{site}}{MSF^{ref}}\right) - \ln\left(\frac{K_\sigma^{site}}{K_\sigma^{ref}}\right) \\ &= \Delta CSR_\sigma + \Delta CSR_{F_{pga}} + \Delta CSR_{r_d} + \Delta CSR_{MSF} + \Delta CSR_{K_\sigma}\end{aligned} \tag{18}$$

where ΔCSR_{σ}, ΔCSR_{Fpga}, ΔCSR_{rd}, ΔCSR_{MSF}, and $\Delta CSR_{K\sigma}$ are site-specific correction factors for stress, soil amplification, shear stress reduction, earthquake magnitude, and overburden pressure, respectively.

2.3.1.2 Correction for Vertical Stress, ΔCSR_{σ}

The relationship for the stress correction factor, ΔCSR_{σ} is defined as:

$$\Delta CSR_{\sigma} = \ln\left[\frac{\left(\sigma_v / \sigma_v'\right)^{site}}{\left(\sigma_v / \sigma_v'\right)^{ref}}\right] \tag{19}$$

If the liquefaction parameter map for CSR^{ref} (%) was developed using the reference soil profile shown in Figure 2-2, then Equation (19) can be simplified as:

$$\Delta CSR_{\sigma} = \ln\left[\frac{\left(\sigma_v / \sigma_v'\right)^{site}}{2}\right] \tag{20}$$

Mayfield et al. (2010) used weight-volume relationships to investigate the possibility of simplifying the stress correction factor in their simplified procedure. By substituting specific gravity and void ratio for the vertical stress terms, and then by assuming that the site-specific void ratio and specific gravity were the same as those used in the reference soil profile, Mayfield et al. developed a simplified equation for their stress correction factor that was simply a function of depth and depth to groundwater. Mayfield et al. demonstrated that this simplified equation was quite insensitive to changes in void ratio, and thus introduced relatively little error into their computed results. A similar investigation was performed with ΔCSR_{σ} in this study to evaluate the possibility of developing a simplified relationship for Equation (20). However, we found that a simplified equation after the manner demonstrated by Mayfield et al. introduces significant error into the computed results of our proposed simplified liquefaction procedure, likely due to the fact

that our proposed procedure is based on a natural logarithm function (i.e. Equation (15)), whereas the Mayfield et al. (2010) simplified procedure is based on a linear relationship.

2.3.1.3 Correction for Soil Amplification, ΔCSR_{Fpga}

The relationship for the soil amplification factor, ΔCSR_{Fpga} is defined as:

$$\Delta CSR_{F_{pga}} = \ln\left(\frac{F_{pga}^{site}}{F_{pga}^{ref}}\right) \tag{21}$$

If the value of F_{pga}^{ref} for the reference soil profile is fixed at 1, then the correction factor for soil amplification can be written as:

$$\Delta CSR_{F_{pga}} = \ln\left(\frac{F_{pga}^{site}}{1}\right) = \ln\left(F_{pga}^{site}\right) \tag{22}$$

Thus the only parameter required to calculate the soil amplification factor is the F_{pga}^{site} value from AASHTO 2012 Table 3.10.3.2-1 corresponding to the site of interest. This table is included here as a reference (Table 2-1). The *PGA* value used to determine F_{pga}^{site} from the table should be calculated from the USGS 2008 (USGS 1996 for Alaska) interactive deaggregation website for the return period of interest (e.g., 2% probability of exceedance in 21 years, T_R = 1039).

If an engineer prefers to use an empirical model for soil amplification, such as the Stewart et al. (2003) model, the ΔCSR_{Fpga} term can be adjusted for the desired model. For example, in the Stewart et al. (2003) model, the median amplification factor F_{pga} is defined as:

$$F_{pga} = \exp\left[a + b\ln\left(PGA_{rock}\right)\right] \tag{23}$$

where PGA_{rock} is in units of g, *a* and *b* are regression coefficients defined by Stewart et al. (2003).

Table 2-1. Values of Site Factor, F_{pga}, at Zero-Period on Acceleration Spectrum (from AASHTO 2012 Table 3.10.3.2-1)

Site Class	Peak Ground Acceleration Coefficient (*PGA*)[1]				
	***PGA* < 0.10**	***PGA* = 0.20**	***PGA* = 0.30**	***PGA* = 0.40**	***PGA* > 0.50**
A	0.8	0.8	0.8	0.8	0.8
B	1.0	1.0	1.0	1.0	1.0
C	1.2	1.2	1.1	1.0	1.0
D	1.6	1.4	1.2	1.1	1.0
E	2.5	1.7	1.2	0.9	0.9
F[2]	*	*	*	*	*

Notes:

[1]Use straight-line interpolation for intermediate values of *PGA*.

[2]Site-specific geotechnical investigation and dynamic site response analysis should be performed for all sites in Site Class F.

Using Equation (23), the correction for the soil amplification factor can be written as:

$$\Delta CSR_{F_{pga}} = \ln\left(\frac{F_{pga}^{site}}{F_{pga}^{ref}}\right) = \ln\left(\frac{\exp\left(a^{site} + b^{site}\ln\left(PGA_{rock}^{site}\right)\right)}{\exp\left(a^{ref} + b^{ref}\ln\left(PGA_{rock}^{ref}\right)\right)}\right)$$
$$= \left(a^{site} + b^{site}\ln\left(PGA_{rock}^{site}\right)\right) - \left(a^{ref} + b^{ref}\ln\left(PGA_{rock}^{ref}\right)\right) \quad (24)$$

There should be no difference between PGA_{rock}^{site} and PGA_{rock}^{ref}, so Equation (24) can be simplified to:

$$\Delta CSR_{F_{pga}} = \left(a^{site} - a^{ref}\right) + \ln\left(PGA_{rock}\right)\left(b^{site} - b^{ref}\right) \quad (25)$$

If the liquefaction parameter map for CSR^{ref} (%) was developed using the reference soil profile shown in Figure 2-2, then a^{ref} = - 0.15, b^{ref} = - 0.13 (see Stewart et al., 2003), and Equation (25) would become:

$$\Delta CSR_{F_{pga}} = \left(a^{site} + 0.15\right) + \ln\left(PGA_{rock}^{site}\right)\left(b^{site} + 0.13\right) \quad (26)$$

2.3.1.4 Correction for Shear Stress Reduction, ΔCSR_{rd}

The shear stress reduction factor, r_d, was defined by Boulanger and Idriss (2012, 2014) as:

$$r_d = \exp\left[\alpha + \beta \cdot M_w\right] \tag{27}$$

$$\alpha = -1.012 - 1.126 \sin\left(\frac{z}{11.73} + 5.133\right) \tag{28}$$

$$\beta = 0.106 + 0.118 \sin\left(\frac{z}{11.28} + 5.142\right) \tag{29}$$

where z represents sample depth in meters and M_w is the mean moment magnitude. Thus the equation for ΔCSR_{rd} becomes:

$$\Delta CSR_{r_d} = \ln\left(\frac{r_d^{site}}{r_d^{ref}}\right) = \ln\left(\frac{\exp\left(\alpha^{site} + \beta^{site} \cdot \mathrm{M}_w^{site}\right)}{\exp\left(\alpha^{ref} + \beta^{ref} \cdot \mathrm{M}_w^{ref}\right)}\right) \tag{30}$$

Both the site soil profile and the reference soil profile experience the same ground motions, so $M_w^{site} = M_w^{ref}$. Therefore, Equation (30) can be written as:

$$\Delta CSR_{r_d} = \left(\alpha^{site} - \alpha^{ref}\right) + M_w^{site}\left(\beta^{site} - \beta^{ref}\right) \tag{31}$$

Mayfield et al. (2010) demonstrated that the r_d term in the Cetin et al. (2004) model is relatively insensitive to the value of M_w for a particular range (M_w = 5.97 to 7.70). This observation allowed the correction factor for r_d to use a standard M_w value of 6.5 for all analyses. In this study, the r_d value from the Boulanger and Idriss (2012) model was found to be quite sensitive to M_w. This sensitivity is clear in Figure 2-4, which illustrates the variability of r_d with depth and M_w (5.5 to 8.0). Due to the significant discrepancy between r_d values for different M_w, the simplified Boulanger and Idriss (2012) method requires M_w^{site} to remain in Equation (31). For the reference soil profile used in this study (Figure 2-2), α^{ref} = -0.3408 and β^{ref} = 0.0385. Thus Equation (31) becomes:

$$\Delta CSR_{r_d} = \left(\alpha^{site} + 0.341\right) + M_w^{site}\left(\beta^{site} - 0.0385\right) \tag{32}$$

Equation (32) can also be written in terms of depth to the site-specific soil layer (in meters) from the ground surface, z^{site} as:

$$\Delta CSR_{r_d} = \left(-0.6712 - 1.126 \sin\left(\frac{z^{site}}{11.73} + 5.133 \right) \right) + M_w^{site} \left(0.0675 + 0.118 \sin\left(\frac{z^{site}}{11.28} + 5.142 \right) \right) \quad (33)$$

where the value of M_w^{site} is the mean moment magnitude from the 2008 (1996 for Alaska) USGS interactive deaggregation website for the return period of interest (e.g., 2% probability of exceedance in 21 years, T_R = 1039). The value of ΔCSR_{rd} varies with depth, and therefore must be calculated for each layer in the site-specific soil profile.

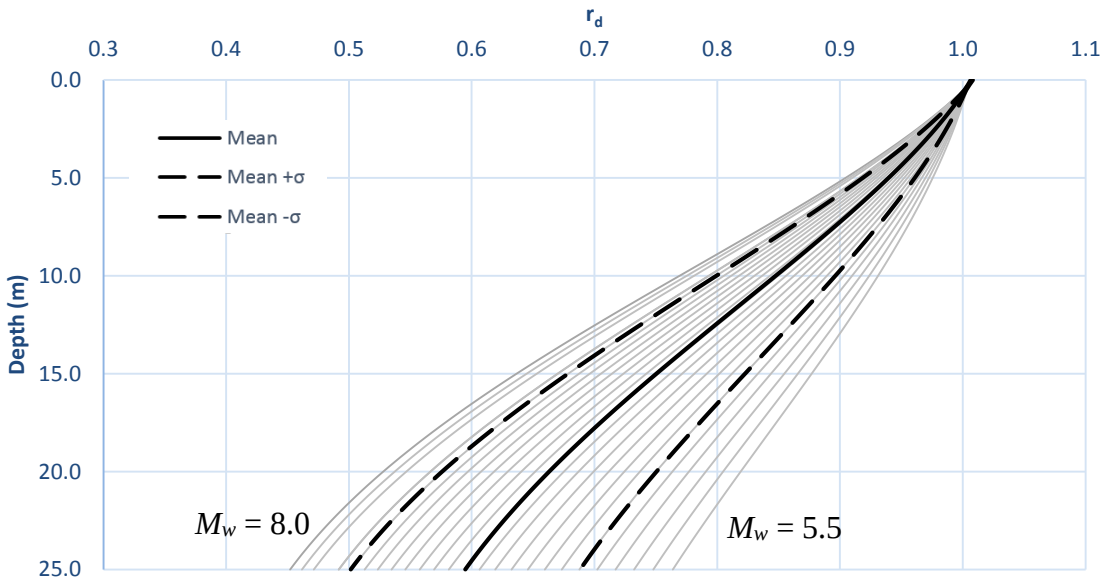

Figure 2-4. Shear stress reduction factor (r_d) vs. depth for a range of M_w values (5.5 to 8.0) according to the Boulanger and Idriss (2012) model.

2.3.1.5 Correction for Magnitude Scaling Factor, ΔCSR_{MSF}

If the *MSF* as calculated in the Idriss and Boulanger (2010, 2012) model is to be used, then there should be no difference in the earthquake magnitude between the reference soil profile and

the actual soil profile. In this case, $MSF^{site} = MSF^{ref}$ which indicates that $\Delta CSR_{MSF} = 0$ and therefore ΔCSR_{MSF} can be excluded from Equation (18).

If the *MSF* as calculated in the updated Boulanger and Idriss (2014) model is to be used, then $MSF = f\left(N_{1,60,cs}\right)$. Because MSF is a function of $N_{1,60,cs}$, it is possible that $MSF^{site} \neq MSF^{ref}$ because it is likely that $\left(N_1\right)_{60,cs}$ varies with depth in the actual soil profile. Thus ΔCSR_{MSF} must be included in Equation (18). Using the equation for *MSF* from the updated Boulanger and Idriss (2014) model, this correction factor can be written as:

$$\Delta CSR_{MSF} = -\ln\left(\frac{MSF^{site}}{MSF^{ref}}\right) = -\ln\left(\frac{1+\left(MSF_{\max}^{site}-1\right)\left(8.64\exp\left(\frac{-M_w^{site}}{4}\right)-1.325\right)}{1+\left(MSF_{\max}^{ref}-1\right)\left(8.64\exp\left(\frac{-M_w^{ref}}{4}\right)-1.325\right)}\right) \tag{34}$$

$$MSF_{\max} = 1.09 + \left(\frac{\left(N_1\right)_{60,cs}}{31.5}\right)^2 \leq 2.2 \tag{35}$$

where $\left(N_1\right)_{60,cs}$ represents the clean sand-equivalent SPT resistance value corrected to 60% efficiency and 1 atm overburden pressure as computed using the equations provided by Idriss and Boulanger (2008, 2010). Note that there is no difference in the magnitude of the ground motions between the reference map and the site. Thus, M_w^{ref} can be replaced with M_w^{site}. Therefore, if the liquefaction parameter map for CSR^{ref} (%) was developed using the reference soil profile shown in Figure 2-2, then $MSF_{\max}^{ref}$ = 1.417 and Equation (34) can be written as:

$$\Delta CSR_{MSF} = -\ln\left[\frac{1+\left(MIN\left\{\left(\frac{\left(N_1\right)_{60,cs}^{site}}{31.5}\right)^2+0.09;\ 1.2\right\}\right)\cdot\left(8.64\exp\left(\frac{-M_w^{site}}{4}\right)-1.325\right)}{3.603\exp\left(\frac{-M_w^{site}}{4}\right)+0.447}\right] \tag{36}$$

The value of ΔCSR_{MSF} must be calculated for each layer in the soil profile because $MSF_{\max}^{site}$ is a function of $(N_1)_{60,cs}$, which likely varies throughout the soil profile. The value of M_w^{site} is the mean moment magnitude from the 2008 (1996 for Alaska) USGS interactive deaggregation website for the return period of interest (e.g., 2% probability of exceedance in 21 years, T_R = 1039). This should be the same value as M_w^{site} used to calculate the ΔCSR_{rd} term in Equation (33).

2.3.1.6 Correction for Overburden Pressure, $\Delta CSR_{K\sigma}$

Both the 2010 and 2014 versions of the Boulanger and Idriss model use the same overburden correction factor, K_σ:

$$K_\sigma = 1 - C_\sigma \ln\left(\frac{\sigma'_v}{P_a}\right) \le 1.1 \tag{37}$$

$$C_\sigma = \frac{1}{18.9 - 2.55\sqrt{(N_1)_{60,cs}}} \le 0.3 \tag{38}$$

where P_a is 1 atmosphere of pressure (i.e. 1 atm, 101.3 kPa, 0.2116 psf). Note that the value $(N_1)_{60,cs}$ must be computed using the equations found in Idriss and Boulanger (2008, 2010). Idriss and Boulanger (2010) commented that the K_σ limit of 1.1 has a somewhat negligible effect. Therefore, the simplified method derived here will not use the restriction on K_σ. However, the limit of 0.3 for values of C_σ will be incorporated. Now the correction term $\Delta CSR_{K\sigma}$ can be written as:

$$\Delta CSR_{K_\sigma} = -\ln\left(\frac{K_\sigma^{site}}{K_\sigma^{ref}}\right) = -\ln\left(\frac{1 - C_\sigma^{site}\ln\left(\frac{(\sigma'_v)^{site}}{P_a}\right)}{1 - C_\sigma^{ref}\ln\left(\frac{(\sigma'_v)^{ref}}{P_a}\right)}\right) \tag{39}$$

If the liquefaction parameter map for CSR^{ref} (%) was developed using the reference soil profile shown in Figure 2-2, then C_σ^{ref} = 0.147, K_σ^{ref} = 1.0672, and Equation (39) would become:

$$\Delta CSR_{K_\sigma} = -\ln\left(\frac{1-\left(MIN\left\{\begin{matrix}0.3\\ \dfrac{1}{18.9-2.55\sqrt{(N_1)_{60,cs}^{site}}}\end{matrix}\right.\right)\cdot\ln\left(\dfrac{(\sigma'_v)^{site}}{P_a}\right)}{1.0672}\right) \quad (40)$$

Note that if $(N_1)_{60,cs}$ is restricted to ≤ 37 blows per foot then the coefficient C_σ as defined in Equation (38) will remain below its maximum value of 0.3.

2.3.1.7 Equations for CSR^{site}, N_{req}^{site}, FS_L, and P_L

Once the $CSR^{ref}(\%)$ is obtained from the appropriate (i.e. hazard-targeted) map and the appropriate correction factors are computed using Equations (20), (22), (33), (36) (neglected if using Idriss and Boulanger 2008 *MSF* instead of the updated Boulanger and Idriss 2014 *MSF*) and (40), the site-specific hazard-targeted CSR^{site} can be computed for site-specific soil layer *i* using the following equation (from Equation (14)):

$$\left(CSR^{site}\right)_i = \exp\left[\ln\left(\frac{CSR^{ref}(\%)}{100}\right)+\left(\Delta CSR_\sigma\right)_i+\left(\Delta CSR_{F_{pga}}\right)_i+\left(\Delta CSR_{r_d}\right)_i+\left(\Delta CSR_{MSF}\right)_i+\left(\Delta CSR_{K_\sigma}\right)_i\right] \quad (41)$$

This $\left(CSR^{site}\right)$ value can then be used to calculate N_{req}^{site}, FS_L, or P_L for site-specific soil layer *i*. To calculate the value of $\left(N_{req}^{site}\right)_i$, solve the following polynomial iteratively (from Equation (13)):

$$0 = \left(\frac{\left(N_{req}^{site}\right)_i}{14.1}\right)+\left(\frac{\left(N_{req}^{site}\right)_i}{126}\right)^2-\left(\frac{\left(N_{req}^{site}\right)_i}{23.6}\right)^3+\left(\frac{\left(N_{req}^{site}\right)_i}{25.4}\right)^4-2.67-\ln\left(\left(CSR^{site}\right)_i\right) \quad (42)$$

Alternatively, the following closed-form regression equation will provide a very close approximation of N_{req}^{site} given CSR^{site} (R^2=0.999):

$$\left(N_{req}^{site}\right)_i = 1.237 \cdot \left(\ln\left(\frac{1}{\left(CSR^{site}\right)_i} \right) \right)^4 - 4.9183 \cdot \left(\ln\left(\frac{1}{\left(CSR^{site}\right)_i} \right) \right)^3 + 1.7624 \cdot \left(\ln\left(\frac{1}{\left(CSR^{site}\right)_i} \right) \right)^2 - 5.4733 \cdot \left(\ln\left(\frac{1}{\left(CSR^{site}\right)_i} \right) \right) + 33.65 \tag{43}$$

Equation (43) is valid for $0.08 \le \left(CSR^{site}\right)_i \le 1.26$. Outside of these bounds, the polynomial should be solved iteratively.

To solve for the uniform-hazard FS_L for the soil layer *i*, use Equation (13) as:

$$\left(FS_L\right)_i = \frac{\left(CRR^{site}\right)_i}{\left(CSR^{site}\right)_i} = \frac{\exp\left[\left(\frac{\left((N_1)_{60,cs}\right)_i}{14.1} \right) + \left(\frac{\left((N_1)_{60,cs}\right)_i}{126} \right)^2 - \left(\frac{\left((N_1)_{60,cs}\right)_i}{23.6} \right)^3 + \left(\frac{\left((N_1)_{60,cs}\right)_i}{25.4} \right)^4 - 2.67 \right]}{\left(CSR^{site}\right)_i} \tag{44}$$

To solve for the uniform hazard P_L for the soil layer *i*, use the following relationship:

$$\left(P_L\right)_i = \Phi\left[-\frac{\ln\left(\frac{\left(CRR^{site}\right)_i}{\left(CSR^{site}\right)_i} \right)}{\sigma_\varepsilon} \right] = \Phi\left[-\frac{\ln\left(\left(FS_L\right)_i\right)}{\sigma_\varepsilon} \right] \tag{45}$$

Where σ_ε is 0.13 if parametric uncertainty (i.e., uncertainty in measuring $(N_1)_{60,cs}$ and estimating seismic loading) is neglected, and σ_ε is 0.277 if parametric uncertainty is considered. Because it is impossible to completely eliminate uncertainty when measuring parameters such as $(N_1)_{60,cs}$ in the field, it is recommended that $\sigma_\varepsilon = 0.277$.

2.4 Empirical Lateral Spread Displacement Model

The simplified lateral spread displacement model is derived from the widely-used empirical lateral spread model originally presented by Bartlett and Youd (1995). Their model was

regressed from a large database of lateral spread case histories from Japan and the western United States, and a large number of parameters related to soil properties, slope geometry, and level of ground motion were statistically evaluated. Bartlett and Youd identified the parameters that produced the best regression, and from those parameters regressed their original empirical predictive relationship. Youd et al. (2002) later updated their original empirical model by using an expanded and corrected version of the 1995 database. The updated Bartlett and Youd empirical model has since been adopted as the state of practice in much of the world, and it is routinely applied on a wide variety of projects in all types of seismic environments. The Youd et al. (2002) updated empirical model is given as:

$$\overline{\log D_H} = b_0 + b_1 M + b_2 \log R^* + b_3 R + b_4 \log W + b_5 \log S + b_6 \log T_{15} + b_7 \log\left(100 - F_{15}\right) + b_8 \log\left(D50_{15} + 0.1\right) \quad (46)$$

where

D_H = median computed permanent lateral spread displacement (m)
M = earthquake moment magnitude
R = the closest horizontal distance from the site to the source (km)
W = the free-face ratio (%)
S = the ground slope (%)
T_{15} = the cumulative thickness (in upper 20 m) of all saturated soil layers with corrected Standard Penetration Test (SPT) blowcounts (i.e., $(N_1)_{60}$) less than 15 blows/foot (m)
F_{15} = the average fines content of the soil comprising T_{15} (%)
$D50_{15}$ = the average mean grain size of the soil comprising T_{15} (mm)

and R* is computed as

$$R^* = R + 10^{0.89M - 5.64} \quad (47)$$

Model coefficients b_0 through b_8 are given in Table 2-2.

Table 2-2 Regression coefficients for the Youd et al. (2002) empirical lateral spread model

Model	b_0	b_1	b_2	b_3	b_4	b_5	b_6	b_7	b_8
Ground slope	-16.213	1.532	-1.406	-0.012	0	0.338	0.540	3.413	-0.795
Free Face	-16.713	1.532	-1.406	-0.012	0.592	0	0.540	3.413	-0.795

The Youd et al (2002) model has recommended values that should be used in the model. Using parameter values outside this range can result in in extrapolating the relationship and predict unrealistic values of lateral displacements. These recommended bounds can be seen in Table 2-3.

Table 2-3 Parameters bounds for the Youd et al (2002) empirical lateral spread model

Variable	Range
D_H	0 to 6.0
M	6.0 to 8.0
R (km)	0.2 to 100
W (%)	1 to 20
S (%)	0.1 to 6
T_{15} (m)	1 to 15

2.4.1 Full Performance-based Lateral Spread Model

Kramer et al. (2007) suggested that performance-based estimates of lateral spread displacement could be computed by modifying an empirical lateral spreading model in such a way so as to insert it directly into a probabilistic seismic hazard analysis (PSHA). Such a modification could be performed by separating the model terms associated with seismic loading (i.e. the Loading Parameter, $\mathscr{L}$) from the model terms associated with local site and geometry conditions (i.e. the Site Parameter, $\mathscr{S}$). Therefore, a modified form of any given empirical lateral spread model could be written as:

$$\mathscr{D} = \mathscr{L} - \mathscr{S} + \varepsilon \tag{48}$$

where $\mathscr{D}$ is the transformed (e.g. log, ln, square root) lateral spread displacement, and $\mathscr{L}, \mathscr{S},$ and ε represent the apparent loading, site, and uncertainty terms.

Following the Kramer et al. (2007) framework, Franke and Kramer (2014) demonstrated how the Youd et al. (2002) empirical model for lateral spread displacement could be adapted to

develop fully probabilistic estimates of lateral spread displacement. The performance-based form of the Youd et al. (2002) was shown to be:

$$\log D_H = \mathscr{L} - \mathscr{S} + \varepsilon \tag{49}$$

where

$$\mathscr{L} = b_1 M + b_2 \log R^* + b_3 R \tag{50}$$

$$\mathscr{S} = -\left(b_0 + b_4 \log W + b_5 \log S + b_6 \log T_{15} + b_7 \log\left(100 - F_{15}\right) + b_8 \log\left(D50_{15} + 0.1\right)\right) \tag{51}$$

$$\varepsilon = \sigma_{\log D_H} \Phi^{-1}\left[P\right] \tag{52}$$

$$\sigma_{\log D_H} = 0.197 \tag{53}$$

If computing the probability of exceeding some given displacement, *d*, Equation (53) can be incorporated as:

$$P\left[D_H > d\right] = 1 - \Phi\left[\frac{\log d - \overline{\log D_H}}{\sigma_{\log D_H}}\right] = 1 - \Phi\left[\frac{\log d - \overline{\log D_H}}{0.197}\right] \tag{54}$$

Because a given site should produce a single value of $\mathscr{S}$ to be used in design, the left side of Equation (49) can be thought of as a simple linear function of $\mathscr{L}$ with a constant y-intercept equal to $\mathscr{S}$ and a data spread characterized by ε, as shown in Figure 2-5. Because $\mathscr{S}$ is considered a constant value in the performance-based analysis, multiple lateral spread hazard curves could be developed for a site for different values of $\mathscr{S}$ (Figure 2-6). Thus, the effect of varying site and/or geometry conditions when computing probabilistic lateral spread displacements could be evaluated.

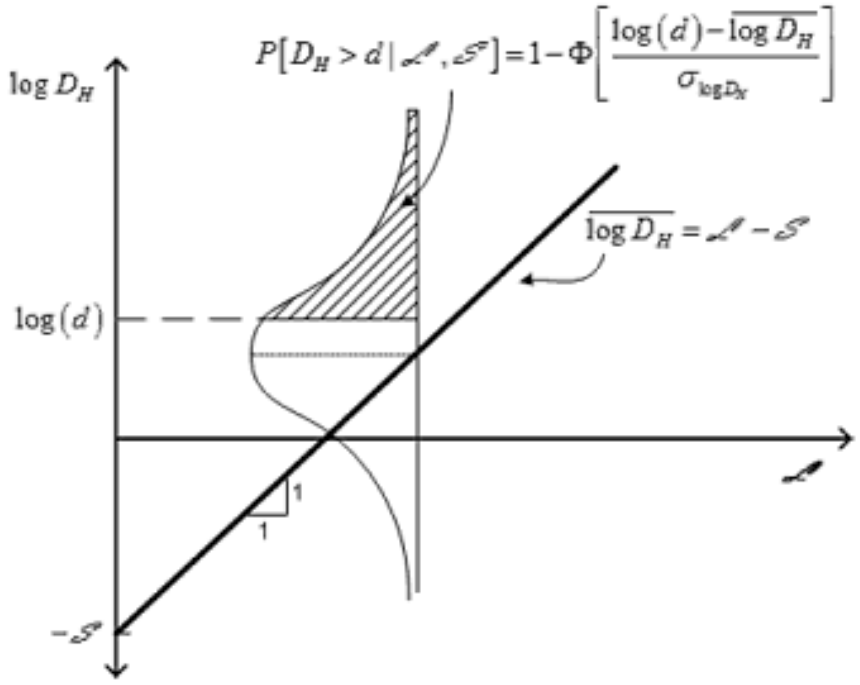

Figure 2-5 Schematic diagram of the fully probabilistic lateral spread model with Youd et al. (2002) (after Franke and Kramer 2013)

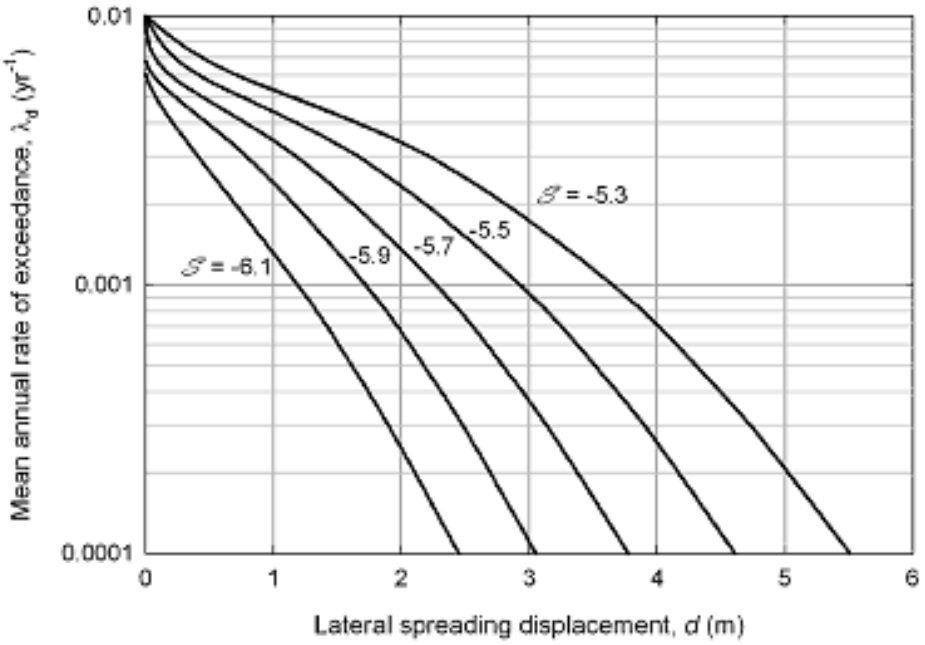

Figure 2-6 Variations of lateral spread hazard curves as a function of the site term, $\mathscr{S}$ (after Kramer et al. 2007)

Though it is not an actual or measurable ground motion parameter, the apparent loading parameter in Equation (50) is a function of magnitude and distance and attenuates in a manner similar to measurable ground motion intensity measures described by traditional Ground Motion Prediction Equations (GMPEs). In the context of the Youd et al. (2002) model, the apparent loading term, therefore, acts in a manner analogous to an Intensity Measure (*IM)*, the variation of whose median value with *M* and *R* is described by Equation (50).

By incorporating Equations (50) and (51) into the probabilistic framework presented in Equation (54) and assigning all of the uncertainty in the Youd et al. (2002) model to the conditional displacement calculation, a performance-based model can be expressed in terms of lateral spread displacement conditional upon the site parameter as:

$$\lambda_{D_H|\mathcal{S}}(d \mid \mathcal{S}) = \sum_{i=1}^{N_{\mathcal{L}}} P\left[D_H > d \mid \mathcal{S}, \mathcal{L}_i\right] \Delta\lambda_{\mathcal{L}_i} \tag{55}$$

where $\lambda_{D_H|\mathcal{S}}(d \mid \mathcal{S})$ is the mean annual rate of exceeding a displacement *d* conditional upon site conditions $\mathcal{S}$, $N_{\mathcal{L}}$ is the number of loading parameter increments required to span the range of possible $\mathcal{L}$ values, and $\Delta\lambda_{\mathcal{L}_i}$ is the increment of the apparent loading parameter in hazard space. For a single source, Equation (55) can also be written as:

$$\lambda_{D_H|\mathcal{S}}\left(d \mid \mathcal{S}\right) = \nu \sum_{i=1}^{N_{\mathcal{L}}} P\left[D_H > d \mid \mathcal{S}, \mathcal{L}_i\right] P\left[\mathcal{L}_i\right] \tag{56}$$

where ν is the mean annual rate of exceeding a minimum magnitude of interest for a given seismic source. Because the loading parameter is a function of magnitude and distance (which are commonly assumed to be independent in PSHA work) and can be affected by multiple seismic sources, Equation (56) can be rewritten as:

$$\lambda_{D_H|\mathcal{S}}\left(d \mid \mathcal{S}\right) = \sum_{i=1}^{N_S} \nu_i \sum_{j=1}^{N_M} \sum_{k=1}^{N_R} P\left[D_H > d \mid \mathcal{S}, M = m_j, R = r_k\right] P\left[M = m_j, R = r_k\right] \tag{57}$$

which is very similar to the PSHA framework commonly used to compute uniform hazard estimates of ground motions. Therefore, Equations (49) through (54) can be incorporated into

common seismic hazard analysis software such as EZ-FRISK or OpenSHA to develop uniform hazard estimates of lateral spread displacement and displacement hazard curves.

2.4.2 Simplified Performance-based Lateral Spread Model

If a generic reference site is used to compute $\mathcal{S}$, then a series of performance-based lateral spread analyses could be performed across a grid to develop contour maps of lateral spread displacement corresponding to various return periods of interest. These maps are called lateral spread reference maps. For example, a reference site for the derivation of the simplified performance-based lateral spread procedure is presented in Figure 2-7. This profile was chosen based on the profile used to develop the full performance-based method to be consistent. Values of 3.0m, 20%, and 0.2mm are computed for the lateral spread parameters T_{15}, F_{15}, and $D50_{15}$, respectively. As shown in Figure 2-7, the geometry of the site constitutes a ground slope condition with ground slope (i.e. S) equal to 1%. The resulting value of $\mathcal{S}$ for the reference site, as computed from Equation (51), is therefore equal to 9.043.

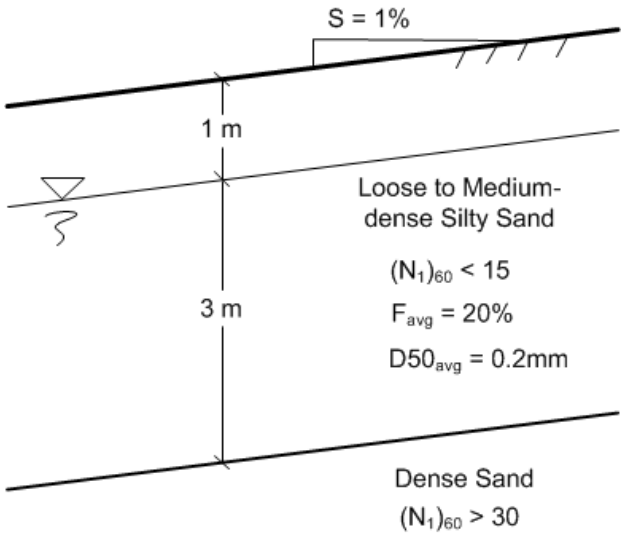

Figure 2-7 Reference soil profile used to derive the simplified performance-based lateral spread approximation

The lateral spread displacement corresponding to the generic reference site could therefore be obtained from the appropriate map and adjusted in order to provide site-specific lateral spread

displacements corresponding to the desired return period. The equation for this site-specific adjustment is given as:

$$\left[\log D_H\right]^{site} = \left[\log D_H\right]^{ref} + \Delta D_H \tag{58}$$

where $\left[\log D_H\right]^{site}$ is the logarithm of the lateral spread displacement adjusted for site-specific conditions, $\left[\log D_H\right]^{ref}$ is the logarithm of the lateral spread displacement corresponding to the reference site (obtained from the map), and ΔD_H is the adjustment factor computed by the engineer. By substituting Equation (49) into Equation (58), the adjustment factor can be written as:

$$\Delta D_H = \left(\mathscr{L} - \mathscr{S}\right)^{site} - \left(\mathscr{L} - \mathscr{S}\right)^{ref} = \left(\mathscr{L}^{site} - \mathscr{L}^{ref}\right) + \left(\mathscr{S}^{ref} - \mathscr{S}^{site}\right) \tag{59}$$

However, because $\mathscr{L}^{site} = \mathscr{L}^{ref}$, Equation (59) can be simplified as:

$$\Delta D_H = \mathscr{S}^{ref} - \mathscr{S}^{site} \tag{60}$$

If Equation (51) is substituted for $\mathscr{S}$, then Equation (60) can be rewritten as:

$$\begin{aligned}\Delta D_H = &-\left[b_0 + b_4 \log W + b_5 \log S + b_6 \log T_{15} + b_7 \log\left(100 - F_{15}\right) + b_8 \log\left(D50_{15} + 0.1\right)\right]^{ref} \\ &+\left[b_0 + b_4 \log W + b_5 \log S + b_6 \log T_{15} + b_7 \log\left(100 - F_{15}\right) + b_8 \log\left(D50_{15} + 0.1\right)\right]^{site}\end{aligned} \tag{61}$$

By simplifying Equation (61) and inserting model coefficients and parameters for the reference site, the adjustment factor can be computed as:

$$\begin{aligned}\Delta D_H = &\, b_0^{site} + b_4^{site} \log\left(W^{site}\right) + b_5^{site} \log\left(S^{site}\right) + 0.540 \log\left(\frac{T_{15}^{site}}{3}\right) \\ &+3.413 \log\left(\frac{100 - F_{15}^{site}}{80}\right) - 0.795 \log\left(\frac{D50_{15}^{site} + 0.1}{0.3}\right) + 16.213\end{aligned} \tag{62}$$

where b_4^{site} and b_5^{site} denote site-specific geometry coefficients dependent on the geometry model (i.e. ground slope or free-face) and are provided in Table 2-4. Parameters with the '*site*' superscript denote site-specific soil and geometry parameters determined from the site-specific soil information provided by the engineer.

Table 2-4 Site-specific geometry coefficients for computing the adjustment factor, ΔD_H

Model	b_0^{site}	b_4^{site}	b_5^{site}
Ground Slope	-16.213	0	0.338
Free Face	-16.713	0.592	0

Once the reference lateral spread displacement is obtained from the appropriate (i.e. hazard-targeted) map and the adjustment factor is computed using Equation (62) and Table 2-4, the site-specific hazard-targeted lateral spread displacement (in meters) can be computed as:

$$D_H^{site} = 10^{\left([\log D_H]^{ref} + \Delta D_H\right)} \tag{63}$$

2.5 Summary

The derivations of the simplified liquefaction triggering and lateral spread displacement models show how to approximate a full performance-based analysis using simple calculations and mapped reference parameters. The simplified liquefaction triggering procedure is based on the Boulanger and Idriss (2012) probabilistic model while the simplified lateral spread displacement model is based on the Youd et al. (2002) empirical model.

3.0 VALIDATION OF THE SIMPLIFIED MODELS

3.1 Overview

The effectiveness of the simplified methods depends on how closely they approximate the results of a complete site-specific probabilistic seismic hazard analysis. In order to show that the simplified method is as accurate as expected, the simplified and full performance-based methods will be performed for ten sites throughout the United States. These sites will be evaluated for three different return periods: 475, 1033, and 2475 years.

3.1.1 Sites used in the Analysis

The sites chosen for the analysis were selected based on the range of seismicity of each site, as well as their distribution across the United States. Table 3-1 lists the location of these sites as well as their latitudes and longitudes.

Table 3-1 Locations used for the validation of the simplified models

Site	Latitude	Longitude
Butte	46.003	-112.533
Charleston	32.726	-79.931
Eureka	40.802	-124.162
Memphis	35.149	-90.048
Portland	45.523	-122.675
Salt Lake City	40.755	-111.898
San Francisco	37.775	-122.418
San Jose	37.339	-121.893
Santa Monica	34.015	-118.492
Seattle	47.53	-122.3

The tools used to validate the liquefaction triggering model did not allow any sites in Alaska at this point, so the site Anchorage, Alaska (Latitude 61.217, Longitude -149.9) was not used in the validation process for that model. However, the tools used to validate the lateral spread displacement model did have the ability to analyze sites in Alaska so the Anchorage site was used in the validation process for that model.

3.2 Simplified Liquefaction Triggering Model Validation

To calculate the site-specific CSR^{site}, an assumed soil profile was applied at each site. The parameters associated with this soil profile are presented in Figure 3-1.

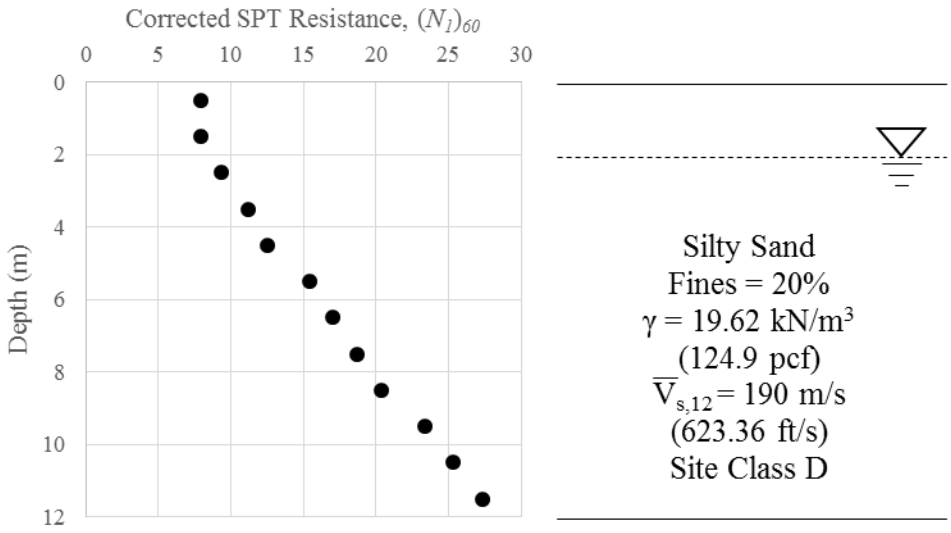

Figure 3-1 Site-specific soil profile used to validate the simplified performance-based model

3.2.1 PBLiquefY

The site-specific analysis for the full performance-based method was performed using PBLiquefY (Franke et al., 2014c). PBLiquefY was also used to create the liquefaction loading maps used to determine the reference value (i.e. CSR^{ref} (%)) necessary for the simplified method. The 2008 USGS ground motion deaggregations were used in both the full and simplified methods.

3.2.2 Validation of the Simplified Performance-Based Cetin et al. (2004) Model

Although the simplified performance-based Cetin et al. (2004) model will not be validated in this report, other publications have verified the use of the simplified Cetin et al. (2004) model (Mayfield et al. 2010; Franke et al 2014d). Mayfield et al. (2010) showed that the computed uniform hazard liquefaction results from the simplified method closely match the liquefaction hazard results from the full performance-based liquefaction analysis at the targeted return period. In future quarterly reports, contour maps of N_{req} from the Cetin et al. (2004) model will be included along with contour maps of CSR^{ref} (%) from the Boulanger and Idriss (2014) model.

3.2.3 Validation of the Simplified Performance-Based Boulanger and Idriss (2012) Model

Using liquefaction loading maps (created using PBLiquefY) and the soil profile selected for the site specific analysis, the value of CSR_{site} was determined for each layer of the site-specific soil profile and for each site using the simplified performance-based method (raw data can be found in the Appendix, Tables A.2 and A.3). These CSR_{site} values were converted to N_{req} values using Equation (42). The resulting N_{req} values are displayed in Figure 3-2 along with the N_{req} values computed using the full performance-based method. Also included in this plot is N_{site}, which is the in-situ clean sand-equivalent SPT resistance of the site soil profile. Note that both the full performance-based and simplified performance-based methods yield almost identical results for each city represented in this analysis. Overall, the difference between the two methods is within an acceptable amount (within 3.41% on average with a maximum difference of 2.25 blow counts for N_{req}).

The direct comparison of the two methods for three different return periods can be seen in Figure 3-3. Each point on this plot represents a single layer in the site soil profile located in one city for one return period (a total of 300 points). As seen in this plot, the simplified method provides a good approximation of the results from a full probabilistic analysis (R^2 value between 0.996 and 0.997) and provides predictions of N_{req} that account for uncertainty in the model parameters without the need for a full probabilistic analysis. It may seem that the high R^2 values are too good to be true; however, it is important to note that this is a mathematically derived relationship and is expected to be closely correlated with the results of a full probabilistic analysis. If these two values (N_{req} from the simplified method and N_{req} from the full method) were randomly selected samples from a natural population, then these R^2 values would be reason for suspicion.

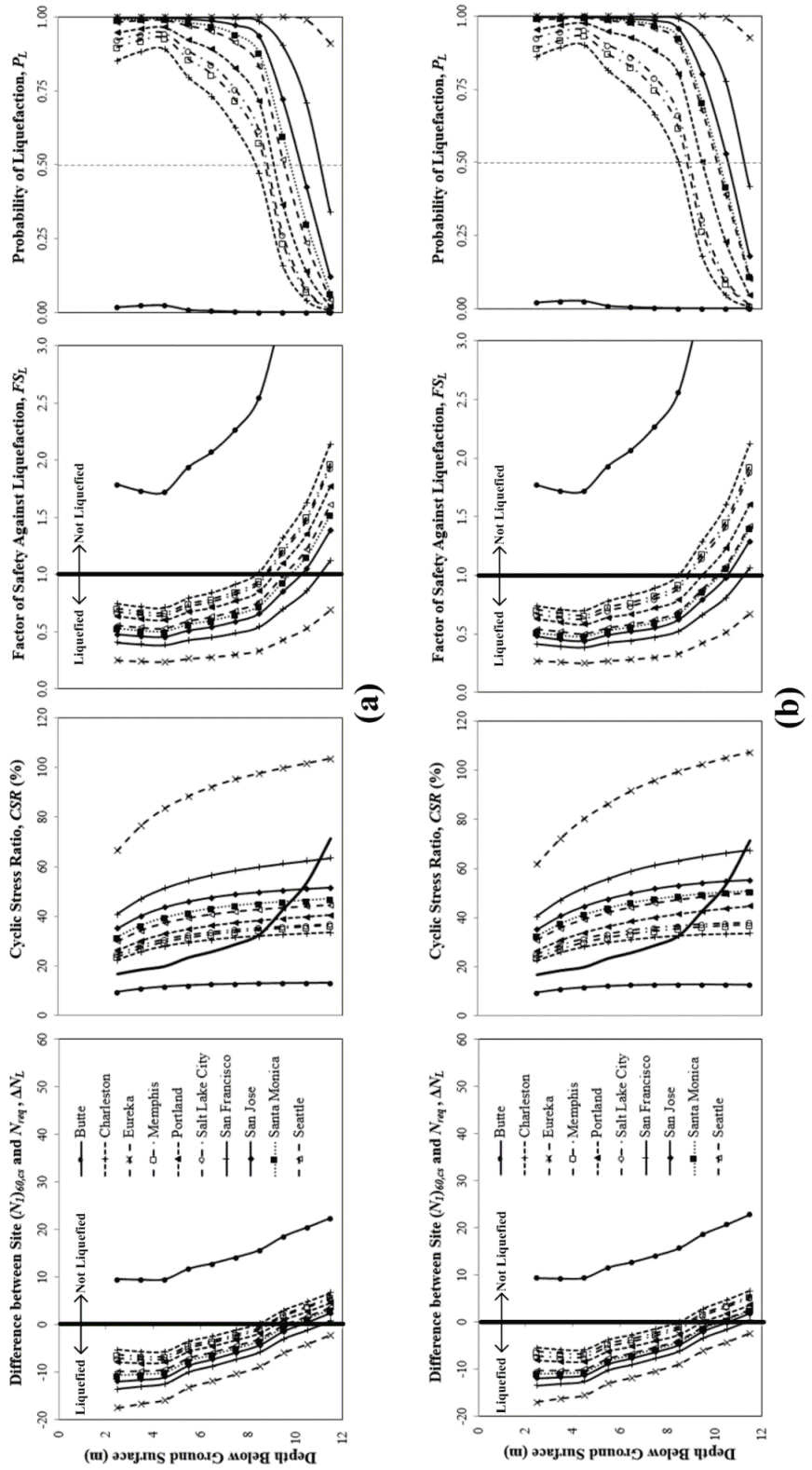

Figure 3-2 ΔN_L, $CSR_{M=7.5,\sigma_v'=1atm}(\%)$, FS_L, **and** P_L **with depth as calculated using (a) the new simplified procedure, and (b) the full performance-based procedure (**T_R **= 1,033 years)**

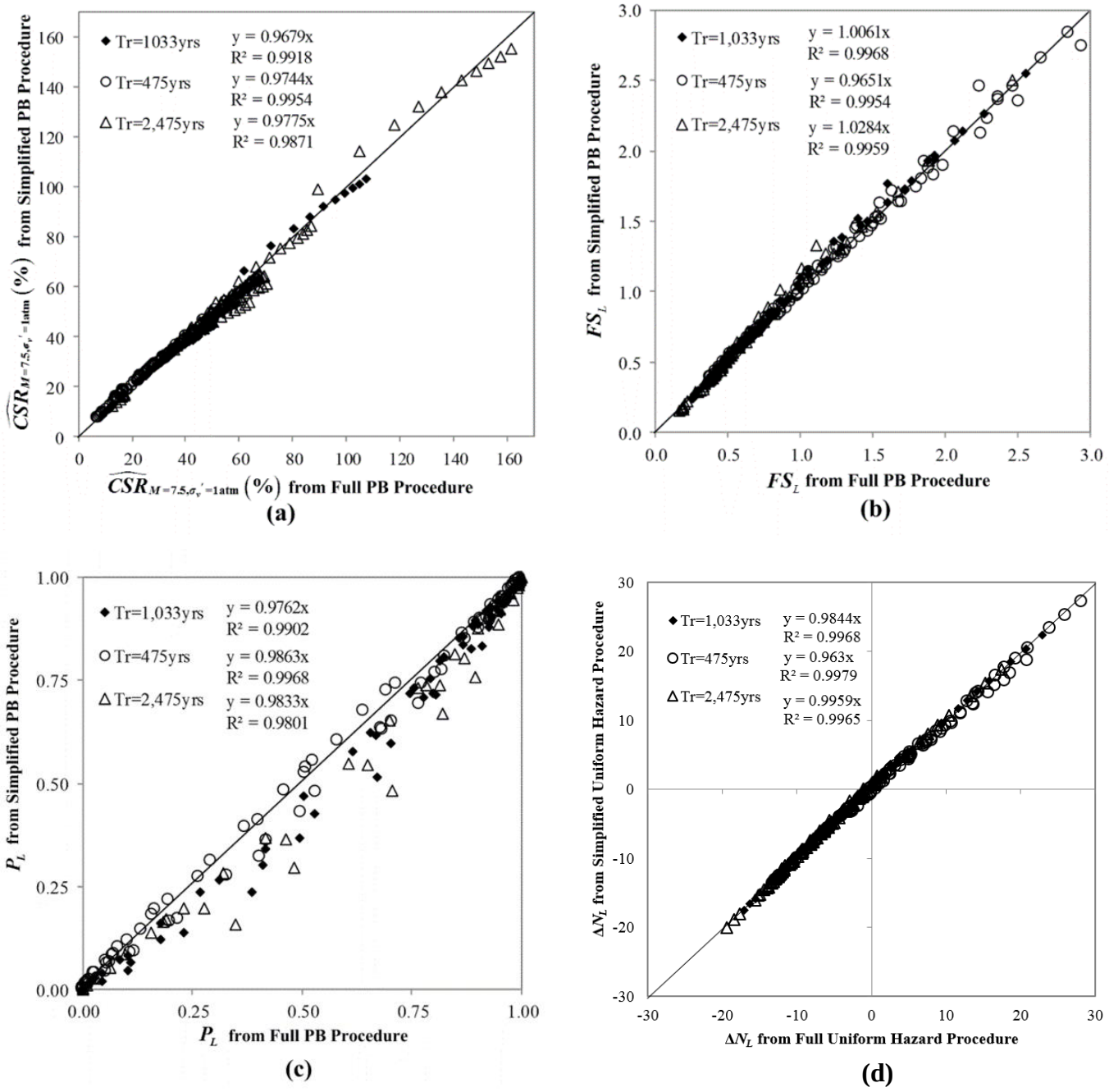

Figure 3-3 Comparative scatter plots for simplified and full performance-based procedures for (a) $CSR_{M=7.5,\sigma_v'=1atm}(\%)$**, (b)** FS_L**, (c)** P_L**, and (d)** ΔN_L

3.2.3.1 Boulanger and Idriss (2014) Updated MSF Term

During the production of this report, a revised Boulanger and Idriss (2014) model was published. This revised model included a new definition of the *MSF* (as explained previously). Though this report discussed the derivation of the simplified performance-based procedure for both the updated Boulanger and Idriss (2014) model and the previous Boulanger and Idriss (2012) model, the remainder of this research will be based on the 2008/2012 version of the *MSF*. This includes validation of the simplified performance-based liquefaction triggering procedure, map development, etc.

3.3 Simplified Lateral Spread Displacement Model Validation

To evaluate the site-specific lateral displacement, a soil profile was assumed for each site. These soil parameters are presented in Figure 3-4. Values of 1.0m, 25%, and 1.0mm were computed for the lateral spread parameters T_{15}, F_{15}, and $D50_{15}$, respectively. As shown in Figure 3-4, the geometry of the site constitutes a ground slope condition with ground slope (i.e. S) equal to 1%. The resulting value of $\mathscr{S}$ for the site, as computed from Equation (51), is therefore equal to 9.846.

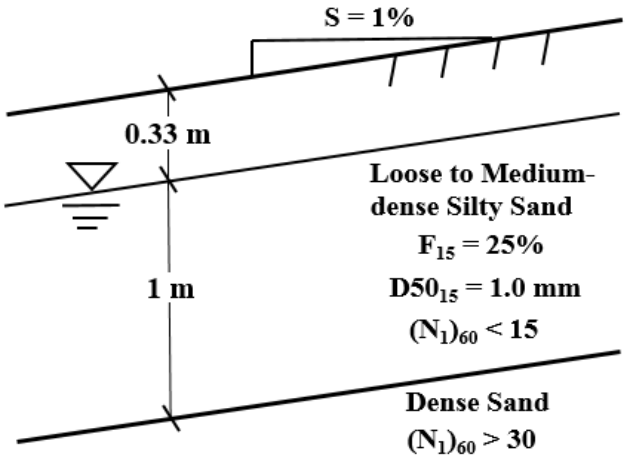

Figure 3-4 Site-specific soil profile used in the simplified lateral spread displacement model validation

3.3.1 EZ-FRISK

To perform the site-specific analysis for both the simplified and full performance-based models, the software EZ-FRISK (Risk Engineering 2013) was utilized. For this analysis, the USGS 2008 seismic source model (Petersen et al. 2008) was used for all locations but Anchorage, Alaska. The 1996 USGS seismic source model was used for that location.

3.3.2 Comparison of Results

Using EZ-FRISK and the soil profile selected for the site specific analysis, the lateral spread displacement was determined for each site using the simplified and full-performance based

models. The results of analysis can be seen in Table 3-2. As can be seen in this table, the results of the analysis for both models resulted in relatively similar results, with the values from the simplified method falling on average within 3.9% of those predicted by full model. The observed discrepancy between the simplified and full performance-based models was no greater than 0.073 m at any site or any return period.

Table 3-2 Lateral spread displacements (m) for the site specific analysis using the two models for the three desired return periods

	Simplified Model			Full PB Model		
Site	**475 Yrs**	**1033 Yrs**	**2475 Yrs**	**475 Yrs**	**1033 Yrs**	**2475 Yrs**
Butte	0.001	0.003	0.008	0.001	0.003	0.008
Charleston	0.001	0.017	0.068	0.001	0.015	0.065
Eureka	0.738	2.321	3.737	0.728	2.248	3.724
Memphis	0.003	0.033	0.067	0.003	0.025	0.065
Portland	0.038	0.152	0.333	0.036	0.152	0.334
Salt Lake City	0.162	0.437	0.726	0.167	0.438	0.726
San Francisco	0.744	1.095	1.493	0.745	1.081	1.492
San Jose	0.312	0.574	0.857	0.312	0.574	0.857
Santa Monica	0.171	0.400	0.719	0.172	0.400	0.719
Seattle	0.054	0.162	0.343	0.053	0.162	0.344
Anchorage	0.045	0.536	1.187	0.045	0.566	1.250

Overall, the difference between the simplified and full performance based model is within an acceptable amount of error (defined by this report as 5%). The closeness of the fit is apparent when the results of both analyses are plotted against each other, which can be seen in Figure 3-5 (these are actual displacement values, not averages). The R^2 values for each return period are larger than 0.9995, indicating that the approximation of the full method is very good. These high R^2 values, as well as the lack of scatter of the results, seem to be too close for a simplified method; however, because this is a mathematically derived relationship it is expected that the results be closely correlated with those of the full probabilistic analysis. If the fit was not so close, than the mathematically derived equation would be suspect.

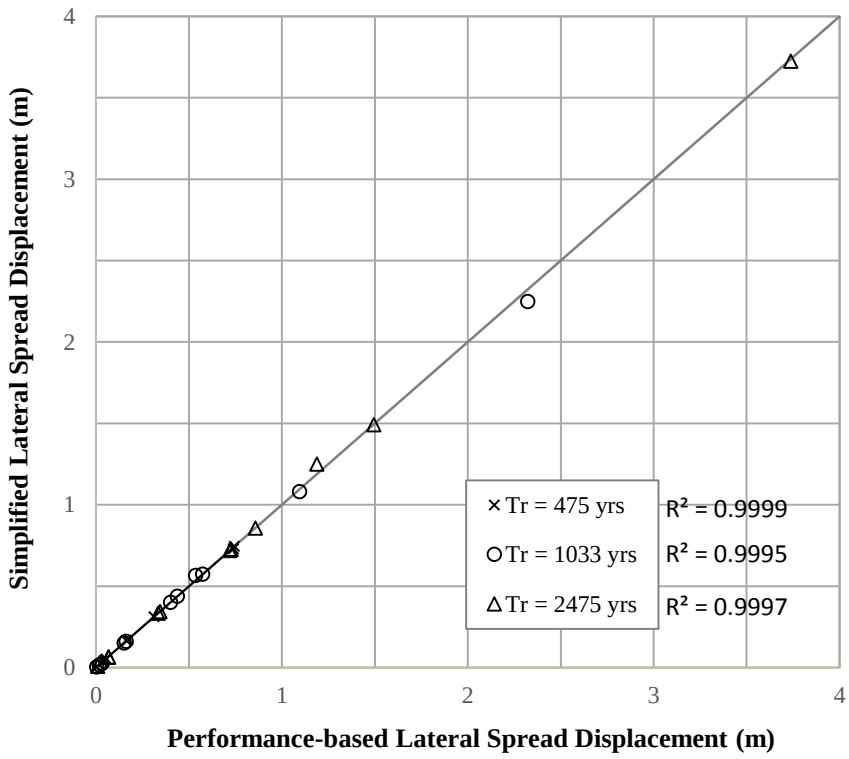

Figure 3-5 Comparison of lateral spread displacements for the simplified and full performance-based models

3.4 Summary

Ten sites throughout the United States were analyzed using both the full and simplified probabilistic procedures for three different return periods: 475, 1033, and 2475 years. Both the simplified liquefaction triggering method and the simplified lateral spread displacement models provided reasonable approximations of their respective full probabilistic methods.

4.0 EVALUATION OF GRID SPACING

4.1 Overview

Because biases due to spacing of grid points in gridded seismic hazard analyses are known to exist, the grid spacing study will evaluate the potential for bias to occur due to grid spacing effects in a gridded probabilistic liquefaction and lateral spread hazard assessment. Because the states involved in this study comprise areas of varying seismicity levels, evaluations will be performed in each of the states to assess the optimum grid spacing for development of liquefaction and lateral spread parameter maps in future tasks.

The grid spacing assessment was performed by comparing interpolated results from a simple 4-point grid placed in various parts of the country with site-specific results. The difference between the interpolated and site-specific results was quantified. By minimizing these computed differences, the optimum grid spacing for the liquefaction parameter maps in each state was obtained.

Note that this grid spacing study does not provide estimates of accuracy between the simplified performance-based method and the full performance-based method. The measurements of error calculated in this grid spacing study reflect only the error involved in interpolation between grid points.

4.2 Performance-based Liquefaction Triggering Evaluation

This section will describe the methods used to derive a correlation between optimum grid spacing and *PGA* for simplified performance-based liquefaction triggering evaluation. The purpose of this correlation was to provide a simple, readily-available, well-defined set of rules for proper grid spacing across the states of interest. This set of rules is necessary because it is impractical to perform an infinite number of full performance-based analyses to create the liquefaction contour maps. It was necessary to determine a finite number of points to analyze. The set of rules created in this grid spacing study was used to define the optimum number of points which would be feasible to analyze in the amount of time given and would yield an acceptable amount of error due to interpolation between analyzed points.

4.2.1 Methodology for Preliminary Study

The preliminary grid spacing study first focused on four cities in areas of varying seismicity: Berkeley, California; Salt Lake City, Utah; Butte, Montana; and Clemson, South Carolina with *PGA* values as shown in Table 4-1. Though Berkeley is not located in one of the funding states for this research, it was used as an extreme in the range of *PGA* values. The more rigorous grid spacing study to follow incorporates a higher number of cities within the funding states. This preliminary study was used to decide whether *PGA* had an effect on optimum grid spacing.

Table 4-1 Cities Used in Preliminary Grid Spacing Study

City	Anchor Point		*PGA* (g) (T_R = 2475 years)
	Latitude	Longitude	
Berkeley, CA	37.872	-122.273	1.1340
Salt Lake City, UT	40.755	-111.898	0.6478
Butte, MT	46.003	-112.533	0.1785
Clemson, SC	34.683	-82.837	0.1439

Using a square grid (like the one shown in Figure 4-1) with the city's anchor point as the center of the square, several grid spacings were tested. This preliminary testing process included grid spacings of 1, 2, 4, 8, 16, 25, 35, and 50 km (0.62, 1.24, 2.49, 4.97, 9.94, 15.5, 21.7 and 31.1 mi). Then a full performance-based liquefaction analysis was performed at each corner point and the center anchor point to solve for Standard Penetration Test (SPT) blowcount (clean-sand equivalent and corrected to 1 atm pressure and 60% hammer efficiency) required to resist liquefaction (i.e. N_{req}) and percent cyclic stress ratio (i.e. *CSR*%) at three return periods (475, 1033, and 2475 years). This process was repeated for each city in the preliminary study.

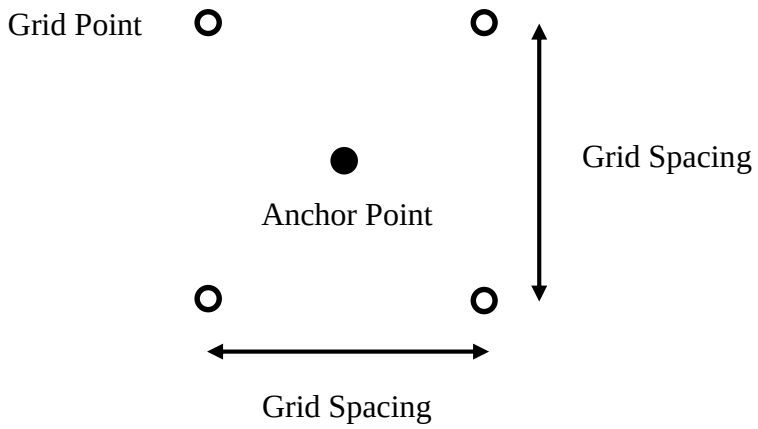

Figure 4-1 Layout of grid points centered on city's anchor point.

An estimate of the liquefaction hazard at the center point (i.e. the interpolated value of either N^{ref}_{req} or CSR^{ref} %) was calculated using the four corner points. This interpolated value was then compared to the actual value of the center point as calculated using a full performance-based liquefaction analysis. The difference between the interpolated value and the true value at the center is called the error term. The error terms were normalized to the actual values at the anchor points by calculating the percent error term as follows:

$$PercentError = \frac{|InterpolatedValue - ActualValue|}{ActualValue} \times 100\% \quad (64)$$

The maximum percent error (i.e. the maximum percent error across all return periods for a given anchor point) became the deciding parameter in selecting optimum grid spacing for a given location. The relationship between maximum percent error and grid spacing was analyzed for each city and is discussed in the following section.

4.2.2 Results of Preliminary Study

The relationship between maximum percent error and grid spacing was analyzed for each city and is displayed in Figure 4-2, Figure 4-3, Figure 4-4, and Figure 4-5. As can be seen in these figures, the relationship between maximum percent error and grid spacing is different for each city. Berkeley had the highest *PGA* value (1.1340g) out of the cities used in this preliminary study and required the smallest grid spacing (approximately 5 km or 3.107 mi) to restrict the maximum

percent error to 5%. On the other hand, the maximum percent error for Clemson, which had the lowest *PGA* value (0.1439g), never exceeded 1% even with 50km (31.07 mi) grid spacing. Based on these graphs, it appears that seismicity (or *PGA*) has an impact on optimum grid spacing.

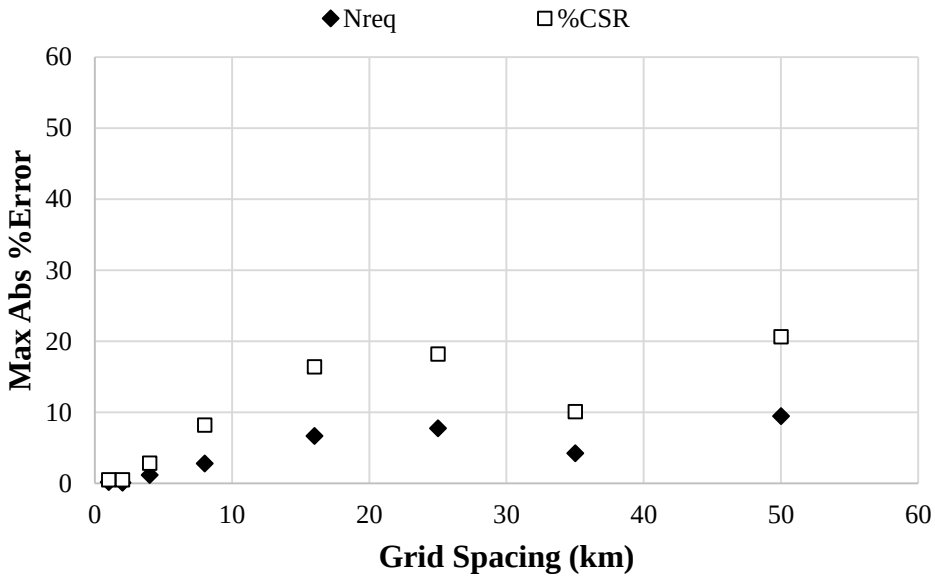

Figure 4-2 Variation of maximum absolute percent error with increasing distance between grid points (Berkeley, CA).

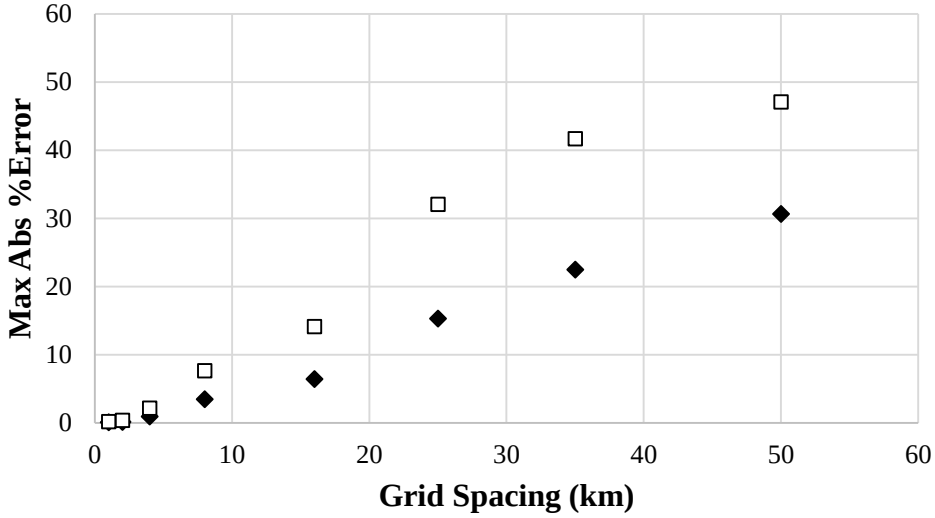

Figure 4-3 Variation of maximum absolute percent error with increasing distance between grid points (Salt Lake City, UT).

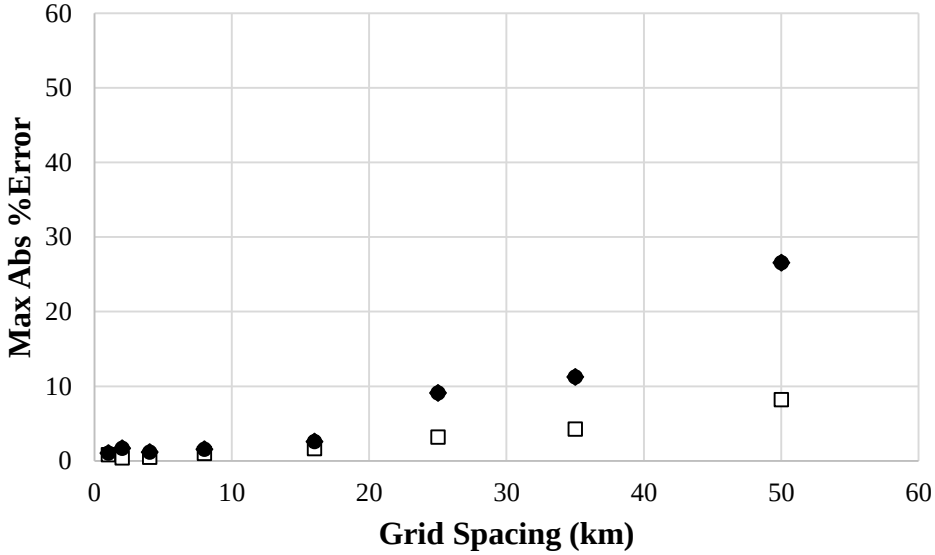

Figure 4-4 Variation of maximum absolute percent error with increasing distance between grid points (Butte, MT).

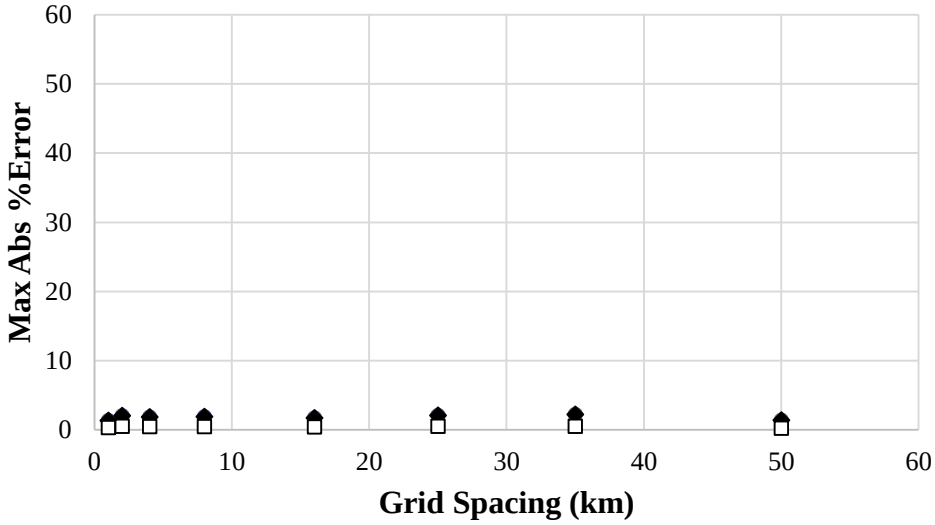

Figure 4-5 Variation of maximum absolute percent error with increasing distance between grid points (Clemson, SC).

4.2.3 Methodology for Grid Spacing Study

Based on the data from the preliminary study, it was hypothesized that *PGA* was a major factor in the relationship between grid spacing and maximum percent error. Specifically, it was hypothesized that as *PGA* increases, the optimum grid spacing decreases. To estimate the effect of *PGA* on optimum grid spacing, a similar study was conducted focusing on 21 cities from a wide range of *PGA* values (Figure 4-6).

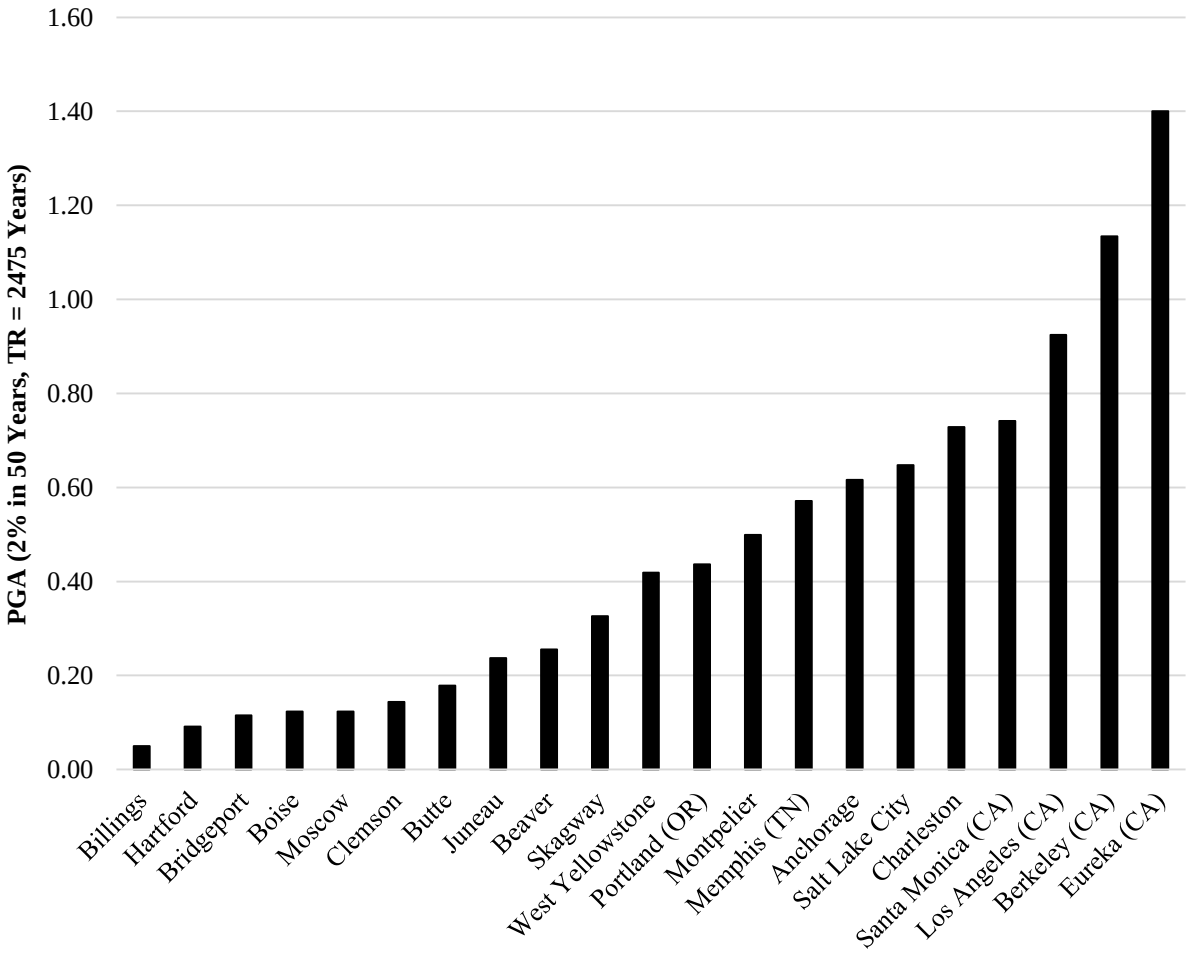

Figure 4-6 Range of *PGA* values for cities included in final grid spacing study.

The desired outcome of the final grid spacing study was to create a correlation between *PGA* and optimum grid spacing in km. An equation for the best-fit trend line alone would not be sufficient, because defining grid points to use in an analysis does not work well with non-integer values for grid spacing and constantly changing distances between points. Therefore, it was necessary to divide the different cities into *PGA* "bins" or defined ranges of values. These bins were determined using the USGS 2008 *PGA* hazard map (T_r = 2475 years) as shown in Figure 4-7. The *PGA* hazard map was chosen because it was clear and readily available as a well-documented definition of which areas in the country had significantly different seismicity levels compared to other areas' seismicity levels. The objective of this study was to determine the optimum grid spacing for each color bin.

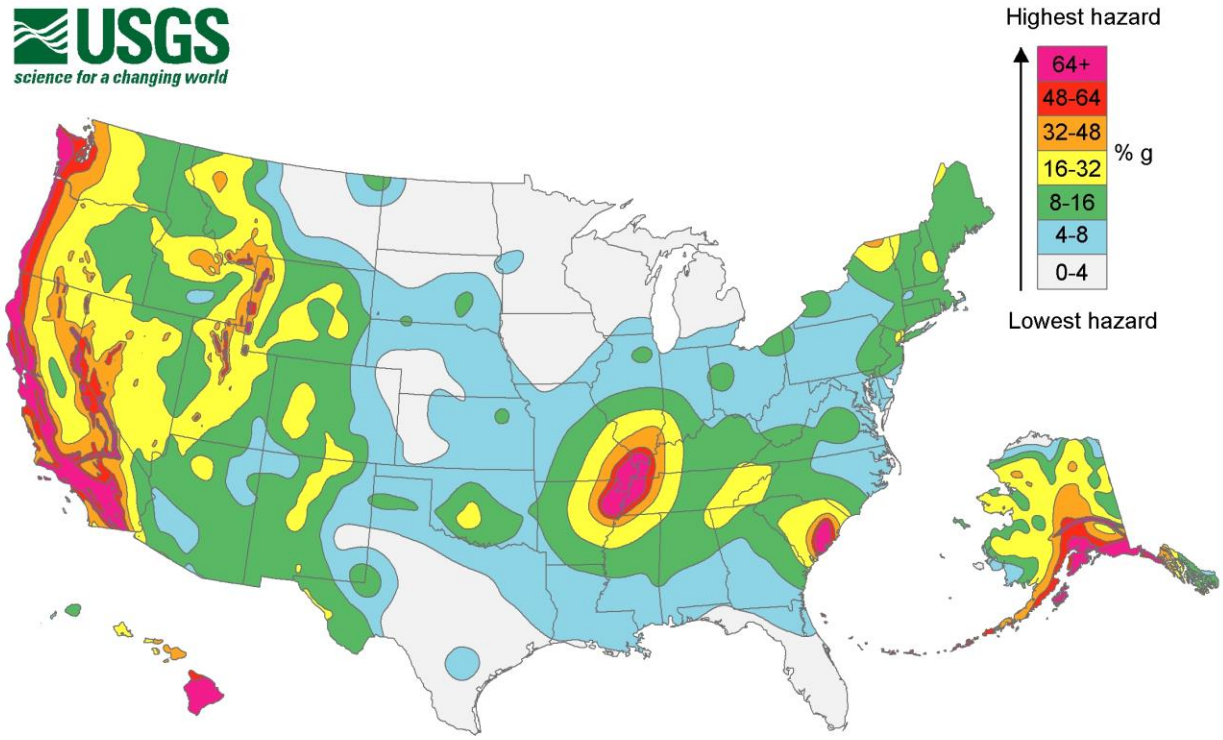

Figure 4-7 USGS 2008 *PGA* hazard map (T_r = 2475 years).

As in the preliminary study, a full performance-based analysis was performed at the anchor point of each city and at the corners of the grid surrounding the anchor point. This was repeated for multiple grid spacings until the percent error was within a reasonable amount. It was determined that "optimum grid spacing" would be defined as the smallest grid spacing (i.e shortest distance between grid points) which yielded a maximum percent error of 5% across all return periods based on *CSR*%. This definition is used because when the maximum percent error based on *CSR*% is limited to 5%, the interpolated value of N_{req} is within 1.5 blow counts of the actual value calculated at the anchor point, as shown in Figure 4-8. This seemed to be a reasonable amount of error, considering the inherent error in obtaining SPT blow counts during soil exploration at a site. If the definition of optimum grid spacing was defined as the smallest grid spacing which yielded a maximum difference of 1.5 blow counts, then the values of percent error based on *CSR*% may be unacceptably high. For example, as shown in Figure 4-8, if the maximum difference in N_{req} is 1.5 blow counts, the percent error in *CSR*% could be as high as 22.5%, which

could cause substantial inaccuracies. Thus the definition of optimum grid spacing was defined based on *CSR*% and not N_{req}.

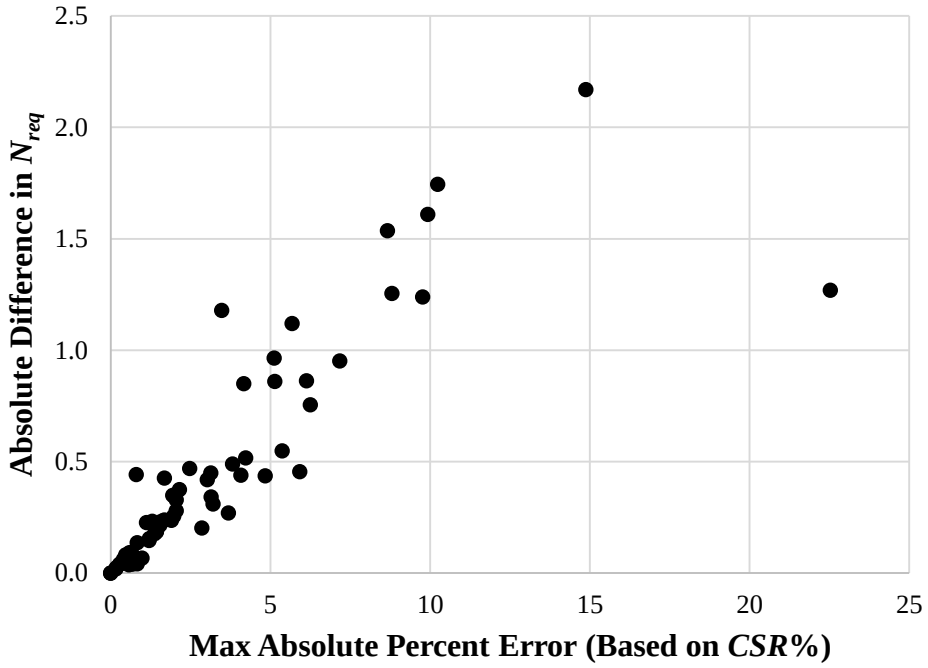

Figure 4-8 Comparison of difference in N_{req} to max absolute percent error based on *CSR*%.

Optimum grid spacing was determined using a plot of maximum percent error vs grid spacing in km. Unique plots were created for each city to determine the optimum grid spacing. Sample plots are provided in Figure 4-9, Figure 4-10, and Figure 4-11. Some cities' data followed a linear trend line while others followed a polynomial trend line. In each case, a reasonable best-fit line was used to determine optimum grid spacing. Some of the cities selected for this study did not reach a maximum percent error of 5%, even when the grid spacing was increased to 50 km (31.07 mi) or more. To avoid extrapolation, such cities (Hartford, CT, *PGA* = 0.0915; Bridgeport, CT, *PGA* = 0.1149; Clemson, SC, *PGA* = 0.1439; Anchorage, AK, *PGA* = 0.6161) were excluded from the final correlation between *PGA* and optimum grid spacing. A description of the final correlation between *PGA* and optimum grid spacing is included in the following section.

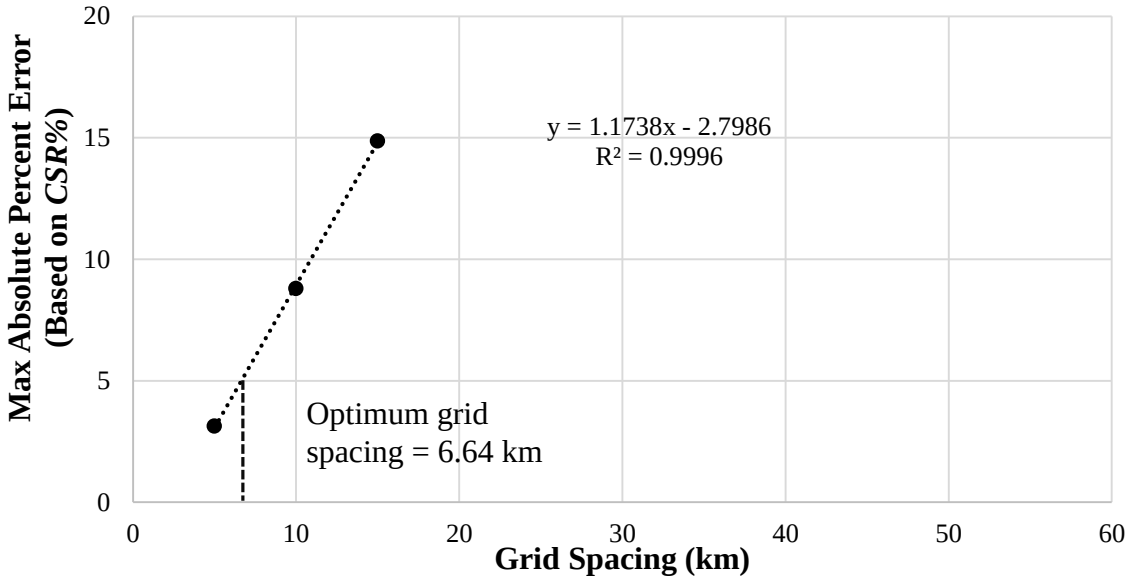

Figure 4-9 Variation of maximum percent error (based on *CSR*%) with increasing distance between grid points for Eureka, CA. (Pink zone, *PGA* = 1.4004)

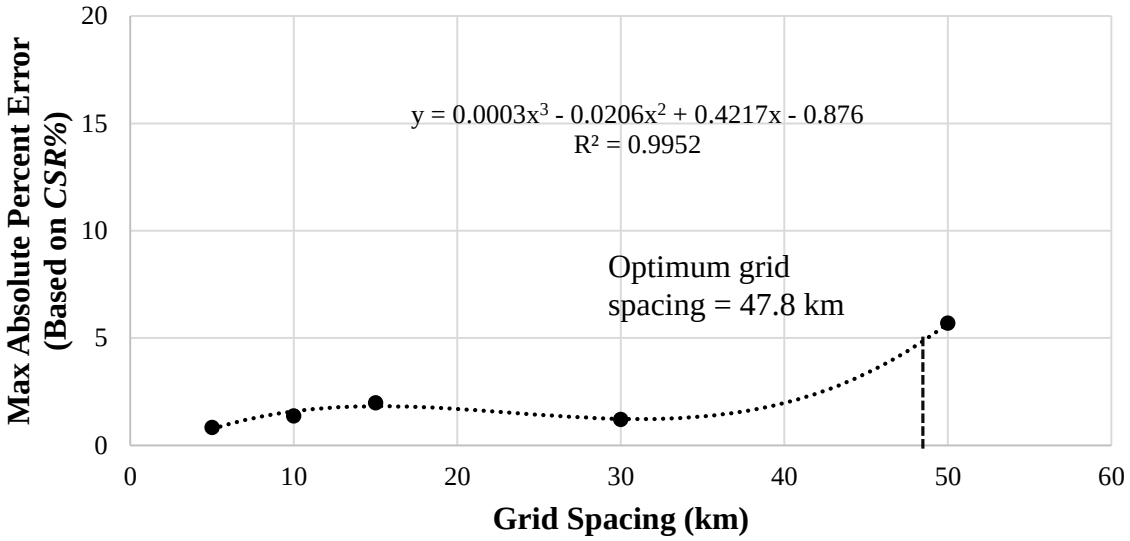

Figure 4-10 Variation of maximum percent error (based on *CSR*%) with increasing distance between grid points for West Yellowstone, MT. (Orange zone, *PGA* = 0.4187)

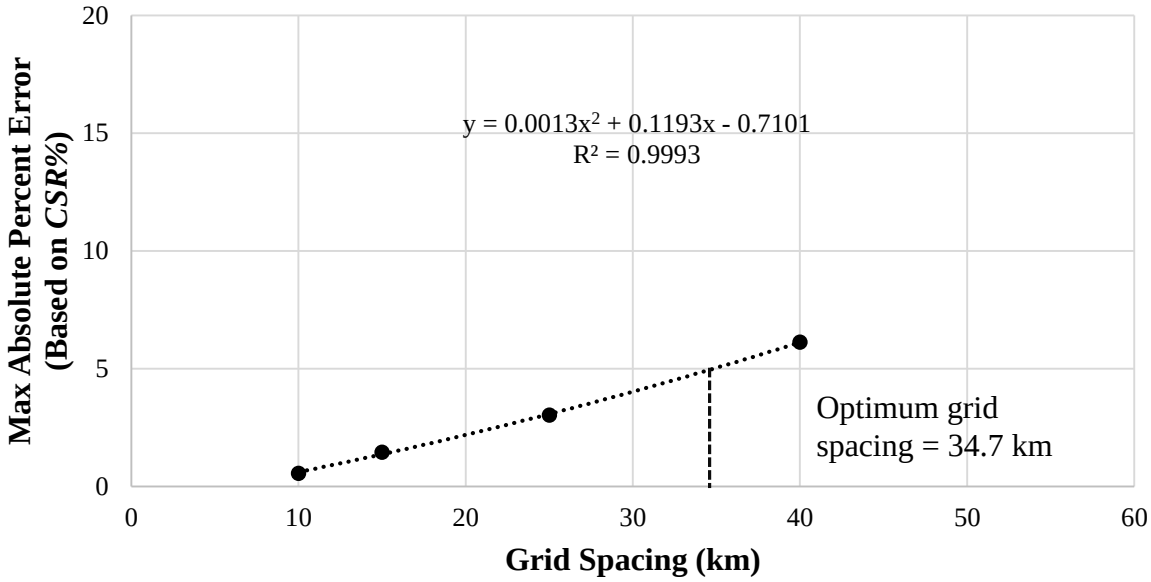

Figure 4-11 Variation of maximum percent error (based on *CSR*%) with increasing distance between grid points for Boise, ID. (Green zone, *PGA* = 0.1232)

4.2.4 *PGA* Correlation

As described in the previous section, optimum grid spacing was determined for each city included in the study that reached at least a maximum percent error of 5% based on *CSR*% (not N_{req}). Optimum grid spacing was then plotted against *PGA* as shown in Figure 4-12. The vertical dashed lines indicate the boundaries between *PGA* bins as defined in the USGS 2008 *PGA* hazard map. The general trend of the points ($R^2 = 0.628$) supports the hypothesis that as *PGA* increases the optimum grid spacing decreases. A hand-drawn lower bound was used to determine the optimum grid spacing based on *PGA*. The lower bound line was chosen as a conservative estimate of optimum grid spacing.

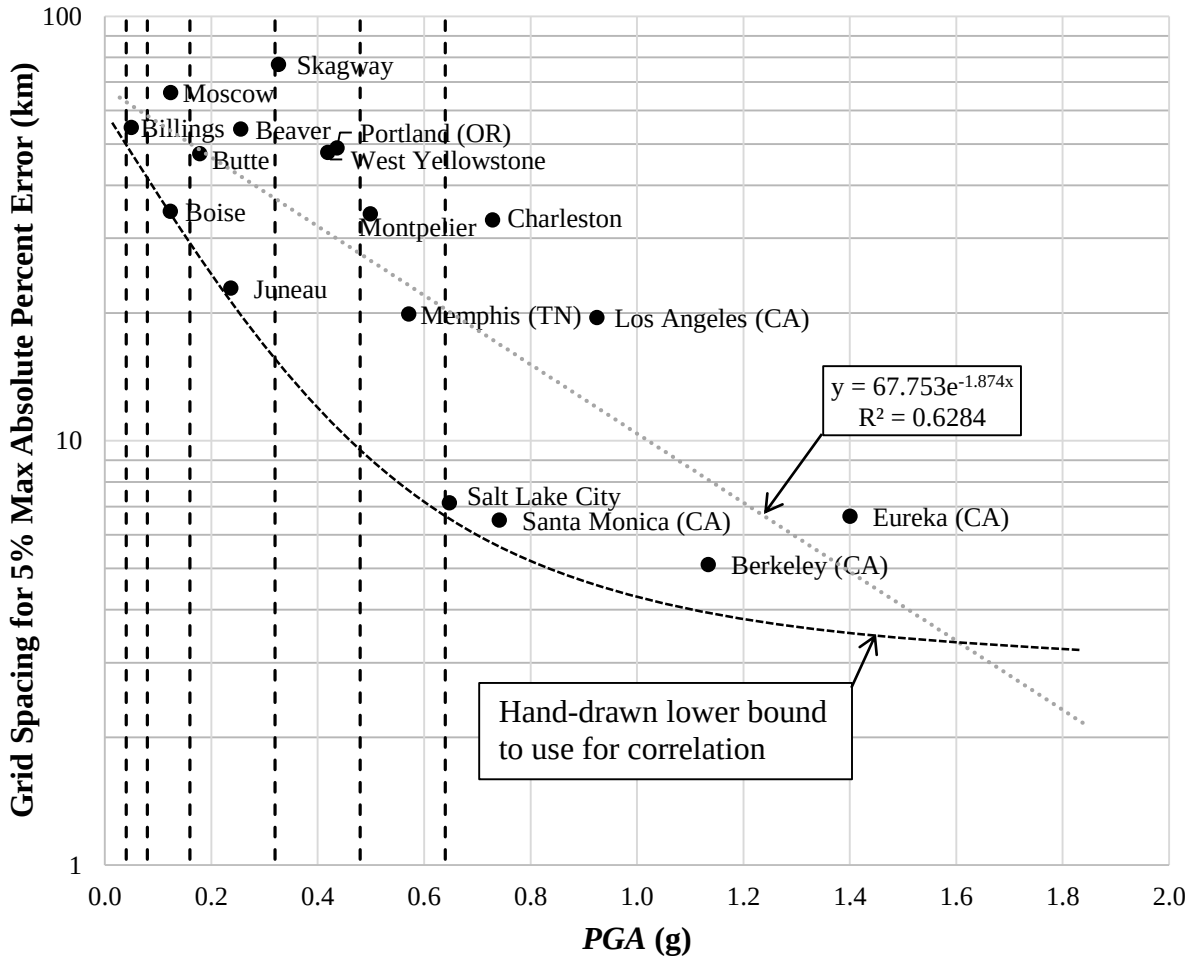

Figure 4-12 Correlation between *PGA* and optimum grid spacing to achieve 5% maximum absolute percent error (based on *CSR*%).

The hand-drawn lower bound shown in Figure 4-12 was used to determine the set of rules for selecting grid spacing in the mapping procedure. Within each *PGA* bin, a lower-bound value for optimum grid spacing was selected. The set of rules includes one optimum grid spacing distance for each *PGA* bin included in the study. Table 4-2 summarizes this set of rules.

Table 4-2 Proposed Set of Rules to Determine Optimum Grid Spacing within a *PGA* Range

PGA	Color	Spacing (km)	Spacing (mi)
0 - 0.04	Gray	50	31.1
0.04 - 0.08	Blue	50	31.1
0.08 - 0.16	Green	30	18.6
0.16 - 0.32	Yellow	20	12.4
0.32 - 0.48	Orange	12	7.5
0.48 - 0.64	Red	8	5.0
0.64+	Pink	4	2.5

In summary, the correlation determined in this study provided a set of rules to use when creating liquefaction loading maps for *CSR*% and liquefaction parameter maps for N_{req}.

4.3 Empirical Lateral Spread Displacement Model

This section will describe the methods used to derive the optimum grid spacing to ensure accuracy of interpolated points determined by the simplified performance-based lateral spread displacement evaluation. To ensure accuracy of the maps, interpolation between grid points must result in values reasonably close to the results of an actual analysis at the same location. It was determined that if the interpolated result was within 5% of an actual analysis at that site, then the result was acceptable.

4.3.1 Methodology for Grid Spacing Study

The methodology used to derive the optimum grid spacing for the simplified lateral spread displacement model began with the selection of three cities in each state that represent three different levels of seismic hazard (with the exception of Connecticut which had essentially uniform hazard across the state). Using the USGS 1996 and 2008 deaggregation websites the PGA at each site was determined for the 2475 year return period. The hazard level at each site as well as the hazard range for each state was found based on the same representation seen in the USGS 2008 PGA hazard map for the 2475 year return period. This map and the subdivision of hazard level can

be seen in Figure 4-7, and a table listing each city with its corresponding *PGA* and hazard zone can be seen in Table 4-3.

Table 4-3 Grid Spacing Analysis Sites and *PGA*

State	Site	*PGA*	Hazard Zone
Alaska	Anchorage	0.618	Red
	Fairbanks	0.414	Orange
	Juneau	0.237	Yellow
Connecticut	Hartford	0.093	Green
	Norwich	0.086	Green
	Danbury	0.121	Green
Idaho	Salmon	0.375	Orange
	Boise	0.136	Green
	Pocatello	0.199	Yellow
Montana	Butte	0.179	Yellow
	Glendive	0.028	Grey
	Billings	0.050	Blue
South Carolina	Charleston	0.733	Pink
	Greenville	0.142	Green
	Columbia	0.225	Yellow
Utah	Salt Lake City	0.665	Pink
	Moab	0.087	Green
	Cedar City	0.285	Yellow

To assess the grid spacing, the reference lateral spread displacement, D_H^{ref}, was found at each city and then four locations surrounding the city at a set grid spacing. Using the city as an anchor point, the four points were selected equidistant from the center creating a square. The grid spacing is then the length of the sides of the square. This arrangement can be seen in Figure 4-1. Using the four surrounding points, a value was interpolated at the center of the points and then compared to the actual value found at the site. This process was repeated for several grid spacings and the % error was calculated. An example of this process can be seen for the city of Charleston, South Carolina at a grid spacing of 15 km (9.32 mi) in Table 4-4.

Table 4-4 Grid Spacing Interpolation Example Calculation for Charleston, South Carolina (32.783, -79.933) at 15 km (9.32 mi) grid spacing.

Grid Spacing - 15 km (9.32 mi)		
Latitude	Longitude	D_H^{ref} (m)
32.850	-80.000	0.829
32.716	-80.000	0.522
32.850	-79.866	0.479
32.716	-79.866	0.333
Interpolated D_H^{ref} (m)		**0.541**
Actual D_H^{ref} (m)		**0.513**
Error (%)		**5.41%**

This process was repeated for each city in the analysis at grid spacings of 5, 10, 15, 20, 25, 30, 40, and 50 km (3.1, 6.21, 9.32, 12.4, 15.5, 18.6, 24.9, and 31.1 mi). The grid spacing, where the error is 5% or less, was then plotted against *PGA* to get an idea of how the grid spacing differs from site to site. This plot can be seen in Figure 4-13.

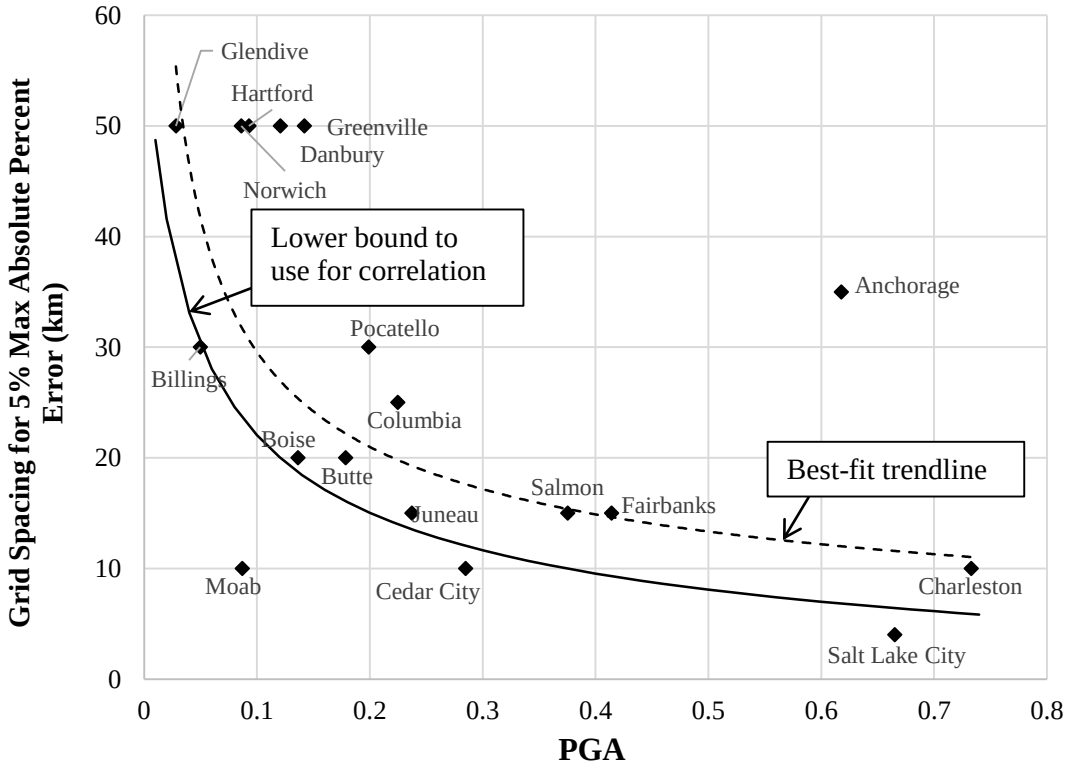

Figure 4-13 Grid spacing based on 5% error plotted against PGA for all sites.

As can be seen in this plot, there is significant scatter of the results. The seismic loading of each location can be very different, so the way that the lateral spread analysis attenuates could be influenced heavily by this. In order to address this uncertainty, a line was fit to the data (dashed line) then a lower bound (solid line) was drawn to represent the minimum grid spacing. This lower envelope was used for all locations, with the exception of Utah and Alaska. Utah was found to require a much finer grid spacing overall and so a specific grid spacing was created to account for this. Alaska was given a slightly coarser grid spacing for two reasons: the first was due to the analysis showing Alaska being overall higher on this plot, and second that Alaska has significantly more surface area than the rest of the states and required more analysis than the rest of the states combined. The value at Moab was considered to be unrepresentative of the overall appropriate grid spacing in Utah, so that point was not incorporated into the proposed grid spacing for Utah. Additionally, the point in Anchorage was not incorporated into the grid spacing for Alaska due to the point also being unrepresentative of the overall grid spacing needs. These proposed grid spacings can be seen in Table 4-5.

Table 4-5 Proposed Grid Spacing for Lateral Spread Analysis Based on *PGA* Zone

PGA	Color	General (km)	Utah (km)	Alaska (km)
0 - 0.04	Gray	40	25	45
0.04 - 0.08	Blue	30	20	35
0.08 - 0.16	Green	20	15	25
0.16 - 0.32	Yellow	15	12	20
0.32 - 0.48	Orange	12	10	15
0.48 - 0.64	Red	8	7	10
0.64+	Pink	5	4	8

4.4 Summary

Based on the analysis outlined here, the grid spacing necessary to maintain accuracy in the interpolated results was found. The grid spacings should result on average 5% difference between

an interpolated value and the result if an analysis were performed at the same site. These grid spacings will be very important in creating the grid of points that will be used in the analysis.

5.0 MAP DEVELOPMENT

5.1 Overview

Now that the optimum grid spacing between points has been determined, the grid points used in the analysis need to be determined, then those points need to be analyzed and the hazard parameters calculated. Once the analysis has been conducted for each grid, than those points will be used to create the liquefaction and lateral spread parameter maps for the target return periods.

This process required the use of several specialized software programs. To create the grid spacing and the maps the Graphical Information System (GIS) software ArcMap, developed by ESRI Incorporated, was used extensively. To perform the simplified liquefaction initiation analysis the software PBLiquefY, developed in house at BYU by Franke et al. (2014), was utilized. To perform the simplified lateral spread displacement analysis, the program EZ-FRISK created by Risk Engineering (2013) was used.

5.2 Creating the Grid Points

The process was started by dividing each state into sections based on the USGS 2008 *PGA* hazard map. This was done using GIS shapefiles downloaded from the USGS website representing the 2008 hazard map. Each *PGA* hazard zone was assigned a grid spacing based on the suggested grid spacing from the previous section. Then using ArcMap, a grid of points with latitude and longitude, was generated for each hazard zone at the specified grid spacing. All the zones were then combined into one general grid for the state.

Additionally, the representatives for each state involved in the research was asked to provide any areas which they felt constituted an "Area of Concern" (AOC). These areas were anywhere that a reduction in grid spacing was thought necessary to provide a more refined hazard surface. Each AOC was then accounted for by modifying the general grid spacing rules to reduce grid spacing in each AOC. This was accomplished differently for the two methods used in this report. For the liquefaction initiation method each AOC was elevated by two hazard levels and the grid spacing for that area was based off the higher hazard. For example, if the AOC was in the "green" section of the hazard map the grid spacing in the AOC would be reduced to that of the

"orange" level. The lateral spread displacement model increased all AOC to the "red" level and used that reduced grid spacing for each example. An example of the subdivision and the overall grid of points for Utah can be seen in Figure 5-1.

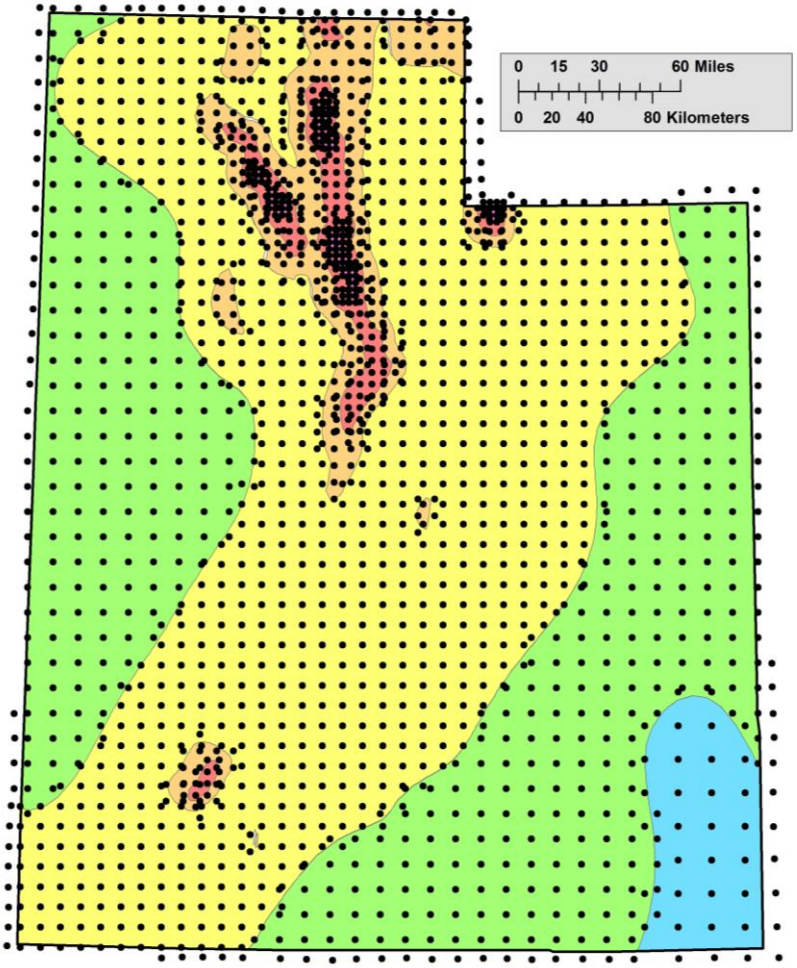

Figure 5-1 Grid points for Utah combined with USGS 2008 PGA hazard map.

5.3 Analysis of the Grid Points

Once the grid points were developed for all the states, the location of each of the points was evaluated for liquefaction and lateral spread hazard using the reference soil profiles discussed in the previous report. Each point was analyzed for the 475, 1033, and 2475 year return periods. Once all of the points for a particular state were successfully run, the results were compiled and then imported back into ArcMap to begin the process of making the parameter maps.

5.3.1 Analysis of the Liquefaction Initiation Model Grid Points

The grid points used in the liquefaction initiation method were analyzed using the USGS 2008 deaggregations for Connecticut, Idaho, Montana, South Carolina, and Utah while the USGS 1996 deaggregations were used for Alaska. The process utilized the ability of PBLiquefY to run multiple sites sequentially.

5.3.2 Analysis of the Lateral Spread Displacement Model Grid Points

Analyzing the grid points in EZ-FRISK requires that a seismic source model be used. To analyze the points in Connecticut, Idaho, Montana, South Carolina, and Utah the USGS 2008 seismic source model was used. For Alaska, the USGS 1998 gridded source model and the USGS 2002 seismic source models were used to analyze the grid points. Only area sources and faults were considered within 300 km of each site, with the exception of subduction zone sources which were considered within 500 km.

5.4 Creation of the Maps

Once the analyzed grid points were imported back into ArcMap the points needed to be turned into a contour map. This was done by converting the individual points into a surface raster using the Kriging tool. This tool interpolates between each point and makes a surface with a value at every point. To ensure that the contours of each state run all the way to the border, the state shape is buffered slightly. The Kriging raster is created based on this buffered shape. Once the Kriging raster is made, the raster surface needs to be converted into a contour.

To make the contour from the Kriging, first the spacing of the contours needs to be determined. It is important that the contour spacing be fine enough that the detail of the map can be read, but far enough apart that the contours can be read. The spacing will vary from map to map based on this process. An example of a Kriging raster and contour for the state of Utah can be seen in Figure 5-2.

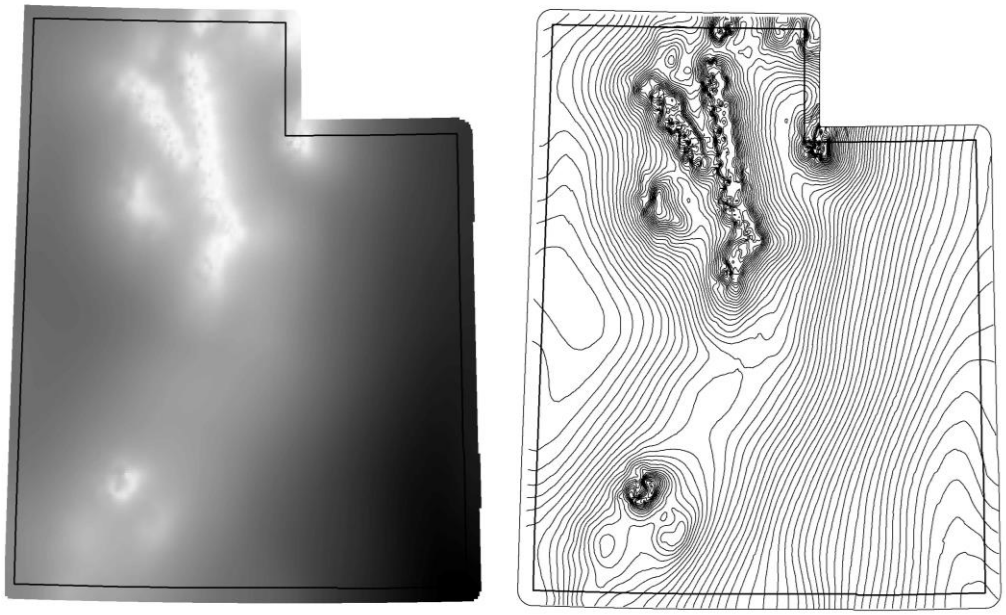

a) b)

Figure 5-2 a) Kriging raster and b) contours for Utah (T_r = 2475 yrs).

Once the proper contour spacing is determined for each map, the contour is labeled and clipped to fit the state shapefile. Then a basemap and reference features are added to provide more detail about the topography to the parameter maps. An example of a completed liquefaction parameter map of N_{req} can be seen in Figure 5-3.

Each model has different parameters represented by the contours on the map. The liquefaction initiation model has two different parameters and therefore two different maps. The first parameter is the reference value of *CSR*% as calculated using the Boulanger and Idriss (2014) model. *CSR* is usually given as a decimal but was changed to a percent to make reading the maps easier. The second parameter is the reference value for N_{req} as calculated using the Cetin et al. (2004) model and is given in units of SPT blowcounts. The lateral spread parameter map shows the reference value of displacement, D_H^{ref} as calculated using the Youd et al. (2002) model, and is given in units of Log (meters). Careful attention needs to be given to the labeling of each map to ensure that map has the correct parameter and that the reference value used in the later steps of the simplified method are accurately read from the contours.

For this report, maps of *CSR*%, N_{req}, and D_H^{ref} were made for each state at the 475, 1033, and 2475 year return periods with the exception of Connecticut. At the 475 and 1033 year return

periods for *CSR*% and the 475 year return period for N_{req}, the maps for Connecticut show no variation in those values and have uniform hazard (N_{req} = 1, *CSR*% = 4.65%) across the state. Consequently, those maps were not included. Additionally, maps for the cities of Anchorage, AK; Boise, ID; Butte, MT; Charleston, SC; and Salt Lake City, UT were created. These maps are provided on the dropbox link previously distributed. Sample liquefaction loading maps and lateral spreading parameter maps can be viewed in Appendix B and C, respectively. The contours were adjusted for each map to make reading it as user friendly as possible.

These maps were provided to show the potential types of parameter maps that can be created. Using the Kriging rasters that will be provided at the culmination of this research, each state can create maps of any area in their state and determine the contour spacing and scale.

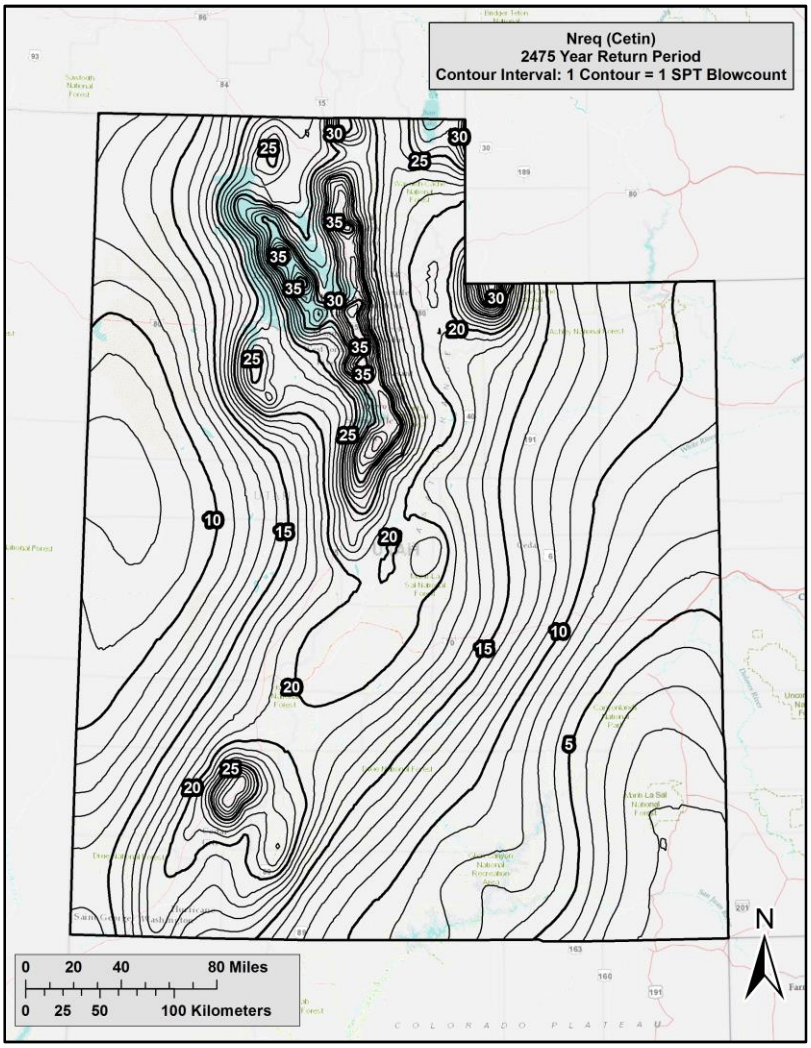

Figure 5-3 N_{req} for Utah (T_r = 2475 years).

5.4.1 Interpreting the File Names

The following section outlines the naming convention for the files provided through the dropbox link.

5.4.1.1 Liquefaction Triggering

Raster – A raster file is a collection of files. Each collection of files is contained in a folder with the following naming convention:

(State)_(parameter type)(return period)_cl
Example: ak_csr475_cl

Notes:

- Three states (Utah, Montana, and Idaho) were analyzed as a combined file. The "State" label for these states is "w" or "w3".
    - "w" stands for the western states analyzed together.
    - "w3" simply indicates that this was the third iteration of the kriging interpolation (two previous iterations were unsuccessful).
- "cl" means that the file has been clipped to the buffered state (or states, in the case of Utah, Montana and Idaho) boundary
- "parameter type" is either "csr", "nrq", "nrc" or "nri".
    - The label "csr" indicates that the raster contains data for *CSR*(%) from the Idriss and Boulanger (2012) method.
    - The labels "nrq" and "nrc" indicate that the raster contains data for N_{req} from the Cetin et al. (2004) method.
    - The label "nri" indicates that the raster contains data for N_{req} from the Idriss and Boulanger (2012) method. This was specially requested for South Carolina, and therefore is not currently provided for other states. These files may be created upon request.

Contour – Contour files are polyline shapefiles with the extension *.shp. These shapefiles are named using the following convention:

(State)_(parameter type)_(return period)_cont
Example: ak_csr_475_cont

Notes:

- "cont" indicates that this is a contour file
- "parameter type" is either csr, nrq, nrc or nri. See the above notes about Raster parameter types.

5.4.1.2 Lateral Spread

Raster – Each file associated with a raster follows the same naming convention:

(State)_(return period)_kriging
Example: ak_475_kriging

5.5 Summary

To create the parameter and hazard maps, the state is subdivided into zones and a grid spacing for each zone is assigned. A grid of points is generated in ArcMap based on this grid spacing. Then the points are analyzed using the specified performance-based analytical software (PBLiquefY, EZ-FRISK). These points are then imported into ArcMap and converted to a Kriging raster that is then used to create a contour of the reference parameter. Sample maps can be seen in the Appendix.

6.0 COMPARISON OF PROBABILISTIC AND DETERMINISTIC ANALYSES

6.1 Overview

This section provides comparisons between the pseudo-probabilistic, deterministic, and simplified performance-based procedures for estimating liquefaction initiation hazard and lateral spread displacement. The purpose of these comparisons is to identify how the deterministic procedure should be used in the proposed simplified procedure.

6.2 Methodology

Three cities of varying seismicity were selected for the comparison study: San Francisco (high seismicity), Salt Lake City (medium seismicity), and Butte (low seismicity). For each city, three analyses were performed: probabilistic (simplified performance-based procedure developed as part of this research), pseudo-probabilistic (AASHTO), and deterministic. A description of each analysis type is provided below.

6.2.1 Simplified Performance-Based Seismic Hazard Analysis

The simplified performance-based procedures involve retrieving a specified liquefaction hazard parameter from a hazard-targeted map developed using full probabilistic analyses. The probabilistic analyses which created the liquefaction loading and lateral spread parameter maps involve creating hazard curves which consider all possible combinations of the required seismic hazard analysis variables and their respective likelihoods. Examples of these variables would be: maximum horizontal ground acceleration, a_{max}, moment magnitude, M_w, or site-to-source distance, R. These processes are discussed in greater detail in the previously submitted update reports: Update Report Year 1 Quarter 1 for the simplified performance-based methods, and Update Report Year 1 Quarter 2 for the development of the liquefaction loading and lateral spread parameter maps.

The parameters used for the comparison of deterministic and simplified methods for this study were: for liquefaction initiation, $CSR\%^{ref}$; and for lateral spread, D_H^{ref}. Each of the parameters were found at the target cities for the 475, 1033, and 2475 year return periods.

6.2.1.1 Simplified Liquefaction Initiation

For the simplified liquefaction initiation procedure the appropriate uniform hazard-targeted liquefaction loading map was identified for each site and values of $CSR\%^{ref}$ were obtained for the necessary return periods. These $CSR\%^{ref}$ values were adjusted for soil characteristics associated with the same assumed soil profile as was used in the validation of the simplified method (shown in Figure 3-1) to estimate $CSR\%^{site}$ values. This same soil profile was used for all three analyses (probabilistic, pseudo-probabilistic, and deterministic). The values of $CSR\%^{site}$ were used to calculate factor of safety against liquefaction (FS_L), and clean-sand equivalent SPT blow count required to resist liquefaction initiation (N_{req}). This process was previously described in greater detail in the derivation of the simplified procedure.

6.2.1.2 Simplified Lateral Spread Displacements

For the simplified performance-based procedure the appropriate lateral spread parameter map was identified for each site and values of D_H^{ref} were obtained for the necessary return periods. Using a generic soil profile (shown in Figure 6-1), the values of D_H^{ref} were corrected and the D_H^{site} was determined for each city at the targeted return periods. The additional analyses (pseudo-probabilistic and deterministic) for the comparison utilized the same soil profile. This process was previously described in greater detail in the derivation of the simplified procedure.

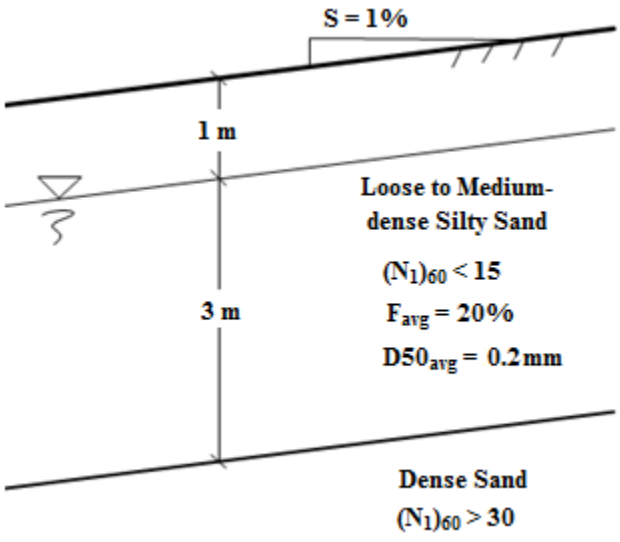

Figure 6-1 Soil profile used for the lateral spread displacement comparison study.

6.2.2 Deterministic Procedure

In the deterministic procedure, ground motions are obtained through a Deterministic Seismic Hazard Analysis (DSHA). A DSHA involves deterministically assessing the seismic sources in the nearby region of the site of interest and identifying the source which produces the highest hazard in the area. The software EZ-FRISK was used to identify the top five seismic sources within 200 km for San Francisco and Salt Lake City. The 2008 USGS Seismic Source Model within EZ-FRISK does not include some smaller faults in low seismic regions, such as Butte. Thus, the governing fault for Butte (Rocker Fault) was identified using the USGS quaternary fault database (USGS et al., 2006). In the case of Salt Lake City and San Francisco, EZ-FRISK provided values of M_w, *PGA*, and *R* for both the 50th (i.e. median) and 84th (i.e. median + σ) percentiles using the New Generation Attenuation (NGA) models for the Western United States (Boore and Atkinson, 2008; Campbell and Bozorgnia, 2008; and Chiou and Youngs, 2008) and weighting schemes shown in Table 6-1. For Butte, the 50th and 84th percentile M_w values were estimated using a correlation with surface rupture length developed by Wells and Coppersmith (1994), and *PGA* was calculated using the same three (NGA) models based on measured dimensions and assumed characteristics of the Rocker Fault. Summaries of the seismic sources considered in this DSHA and details of the Rocker Fault calculations are provided in Tables D.1 and D.2, respectively, in the Appendix. Once the model inputs have been determined through the DSHA they are entered into the respective empirical liquefaction hazard models. A summary of the governing input variables utilized in the deterministic liquefaction initiation and lateral spread displacement models are provided in Table 6-2.

Table 6-1 NGA model weights used in the deterministic procedure.

Attenuation Model	Weight
Boore & Atkinson (2008)	0.333
Campbell & Bozorgnia (2008)	0.333
Chiou & Youngs (2008)	0.333

Table 6-2 Input variables used in the deterministic models (a_{max} calculated using F_{pga} from AASHTO code).

Location	Latitude	Longitude	Distance [km]	Mean M_w	Median (50%)		Median + σ (84%)	
					PGA	a_{max}	*PGA*	a_{max}
Butte	46.003	-112.533	4.92	6.97	0.5390	0.5390	0.9202	0.9202
Salt Lake City	40.755	-111.898	1.02	7.00	0.5911	0.5911	1.005	1.005
San Francisco	37.775	-122.418	12.4	8.05	0.3175	0.3754	0.5426	0.5426

6.2.2.1 Liquefaction Initiation

Estimations of liquefaction initiation potential (FS_L, N_{req}, and *CSR*%) were calculated deterministically using equations from the Idriss and Boulanger (2008) liquefaction triggering model. *CSR*% is found using the following equation:

$$CSR(\%) = 0.65\frac{a_{\max}}{g}\frac{\sigma_v}{\sigma_v'}(r_d)\frac{1}{(MSF)}\frac{1}{K_\sigma}(100\%) \tag{65}$$

where σ_v is the total vertical stress in the soil; σ_v' is the effective vertical stress in the soil; $a_{\max}/g$ is the peak ground surface acceleration as a fraction of gravity; MSF is the magnitude scaling factor as computed according to Idriss and Boulanger (2008); r_d is the depth reduction factor according to Idriss and Boulanger (2008); and K_σ the depth correction factor and is computed according to Idriss and Boulanger (2008). FS_L is calculated as:

$$FS_L = \frac{CRR}{CSR} = \frac{100 \cdot CRR}{CSR(\%)} \tag{66}$$

$$CRR_{P_L=50\%} = \exp\left[\left(\frac{(N_1)_{60,cs}}{14.1}\right) + \left(\frac{(N_1)_{60,cs}}{126}\right)^2 - \left(\frac{(N_1)_{60,cs}}{23.6}\right)^3 + \left(\frac{(N_1)_{60,cs}}{25.4}\right)^4 - 2.8\right] \tag{67}$$

where $(N_1)_{60,cs}$ represents the clean sand-equivalent SPT resistance value corrected to 60% efficiency and 1 atm overburden pressure as computed using the equations provided by Idriss and Boulanger (2008, 2010). N_{req} is solved iteratively from the following polynomial:

$$0 = \left(\frac{N_{req}}{14.1}\right) + \left(\frac{N_{req}^{\ 2}}{126}\right) - \left(\frac{N_{req}^{\ 3}}{23.6}\right) + \left(\frac{N_{req}^{\ 4}}{25.4}\right) - 2.8 - \ln(CSR) \tag{68}$$

6.2.2.2 Lateral Spread Displacement

Estimations of lateral spread displacement for the deterministic process were found using the equation from the Youd et al (2002) empirical lateral spread model. The model is a regression based on seismic loading parameters and site specific soil parameters. The seismic loading inputs are shown in Table 6-2, and the site specific soil inputs were drawn from the soil profile seen in Figure 6-1. With these values the lateral spread displacement, D_H, is found using the following equation:

$$\begin{aligned}\overline{\log D_H} = {} & b_0 + b_1 M + b_2 \log R^* + b_3 R + b_4 \log W + b_5 \log S \\ & + b_6 \log T_{15} + b_7 \log(100 - F_{15}) + b_8 \log(D50_{15} + 0.1)\end{aligned} \tag{69}$$

where D_H is the median computed permanent lateral spread displacement (m), M is the earthquake moment magnitude, R is the closest horizontal distance from the site to the source (km), W is the free-face ratio (%), S is the ground slope (%), T_{15} is the cumulative thickness (in upper 20 m) of all saturated soil layers with corrected Standard Penetration Test (SPT) blowcounts (i.e., $(N_1)_{60}$) less than 15 blows/foot (m), F_{15} is the average fines content of the soil comprising T_{15} (%), $D50_{15}$ is the average mean grain size of the soil comprising T_{15} (mm), and R* which is computed as:

$$R^* = R + 10^{0.89M - 5.64} \tag{70}$$

The model coefficients b_0 through b_8 are given in Table 2-2.

6.2.3 Pseudo-probabilistic Seismic Hazard Analysis

In the pseudo-probabilistic procedure, the variables used in the empirical liquefaction hazard models are obtained from a Probabilistic Seismic Hazard Analysis (PSHA). Then these

variables are used in the same deterministic procedure outlined previously for both the liquefaction initiation and lateral spread displacements. To find these variables using a PSHA the USGS 2008 interactive deaggregation website (USGS 2008) was utilized. This procedure involved entering the latitude and longitude of the target cities, then selecting the return period for the analysis. Using this tool, the mean magnitude (M_w), peak ground acceleration (PGA) for rock, and source-to-site distance (R) were obtained for a return period of 1,039 years for each city of interest. The resulting values are summarized in Table 6-3.

Table 6-3 Input values found using USGS 2008 Deaggregations (T_R = 1,039 years).

Location	Latitude	Longitude	Distance (km)	Mean M_w	PGA	F_{pga}
Butte	46.003	-112.533	24.9	6.03	0.1206	1.559
Salt Lake City	40.755	-111.898	4.20	6.84	0.4030	1.097
San Francisco	37.775	-122.418	12.0	7.38	0.5685	1.000

6.3 Results

Each city was evaluated using the three analysis types discussed previously (probabilistic, pseudo-probabilistic, and deterministic). The following plots allow comparisons between the three methods and help explain the purpose of deterministic analyses within the proposed simplified performance-based procedures.

6.3.1 Performance-based Liquefaction Triggering Assessment

6.3.1.1 Pseudo-probabilistic vs. Simplified Performance-based

In each of the three cities analyzed, the results from the pseudo-probabilistic procedure suggested greater liquefaction hazard than the results from the performance-based procedure. The direct comparison of both methods is provided in Figure 6-2.

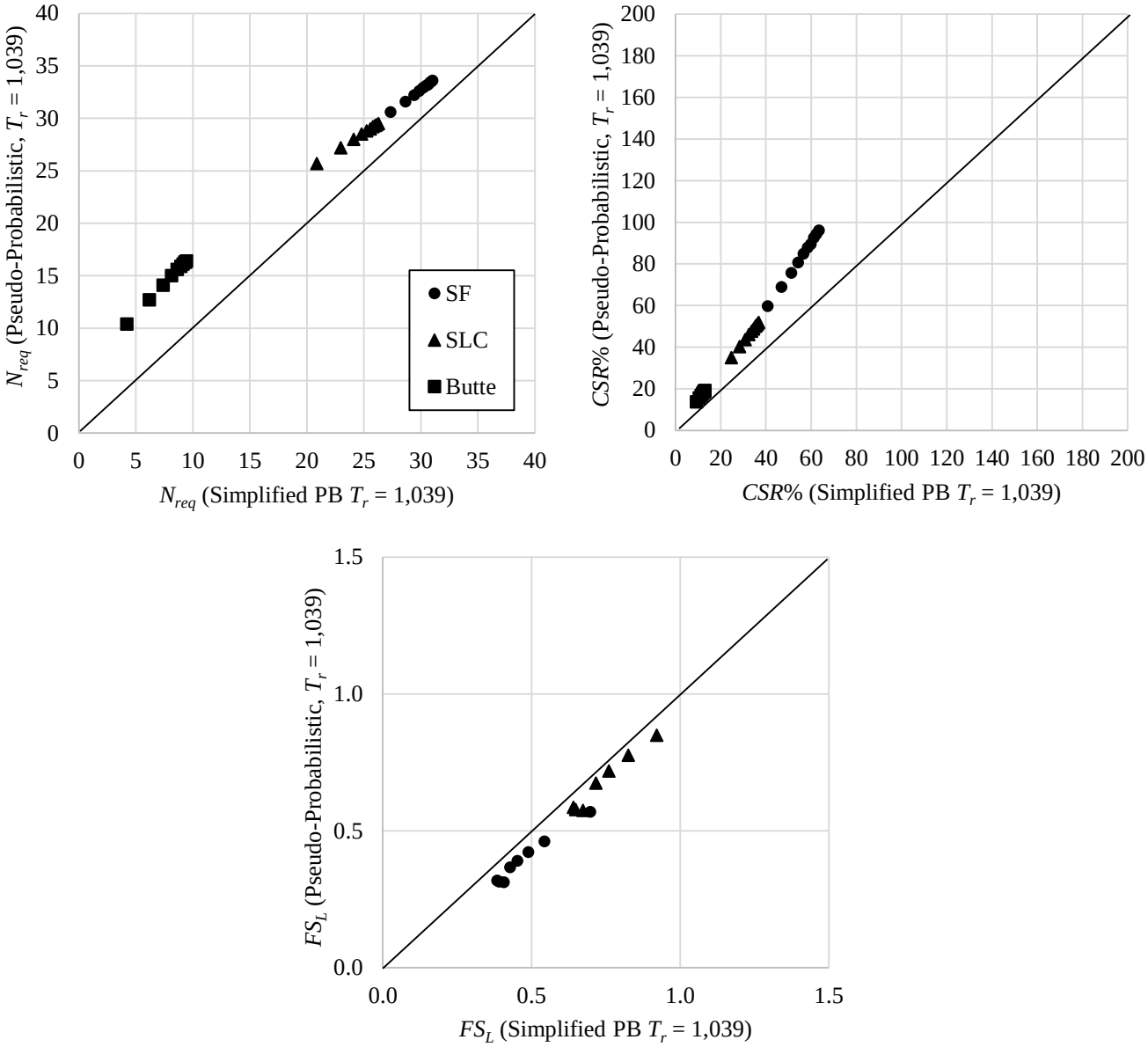

Figure 6-2 Comparison of pseudo-probabilistic and simplified performance-based values of N_{req}, *CSR*%, and FS_L.

6.3.1.2 Deterministic vs. Simplified Performance-based

Direct comparison plots (Figure 6-3 through Figure 6-5) show that the deterministic analyses frequently over-predicted liquefaction hazard. This over-prediction is especially evident in the case of Butte where the simplified performance-based method estimated N_{req} values as low as 3.1% of the deterministic N_{req} values. This discrepancy could be because the likelihood of the

large Rocker Fault near Butte rupturing and achieving the 50% ground motion is very low. Therefore, in the simplified performance-based approach (which incorporates likelihoods of seismic events in the calculations), the associated N_{req} is much lower. These comparison plots also highlight the significant discrepancy between the 50th and 84th percentile ground motions. In the case of San Francisco at the 2,475-year return period, the 50th percentile ground motions under-predict N_{req} while the 84th percentile ground motions over-predict N_{req}. This discrepancy produces a dilemma for the engineer who has to decide which ground motions appropriately characterize the liquefaction hazard for the given site. However, the simplified performance-based procedure does not depend on this decision and can provide a more consistent estimate of liquefaction hazard.

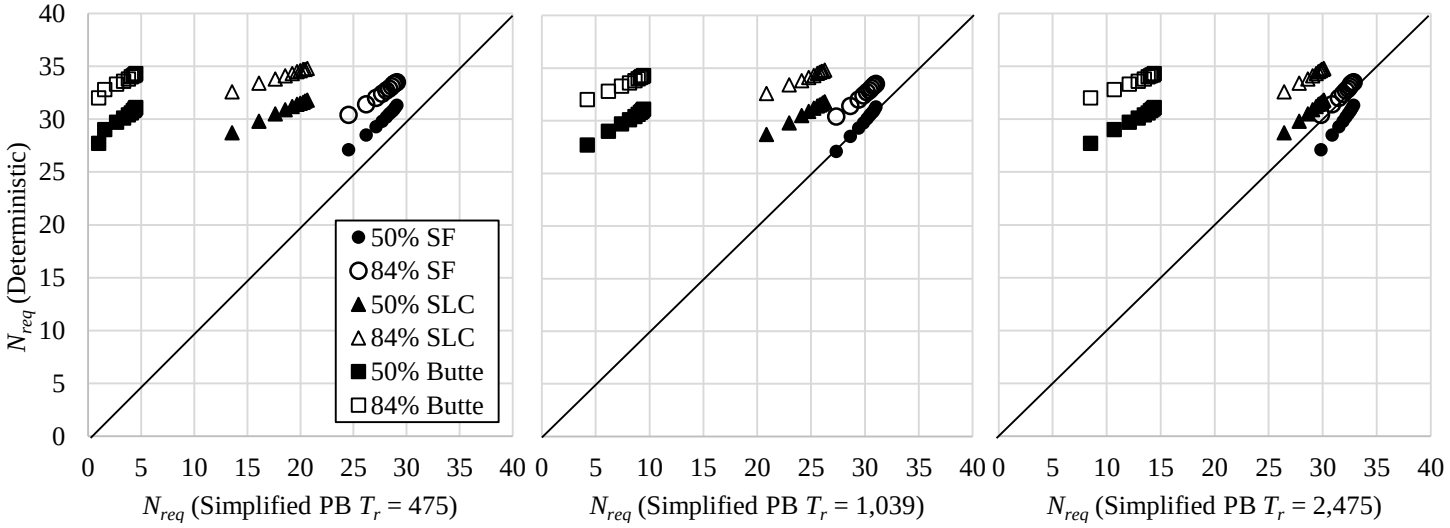

Figure 6-3 Comparison of deterministic and simplified performance-based values of N_{req}.

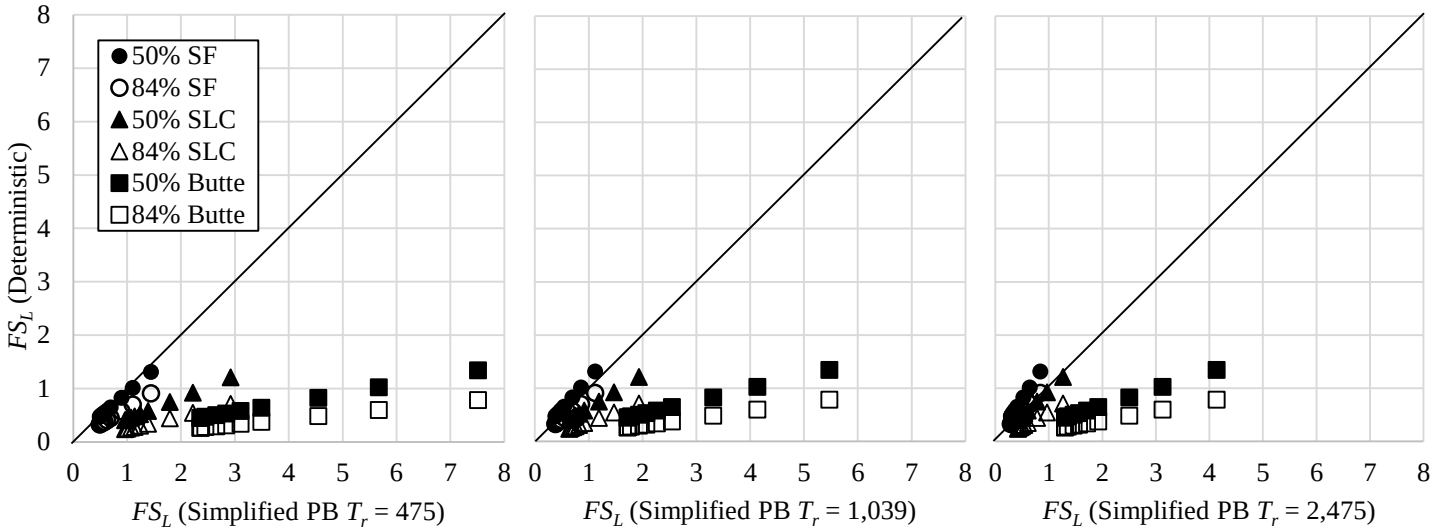

Figure 6-4 Comparison of deterministic and simplified performance-based values of FS_L.

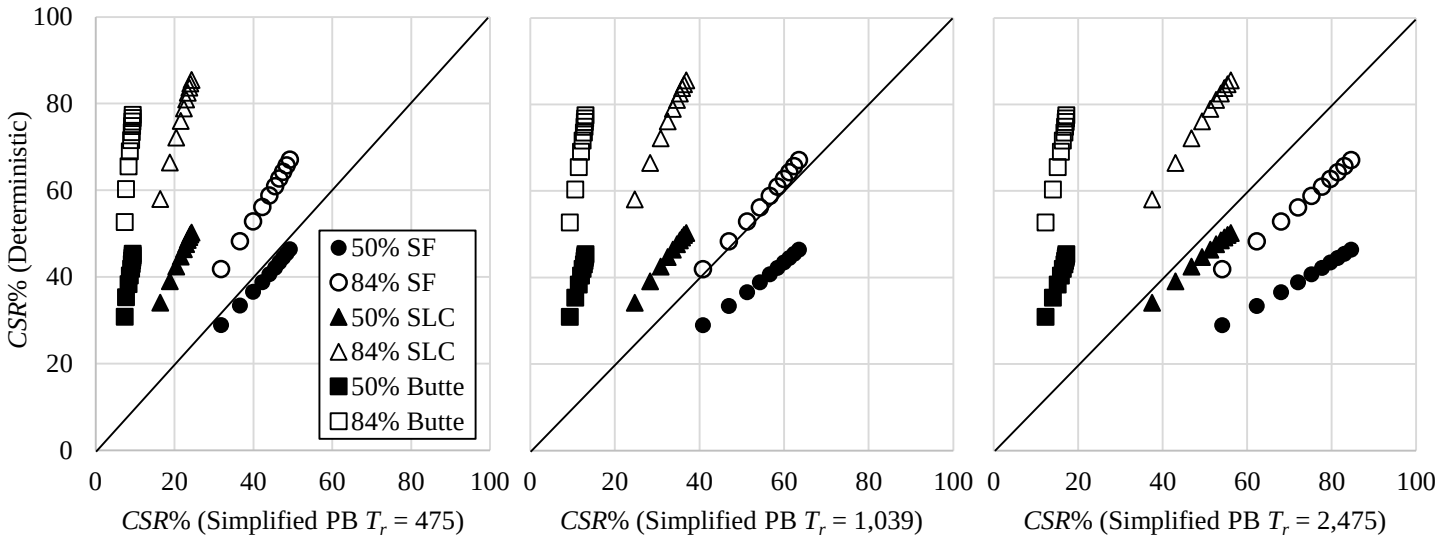

Figure 6-5 Comparison of deterministic and simplified performance-based values of *CSR*%.

6.3.2 Empirical Lateral Spread Displacement Model

Once the analysis of the different methods was completed, the data was examined and several charts were created, one for each city. These charts compare, side by side, the results of the simplified, pseudo-probabilistic, and deterministic analyses. These charts can be seen in Figure 6-6, Figure 6-7, and Figure 6-8.

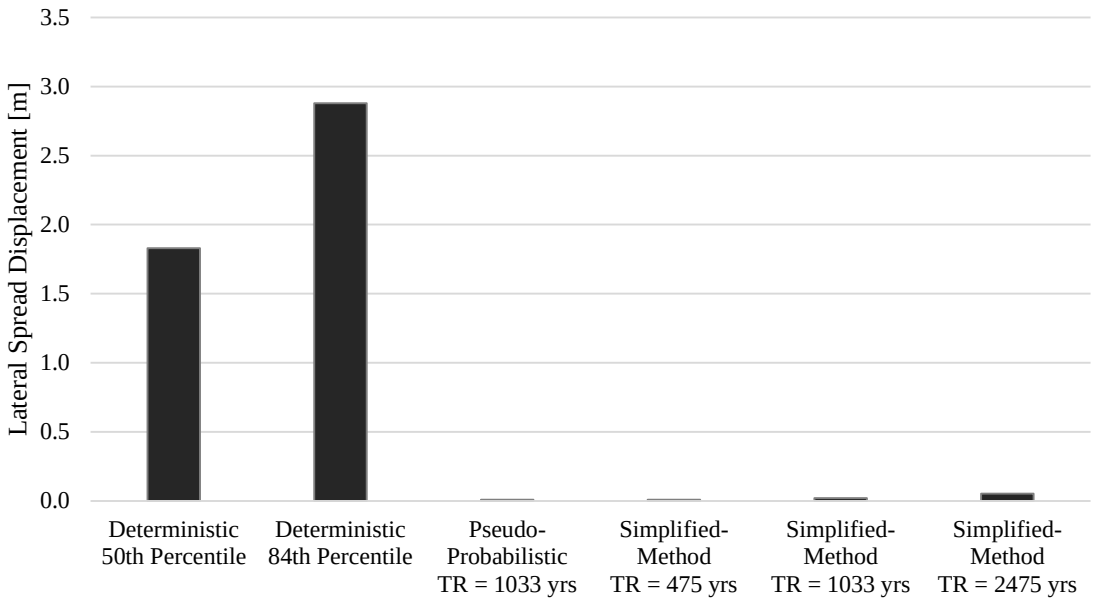

Figure 6-6 Comparison of Deterministic, Pseudo-probabilistic, and Simplified methods for Butte, MT (Latitude 46.033, Longitude -112.533).

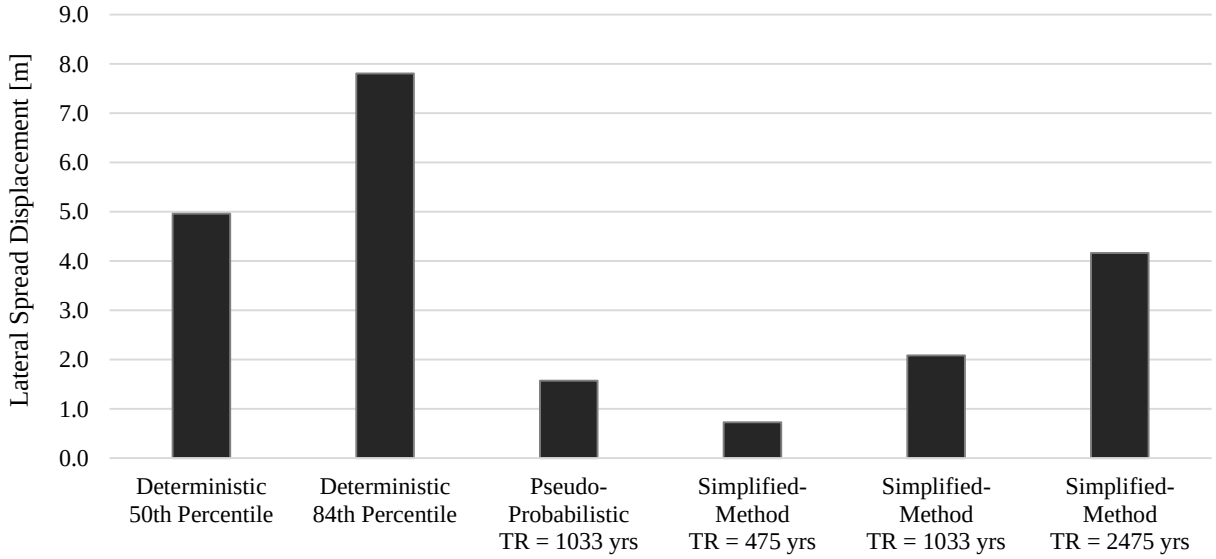

Figure 6-7 Comparison of Deterministic, Pseudo-probabilistic, and Simplified methods for Salt Lake City, UT (Latitude 40.755, Longitude -111.898).

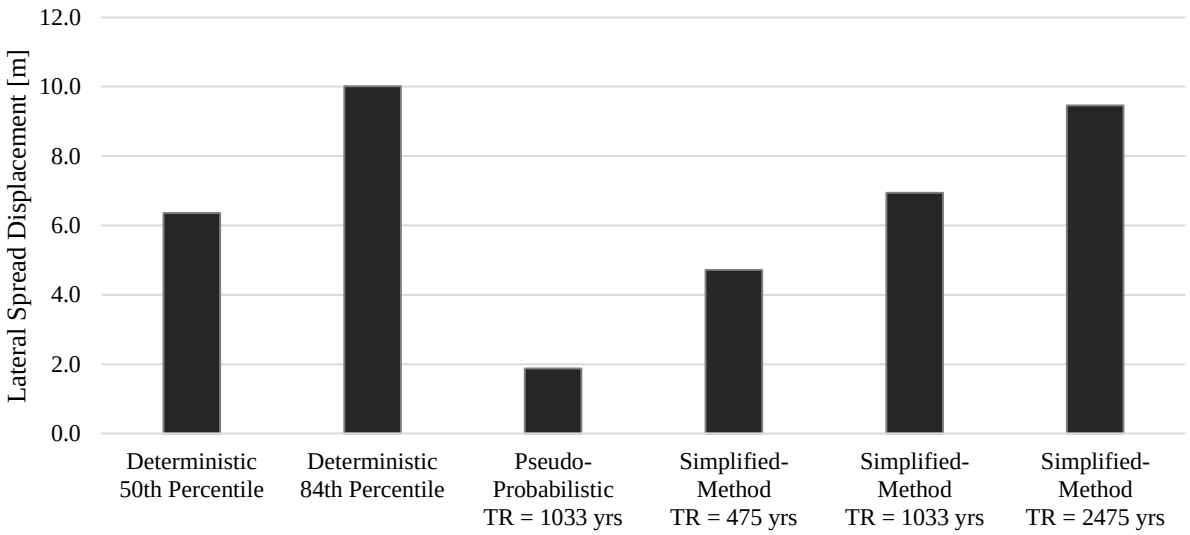

Figure 6-8 Comparison of Deterministic, Pseudo-probabilistic, and Simplified methods for San Francisco, CA (Latitude 37.775, Longitude -122.418).

The different cities are associated with regions of differing seismicity, and the deterministic comparisons with the simplified results yield some interesting conclusions. In the city with low seismicity, Butte seen in Figure 6-6, the deterministic method massively over-predicts the displacements predicted by the simplified and pseudo-probabilistic methods. This result can be attributed to the deterministic procedure not accounting for the likelihood of the Rocker fault rupturing, and predicts a displacement that may have an extremely low probability of occurring. The medium seismicity city, Salt Lake City seen in Figure 6-7, shows as well that the deterministic method predicts displacements higher than the simplified and pseudo-probabilistic procedures. In San Francisco, the high seismicity city, the results are much more similar at the 2475 return period, as can be seen in Figure 6-8. In this area the simplified method for the 2475 year return period predicts a slightly higher displacement than the deterministic mean value. The deterministic 84th percentile still predicts a higher value than the simplified method at the 2475 year return period.

6.4 Summary

The results of this study, for both the liquefaction initiation and lateral spread displacement, show that deterministic methods severely over-predicted liquefaction hazard in Butte—an area of low seismicity. The deterministic results also slightly over-predicted liquefaction hazards at high return periods in Salt Lake City—an area of medium seismicity. In San Francisco—an area of high seismicity—the deterministic methods slightly under-predicted liquefaction hazard when considering the 50th percentile ground motions in the deterministic method and the 2,475-year return period in the simplified performance-based procedures. These results suggest that the deterministic results could be used as an upper-bound in areas of high seismicity, but in areas of low seismicity, the deterministic analysis could be optional. Engineers performing analyses in areas of medium to high seismicity could choose to use a deterministic analysis as a "reality check" against the simplified performance-based results. If both deterministic and performance-based methods are considered, the *lower* result is the governing value. When deciding whether the deterministic or performance-based results should be accepted, engineers should apply the following rule: the *lower hazard* governs (i.e. lowest value of N_{req}, CSR%, P_L, and D_h, highest value of FS_L).

This rule may seem counter-intuitive, but the idea is not completely foreign—when developing a spectral acceleration design envelope, the lower of the deterministic and probabilistic values is the governing acceleration. Likewise, in a liquefaction hazard analysis, the lower value governs. If the deterministic value is lower than the performance-based value, the combination of multiple seismic sources in the performance-based analysis may suggest greater liquefaction hazard than would be caused by a single, nearby, governing fault. Therefore, the deterministic analysis provides a type of "reality check" against the performance-based analysis, and the deterministic results should be accepted. If the performance-based value is lower than the deterministic value, the nearby governing fault may have a significantly low likelihood of rupturing and achieving the 50th or 84th percentile ground motions. In this case, the deterministic results could be considered too extreme (especially for some projects which do not need to be designed to withstand such large events). Therefore, the performance-based results should be accepted as a representation of the more *likely* liquefaction hazard.

7.0 DEVELOPMENT OF THE SIMPLIFIED LIQUEFACTION ASSESSMENT TOOL

7.1 Overview

This section explains the components of the simplified liquefaction assessment tool and provides some guidance for how the tool should be used.

7.2 Description of Tool Components

7.2.1 Inputs

This section of the spreadsheet is the starting place of the analysis. Here, the user may select which analyses and options he or she would prefer and enter the soil profile information, mapped reference values, and other parameters which are necessary for the simplified performance-based procedure. At the bottom of the sheet, there is a section for deterministic inputs if the user would like to consider a deterministic analysis as well.

7.2.2 Map Help

This section shows an example of a $\log[D_H^{ref}]$ map and shows how to retrieve the mapped liquefaction loading value or lateral spread displacement value.

7.2.3 Simplified Performance-based Liquefaction Triggering

7.2.3.1 PB Liquefaction Initiation

This section of the spreadsheet shows the calculations for the simplified performance-based liquefaction initiation procedure. The Boulanger and Idriss (2012) model is simplified as derived in the Year 1 Quarter 1 report of this research. The Cetin et al. (2004) model is simplified as derived in the Mayfield et al. (2010) publication. This section also provides the calculations for correcting field SPT blow counts to values of $(N_1)_{60,cs}$. The user is not required to do anything on this page. This section is simply for reference if the engineer would like to see the calculation process.

7.2.3.2 Deterministic Liquefaction Initiation

This section of the spreadsheet calculates deterministic liquefaction initiation values. The formulas from the deterministic Idriss and Boulanger (2008) model and from the deterministic Cetin et al. (2004) model are used here. The user is not required to do anything on this page. This section is simply for reference if the engineer would like to see the calculation process.

7.2.4 Simplified Performance-based Lateral Spread Displacement

This portion of the spreadsheet determines the simplified and deterministic lateral spread displacements based on the Youd et al (2002) empirical model and the simplified procedure developed in this study. The deterministic and simplified equations can be seen on this page, and all lateral spread calculations are performed on this page. This sheet does not require any input from the user, the calculations are performed when the "Analyze" button on the input page is clicked. This section is to provide a reference to the engineer.

7.2.5 Final Summary

This section shows the final results of the analyses chosen on the *Inputs* tab. The format of this section is already set up for easy printing. The headers of each page are associated with the project information entered on the *Inputs* tab. The first page provides a summary of inputs from the *Inputs* tab to facilitate easy checking of the inputs. The following pages show the results of the analyses. To print only the pages with the user-specified analyses, return to the *Inputs* tab and click the "Print Final Summary" button. The print preview window will appear and show only the user-specified analyses.

7.2.6 References

This section provides references for the models used in this spreadsheet and further guidance for using this spreadsheet.

7.3 Suggested Simplified Procedure

The following sections describe the suggested simplified procedure for assessing liquefaction triggering hazard and lateral spread displacement.

7.3.1 Simplified Performance-based Liquefaction Triggering

1) Select an appropriate return period (T_R) for your project (this may depend on the intended use of the building, code requirements, etc.).
2) Retrieve the reference liquefaction loading value (i.e. N_{req}^{ref} or *CSR*%) from the map with the desired return period and model (i.e. Cetin et al, 2004 or Boulanger and Idriss, 2012). Note that provided N_{req}^{ref} maps are based on the Cetin et al. model and *CSR*% maps are based on the Boulanger and Idriss model.
3) Open the simplified performance-based liquefaction assessment tool (provided as part of this report). Enter the required soil profile information into the *Inputs* tab. Required values include depth to center of the sublayer, field SPT blowcount, unit weight (γ), fines content in percent, and thickness of each sublayer. An optional parameter is K_{DR}, a correction factor for age of sand deposits from Hayati and Andrus (2009). This value is not required, but may be used to increase the CRR of particular soil layers. Enter the hammer information, which is used for $(N_1)_{60,cs}$ corrections.
    a. Soil profile information can be entered in either SI or English customary units. Select the desired option by clicking the associated toggle above the soil profile table.
    b. Even though the zone of interest to the user may not include sublayers near the ground surface, all sublayers above the zone of interest must be included in the inputs tab so that the effective stress calculations will work properly. In other words, begin at the ground surface and include all sublayers down to the end of the zone of interest.
4) On the *Inputs* tab under "Analysis Selections", select the desired models and analyses. If the user wishes to use a deterministic analysis as an upper-bound to the performance-based results, the user should select the appropriate deterministic checkbox.

5) On the *Inputs* tab, enter liquefaction triggering parameters to be used in the simplified performance-based correction factors (derived in the Year 1 Quarter 1 report). The calculations will be performed in the spreadsheet automatically, but a few parameters must be provided by the user:

   a. *PGA*: Peak Ground Acceleration should be retrieved from the 2008 (or 1996, for Alaska) USGS Interactive Deaggregation website (http://geohazards.usgs.gov/deaggint/2008/) at the return period specified in step 1. Note that the website uses exceedance probabilities instead of return periods. Use Table 7-1 to convert return periods to exceedance probabilities.

Table 7-1. Conversions between Return Period and Exceedance Probability for use in the USGS interactive deaggregations website.

	Exceedance Probability	
Return Period	**Percent**	**Years**
475	10	50
1,039 (1,033)	2 (7)	21 (75)
2,475	2	50

   After entering the latitude and longitude of the site, exceedance probability, Spectral Period of 0.0 seconds, and $V_{s,30}$ of 760 m/s, retrieve the *PGA* from the output report. This value is necessary for estimating the F_{pga}. An example of where this number is located in the output report is provided in the *References* tab of the spreadsheet.

   b. F_{pga}: If the user checks the "Calculate F_{pga} automatically" checkbox, the spreadsheet will calculate F_{pga} according to the 2012 AASHTO code. However, this cannot be done if the Site Class is F (see notes about Site Class below), and therefore, the user must specify an F_{pga} value based on a site response analysis.

   c. M_w: The mean moment magnitude (M_w) is used to calculate the MSF correction factor as discussed in the Year 1 Quarter 1 report. The value for M_w is found in the same output report created to find the *PGA* value. An example of where this number is located in the output report is provided in the *References* tab of the spreadsheet.

d. $V_{s,12}$: The shear wave velocity in the upper 12m (40 ft) is only required when using the Cetin et al (2004) model. For further guidance in calculating this value, see the *References* tab of the spreadsheet.

e. Site Class: The site class is necessary for calculating the F_{pga}. Site class is determined based on soil type and soil properties. See the *References* tab of the spreadsheet for further help in determining site class.

6) On the *Inputs* tab under "Mapped Reference Values", enter the mapped values retrieved as part of step 2. At least one of the two parameters ($CSR(\%)^{ref}$ or $N_{req}{}^{ref}$) is necessary for analysis, but be aware of which model each of these parameters is associated with (see step 2). Also report the return period associated with the chosen map (this value will not be used in any calculations, but will be displayed on the final summary page for reference).

7) If the user wishes to use a deterministic analysis as an upper-bound to the performance-based results, the user should enter the deterministic values of *PGA*, M_w, and percentile of the *PGA* to be considered. This percentile value is used in the calculation of *CRR*, where the P_L value in the *CRR* equation is equal to (1 – percentile/100%) . The user must also specify a site class for the soil or provide a user-defined value for F_{pga}.

   a. Deterministic values of *PGA* and M_w should be assessed by an experienced individual with proper training in deterministic seismic hazard analysis (DSHA).

   b. It is suggested (as explained previously in this report) that a deterministic analysis should be considered when the engineer suspects that the project could benefit from a deterministic cap. In areas of low seismicity, this is likely unnecessary.

8) Several checkboxes are displayed near the top of the *Inputs* tab which allow the user to select which analyses (liquefaction initiation, settlement, lateral spread, or seismic slope stability), models (Cetin et al or Boulanger and Idriss), and options (P_L or FS_L) the user would like to consider. Select the desired analyses, models, and options before proceeding to the next step.

9) Once everything is correctly entered into the *Inputs* tab, click "Analyze". The calculations will be displayed on the *PB Liquefaction Initiation* and *Det. Liquefaction Initiation* tabs.
10) The *Final Summary* tab displays plots, tables and a summary of inputs in a printable format. The headers of these pages will reflect information such as company name, project name/number, date, etc. entered at the top of the *Inputs* tab.

7.3.2 Simplified Performance-based Lateral Spread Displacement

1) Select an appropriate return period (T_R) for your project (this may depend on the intended use of the building, code requirements, etc.).
2) Retrieve the logged reference lateral spread value (D_H^{ref}) from the map with the desired return period.
3) Open the simplified performance-based liquefaction hazard assessment tool (provided as part of this report). Enter the required soil profile information into the *Inputs* tab. Required values include T_{15} (cumulative thickness of sand or gravel layers with SPT blow counts less than 15), W or S (which are terms based on site geometry), D_{50} (the mean grain size of the T_{15} layers), and F_{15} (the fines content of the T_{15} layers).
   a. The user must choose whether the analysis is for the Free Face or Ground Slope conditions.
   b. Soil profile information can be entered in either SI or English customary units. Select the desired option by clicking the associated toggle above the soil profile table.
4) On the *Inputs* tab under "Analysis Selections", select the desired models and analyses. If the user wishes to use a deterministic analysis as an upper-bound to the performance-based results, the user should select the appropriate deterministic checkbox.
5) On the *Inputs* tab under "Mapped Reference Values", enter the mapped values retrieved as part of step 2. Also report the return period associated with the chosen map (this value will not be used in any calculations, but will be displayed on the final summary page for reference).
6) If the user wishes to use a deterministic analysis as an upper-bound to the performance-based results, the user should enter the deterministic values of M_w (moment magnitude

of fault), R (source-to-site distance), and percentile of the M_w to be considered. This percentile value is required for the deterministic calculations.

   a. Deterministic values of M_w and R should be assessed by an experienced individual with proper training in deterministic seismic hazard analysis (DSHA).
   b. It is suggested (as explained previously in this report) that a deterministic analysis should be considered when the engineer suspects that the project could benefit from a deterministic cap. In areas of low seismicity, this is likely unnecessary.

7) Several checkboxes are displayed near the top of the *Inputs* tab which allow the user to select which analyses (liquefaction initiation, settlement, lateral spread, or seismic slope stability), models (Cetin et al or Boulanger and Idriss), and options (P_L or FS_L) the user would like to consider. Select the desired analyses, models, and options before proceeding to the next step.
8) Once everything is correctly entered into the *Inputs* tab, click "Analyze". The calculations will be displayed on the *Lateral Spread* tab.
9) The *Final Summary* tab displays plots, tables and a summary of inputs in a printable format. The headers of these pages will reflect information such as company name, project name/number, date, etc. entered at the top of the *Inputs* tab.

7.4 Summary

This section introduced the simplified performance-based liquefaction assessment tool, described the various components and aspects of the tool, and provided step-by-step instructions for the user to use the tool. With this tool and description, the engineer will be able to use the simplified methods developed in the study without additional training or expertise.

8.0 CONCLUSIONS

8.1 Summary

The purpose of the research performed was to provide the benefit of the full performance-based probabilistic earthquake hazard analysis, without requiring special software, training, and experience. To accomplish this goal, simplified models of liquefaction triggering and lateral spread displacements were developed that reasonably approximate the results of full performance-based analyses. The objective of this report was to introduce the original models used to determine earthquake hazards (i.e. liquefaction triggering and lateral spread displacement), provide in-depth derivations that demonstrate the development of the simplified methods, validate the simplified models by performing a site-specific analysis for several different sites using the simplified and full models, determine sufficient grid spacings for the development of the liquefaction parameter maps, develop the liquefaction parameter maps for the targeted states at the 475, 1033, and 2475 year return periods, compare the results of the simplified methods against deterministic and pseudo-probabilistic procedures, and then introduce a tool for performing the calculations for the simplified methods.

8.2 Findings

8.2.1 Derivation of the Simplified Procedures

The derivations of the simplified liquefaction triggering and lateral spread displacement models show how to approximate a full performance-based analysis using simple calculations and mapped reference parameters. The simplified liquefaction triggering procedure is based on the Boulanger and Idriss (2012) probabilistic model while the simplified lateral spread displacement model is based on the Youd et al. (2002) empirical model.

8.2.2 Validation of the Simplified Procedures

Ten sites throughout the United States were analyzed using both the full and simplified probabilistic procedures for three different return periods: 475, 1033, and 2475 years. Both the

simplified liquefaction triggering method and the simplified lateral spread displacement models provided reasonable approximations of their respective full probabilistic methods. This shows that the simplified procedures derived in this report can be used to approximate the results of a full probabilistic procedure without the need for special software, training, and experience.

8.2.3 Evaluation of Grid Spacing

A grid spacing necessary to maintain accuracy in the interpolated results was found for the liquefaction triggering and lateral spread displacement models. These grid spacings resulted on average with a 5% difference between an interpolated value and the result if an analysis were performed at the same site. These grid spacings were very important in creating the grid of points that was used in the analysis.

8.2.4 Map Development

The liquefaction parameter maps were developed for each state by subdividing them into zones and assigning a grid spacing for each zone. The grid points were then generated in ArcMap based on this grid spacing. The points were analyzed using the specified performance-based analytical software (PBLiquefY, EZ-FRISK), then imported into ArcMap and converted to a Kriging raster that is then used to create a contour of the specific reference parameter.

8.2.5 Comparison with Deterministic Procedures

The results of this study show, for the 475 and 2475 year return periods for both the liquefaction initiation and lateral spread displacement, that deterministic methods severely over-predicted liquefaction hazard in areas of low seismicity. The deterministic results slightly over-predicted liquefaction hazards in areas of medium seismicity. And in areas of high seismicity the deterministic methods slightly under-predicted liquefaction hazard. These results suggest that the deterministic results could be used as an upper-bound in areas of high seismicity, but in areas of low seismicity, the deterministic analysis could be optional. Engineers performing analyses in areas of medium to high seismicity could choose to use a deterministic analysis as a "reality check" against the simplified performance-based results.

8.3 Limitations and Challenges

During the production of this report, a revised Boulanger and Idriss (2014) model was published. This revised model included a new definition of the *MSF* (as explained previously). Though this report discussed the derivation of the simplified performance-based procedure for both the updated Boulanger and Idriss (2014) model and the previous Boulanger and Idriss (2012) model, the 2012 version of the *MSF* was used throughout the report.

REFERENCES

Bartlett, S.F., and Youd, T.L. (1995). Empirical prediction of liquefaction-induced lateral spread. *J. Geotech. Eng.*, 121(4), 316-329.

Boulanger, R. W., and Idriss, I. M. (2012). Probabilistic standard penetration test-based liquefaction-triggering procedure. *J. Geotech. Geoenviron. Eng.*, 10.1061/(ASCE)GT.1943-5606.0000700, 1185–1195.

Boulanger, R. W., and Idriss, I. M. (2014). CPT and SPT based liquefaction triggering procedures. *Rep. UCD/CGM-14/01*, Dept. of Civil and Environmental Engineering, Univ. of California–Davis, Davis, CA.

Cetin, K. O., et al. (2004). Standard penetration test-based probabilistic and deterministic assessment of seismic soil liquefaction potential. *J. Geotech. Geoenviron. Eng*., 10.1061/(ASCE)1090-0241(2004)130:12(1314), 1314–1340.

Cornell, C.A., and Krawinkler, H. (2000). Progress and challenges in seismic performance assessment. *PEER News,* April, 1-3.Deierlein, G.G., Krawinkler, H., and Cornell, C.A. (2003). A framework for performance-based earthquake engineering, Proc., 2003 Pacific Conference on Earthquake Engineering.

Franke, K. and Wright, A. (2013) An Alternative Performance-Based Liquefaction Initiation Procedure for the Standard Penetration Test. *Geo-Congress 2013*, 10.1061/9780784412787.086, 846-849.

Franke, K.W. and Kramer, S.L. (2014). A procedure for the empirical evaluation of lateral spread displacement hazard curves. *J. Geotech. Geoenviron. Eng.*, ASCE, 140(1), 110-120.

Franke, K.W., Lingwall, B.N., Youd, T.L. (2014a). Sensitivity of empirical liquefaction assessment to seismic loading in areas of low seismicity and its implications for sustainability, Geo-Congress 2014 Technical Papers, p. 1284-1293.

Franke, K., Wright, A., and Ekstrom, L. (2014b). Comparative Study between Two Performance-Based Liquefaction Triggering Models for the Standard Penetration Test. *J. Geotech. Geoenviron. Eng.* , 10.1061/(ASCE)GT.1943-5606.0001094 , 04014010.

Franke, K.W., Wright, A.D., and Hatch, C.K. (2014c). PBLiquefY: A new analysis tool for the performance-based evaluation of liquefaction triggering. Proceedings, 10th National Conference on Earthquake Engineering, Paper No. 87, EERI, Oakland, CA.

Franke, K.W., Mayfield, R.T., and Wright, A.D. (2014d). Simplified uniform hazard analysis for bridges, *Transportation Research Record*, TRB, in press, Washington D.C.

Idriss, I.M., and Boulanger, R.W. (2008). *Soil liquefaction during earthquakes.* Monograph MNO-12, Earthquake Engineering Research Institute, Oakland, CA 261 pp.

Idriss, I. M., and Boulanger, R. W. (2010). SPT-based liquefaction triggering procedures. *Rep. UCD/CGM-10/02,* Dept. of Civil and Environmental Engineering, Univ. of California–Davis, Davis, CA.

Kramer, S.L. (2008). Evaluation of liquefaction hazards in Washington State. WSDOT Report WA-RD 668.1, 152 pp.

Kramer, S.K., Franke, K.W., Huang, Y.-M., and Baska, D. (2007). Performance-based evaluation of lateral spreading displacement. *Proceedings, 4th International Conference on Earthquake Geotechnical Engineering,* Paper No. 1208, Thessaloniki, Greece, June 2007.

Krawinkler, H. (2002). A general approach to seismic performance assessment, Proc., Int. Conf. on Advances and New Challenges in Earthquake Engineering Research, ICANCEER, Hong Kong.

Mayfield, R. T., Kramer, S. L., and Huang, Y.-M. (2010). Simplified approximation procedure for performance-based evaluation of liquefaction potential. *J. Geotech. Geoenviron. Eng*., 10.1061/(ASCE) GT.1943-5606.0000191, 140–150.

Petersen, Mark D., Frankel, Arthur D., Harmsen, Stephen C., Mueller, Charles S., Haller, Kathleen M., Wheeler, Russell L., Wesson, Robert L., Zeng, Yuehua, Boyd, Oliver S., Perkins, David M., Luco, Nicolas, Field, Edward H., Wills, Chris J., and Rukstales, Kenneth S. (2008). Documentation for the 2008 Update of the United States National Seismic Hazard Maps. Open-File Report 2008–1128, United States Geological Survey, Denver, CO: available at website: http://pubs.usgs.gov/of/2008/1128/.

Risk Engineering. (2013). EZ-FRISK, ver. 7.60. Boulder, Colorado.

Seed, H.B. (1979). Soil liquefaction and cyclic mobility evaluation for level ground during earthquakes. *J. Geotech. Eng. Div*., 105(GT2), p. 201-255.

Seed, H.B. and Idriss, I.M. (1971). Simplified procedure for evaluating soil liquefaction potential," *J. Soil Mech. and Found. Div*., 97(SM9), p. 1249-1273.

Seed, H.B. and Idriss, I.M. (1982). *Ground Motions and Soil Liquefaction During Earthquakes.* EERI, Oakland, CA, 134 pp.

Seed, H.B., Tokimatsu, K., Harder, L.F. Jr., and Chung, R. (1985). Influence of SPT procedures in soil liquefaction resistance evaluations, *J. Geotech. Eng*., 111(12), p. 1425-1445.

Stewart, J.P., Liu, A.H., and Choi, Y. (2003). Amplification factors for spectral acceleration in tectonically active regions. *Bull. Seismol. Soc. Am.,* 93(7): 332-352.

USGS. (2008). "USGS 2008 interactive deaggregation." https://geohazards.usgs.gov/deaggint/2008/ (March 26, 2014).

Youd, T.L., Hansen, C.M., and Bartlett, S.F. (2002). Revised multilinear regression equations for prediction of lateral spread displacement. *J. Geotech. Geoenviron. Eng.,* ASCE. 128(12), 1007-1017.

APPENDIX A: Supplementary Validation Data

The following tables are supplementary to the validation results of this report but are too lengthy to include in the body of the text. The values in Table A-1 are values used in the calculation of CSR^{site} for each of the ten cities in the study. The values of $\%CSR^{ref}$ were retrieved from the hazard-targeted liquefaction parameter maps created using PBLiquefY. The values of mean *M* and *PGA* were retrieved from the 2008 USGS deaggregation website. Values of F_{pga} were interpolated from AASHTO 2012 Table 3.10.3.2-1. Table A-2 displays the results of the simplified liquefaction triggering procedure while Table A-3 displays the results of the full probabilistic liquefaction triggering procedure.

Depth conversions: 2.5 m (8.20 ft), 3.5 m (11.48 ft), 4.5 m (14.76 ft), 5.5 m (18.04 ft), 6.5 m (21.33 ft), 7.5 m (24.61 ft), 8.5 m (27.89 ft), 9.5 m (31.17 ft), 10.5 m (34.45 ft), 11.5 m (37.73 ft)

Table A-1 Parameters Used in Simplified Liquefaction Triggering Procedure

Location	T_R = 1033				T_R = 475				T_R = 2475			
	$\%CSR^{ref}$	Mean *M*	*PGA*	F_{pga}	$\%CSR^{ref}$	Mean *M*	*PGA*	F_{pga}	$\%CSR^{ref}$	Mean *M*	*PGA*	F_{pga}
Butte	10.37	6.03	0.1206	1.559	7.434	6.03	0.0834	1.600	14.671	6.05	0.1785	1.443
Charleston	33.46	6.87	0.3680	1.132	12.750	6.61	0.1513	1.497	66.794	7.00	0.7287	1.000
Eureka	109.64	7.40	0.9662	1.000	67.819	7.33	0.6154	1.000	162.159	7.45	1.4004	1.000
Memphis	34.73	7.19	0.3346	1.165	14.811	6.98	0.1604	1.479	61.245	7.24	0.5711	1.000
Portland	37.08	7.29	0.2980	1.204	23.485	7.24	0.1990	1.402	55.225	7.31	0.4366	1.063
Salt Lake City	38.09	6.84	0.4030	1.097	20.724	6.75	0.2126	1.375	62.332	6.90	0.6717	1.000
San Francisco	68.49	7.38	0.5685	1.000	50.860	7.31	0.4394	1.061	90.113	7.44	0.7254	1.000
San Jose	57.89	6.67	0.5627	1.000	45.322	6.66	0.4560	1.044	72.345	6.66	0.6911	1.000
Santa Monica	52.70	6.79	0.5372	1.000	37.984	6.74	0.3852	1.115	71.788	6.84	0.7415	1.000
Seattle	47.29	6.82	0.4444	1.056	32.213	6.75	0.3110	1.189	67.879	6.88	0.6432	1.000

Table A-2 Results from Simplified Liquefaction Triggering Procedure

			T_R = 1033 Simple PB (Idriss & Boulanger)				T_R = 475 Simple PB (Idriss & Boulanger)				T_R = 2475 Simple PB (Idriss & Boulanger)			
	Depth (m)	$N_{1,60,cs}$ site	N_{req}	$\%CSR^{site}$	FS_L	P_L	N_{req}	$\%CSR^{site}$	FS_L	P_L	N_{req}	$\%CSR^{site}$	FS_L	P_L
Butte	2.5	13.78	4.568	9.528	1.747	0.022	1.000	7.434	2.375	0.002	8.740	12.467	1.335	0.148
	3.5	15.62	6.554	10.867	1.691	0.029	2.029	7.994	2.299	0.001	10.965	14.223	1.292	0.177
	4.5	16.95	7.780	11.749	1.681	0.030	3.144	8.642	2.285	0.001	12.344	15.377	1.284	0.183
	5.5	19.87	8.522	12.301	1.892	0.011	3.811	9.049	2.572	0.000	13.178	16.104	1.445	0.092
	6.5	21.47	9.030	12.688	2.021	0.006	4.266	9.335	2.748	0.000	13.749	16.615	1.544	0.059
	7.5	23.12	9.356	12.940	2.213	0.002	4.553	9.518	3.008	0.000	14.111	16.945	1.690	0.029
	8.5	24.83	9.553	13.094	2.487	0.001	4.729	9.633	3.381	0.000	14.336	17.153	1.899	0.010
	9.5	27.79	9.685	13.197	3.238	0.000	4.846	9.709	4.401	0.000	14.484	17.291	2.471	0.001
	10.5	29.76	9.772	13.265	4.036	0.000	4.921	9.757	5.486	0.000	14.581	17.382	3.080	0.000
	11.5	31.81	9.848	13.325	5.346	0.000	4.990	9.803	7.268	0.000	14.669	17.465	4.079	0.000
Charleston	2.5	13.78	18.765	21.832	0.762	0.836	6.850	11.076	1.503	0.071	26.706	38.365	0.434	0.999
	3.5	15.62	21.090	25.043	0.734	0.868	9.023	12.683	1.449	0.090	28.077	44.043	0.417	0.999
	4.5	16.95	22.393	27.241	0.725	0.877	10.406	13.769	1.434	0.097	28.842	47.955	0.412	0.999
	5.5	19.87	23.158	28.716	0.810	0.776	11.284	14.485	1.606	0.044	29.299	50.607	0.460	0.997
	6.5	21.47	23.688	29.836	0.860	0.708	11.919	15.016	1.708	0.027	29.620	52.638	0.487	0.995
	7.5	23.12	24.052	30.657	0.934	0.597	12.362	15.393	1.860	0.013	29.846	54.151	0.529	0.989
	8.5	24.83	24.312	31.273	1.041	0.442	12.676	15.664	2.079	0.004	30.011	55.306	0.589	0.972
	9.5	27.79	24.519	31.781	1.344	0.143	12.921	15.878	2.691	0.000	30.145	56.276	0.759	0.840
	10.5	29.76	24.691	32.215	1.662	0.033	13.120	16.053	3.335	0.000	30.259	57.122	0.937	0.593
	11.5	31.81	24.855	32.643	2.182	0.002	13.310	16.221	4.392	0.000	30.368	57.957	1.229	0.228
Eureka	2.5	13.78	30.898	62.315	0.267	1.000	26.775	38.616	0.431	0.999	33.360	92.041	0.181	1.000
	3.5	15.62	31.855	71.732	0.256	1.000	28.158	44.432	0.414	0.999	34.124	105.987	0.173	1.000
	4.5	16.95	32.412	78.334	0.252	1.000	28.938	48.494	0.407	0.999	34.576	115.783	0.171	1.000
	5.5	19.87	32.757	82.929	0.281	1.000	29.413	51.310	0.454	0.998	34.860	122.624	0.190	1.000
	6.5	21.47	33.008	86.554	0.296	1.000	29.754	53.520	0.479	0.996	35.069	128.038	0.200	1.000
	7.5	23.12	33.193	89.368	0.320	1.000	30.000	55.226	0.518	0.991	35.223	132.260	0.216	1.000
	8.5	24.83	33.334	91.620	0.355	1.000	30.187	56.581	0.576	0.977	35.342	135.660	0.240	1.000
	9.5	27.79	33.453	93.596	0.457	0.998	30.343	57.761	0.740	0.862	35.443	138.653	0.308	1.000
	10.5	29.76	33.559	95.388	0.561	0.981	30.479	58.825	0.910	0.633	35.533	141.378	0.379	1.000
	11.5	31.81	33.661	97.183	0.733	0.869	30.611	59.888	1.190	0.265	35.620	144.113	0.494	0.995
Memphis	2.5	13.78	19.764	23.120	0.720	0.882	8.898	12.588	1.322	0.157	25.676	34.955	0.476	0.996
	3.5	15.62	22.022	26.578	0.692	0.909	11.242	14.450	1.272	0.193	27.188	40.195	0.457	0.998
	4.5	16.95	23.285	28.978	0.681	0.917	12.754	15.731	1.255	0.206	28.034	43.841	0.450	0.998
	5.5	19.87	24.039	30.628	0.760	0.839	13.730	16.598	1.402	0.111	28.543	46.355	0.502	0.994
	6.5	21.47	24.570	31.908	0.804	0.785	14.452	17.261	1.486	0.076	28.906	48.315	0.531	0.989
	7.5	23.12	24.946	32.882	0.871	0.691	14.974	17.755	1.613	0.042	29.166	49.812	0.575	0.977
	8.5	24.83	25.225	33.645	0.968	0.547	15.361	18.129	1.796	0.017	29.361	50.991	0.639	0.947
	9.5	27.79	25.454	34.299	1.246	0.214	15.681	18.444	2.317	0.001	29.523	52.009	0.822	0.761
	10.5	29.76	25.652	34.882	1.535	0.061	15.955	18.718	2.860	0.000	29.663	52.918	1.012	0.483
	11.5	31.81	25.841	35.461	2.009	0.006	16.220	18.986	3.752	0.000	29.799	53.825	1.324	0.156

			T_R = 1033 Simple PB (Idriss & Boulanger)				T_R = 475 Simple PB (Idriss & Boulanger)				T_R = 2475 Simple PB (Idriss & Boulanger)			
	Depth (m)	$N_{1,60,cs}$ site	N_{req}	$\%CSR^{site}$	FS_L	P_L	N_{req}	$\%CSR^{site}$	FS_L	P_L	N_{req}	$\%CSR^{site}$	FS_L	P_L
Portland	2.5	13.78	21.346	25.447	0.654	0.937	16.028	18.792	0.886	0.669	25.152	33.443	0.498	0.994
	3.5	15.62	23.426	29.272	0.628	0.954	18.582	21.609	0.851	0.721	26.736	38.474	0.478	0.996
	4.5	16.95	24.583	31.940	0.618	0.959	20.091	23.570	0.838	0.739	27.621	41.987	0.470	0.997
	5.5	19.87	25.274	33.783	0.689	0.911	21.011	24.920	0.934	0.598	28.155	44.417	0.524	0.990
	6.5	21.47	25.765	35.227	0.728	0.874	21.668	25.975	0.987	0.518	28.537	46.324	0.554	0.984
	7.5	23.12	26.116	36.336	0.788	0.805	22.137	26.780	1.069	0.405	28.812	47.790	0.599	0.968
	8.5	24.83	26.379	37.213	0.875	0.685	22.486	27.413	1.188	0.267	29.019	48.953	0.665	0.929
	9.5	27.79	26.597	37.974	1.125	0.335	22.775	27.960	1.528	0.063	29.192	49.965	0.855	0.714
	10.5	29.76	26.786	38.657	1.385	0.120	23.025	28.449	1.882	0.011	29.342	50.874	1.052	0.427
	11.5	31.81	26.968	39.341	1.811	0.016	23.265	28.937	2.462	0.001	29.488	51.785	1.376	0.125
Salt Lake City	2.5	13.78	20.465	24.103	0.691	0.909	13.594	16.475	1.010	0.485	25.979	35.895	0.464	0.997
	3.5	15.62	22.608	27.641	0.665	0.930	16.118	18.883	0.973	0.539	27.431	41.183	0.446	0.998
	4.5	16.95	23.789	30.059	0.657	0.935	17.651	20.521	0.962	0.555	28.235	44.806	0.441	0.998
	5.5	19.87	24.479	31.680	0.735	0.867	18.585	21.613	1.077	0.395	28.712	47.246	0.493	0.995
	6.5	21.47	24.955	32.906	0.779	0.816	19.242	22.432	1.143	0.314	29.044	49.099	0.522	0.990
	7.5	23.12	25.282	33.804	0.847	0.726	19.694	23.025	1.244	0.216	29.275	50.466	0.567	0.980
	8.5	24.83	25.513	34.472	0.945	0.581	20.012	23.460	1.388	0.118	29.442	51.493	0.632	0.951
	9.5	27.79	25.698	35.022	1.220	0.236	20.263	23.812	1.794	0.017	29.576	52.346	0.816	0.768
	10.5	29.76	25.851	35.491	1.508	0.069	20.470	24.109	2.220	0.002	29.687	53.078	1.009	0.488
	11.5	31.81	25.996	35.950	1.982	0.007	20.667	24.399	2.920	0.000	29.795	53.798	1.324	0.155
San Francisco	2.5	13.78	26.864	38.946	0.427	0.999	24.088	30.742	0.541	0.987	29.389	51.161	0.325	1.000
	3.5	15.62	28.240	44.826	0.410	0.999	25.811	35.367	0.520	0.991	30.490	58.910	0.312	1.000
	4.5	16.95	29.017	48.943	0.403	0.999	26.769	38.596	0.512	0.992	31.124	64.350	0.307	1.000
	5.5	19.87	29.491	51.807	0.449	0.998	27.346	40.831	0.570	0.979	31.516	68.146	0.341	1.000
	6.5	21.47	29.833	54.061	0.474	0.996	27.757	42.583	0.602	0.966	31.802	71.150	0.360	1.000
	7.5	23.12	30.081	55.810	0.513	0.992	28.053	43.931	0.652	0.939	32.011	73.488	0.390	1.000
	8.5	24.83	30.270	57.205	0.569	0.979	28.275	45.000	0.724	0.878	32.171	75.370	0.432	0.999
	9.5	27.79	30.429	58.427	0.731	0.871	28.460	45.929	0.930	0.603	32.307	77.025	0.555	0.983
	10.5	29.76	30.568	59.533	0.899	0.649	28.622	46.766	1.145	0.313	32.427	78.532	0.682	0.917
	11.5	31.81	30.702	60.642	1.175	0.280	28.777	47.602	1.497	0.073	32.544	80.043	0.890	0.663
San Jose	2.5	13.78	25.188	33.542	0.496	0.994	22.491	27.421	0.607	0.964	27.607	41.926	0.397	1.000
	3.5	15.62	26.722	38.422	0.478	0.996	24.368	31.409	0.585	0.973	28.854	48.023	0.383	1.000
	4.5	16.95	27.562	41.734	0.473	0.997	25.390	34.113	0.579	0.976	29.546	52.158	0.379	1.000
	5.5	19.87	28.051	43.924	0.530	0.989	25.981	35.900	0.648	0.941	29.953	54.892	0.424	0.999
	6.5	21.47	28.387	45.558	0.563	0.981	26.385	37.232	0.689	0.911	30.233	56.928	0.451	0.998
	7.5	23.12	28.614	46.728	0.613	0.961	26.656	38.185	0.750	0.851	30.423	58.385	0.490	0.995
	8.5	24.83	28.773	47.576	0.685	0.914	26.845	38.875	0.838	0.739	30.556	59.438	0.548	0.985
	9.5	27.79	28.895	48.252	0.886	0.670	26.991	39.425	1.084	0.386	30.659	60.278	0.709	0.893
	10.5	29.76	28.995	48.814	1.097	0.370	27.108	39.880	1.342	0.144	30.742	60.975	0.878	0.681
	11.5	31.81	29.089	49.359	1.443	0.093	27.220	40.320	1.767	0.020	30.821	61.649	1.156	0.301

			T_R = 1033 Simple PB (Idriss & Boulanger)				T_R = 475 Simple PB (Idriss & Boulanger)				T_R = 2475 Simple PB (Idriss & Boulanger)			
	Depth (m)	$N_{1,60,cs}$ site	N_{req}	$\%CSR^{site}$	FS_L	P_L	N_{req}	$\%CSR^{site}$	FS_L	P_L	N_{req}	$\%CSR^{site}$	FS_L	P_L
Santa Monica	2.5	13.78	23.956	30.437	0.547	0.985	20.730	24.493	0.680	0.918	27.485	41.406	0.402	0.999
	3.5	15.62	25.656	34.894	0.527	0.990	22.832	28.070	0.655	0.937	28.756	47.486	0.387	1.000
	4.5	16.95	26.586	37.933	0.521	0.991	23.985	30.504	0.647	0.942	29.465	51.641	0.382	1.000
	5.5	19.87	27.130	39.964	0.582	0.975	24.655	32.124	0.724	0.878	29.886	54.427	0.428	0.999
	6.5	21.47	27.505	41.493	0.618	0.959	25.114	33.338	0.769	0.828	30.180	56.534	0.454	0.998
	7.5	23.12	27.762	42.606	0.672	0.924	25.426	34.217	0.837	0.740	30.384	58.076	0.493	0.995
	8.5	24.83	27.944	43.427	0.750	0.851	25.644	34.860	0.934	0.597	30.529	59.225	0.550	0.985
	9.5	27.79	28.088	44.098	0.969	0.545	25.816	35.382	1.208	0.248	30.645	60.169	0.710	0.892
	10.5	29.76	28.207	44.666	1.199	0.257	25.955	35.818	1.495	0.073	30.742	60.973	0.878	0.681
	11.5	31.81	28.320	45.220	1.575	0.050	26.088	36.244	1.966	0.007	30.835	61.763	1.153	0.303
Seattle	2.5	13.78	23.208	28.820	0.578	0.976	19.016	22.145	0.752	0.849	26.908	39.111	0.426	0.999
	3.5	15.62	25.007	33.047	0.556	0.983	21.304	25.380	0.724	0.878	28.247	44.864	0.410	0.999
	4.5	16.95	25.991	35.934	0.550	0.985	22.577	27.583	0.716	0.886	28.993	48.806	0.405	0.999
	5.5	19.87	26.566	37.864	0.615	0.961	23.320	29.050	0.801	0.788	29.436	51.455	0.452	0.998
	6.5	21.47	26.964	39.323	0.652	0.939	23.830	30.151	0.851	0.720	29.745	53.465	0.480	0.996
	7.5	23.12	27.237	40.389	0.709	0.893	24.176	30.948	0.925	0.611	29.960	54.942	0.521	0.991
	8.5	24.83	27.431	41.180	0.791	0.801	24.419	31.533	1.033	0.454	30.114	56.050	0.581	0.975
	9.5	27.79	27.584	41.828	1.022	0.469	24.610	32.008	1.335	0.148	30.238	56.967	0.750	0.850
	10.5	29.76	27.711	42.380	1.263	0.200	24.765	32.406	1.652	0.035	30.342	57.752	0.927	0.608
	11.5	31.81	27.833	42.920	1.660	0.034	24.913	32.795	2.172	0.003	30.441	58.524	1.217	0.239

Table A-3 Results from Full Probabilistic Liquefaction Triggering Procedure

			T_R = 1033 Full PB (Idriss & Boulanger)				T_R = 475 Full PB (Idriss & Boulanger)				T_R = 2475 Full PB (Idriss & Boulanger)			
	Depth (m)	$N_{1,60,cs}$ site	N_{req}	$\%CSR^{site}$	FS_L	P_L	N_{req}	$\%CSR^{site}$	FS_L	P_L	N_{req}	$\%CSR^{site}$	FS_L	P_L
Butte	2.5	13.78	4.38	9.408	1.77	0.020	1	7.434	2.24	0.002	8.89	12.581	1.32	0.156
	3.5	15.62	6.29	10.682	1.72	0.025	1.62	7.767	2.37	0.001	11.09	14.325	1.28	0.184
	4.5	16.95	7.47	11.522	1.72	0.026	2.65	8.350	2.37	0.001	12.47	15.486	1.28	0.190
	5.5	19.87	8.21	12.067	1.93	0.009	3.29	8.730	2.67	0.000	13.36	16.266	1.43	0.098
	6.5	21.47	8.68	12.421	2.07	0.004	3.68	8.968	2.86	0.000	13.91	16.761	1.53	0.062
	7.5	23.12	8.94	12.619	2.27	0.002	3.88	9.092	3.15	0.000	14.27	17.092	1.68	0.031
	8.5	24.83	9.07	12.719	2.56	0.000	3.96	9.142	3.56	0.000	14.46	17.269	1.89	0.011
	9.5	27.79	9.09	12.735	3.36	0.000	3.95	9.136	4.68	0.000	14.52	17.325	2.47	0.001
	10.5	29.76	9.02	12.681	4.22	0.000	3.87	9.086	5.89	0.000	14.48	17.287	3.10	0.000
	11.5	31.81	8.9	12.589	5.66	0.000	3.73	8.999	7.92	0.000	14.37	17.185	4.15	0.000
Charleston	2.5	13.78	19.25	22.443	0.74	0.860	6.38	10.745	1.55	0.057	26.94	39.232	0.42	0.999
	3.5	15.62	21.54	25.762	0.71	0.889	8.39	12.202	1.51	0.070	28.37	45.472	0.40	0.999
	4.5	16.95	22.85	28.104	0.70	0.899	9.63	13.154	1.50	0.071	29.2	50.012	0.39	1.000
	5.5	19.87	23.68	29.819	0.78	0.815	10.42	13.781	1.69	0.029	29.75	53.497	0.44	0.999
	6.5	21.47	24.23	31.076	0.83	0.756	10.9	14.170	1.81	0.016	30.13	56.163	0.46	0.998
	7.5	23.12	24.6	31.984	0.89	0.655	11.18	14.399	1.99	0.007	30.41	58.281	0.49	0.995
	8.5	24.83	24.86	32.654	1.00	0.504	11.3	14.498	2.25	0.002	30.61	59.879	0.54	0.986
	9.5	27.79	25.03	33.108	1.29	0.179	11.31	14.507	2.95	0.000	30.76	61.127	0.70	0.902
	10.5	29.76	25.13	33.381	1.60	0.044	11.22	14.432	3.71	0.000	30.86	61.984	0.86	0.702
	11.5	31.81	25.19	33.547	2.12	0.003	11.06	14.300	4.98	0.000	30.94	62.684	1.14	0.322
Eureka	2.5	13.78	30.81	61.553	0.27	1.000	27.15	40.044	0.42	0.999	33.2	89.482	0.19	1.000
	3.5	15.62	31.88	72.010	0.26	1.000	28.59	46.600	0.39	1.000	34.08	105.096	0.18	1.000
	4.5	16.95	32.55	80.128	0.25	1.000	29.44	51.481	0.38	1.000	34.66	117.738	0.17	1.000
	5.5	19.87	32.98	86.133	0.27	1.000	30	55.225	0.42	0.999	35.02	126.741	0.18	1.000
	6.5	21.47	33.33	91.557	0.28	1.000	30.4	58.203	0.44	0.998	35.34	135.607	0.19	1.000
	7.5	23.12	33.58	95.759	0.30	1.000	30.7	60.622	0.47	0.997	35.58	142.853	0.20	1.000
	8.5	24.83	33.78	99.337	0.33	1.000	30.93	62.596	0.52	0.991	35.75	148.324	0.22	1.000
	9.5	27.79	33.93	102.156	0.42	0.999	31.11	64.217	0.67	0.929	35.89	153.055	0.28	1.000
	10.5	29.76	34.07	104.896	0.51	0.992	31.25	65.527	0.82	0.767	36.01	157.281	0.34	1.000
	11.5	31.81	34.18	107.127	0.67	0.930	31.36	66.588	1.07	0.404	36.13	161.673	0.44	0.998
Memphis	2.5	13.78	20.09	23.568	0.71	0.895	8.43	12.232	1.36	0.133	26.17	36.513	0.46	0.998
	3.5	15.62	22.35	27.163	0.68	0.921	10.62	13.942	1.32	0.159	27.73	42.462	0.43	0.999
	4.5	16.95	23.66	29.775	0.66	0.931	11.99	15.076	1.31	0.165	28.64	46.863	0.42	0.999
	5.5	19.87	24.5	31.733	0.73	0.869	12.9	15.859	1.47	0.083	29.24	50.252	0.46	0.997
	6.5	21.47	25.08	33.244	0.77	0.826	13.49	16.382	1.57	0.053	29.67	52.963	0.48	0.996
	7.5	23.12	25.49	34.403	0.83	0.746	13.87	16.725	1.71	0.026	29.98	55.083	0.52	0.991
	8.5	24.83	25.8	35.334	0.92	0.616	14.08	16.917	1.93	0.009	30.23	56.904	0.57	0.978
	9.5	27.79	26.02	36.025	1.19	0.269	14.18	17.009	2.51	0.000	30.43	58.437	0.73	0.871
	10.5	29.76	26.18	36.546	1.46	0.084	14.17	17.000	3.15	0.000	30.58	59.634	0.90	0.652
	11.5	31.81	26.3	36.946	1.93	0.009	14.1	16.935	4.21	0.000	30.69	60.539	1.18	0.278

			T_R = 1033 Full PB (Idriss & Boulanger)				T_R = 475 Full PB (Idriss & Boulanger)				T_R = 2475 Full PB (Idriss & Boulanger)			
	Depth (m)	$N_{1,60,cs}$ site	N_{req}	$\%CSR^{site}$	FS_L	P_L	N_{req}	$\%CSR^{site}$	FS_L	P_L	N_{req}	$\%CSR^{site}$	FS_L	P_L
Portland	2.5	13.78	21.9	26.367	0.63	0.952	15.62	18.383	0.91	0.640	25.97	35.866	0.46	0.997
	3.5	15.62	24.02	30.584	0.60	0.967	18.2	21.153	0.87	0.694	27.61	41.939	0.44	0.999
	4.5	16.95	25.27	33.771	0.58	0.974	19.78	23.142	0.85	0.717	28.59	46.600	0.42	0.999
	5.5	19.87	26.09	36.251	0.64	0.945	20.82	24.628	0.94	0.581	29.25	50.312	0.46	0.997
	6.5	21.47	26.68	38.271	0.67	0.926	21.56	25.795	0.99	0.508	29.74	53.429	0.48	0.996
	7.5	23.12	27.13	39.965	0.72	0.886	22.09	26.698	1.07	0.400	30.11	56.017	0.51	0.992
	8.5	24.83	27.48	41.387	0.79	0.806	22.48	27.402	1.19	0.266	30.43	58.437	0.56	0.983
	9.5	27.79	27.76	42.595	1.00	0.495	22.77	27.949	1.53	0.063	30.69	60.539	0.71	0.896
	10.5	29.76	27.99	43.638	1.23	0.230	22.99	28.379	1.89	0.011	30.89	62.245	0.86	0.707
	11.5	31.81	28.18	44.537	1.60	0.045	23.15	28.701	2.48	0.001	31.08	63.942	1.11	0.348
Salt Lake City	2.5	13.78	21.06	24.996	0.67	0.929	13.29	16.203	1.03	0.461	26.28	36.878	0.45	0.998
	3.5	15.62	23.18	28.762	0.64	0.947	15.77	18.532	0.99	0.512	27.78	42.684	0.43	0.999
	4.5	16.95	24.38	31.438	0.63	0.953	17.29	20.120	0.98	0.527	28.65	46.916	0.42	0.999
	5.5	19.87	25.13	33.381	0.70	0.904	18.28	21.247	1.10	0.371	29.21	50.072	0.46	0.997
	6.5	21.47	25.65	34.877	0.74	0.866	18.94	22.050	1.16	0.293	29.6	52.504	0.49	0.995
	7.5	23.12	25.99	35.930	0.80	0.794	19.38	22.611	1.27	0.197	29.87	54.314	0.53	0.990
	8.5	24.83	26.24	36.745	0.89	0.668	19.66	22.981	1.42	0.104	30.07	55.727	0.58	0.974
	9.5	27.79	26.41	37.320	1.15	0.313	19.83	23.210	1.84	0.014	30.22	56.829	0.75	0.848
	10.5	29.76	26.52	37.702	1.42	0.103	19.9	23.305	2.30	0.001	30.33	57.662	0.93	0.606
	11.5	31.81	26.58	37.913	1.88	0.011	19.91	23.319	3.06	0.000	30.39	58.125	1.23	0.231
San Francisco	2.5	13.78	27.22	40.322	0.41	0.999	24.51	31.758	0.52	0.990	29.39	51.169	0.33	1.000
	3.5	15.62	28.66	46.969	0.39	1.000	26.25	36.778	0.50	0.994	30.6	59.797	0.31	1.000
	4.5	16.95	29.5	51.861	0.38	1.000	27.26	40.482	0.49	0.995	31.32	66.199	0.30	1.000
	5.5	19.87	30.04	55.511	0.42	0.999	27.91	43.270	0.54	0.987	31.81	71.239	0.33	1.000
	6.5	21.47	30.47	58.752	0.44	0.999	28.38	45.522	0.56	0.981	32.16	75.235	0.34	1.000
	7.5	23.12	30.76	61.127	0.47	0.997	28.71	47.237	0.61	0.965	32.46	78.955	0.36	1.000
	8.5	24.83	30.97	62.950	0.52	0.991	28.95	48.560	0.67	0.925	32.67	81.736	0.40	1.000
	9.5	27.79	31.16	64.680	0.66	0.933	29.15	49.716	0.86	0.708	32.82	83.819	0.51	0.993
	10.5	29.76	31.31	66.102	0.81	0.777	29.3	50.615	1.06	0.420	32.94	85.545	0.63	0.955
	11.5	31.81	31.43	67.278	1.06	0.418	29.41	51.294	1.39	0.118	33.04	87.027	0.82	0.765
San Jose	2.5	13.78	25.67	34.937	0.48	0.996	23	28.399	0.59	0.973	27.74	42.506	0.39	1.000
	3.5	15.62	27.25	40.442	0.45	0.998	24.89	32.734	0.56	0.981	29.08	49.306	0.37	1.000
	4.5	16.95	28.16	44.441	0.44	0.998	25.95	35.803	0.55	0.984	29.88	54.383	0.36	1.000
	5.5	19.87	28.75	47.453	0.49	0.995	26.64	38.127	0.61	0.963	30.44	58.516	0.40	1.000
	6.5	21.47	29.15	49.716	0.52	0.992	27.09	39.809	0.64	0.944	30.79	61.382	0.42	0.999
	7.5	23.12	29.46	51.607	0.55	0.983	27.41	41.095	0.70	0.904	31.04	63.578	0.45	0.998
	8.5	24.83	29.67	52.963	0.62	0.960	27.63	42.026	0.77	0.821	31.28	65.814	0.50	0.994
	9.5	27.79	29.82	53.971	0.79	0.800	27.78	42.684	1.00	0.498	31.45	67.478	0.63	0.950
	10.5	29.76	29.92	54.662	0.98	0.530	27.88	43.133	1.24	0.218	31.57	68.694	0.78	0.816
	11.5	31.81	29.99	55.154	1.29	0.178	27.93	43.362	1.64	0.037	31.65	69.526	1.03	0.465

			T_R = 1033 Full PB (Idriss & Boulanger)				T_R = 475 Full PB (Idriss & Boulanger)				T_R = 2475 Full PB (Idriss & Boulanger)			
	Depth (m)	$N_{1,60,cs}$ site	N_{req}	$\%CSR^{site}$	FS_L	P_L	N_{req}	$\%CSR^{site}$	FS_L	P_L	N_{req}	$\%CSR^{site}$	FS_L	P_L
Santa Monica	2.5	13.78	24.77	32.419	0.51	0.992	21.24	25.278	0.66	0.934	27.6	41.896	0.40	1.000
	3.5	15.62	26.46	37.492	0.49	0.995	23.34	29.092	0.63	0.951	28.94	48.504	0.38	1.000
	4.5	16.95	27.43	41.178	0.48	0.996	24.53	31.808	0.62	0.957	29.75	53.497	0.37	1.000
	5.5	19.87	28.02	43.778	0.53	0.989	25.28	33.799	0.69	0.911	30.28	57.281	0.41	0.999
	6.5	21.47	28.47	45.978	0.56	0.982	25.78	35.272	0.73	0.875	30.65	60.207	0.43	0.999
	7.5	23.12	28.76	47.507	0.60	0.966	26.13	36.382	0.79	0.806	30.89	62.245	0.46	0.997
	8.5	24.83	28.97	48.674	0.67	0.927	26.38	37.217	0.88	0.685	31.08	63.942	0.51	0.993
	9.5	27.79	29.13	49.598	0.86	0.705	26.55	37.807	1.13	0.329	31.24	65.432	0.65	0.938
	10.5	29.76	29.24	50.252	1.06	0.410	26.65	38.163	1.40	0.111	31.35	66.490	0.81	0.783
	11.5	31.81	29.32	50.737	1.40	0.110	26.71	38.379	1.86	0.013	31.43	67.278	1.06	0.418
Seattle	2.5	13.78	24.06	30.676	0.54	0.986	19.42	22.663	0.73	0.867	27.4	41.053	0.41	0.999
	3.5	15.62	25.87	35.551	0.52	0.991	21.72	26.061	0.71	0.896	28.82	47.835	0.38	1.000
	4.5	16.95	26.92	39.157	0.50	0.993	23.04	28.479	0.69	0.907	29.67	52.963	0.37	1.000
	5.5	19.87	27.61	41.939	0.55	0.983	23.88	30.264	0.77	0.829	30.24	56.979	0.41	0.999
	6.5	21.47	28.09	44.107	0.58	0.975	24.45	31.609	0.81	0.775	30.66	60.290	0.43	0.999
	7.5	23.12	28.45	45.876	0.62	0.956	24.84	32.602	0.88	0.680	30.96	62.861	0.46	0.998
	8.5	24.83	28.72	47.291	0.69	0.911	25.11	33.326	0.98	0.533	31.22	65.243	0.50	0.994
	9.5	27.79	28.92	48.391	0.88	0.673	25.3	33.856	1.26	0.200	31.43	67.278	0.64	0.949
	10.5	29.76	29.09	49.364	1.08	0.385	25.43	34.228	1.56	0.053	31.6	69.004	0.78	0.820
	11.5	31.81	29.22	50.132	1.42	0.102	25.5	34.432	2.07	0.004	31.73	70.374	1.01	0.482

APPENDIX B: Sample Liquefaction Loading Maps

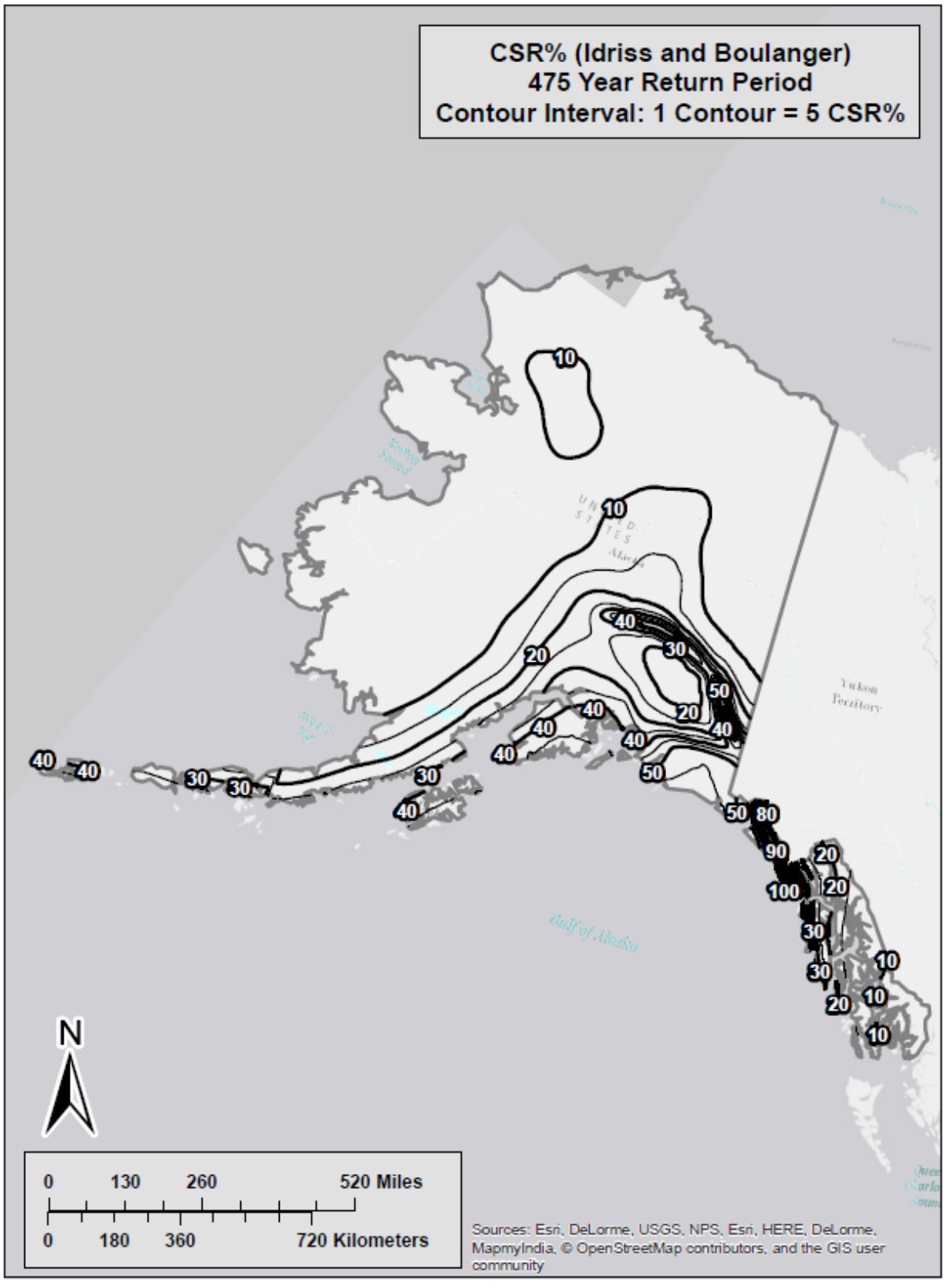

Figure B-1 Liquefaction Triggering ($CSR\%^{ref}$) Map for Alaska (T_r = 475)

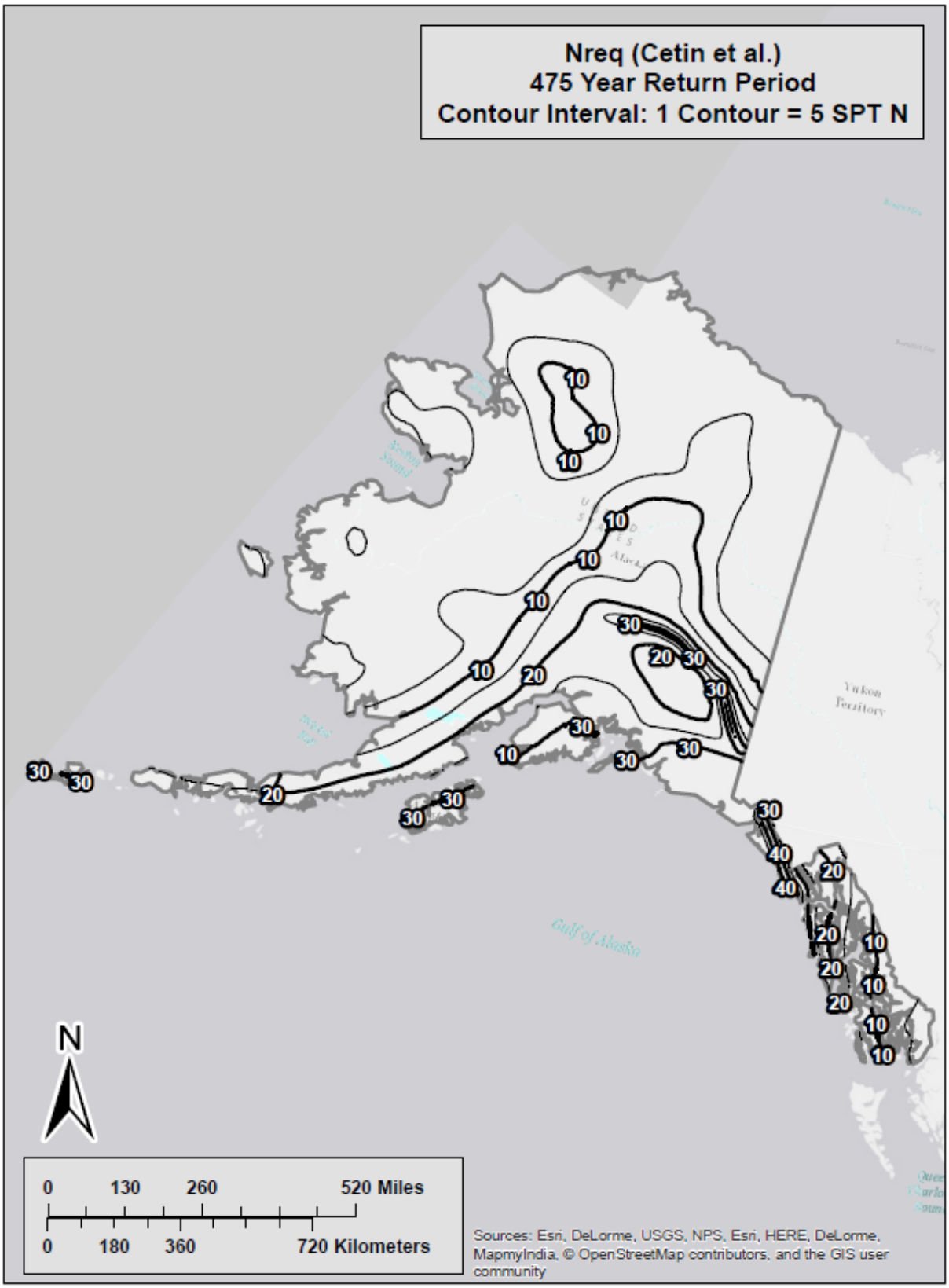

Figure B-2 Liquefaction Triggering (N_{req}^{ref}) Map for Alaska (T_r = 475)

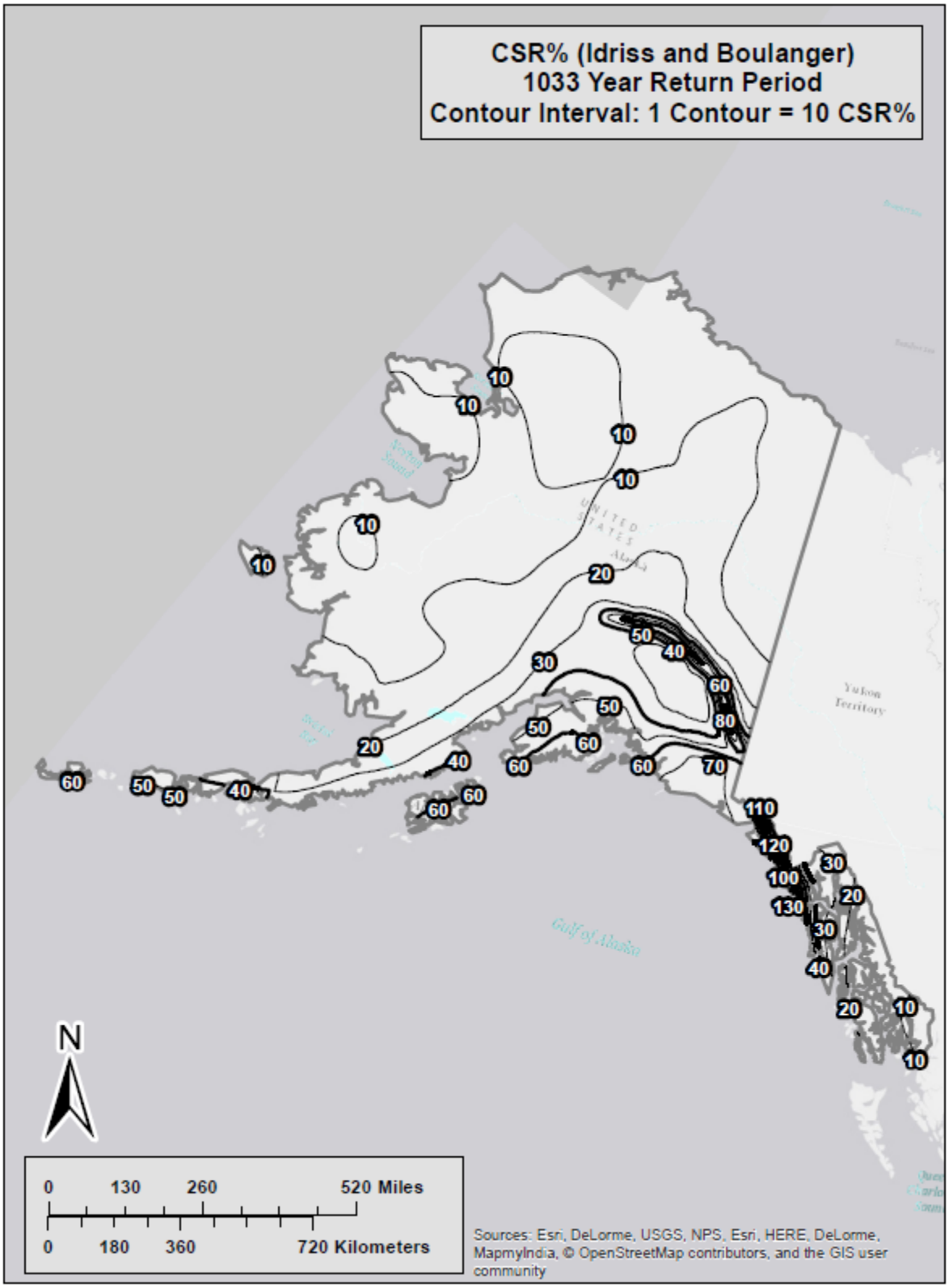

Figure B-3 Liquefaction Triggering ($CSR\%^{ref}$) Map for Alaska (T_r = 1,033)

Figure B-4 Liquefaction Triggering (N_{req}^{ref}) Map for Alaska (T_r = 1,033)

Figure B-5 Liquefaction Triggering ($CSR\%^{ref}$) Map for Alaska (T_r = 2,475)

Figure B-6 Liquefaction Triggering (N_{req}^{ref}) Map for Alaska (T_r = 2,475)

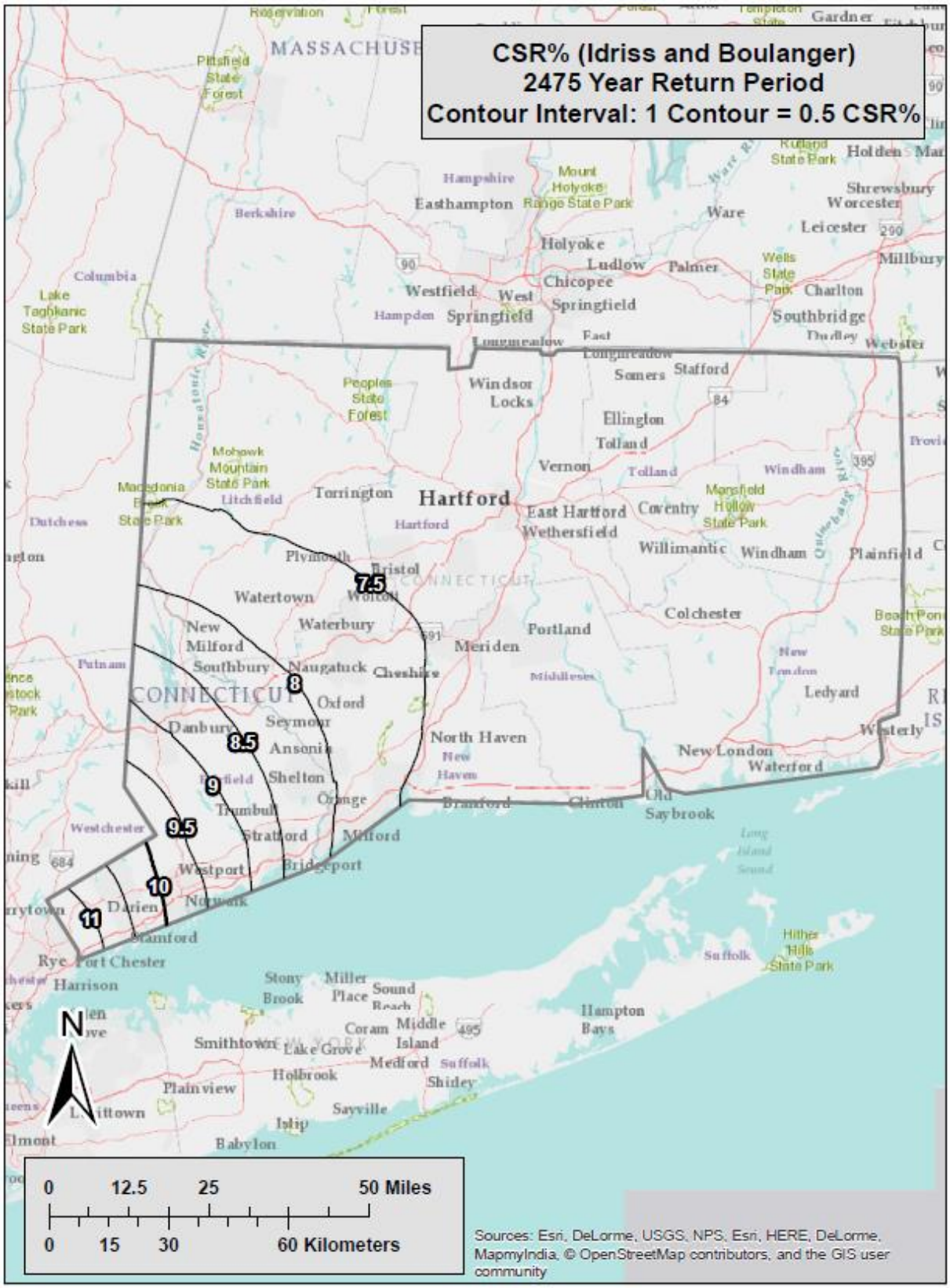

Figure B-7 Liquefaction Triggering ($CSR\%^{ref}$) Map for Connecticut (T_r = 2,475)

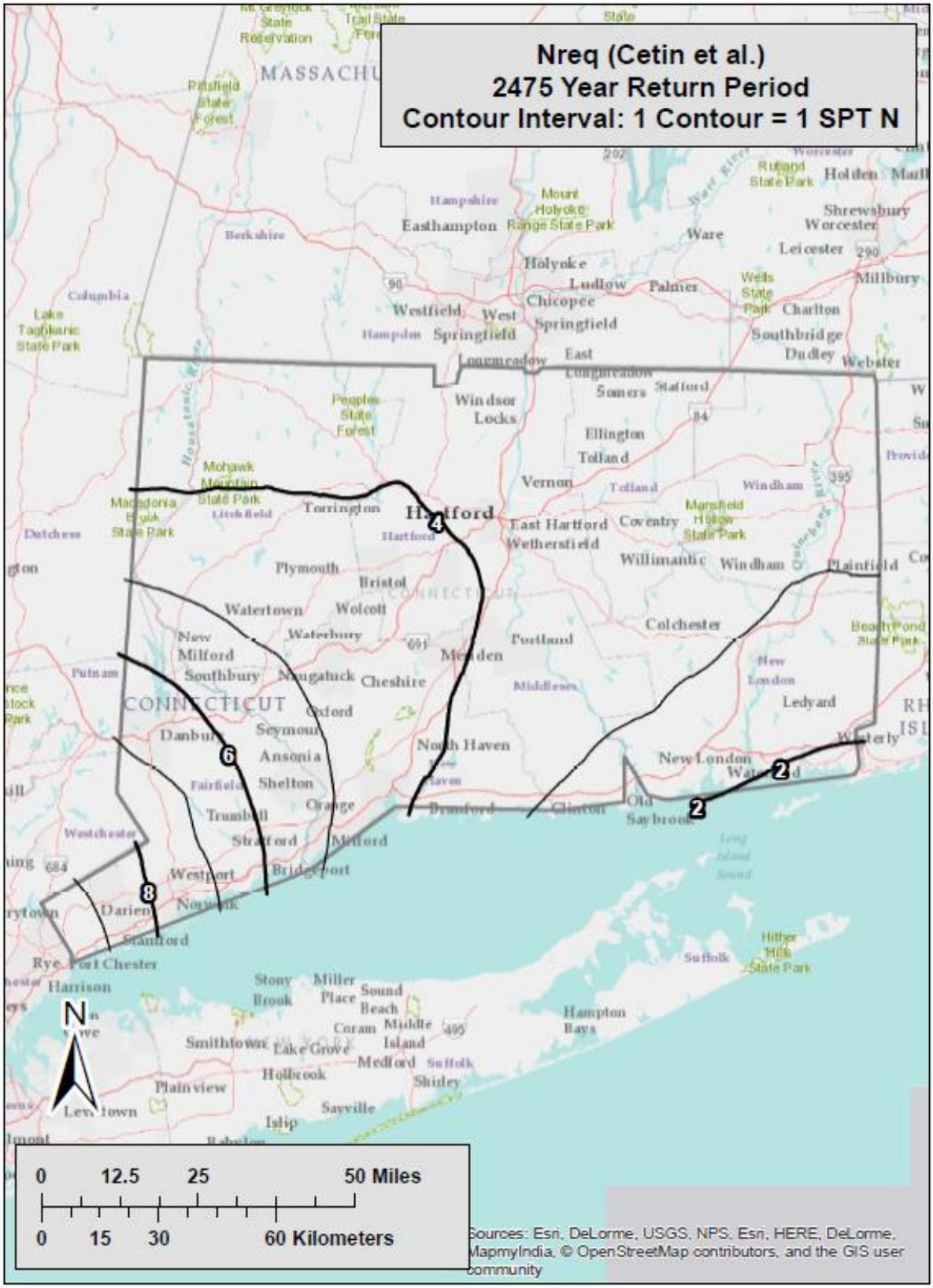

Figure B-8 Liquefaction Triggering (N_{req}^{ref}) Map for Connecticut (T_r = 2,475)

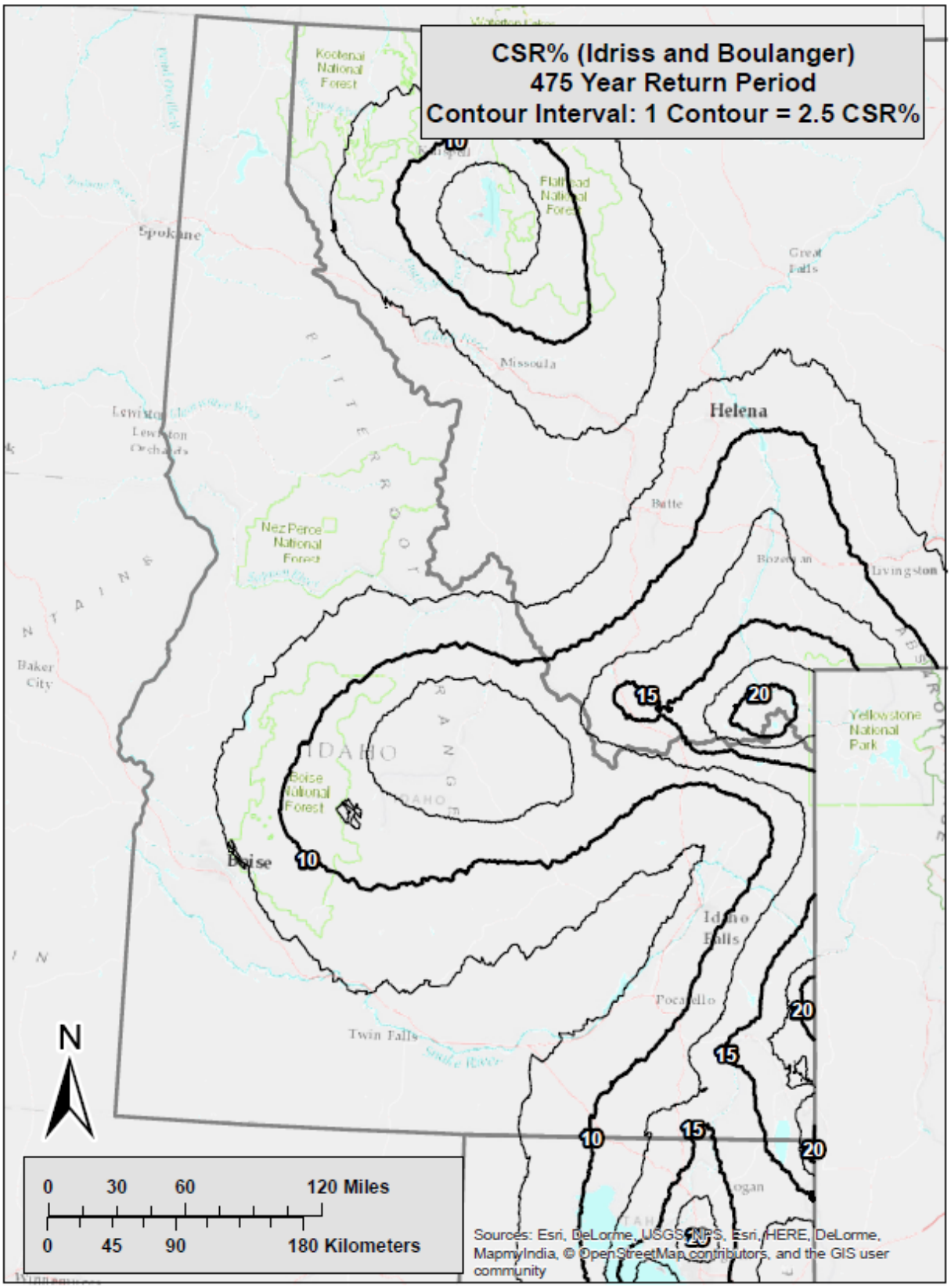

Figure B-9 Liquefaction Triggering ($CSR\%^{ref}$) Map for Idaho (T_r = 475)

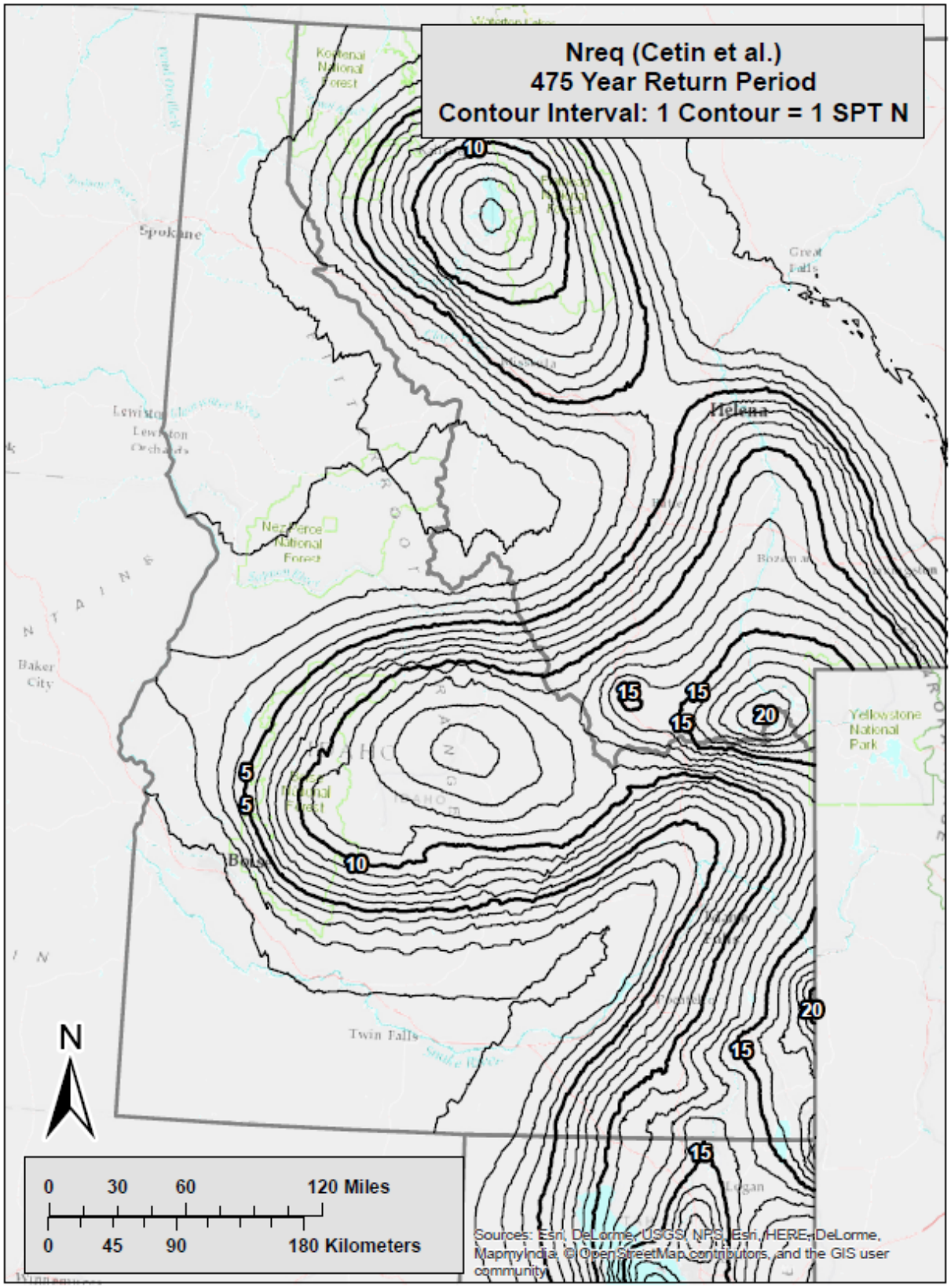

Figure B-10 Liquefaction Triggering (N_{req}^{ref}) Map for Idaho (T_r = 475)

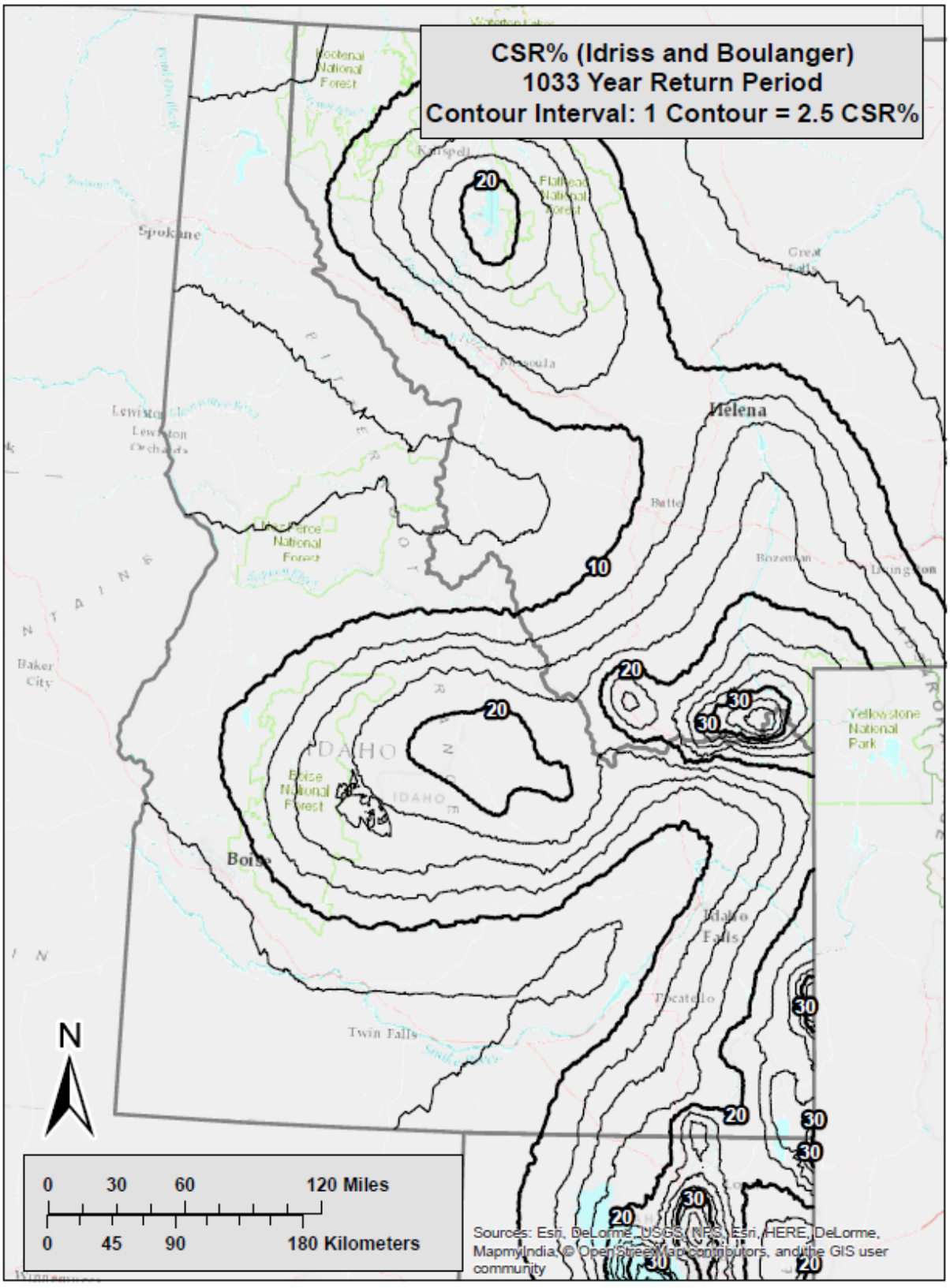

Figure B-11 Liquefaction Triggering ($CSR\%^{ref}$) Map for Idaho (T_r = 1,033)

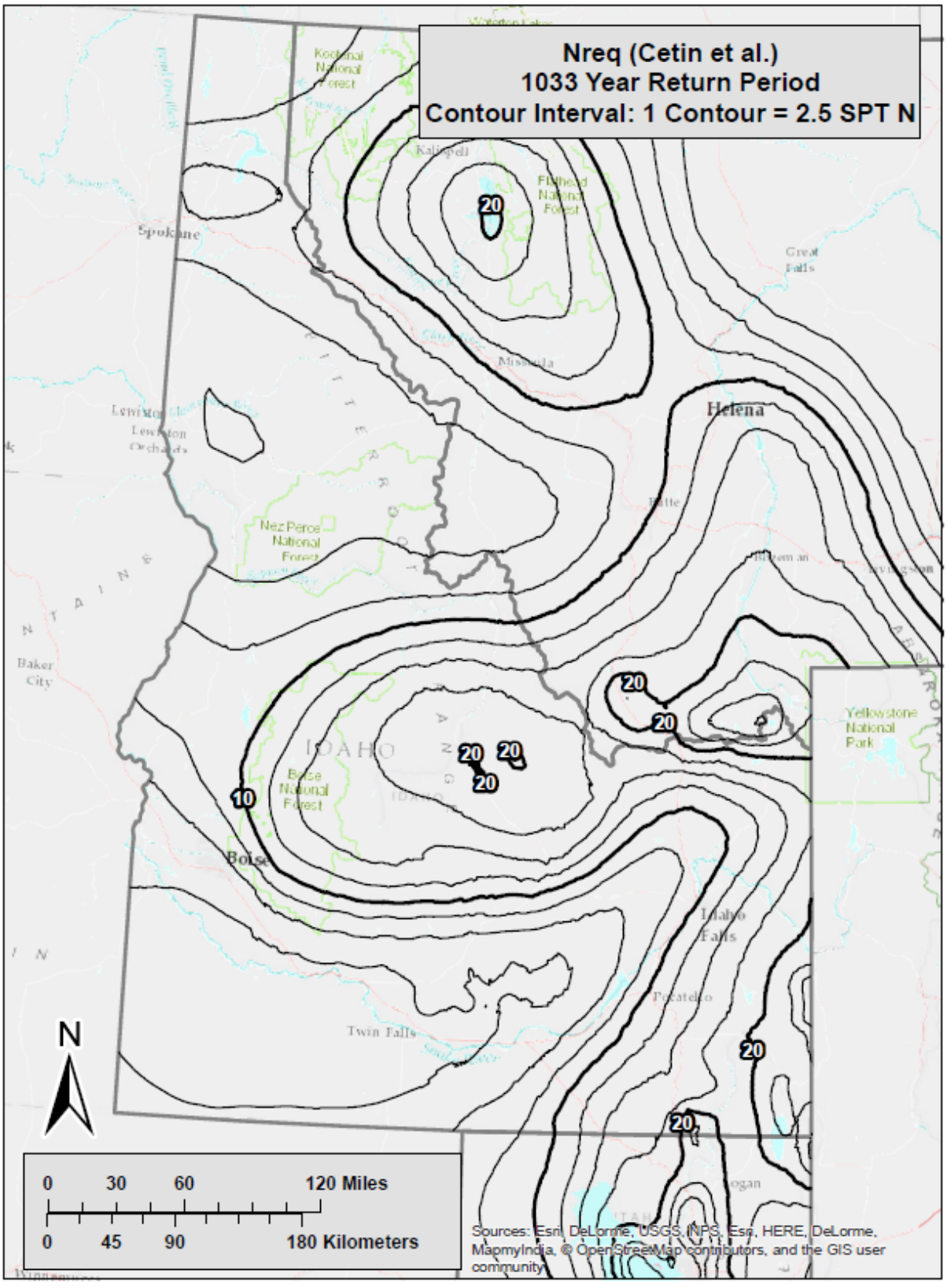

Figure B-12 Liquefaction Triggering (N_{req}^{ref}) Map for Idaho (T_r = 1,033)

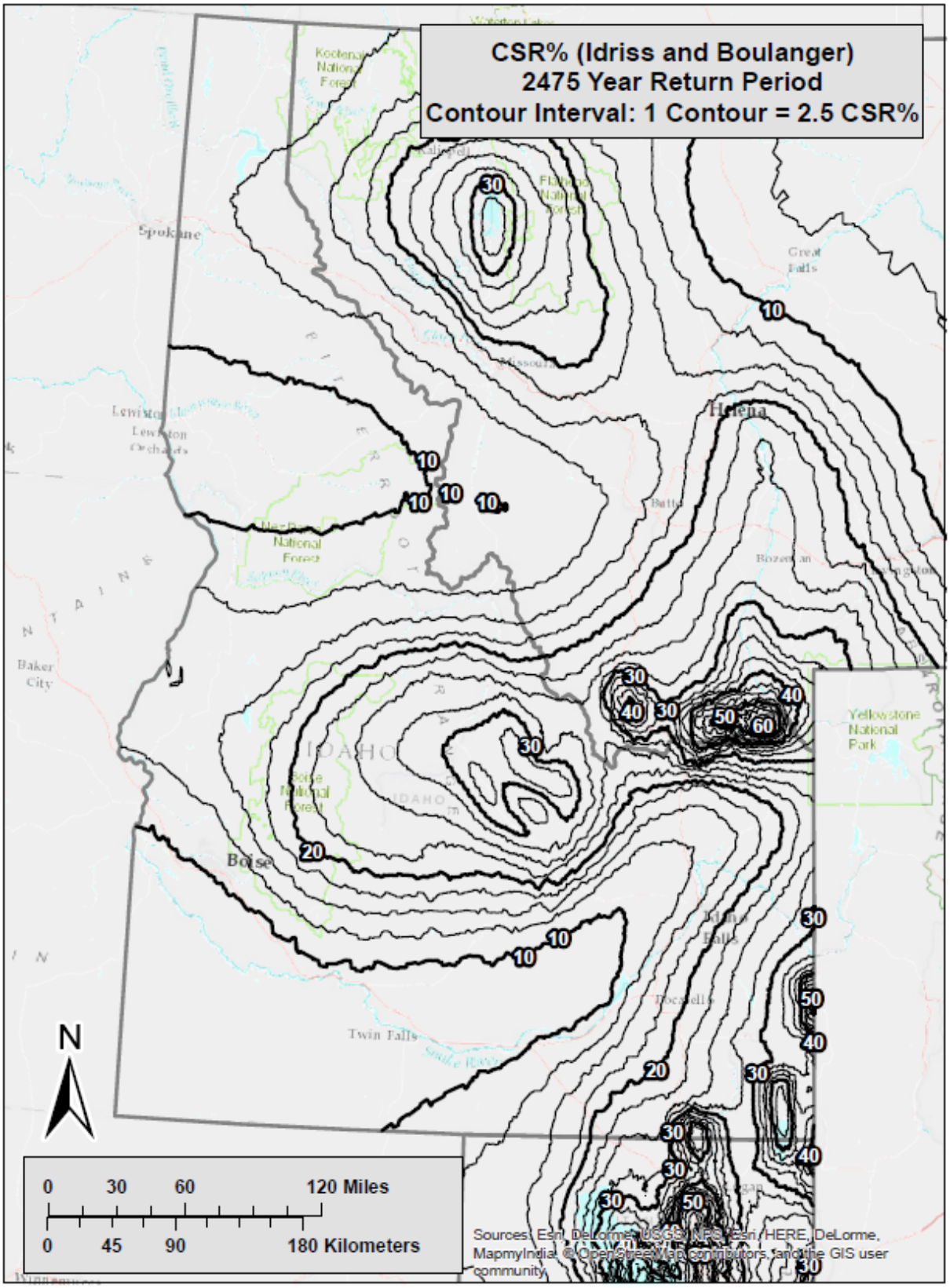

Figure B-13 Liquefaction Triggering ($CSR\%^{ref}$) Map for Idaho (T_r = 2,475)

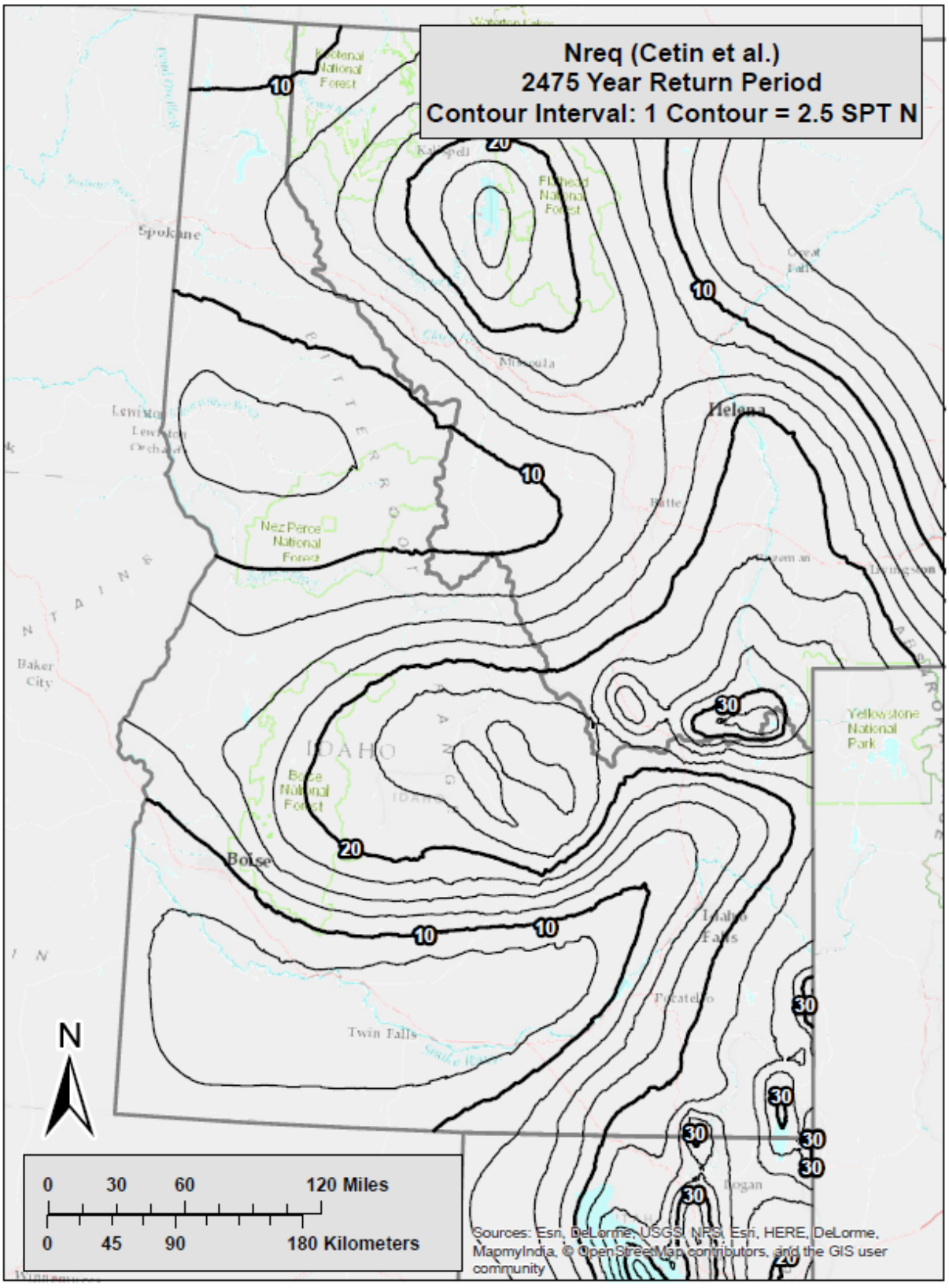

Figure B-14 Liquefaction Triggering (N_{req}^{ref}) Map for Idaho (T_r = 2,475)

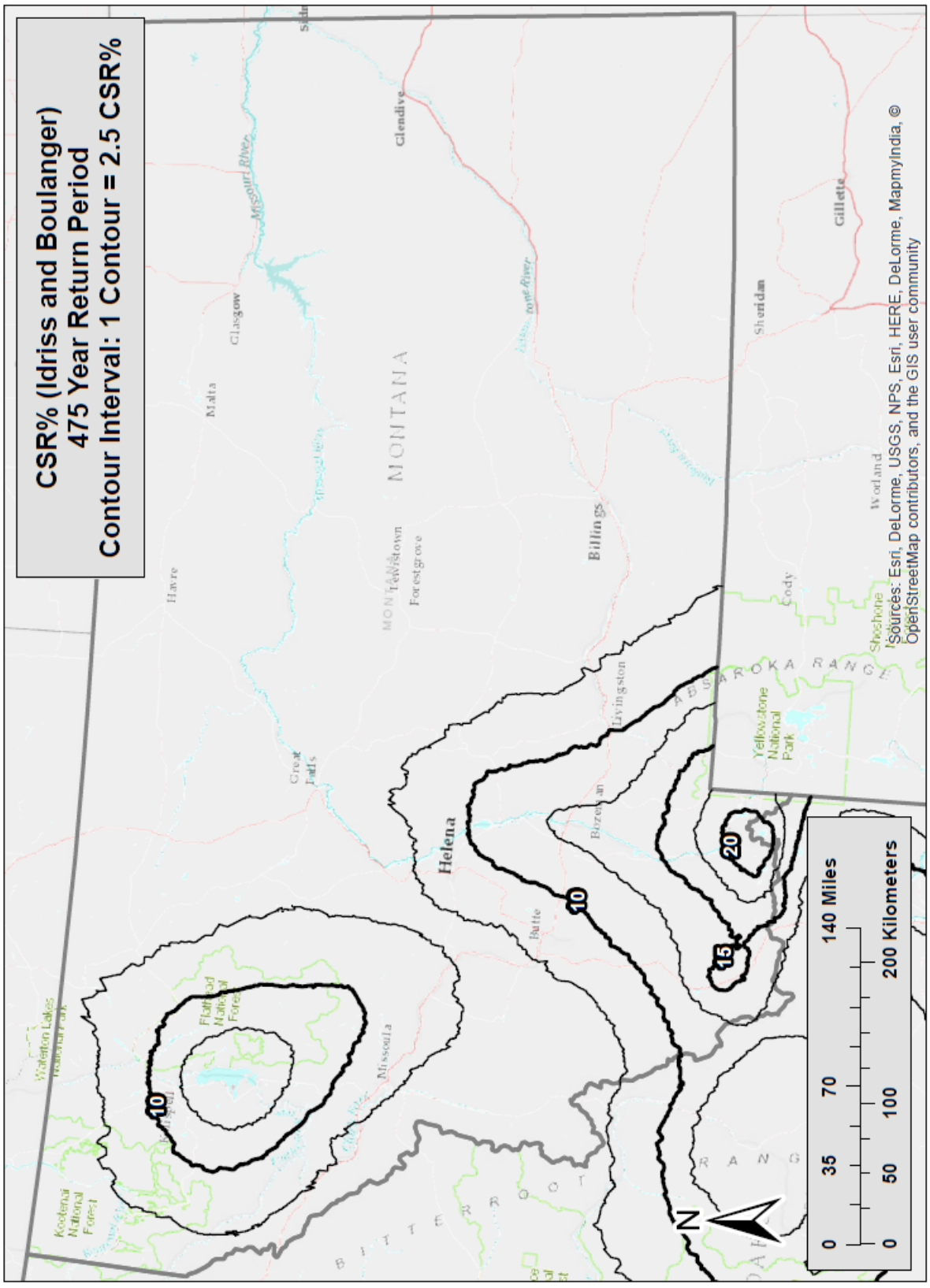

Figure B-15 Liquefaction Triggering ($CSR\%^{ref}$) Map for Montana (T_r = 475)

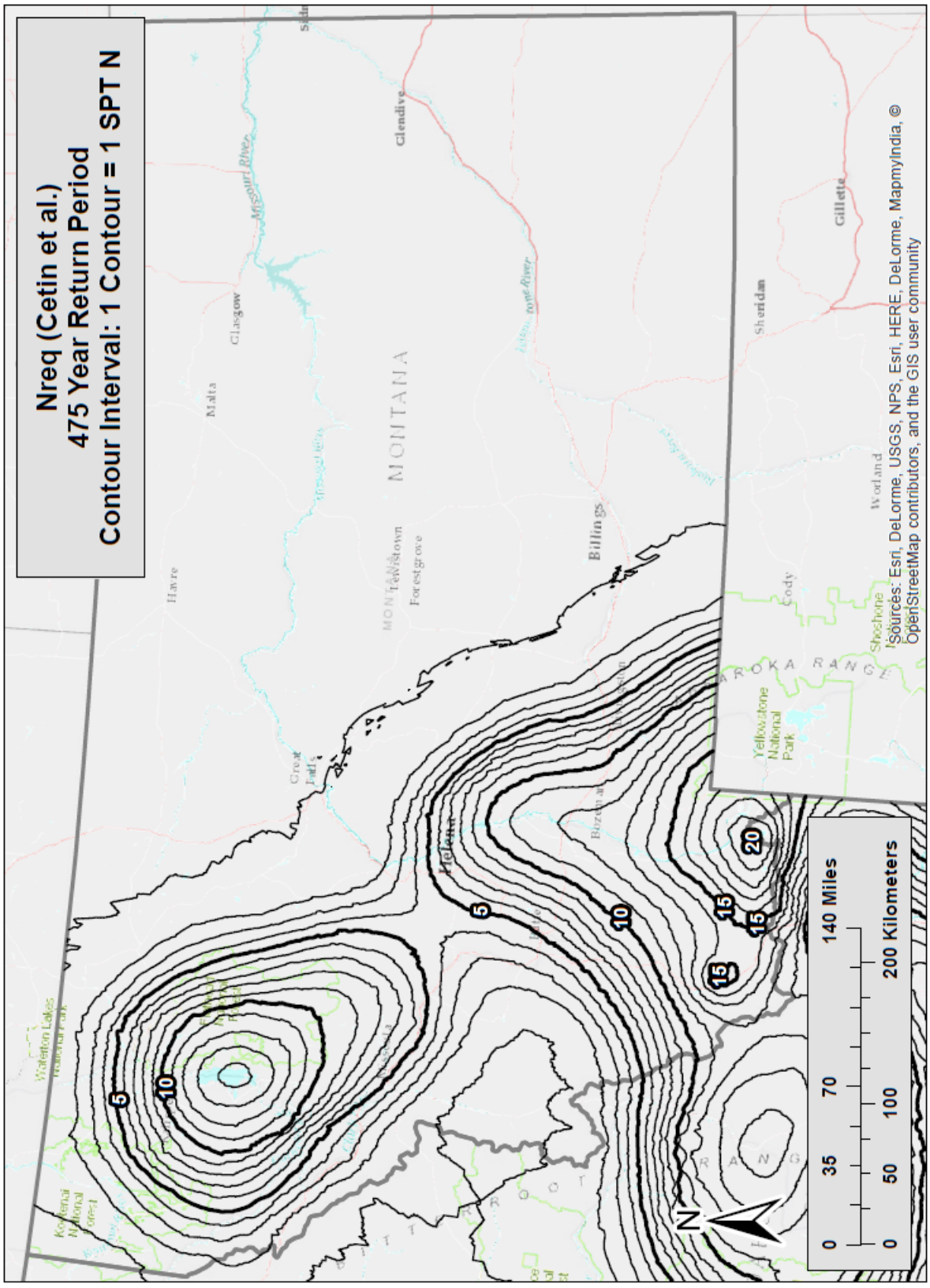

Figure B-16 Liquefaction Triggering (N_{req}^{ref}) Map for Montana (T_r = 475)

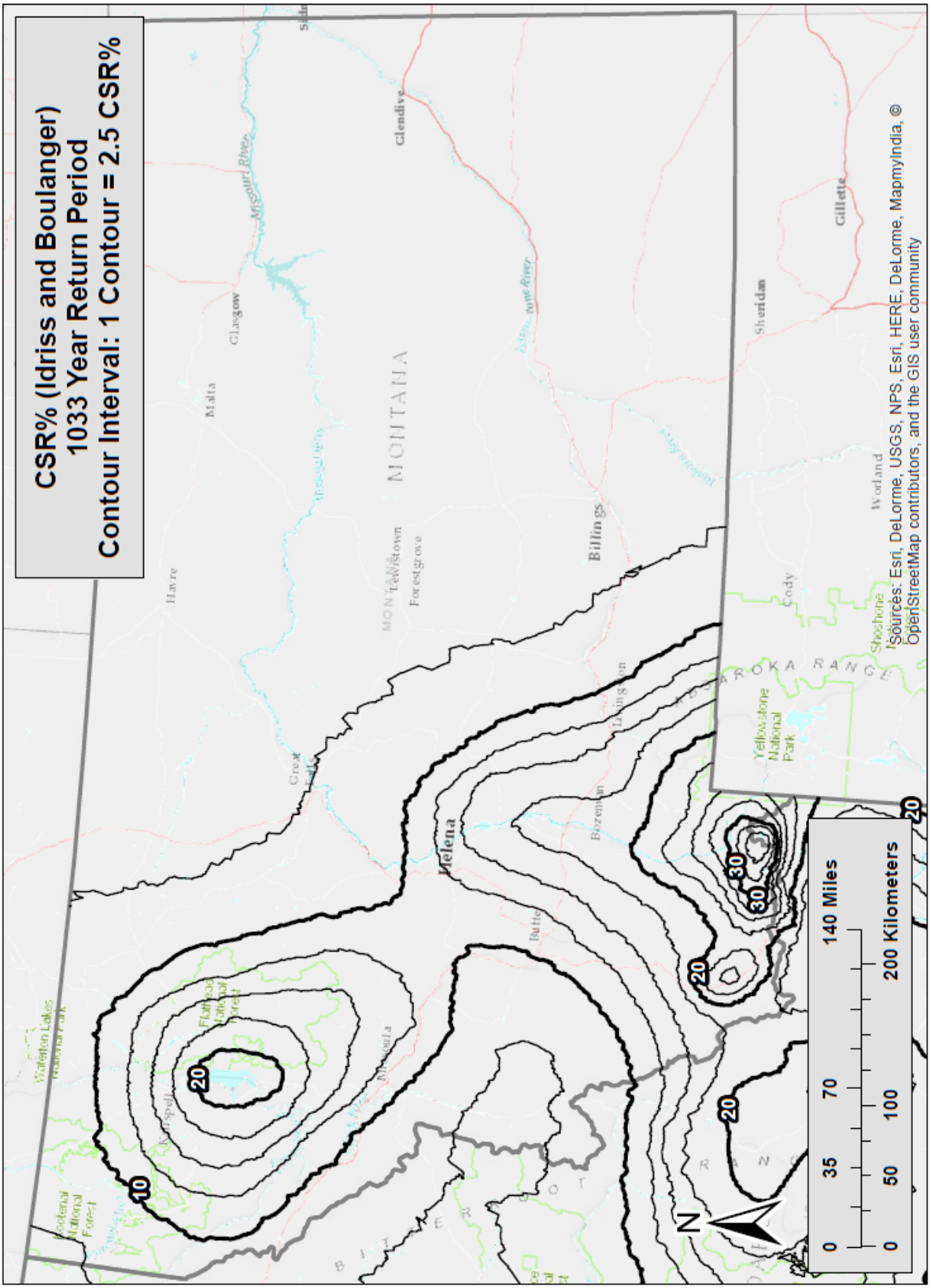

Figure B-17 Liquefaction Triggering ($CSR\%^{ref}$) Map for Montana (T_r = 1,033)

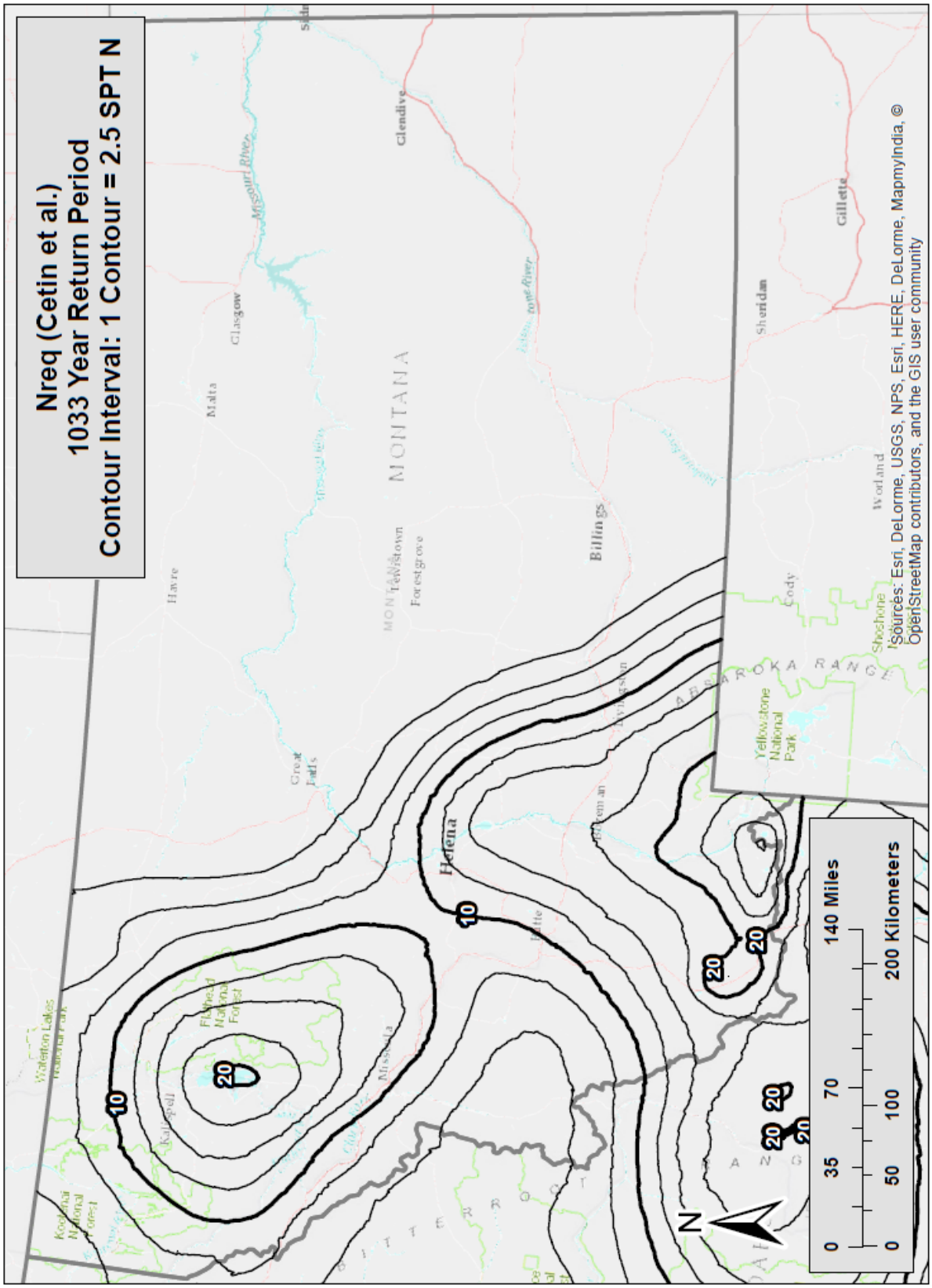

Figure B-18 Liquefaction Triggering (N_{req}^{ref}) Map for Montana (T_r = 1,033)

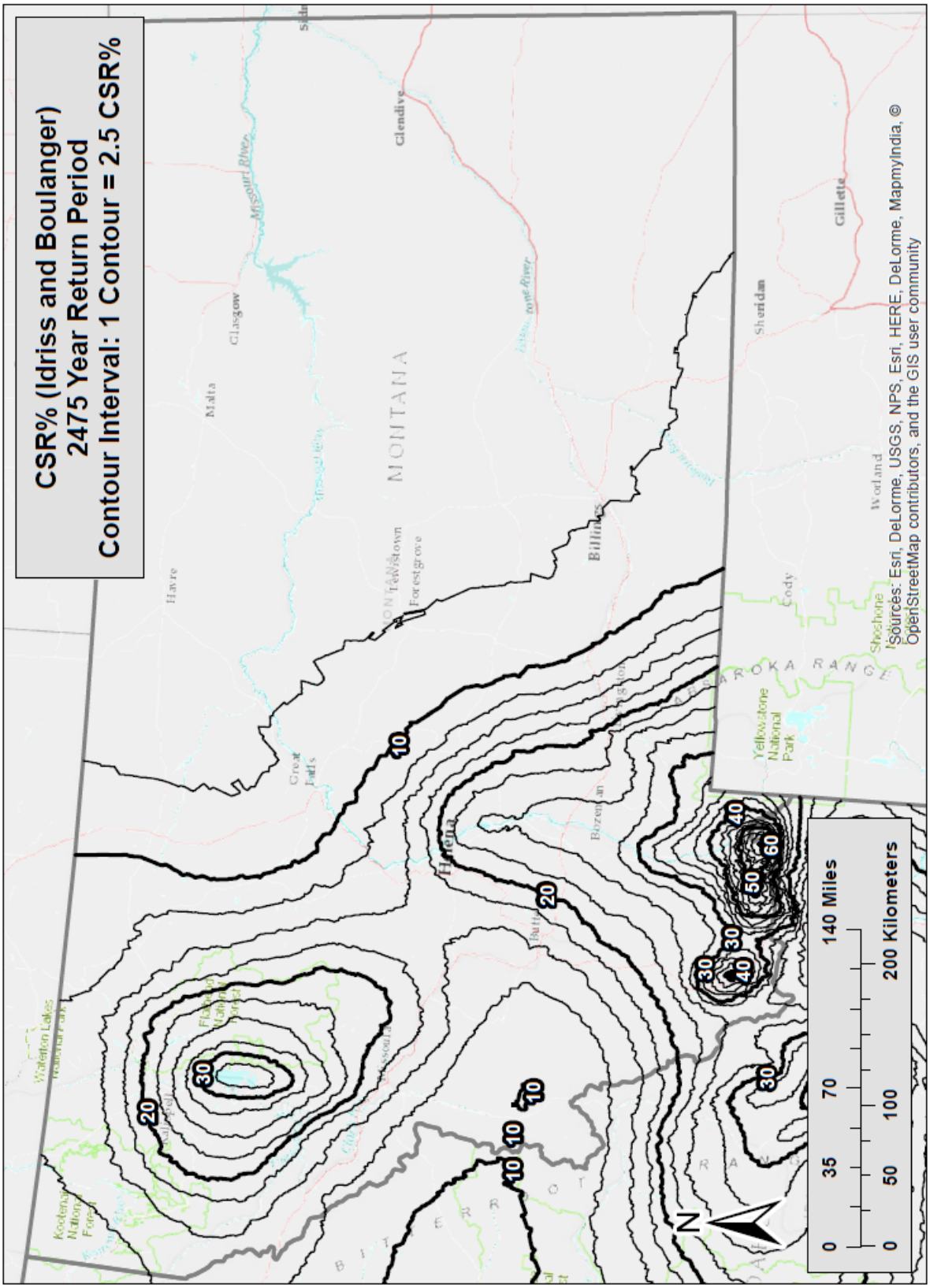

Figure B-19 Liquefaction Triggering ($CSR\%^{ref}$) Map for Montana (T_r = 2,475)

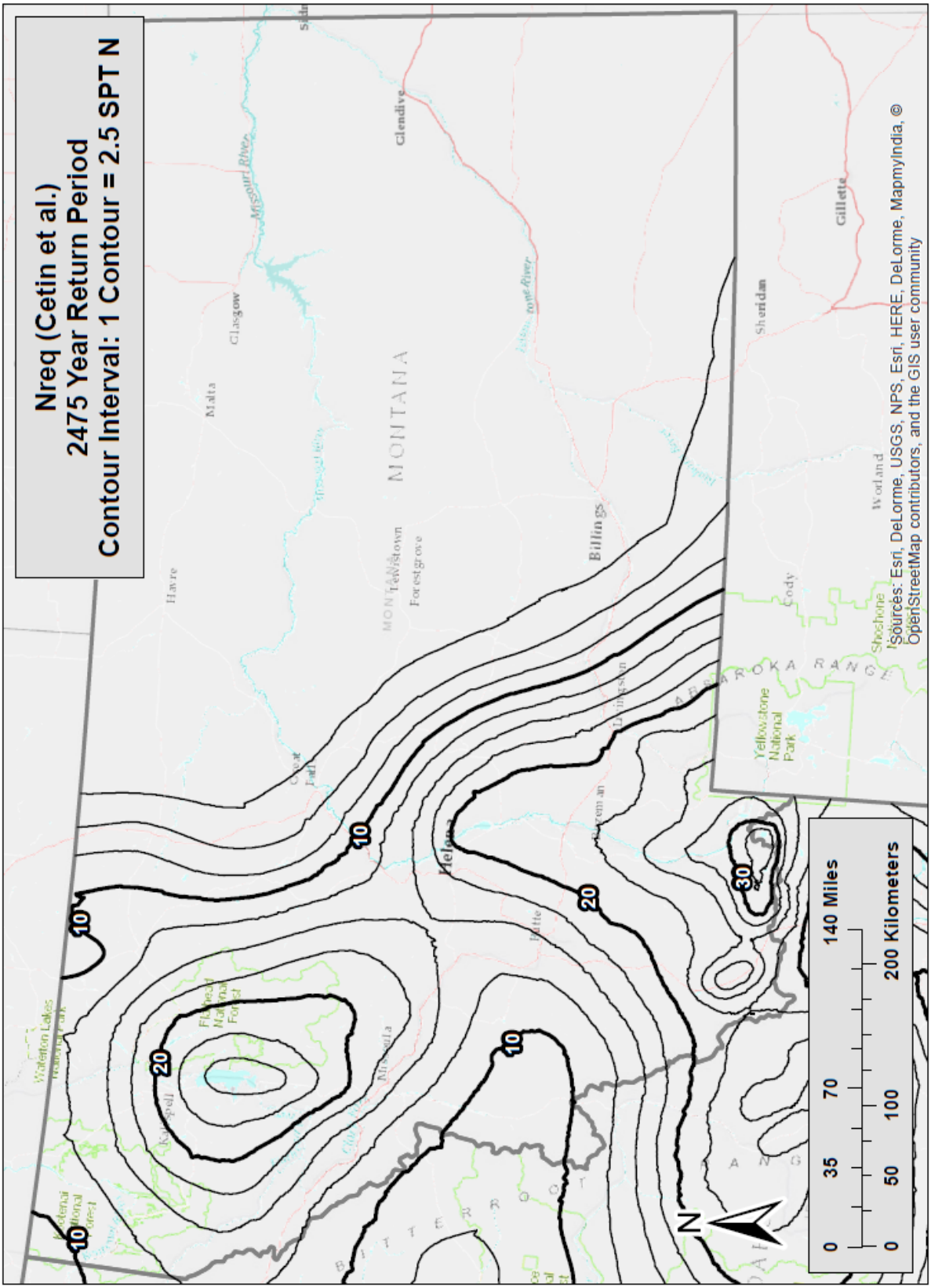

Figure B-20 Liquefaction Triggering (N_{req}^{ref}) Map for Montana (T_r = 2,475)

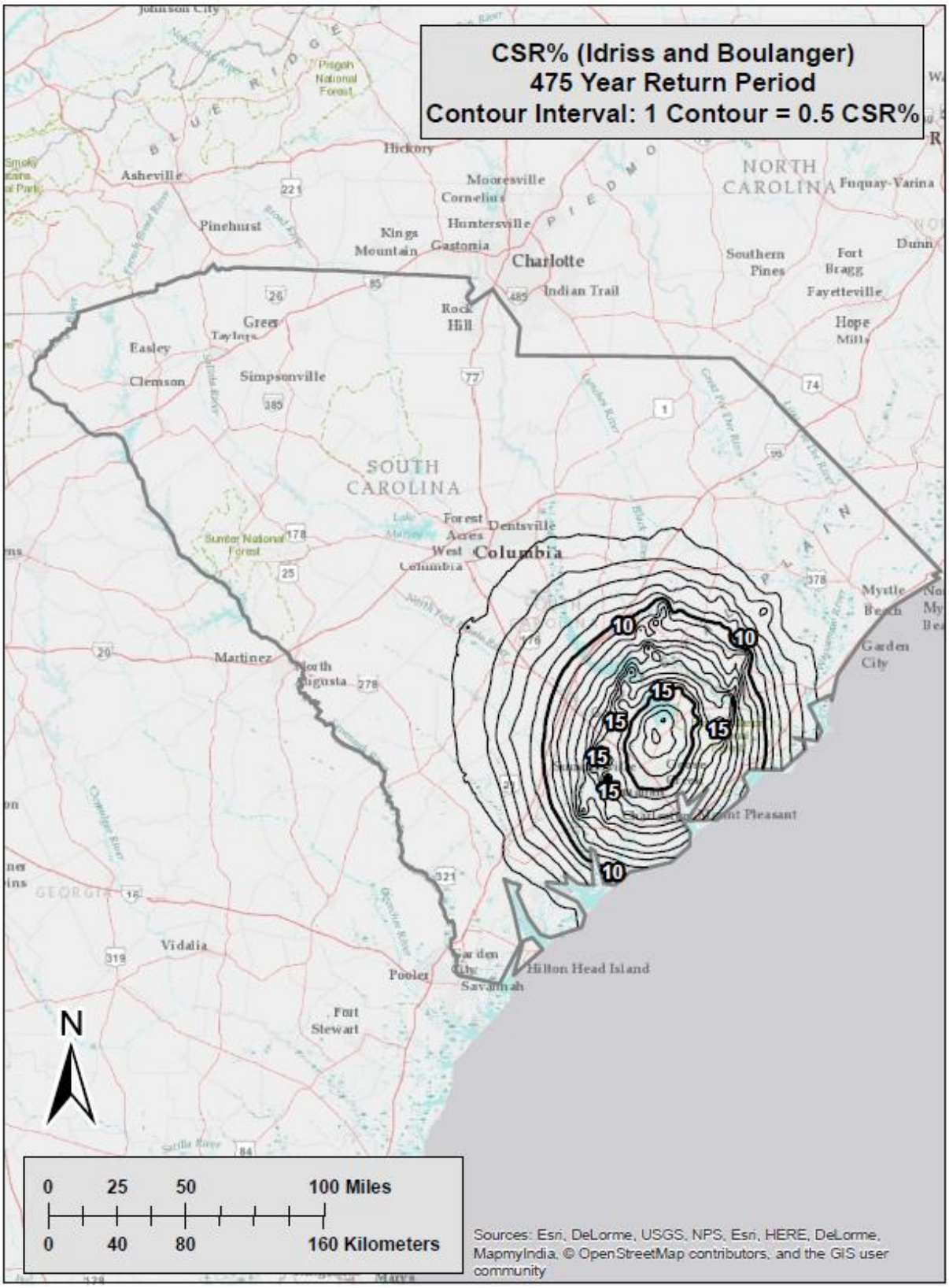

Figure B-21 Liquefaction Triggering ($CSR\%^{ref}$) Map for South Carolina (T_r = 475)

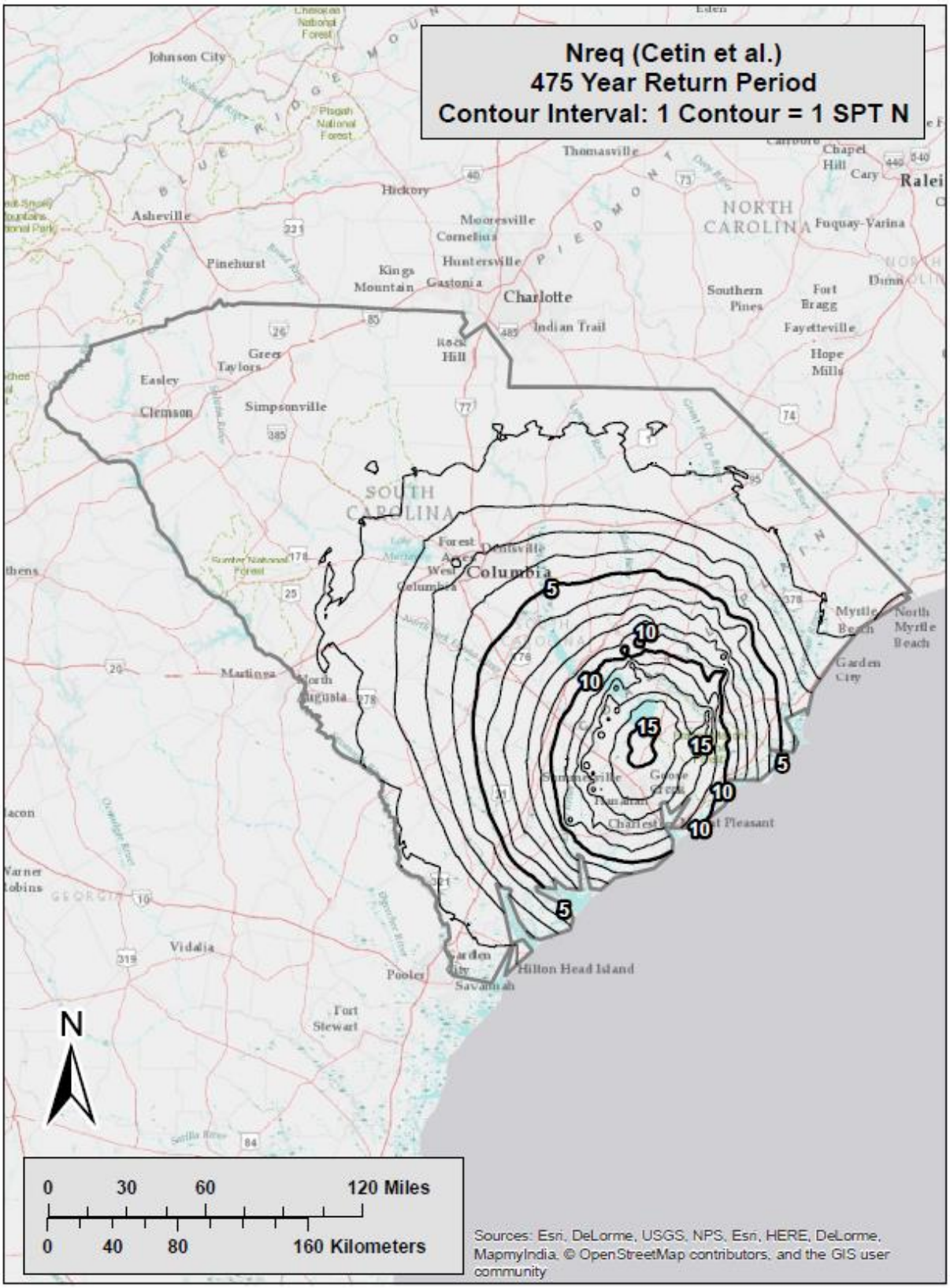

Figure B-22 Liquefaction Triggering ($N_{req}^{ref,\ Cetin}$) Map for South Carolina (T_r = 475)

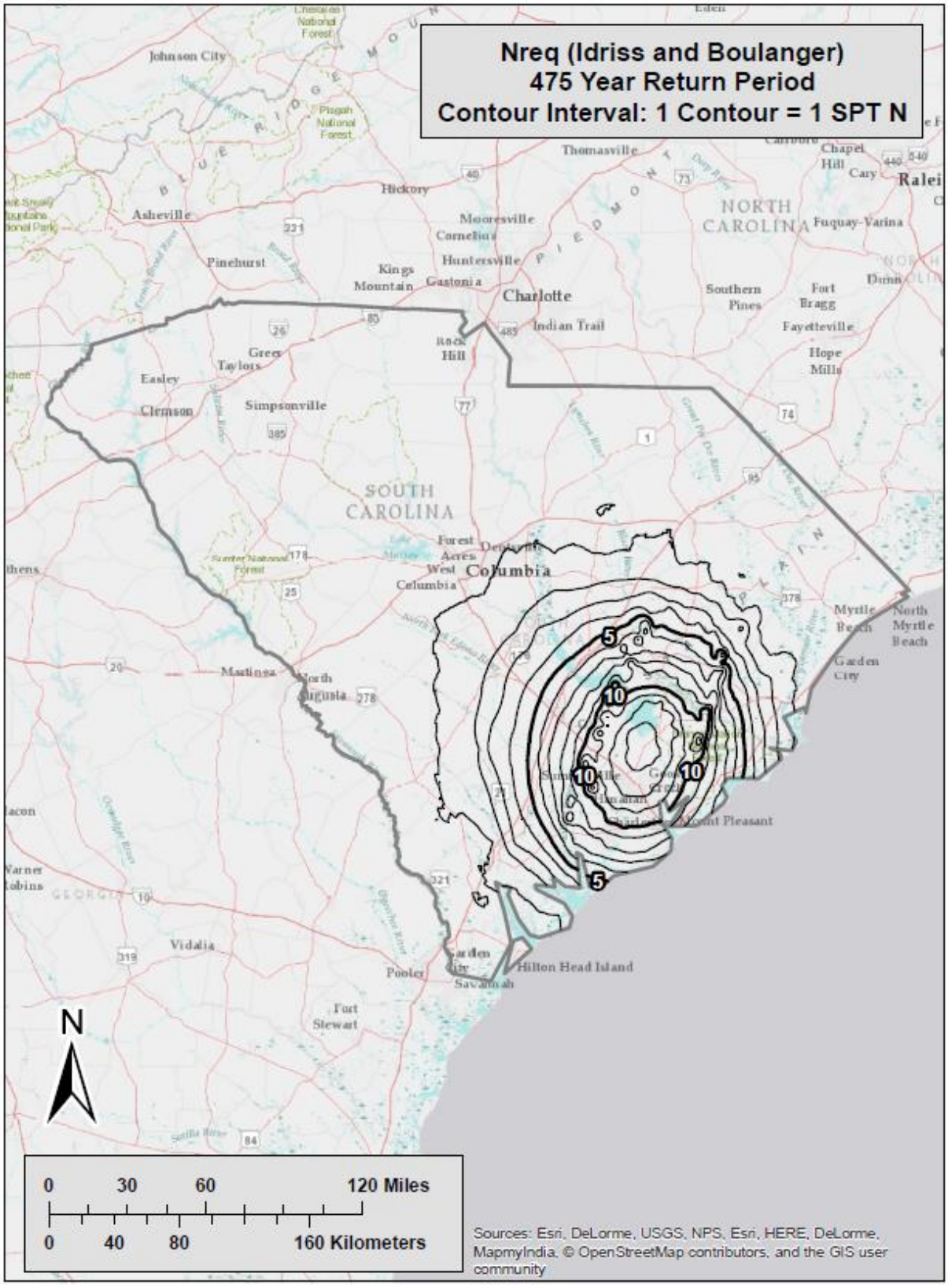

Figure B-23 Liquefaction Triggering ($N_{req}^{ref,\ Idriss}$) Map for South Carolina (T_r = 475)

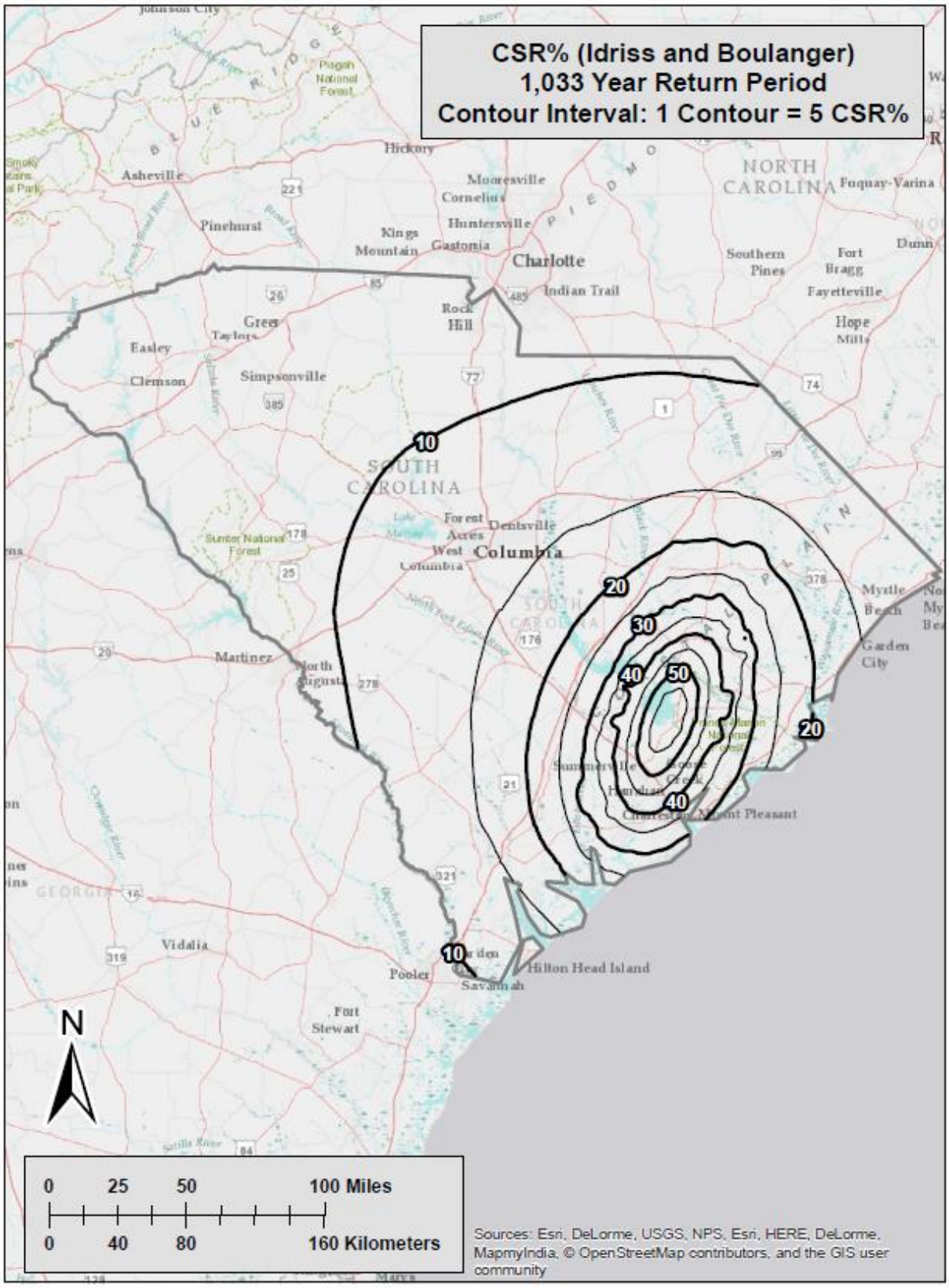

Figure B-24 Liquefaction Triggering ($CSR\%^{ref}$) Map for South Carolina (T_r = 1,033)

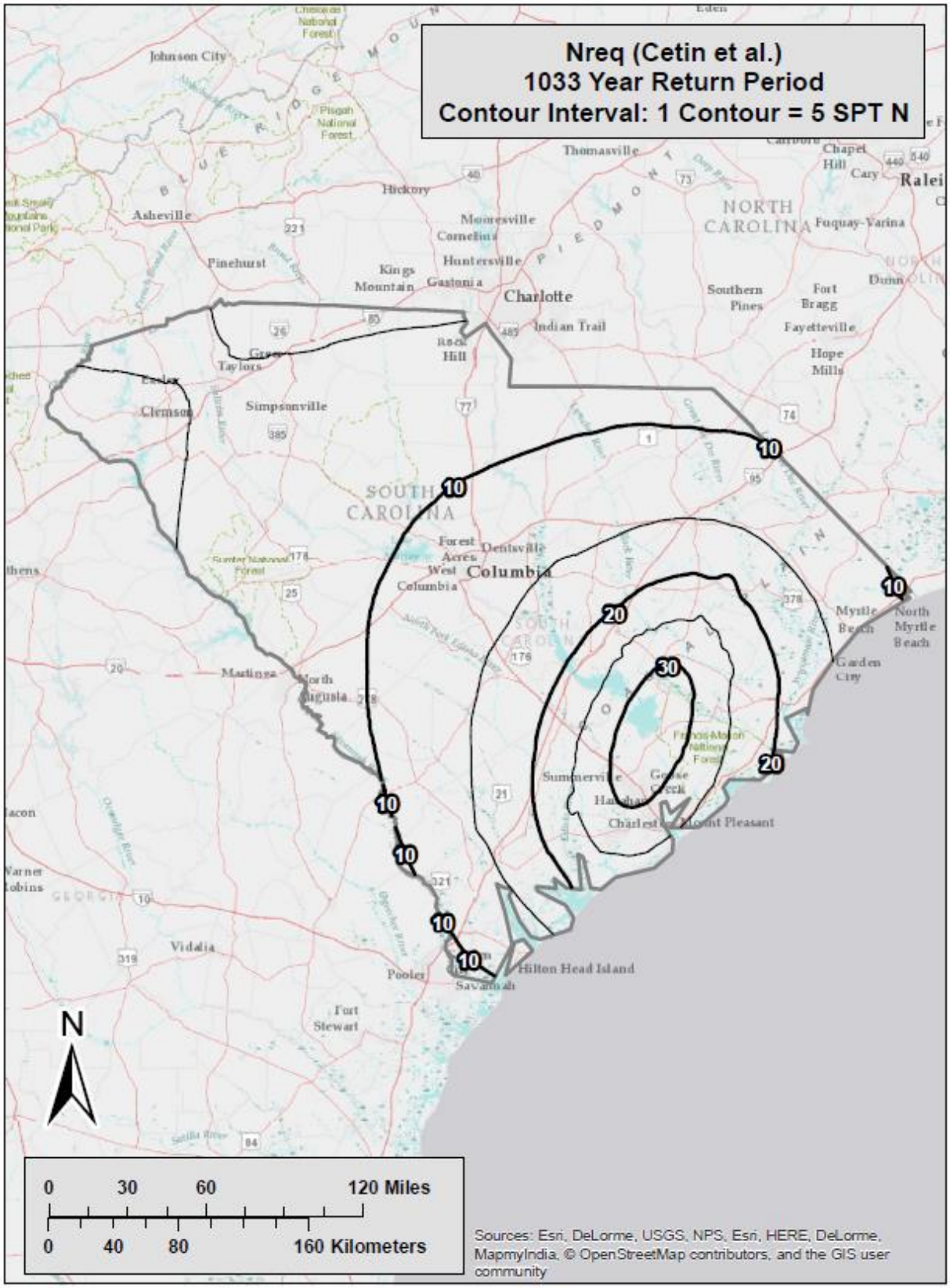

Figure B-25 Liquefaction Triggering ($N_{req}^{ref,Cetin}$) Map for South Carolina (T_r = 1,033)

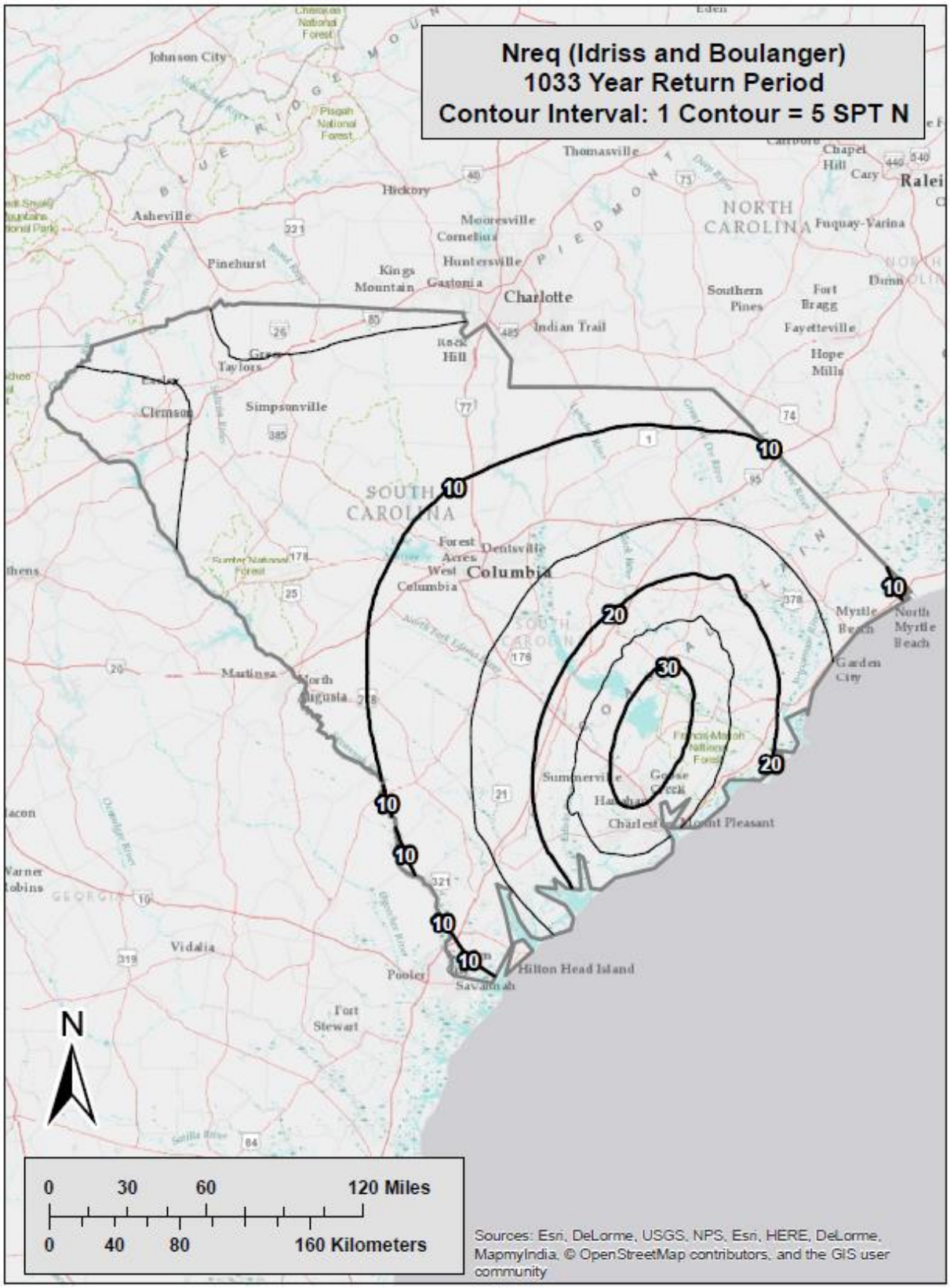

Figure B-26 Liquefaction Triggering ($N_{req}^{ref,Idriss}$) Map for South Carolina (T_r = 1,033)

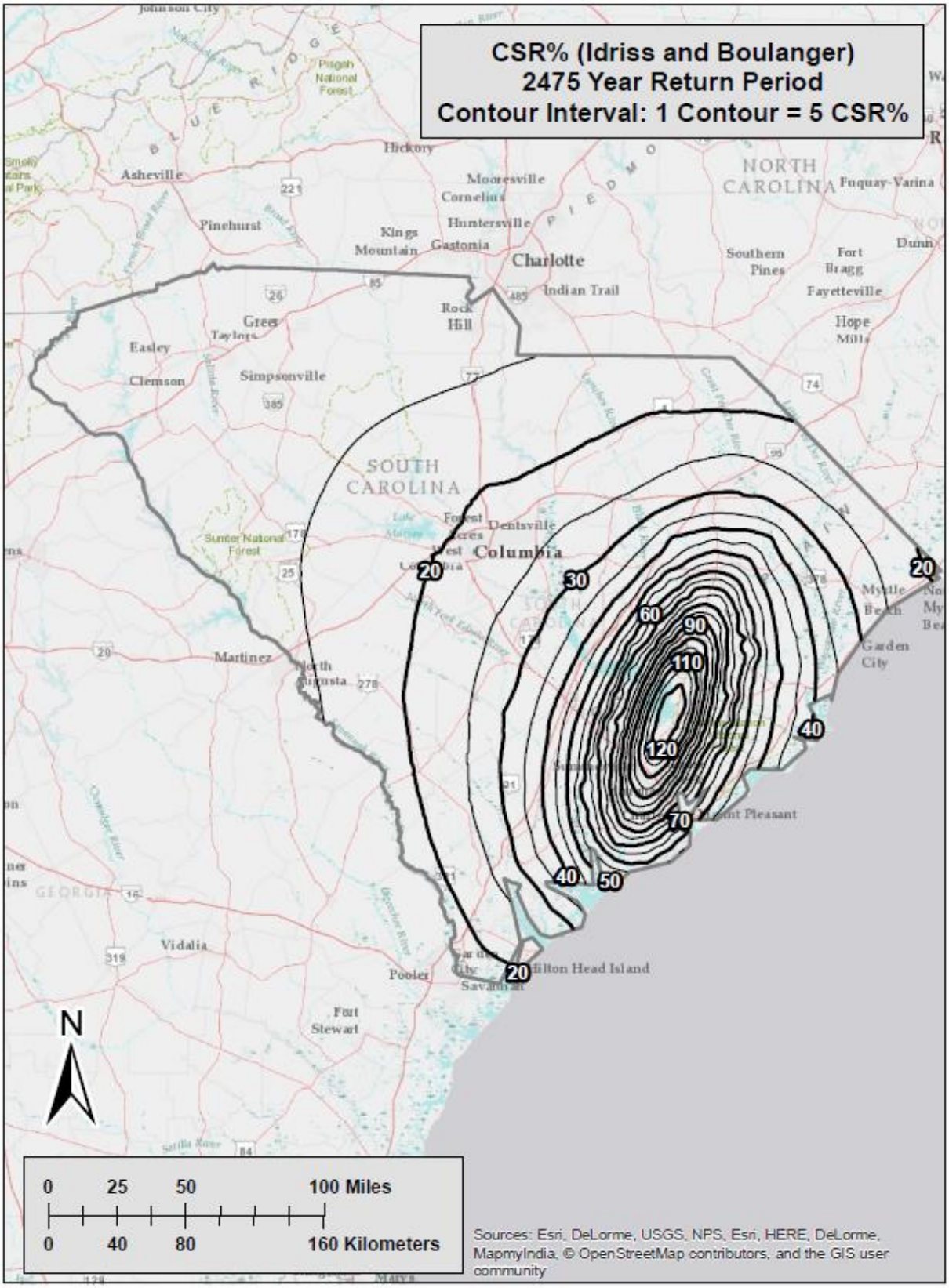

Figure B-27 Liquefaction Triggering ($CSR\%^{ref}$) Map for South Carolina (T_r = 2,475)

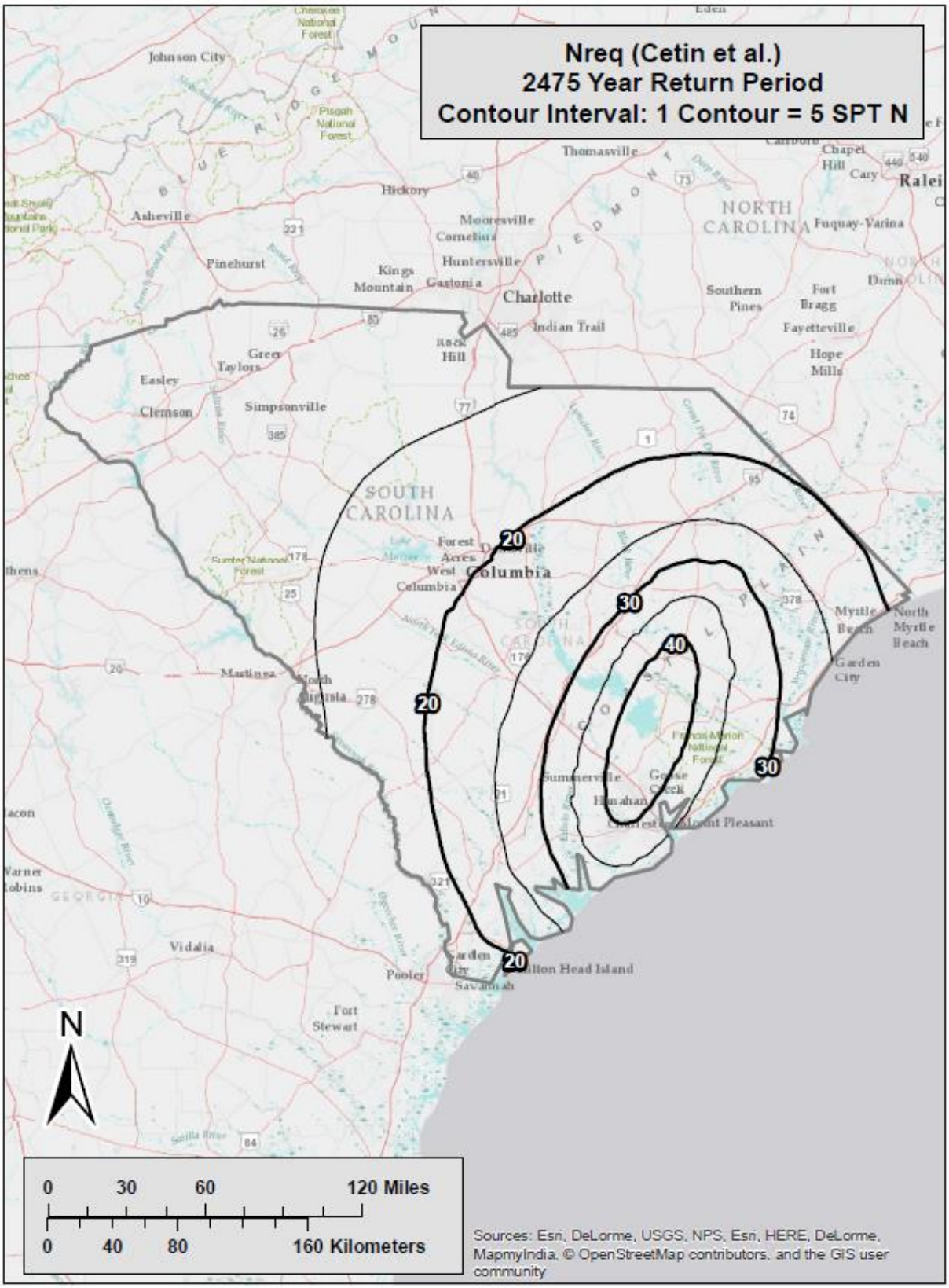

Figure B-28 Liquefaction Triggering ($N_{req}^{ref,Cetin}$) Map for South Carolina (T_r = 2,475)

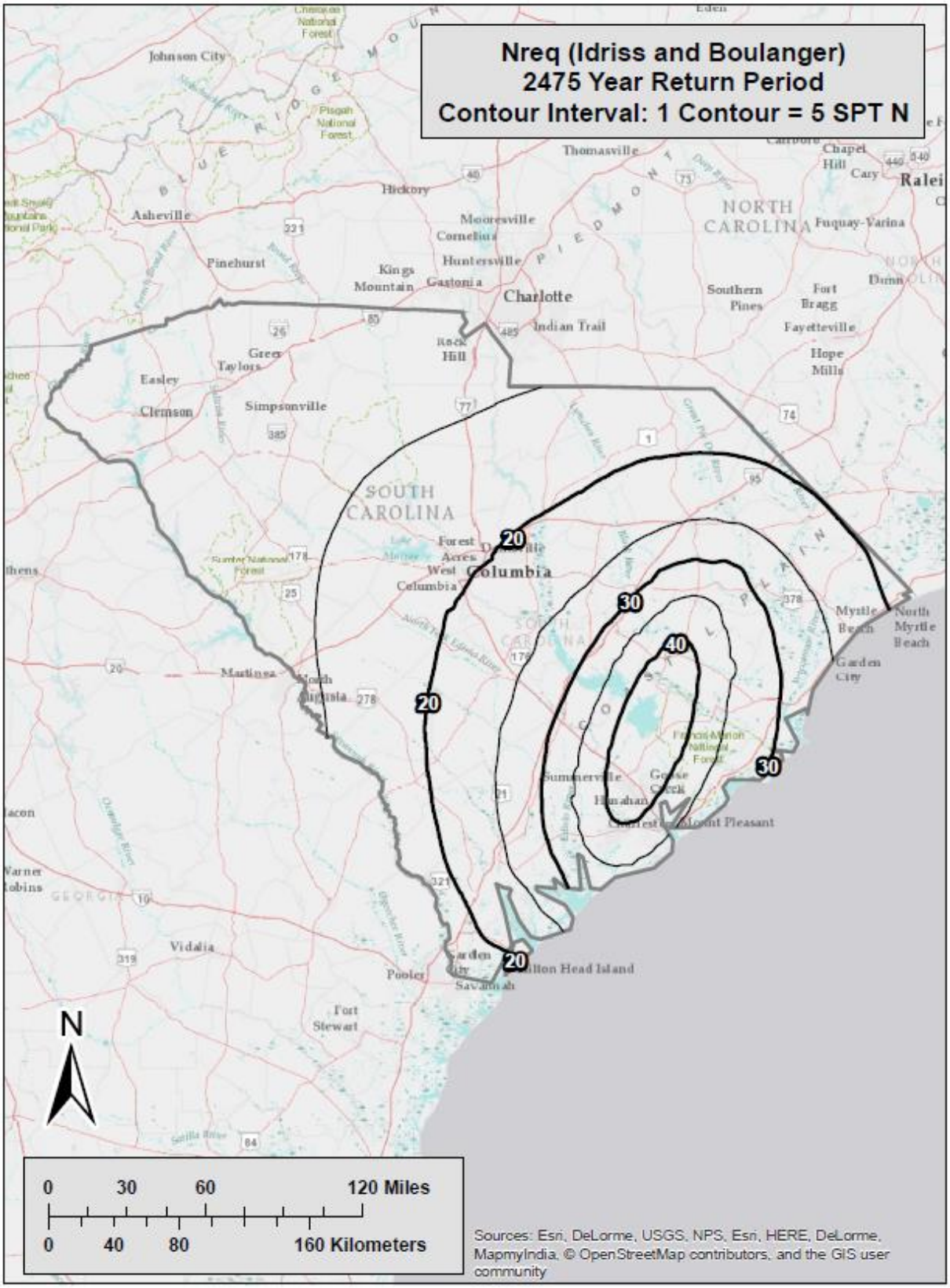

Figure B-29 Liquefaction Triggering ($N_{req}^{ref,Idriss}$) Map for South Carolina (T_r = 2,475)

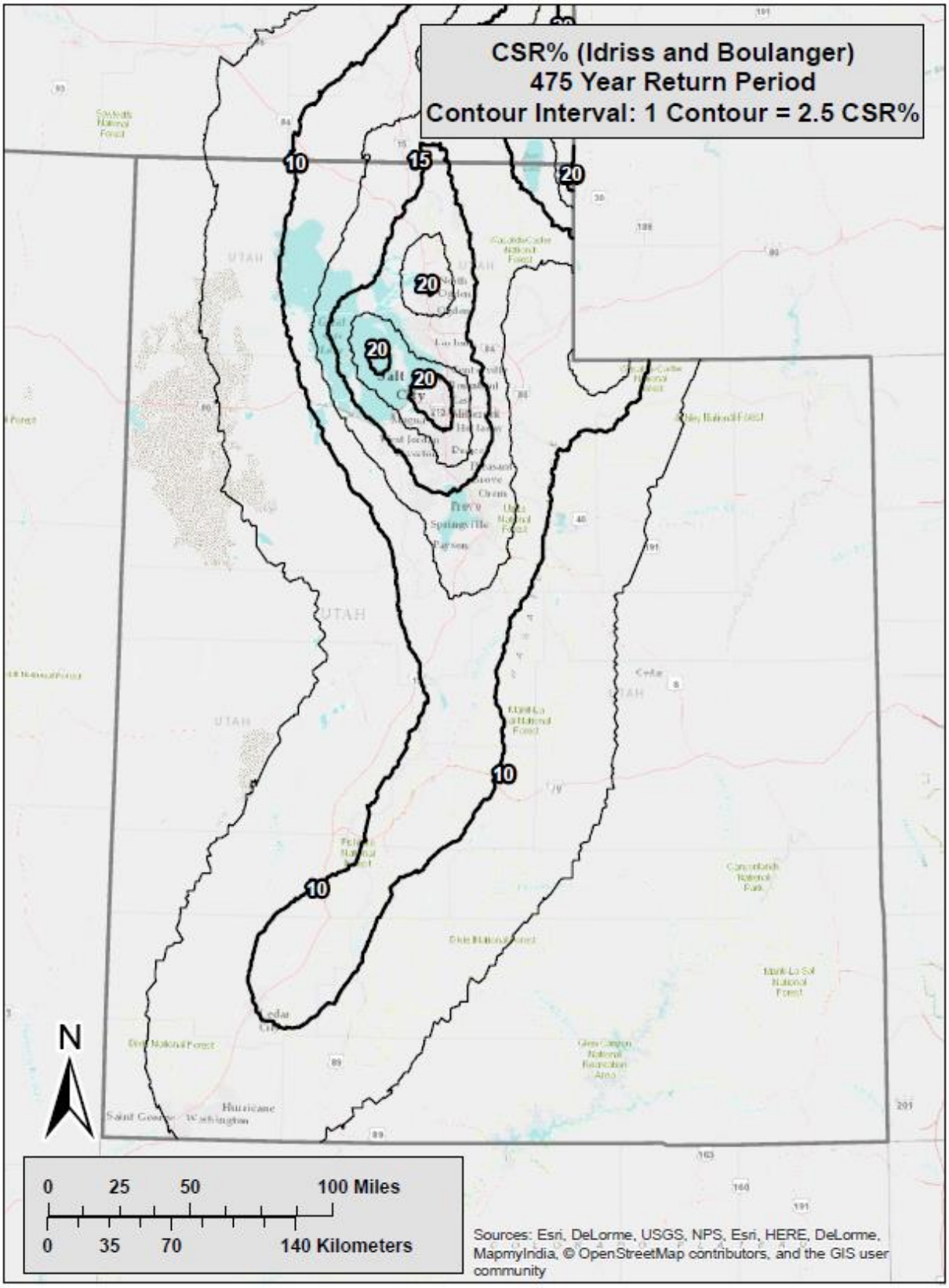

Figure B-30 Liquefaction Triggering ($CSR\%^{ref}$) Map for Utah (T_r = 475)

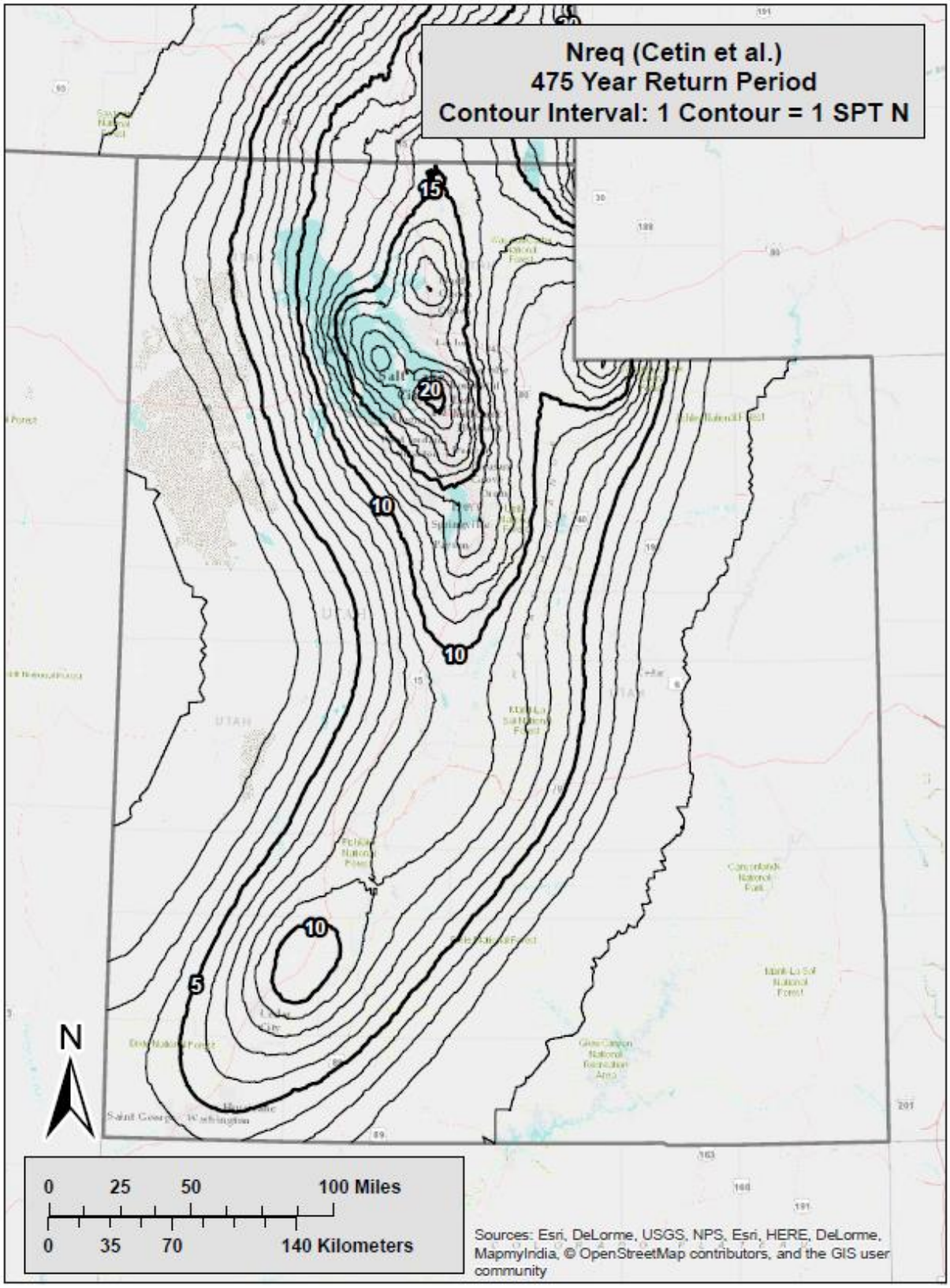

Figure B-31 Liquefaction Triggering (N_{req}^{ref}) Map for Utah (T_r = 475)

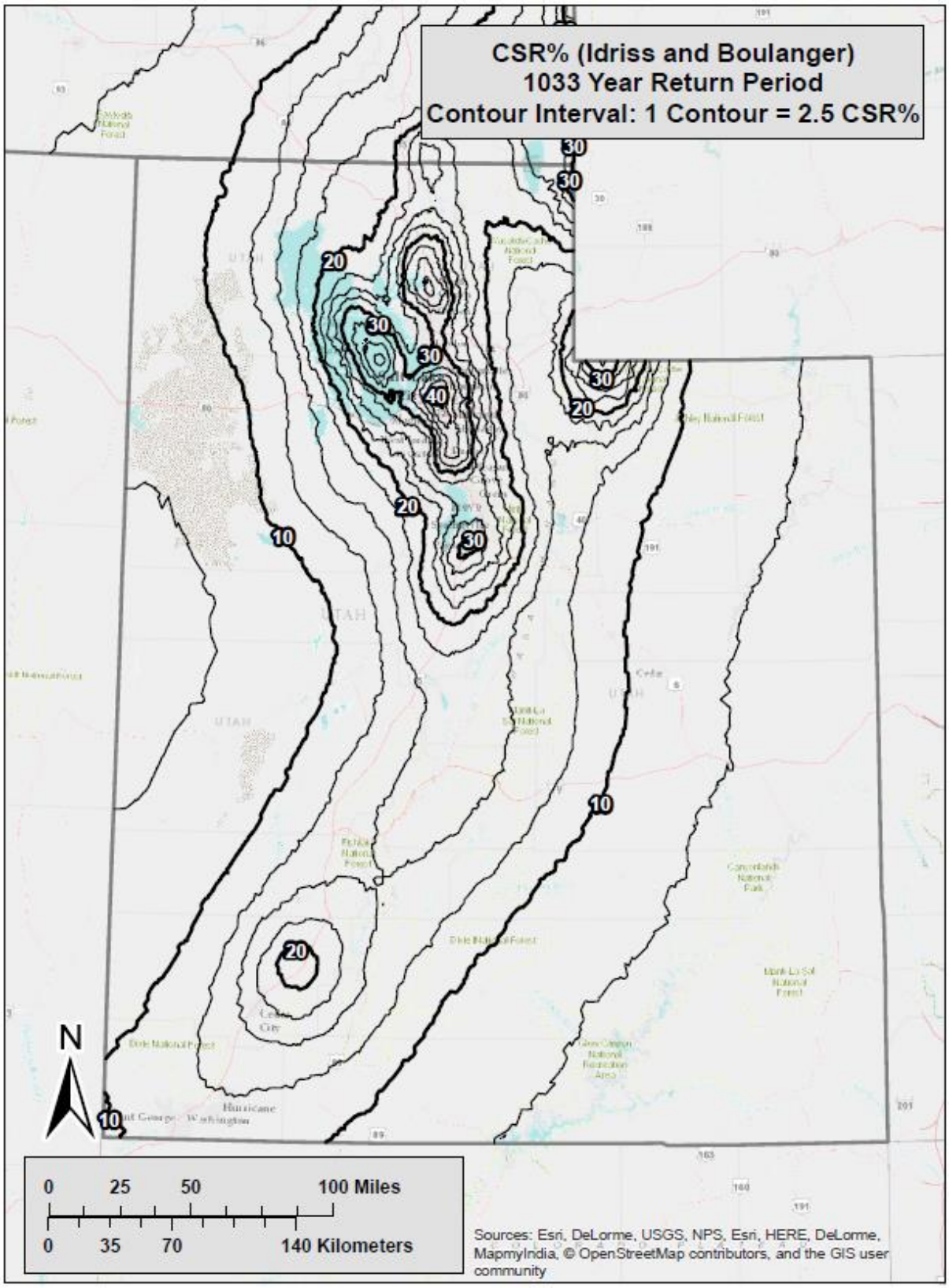

Figure B-32 Liquefaction Triggering ($CSR\%^{ref}$) Map for Utah (T_r = 1,033)

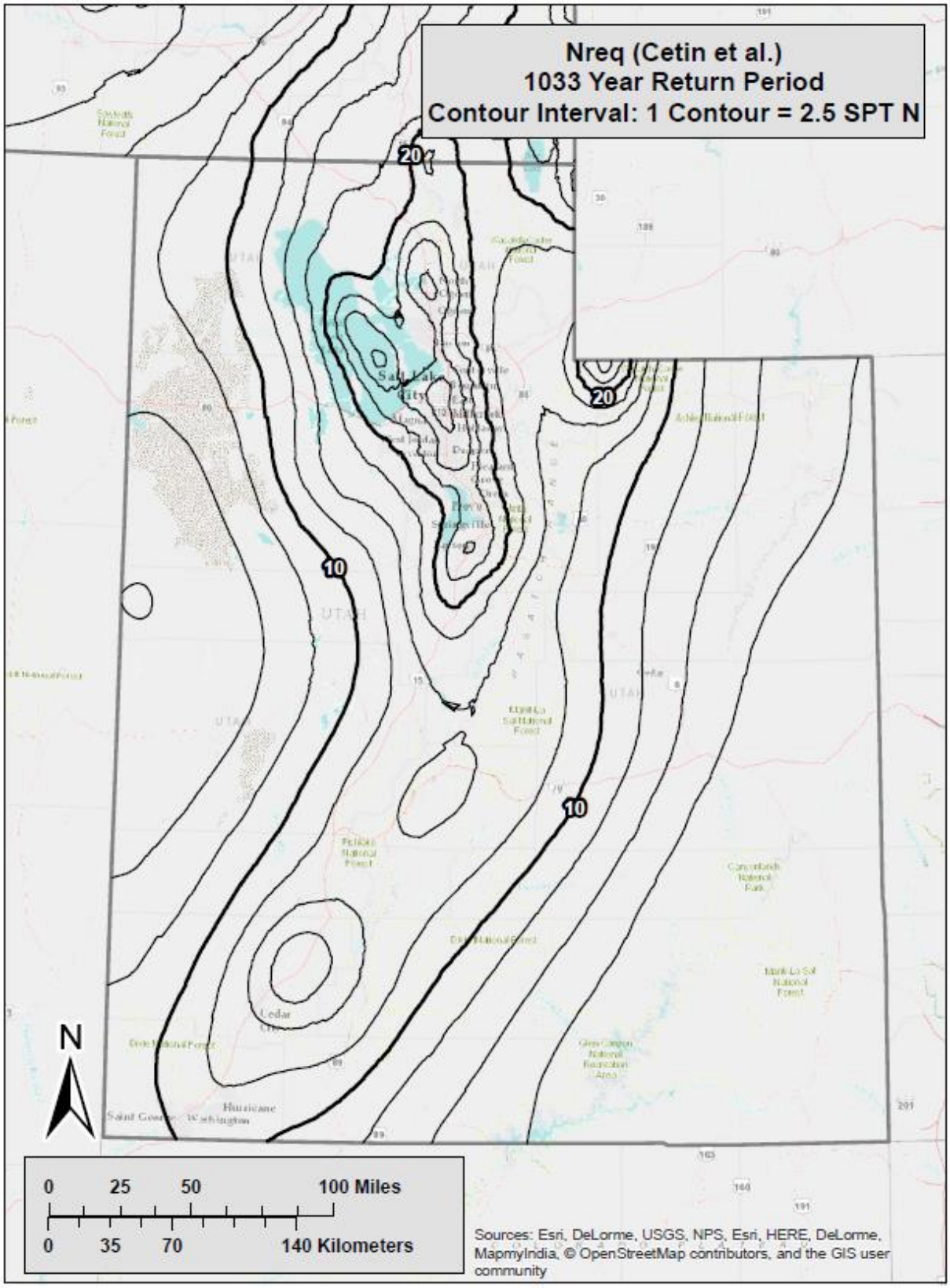

Figure B-33 Liquefaction Triggering (N_{req}^{ref}) Map for Utah (T_r = 1,033)

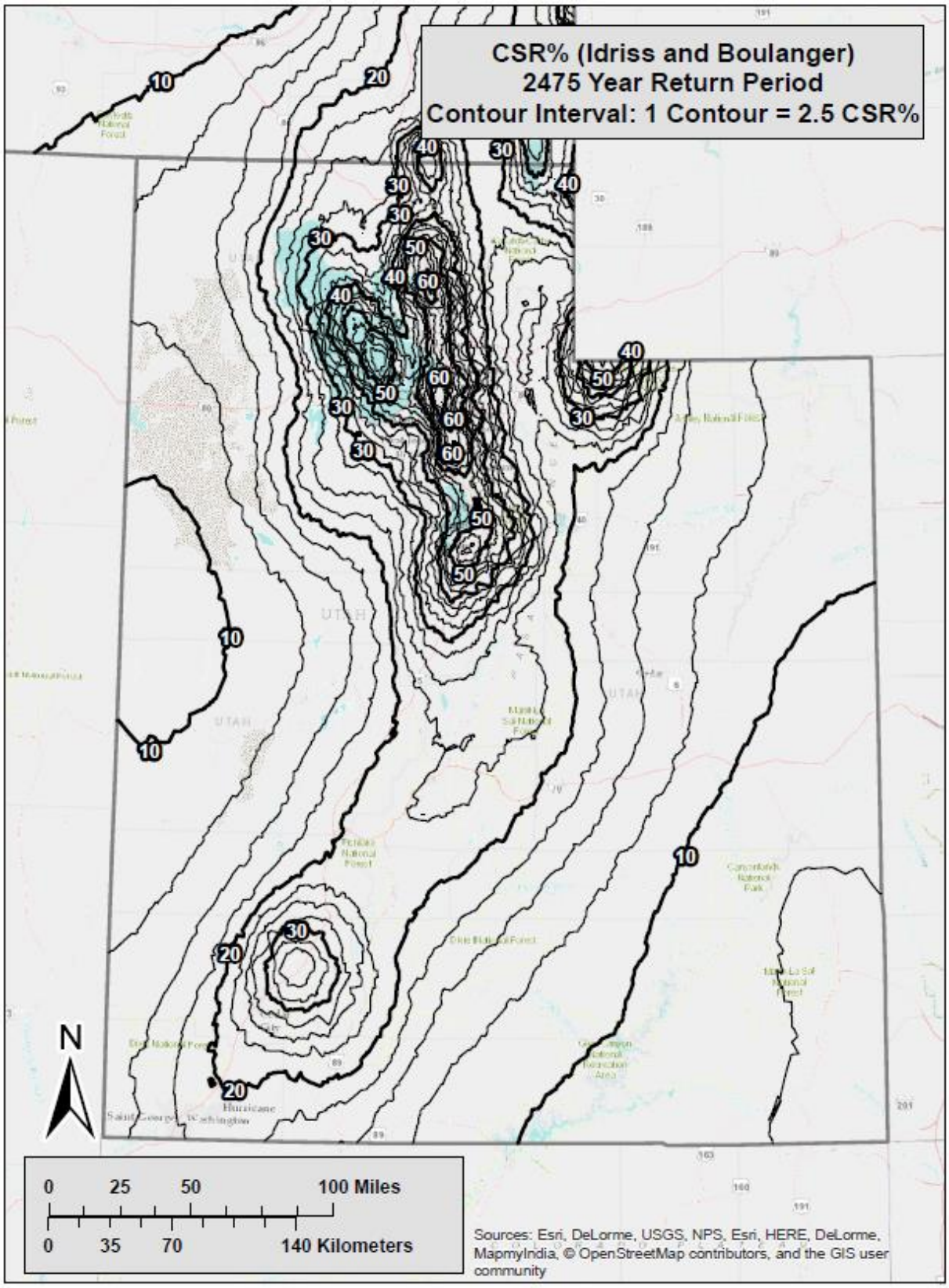

Figure B-34 Liquefaction Triggering ($CSR\%^{ref}$) Map for Utah (T_r = 2,475)

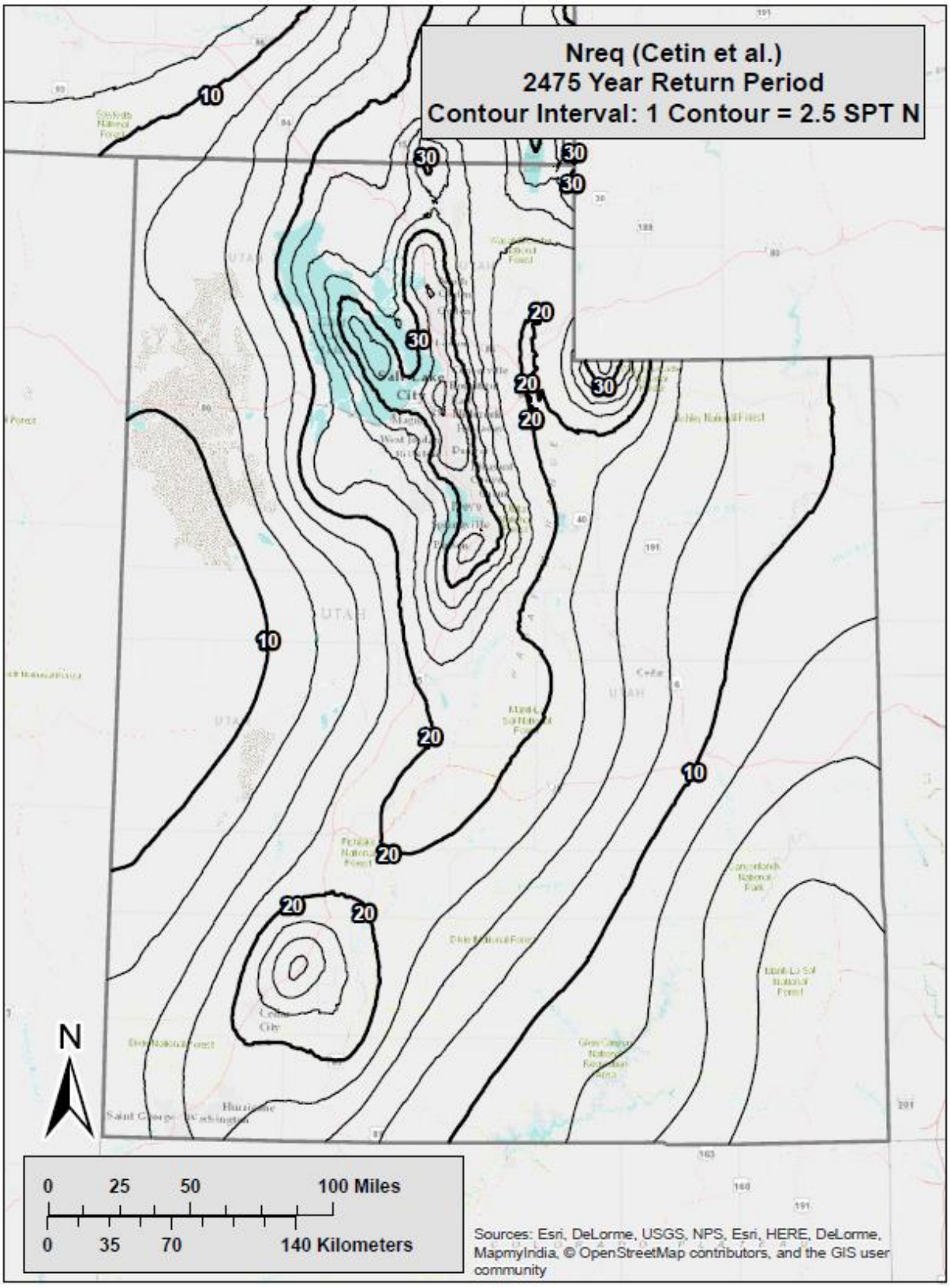

Figure B-35 Liquefaction Triggering (N_{req}^{ref}) Map for Utah (T_r = 2,475)

APPENDIX C: Sample Lateral Spread Parameter Maps

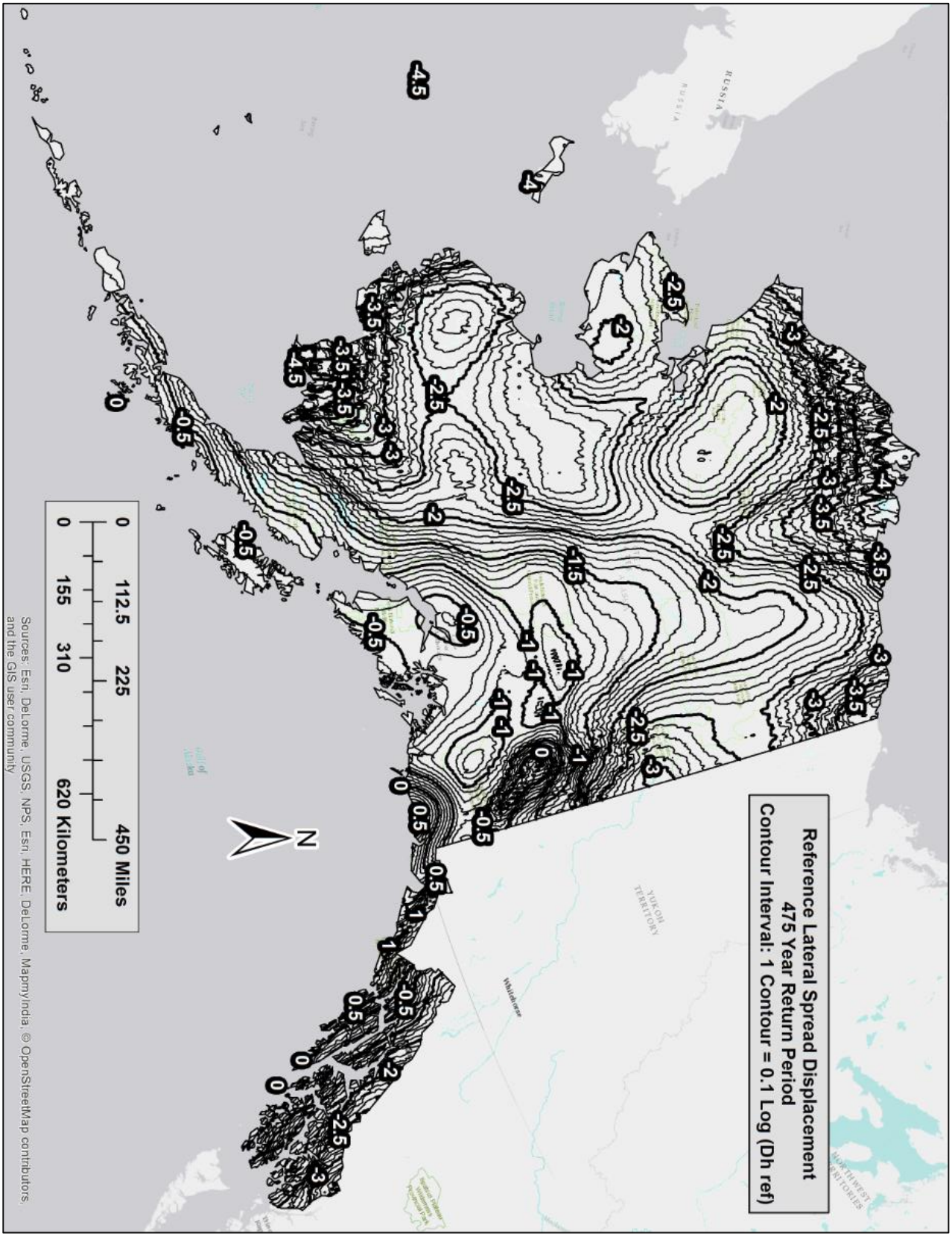

Figure C-1 Lateral Spread Parameter (D_H^{ref}) Map for Alaska (T_r = 475)

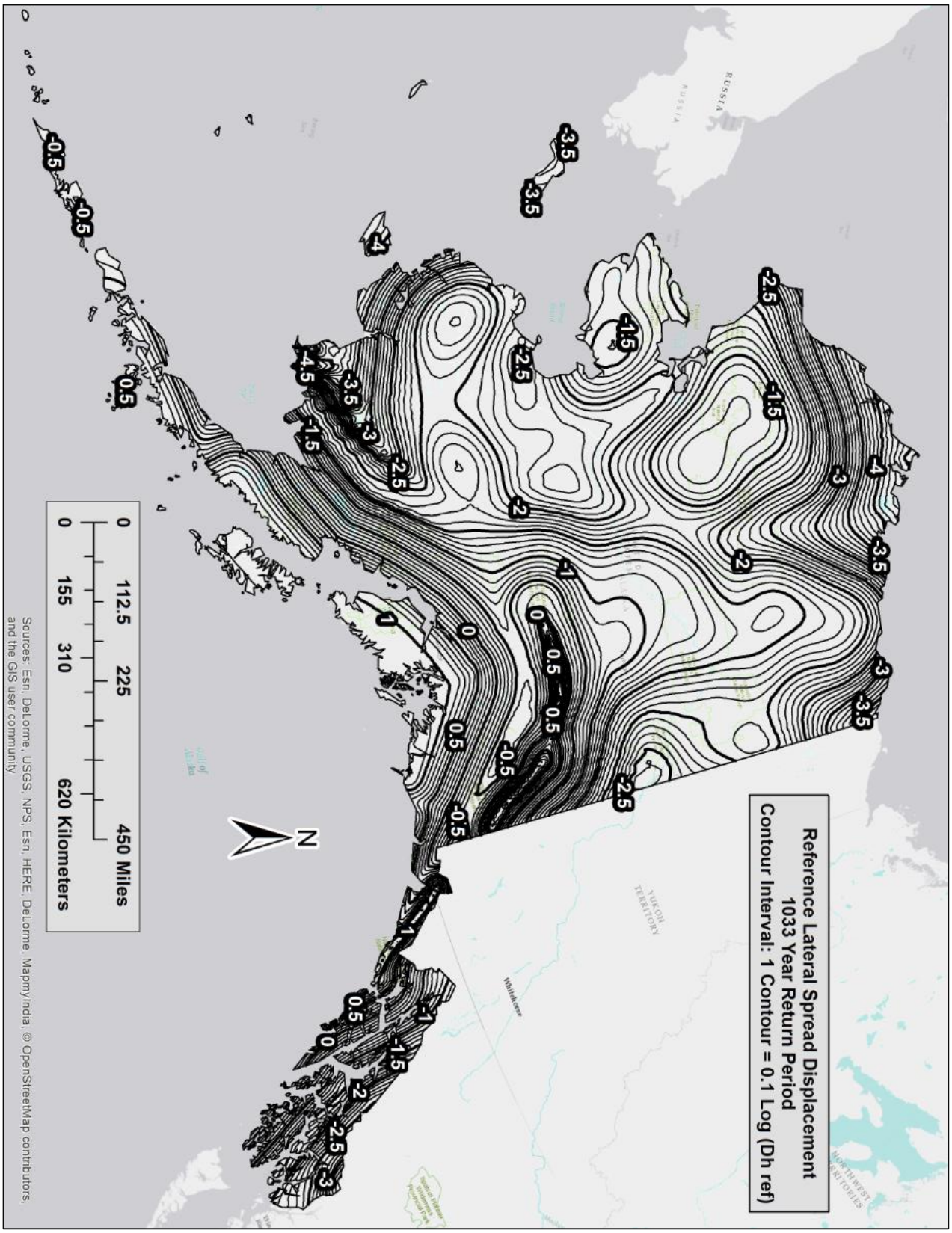

Figure C-2 Lateral Spread Parameter (D_H^{ref}) Map for Alaska (T_r = 1,033)

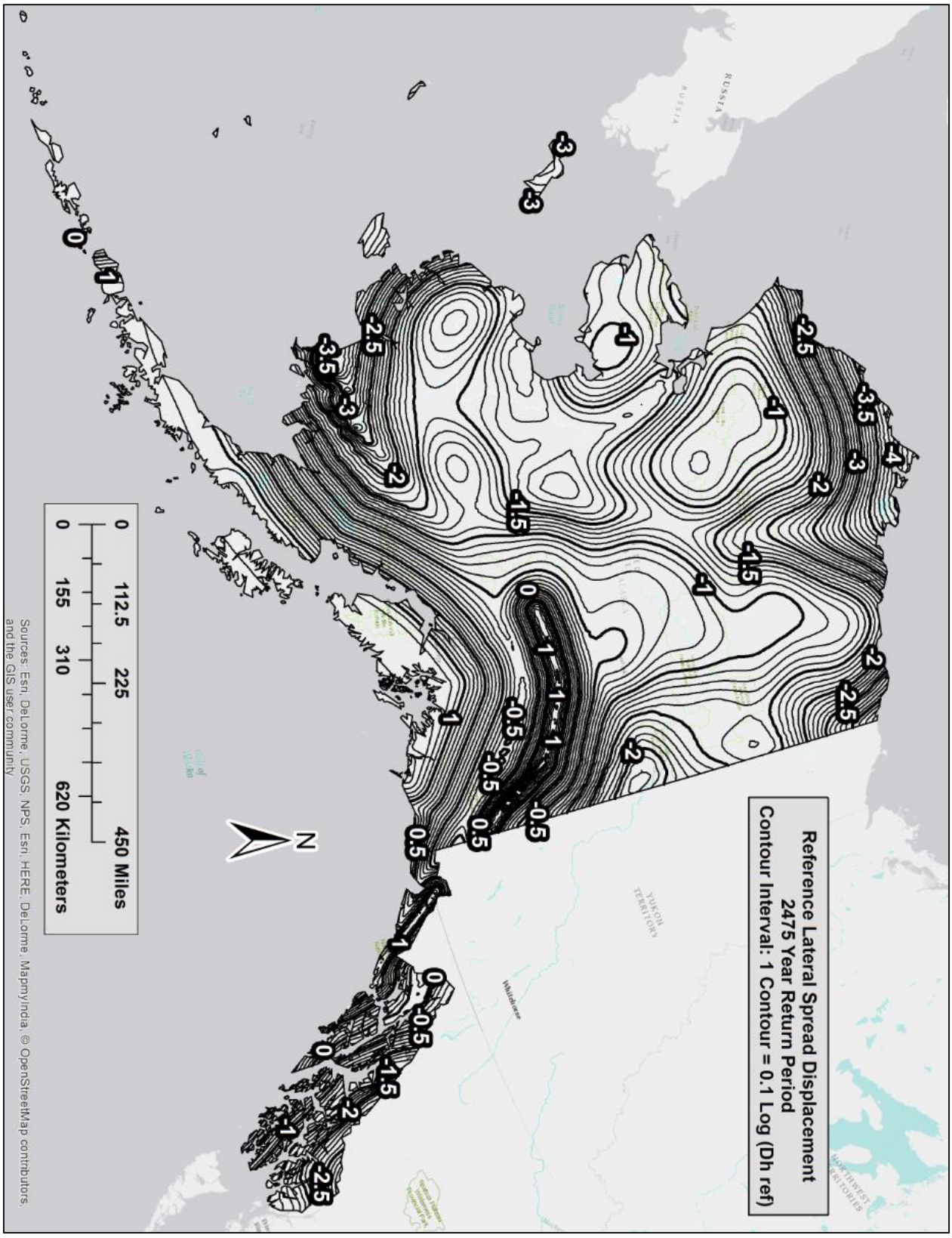

Figure C-3 Lateral Spread Parameter (D_H^{ref}) Map for Alaska (T_r = 2,475)

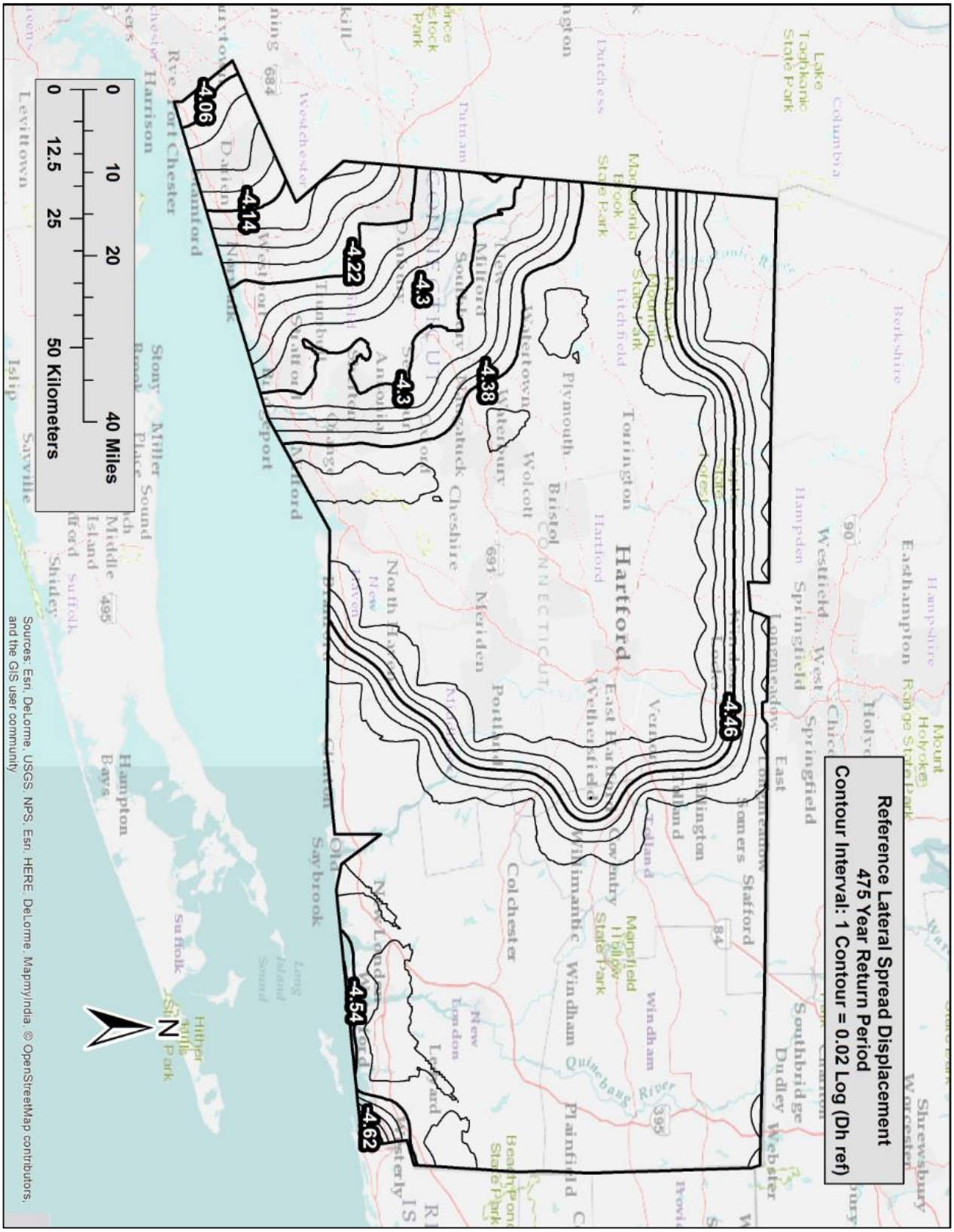

Figure C-4 Lateral Spread Parameter (D_H^{ref}) Map for Connecticut (T_r = 475)

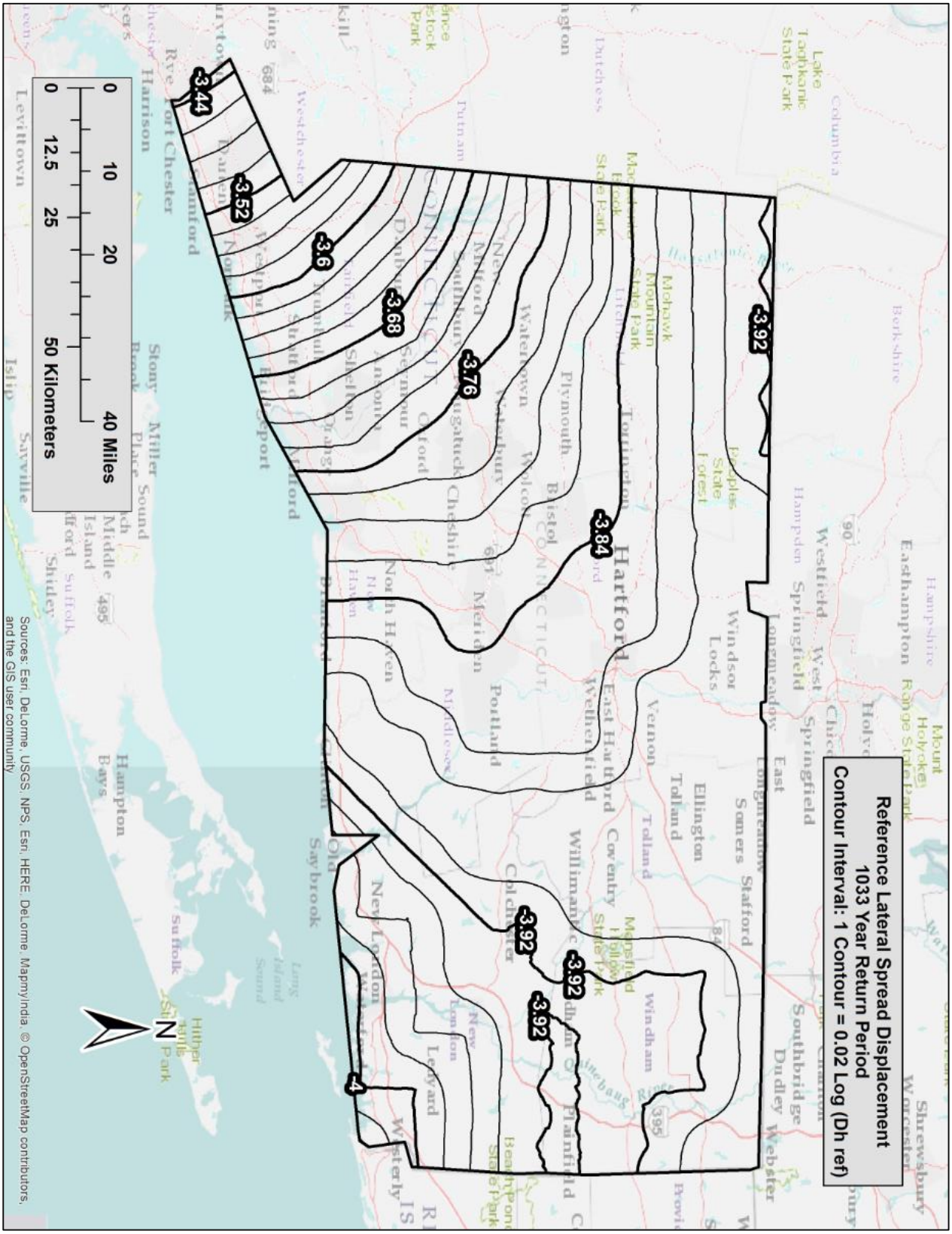

Figure C-5 Lateral Spread Parameter (D_H^{ref}) Map for Connecticut (T_r = 1,033)

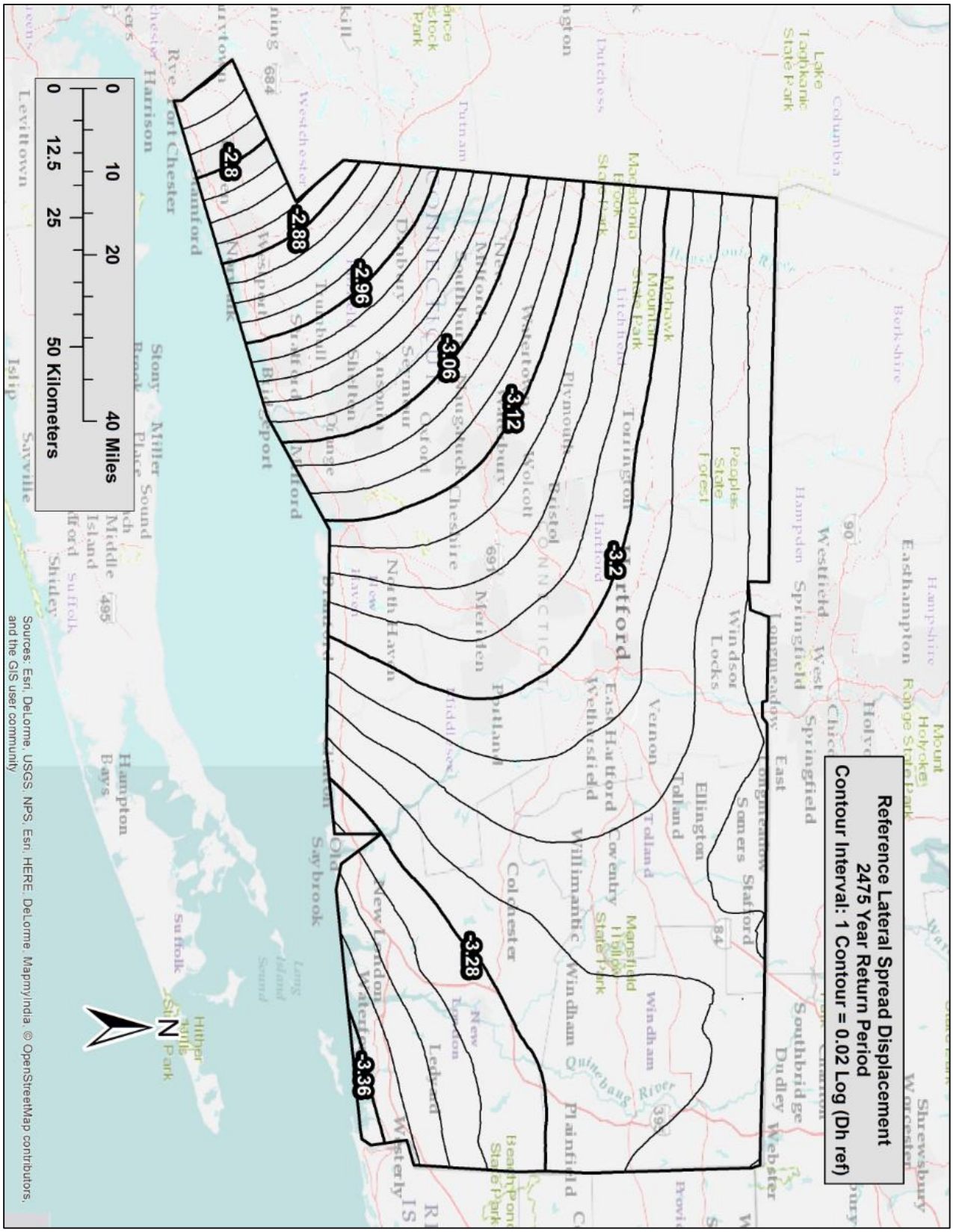

Figure C-6 Lateral Spread Parameter (D_H^{ref}) Map for Connecticut (T_r = 2,475)

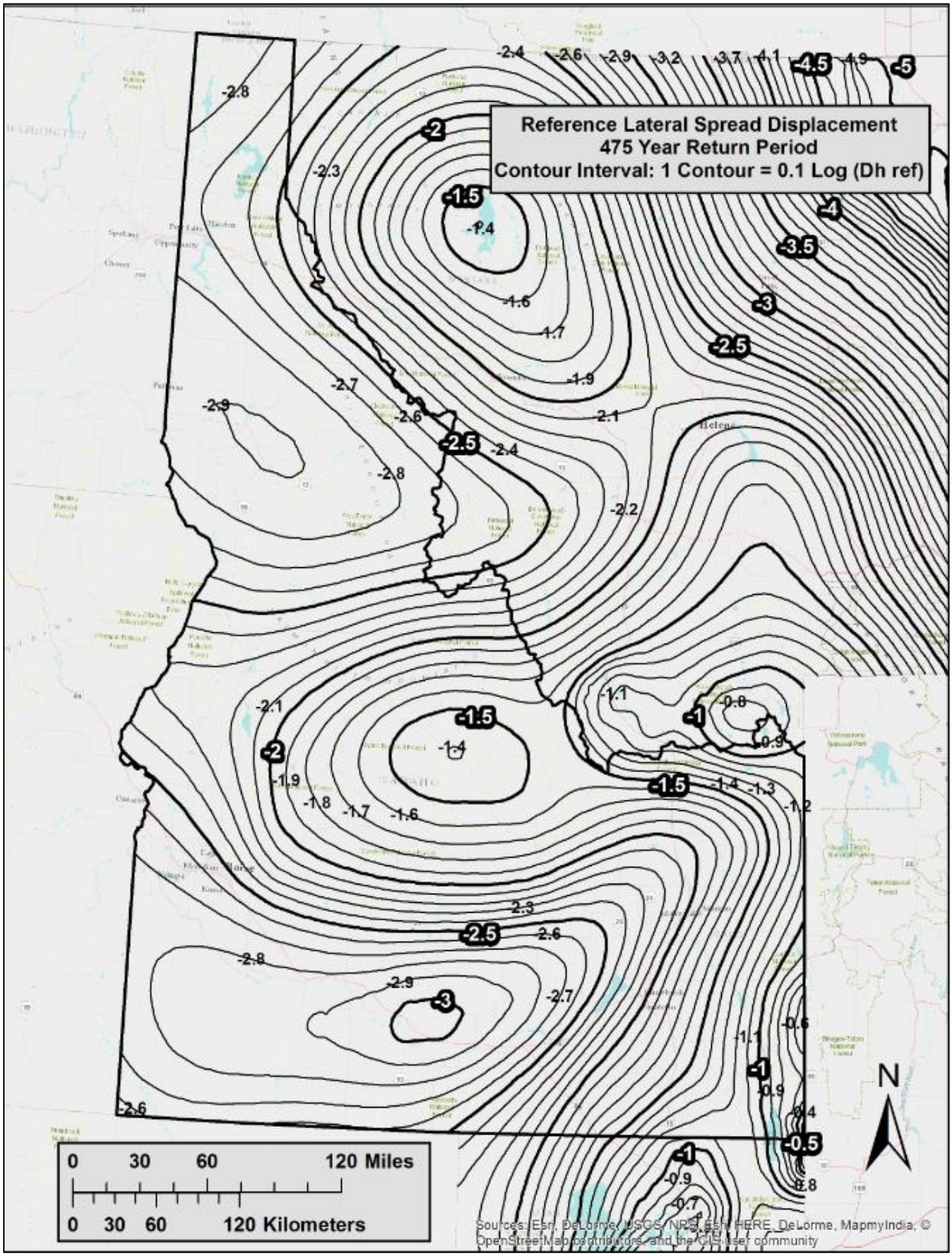

Figure C-7 Lateral Spread Parameter ($D_H{}^{ref}$) Map for Idaho (T_r = 475)

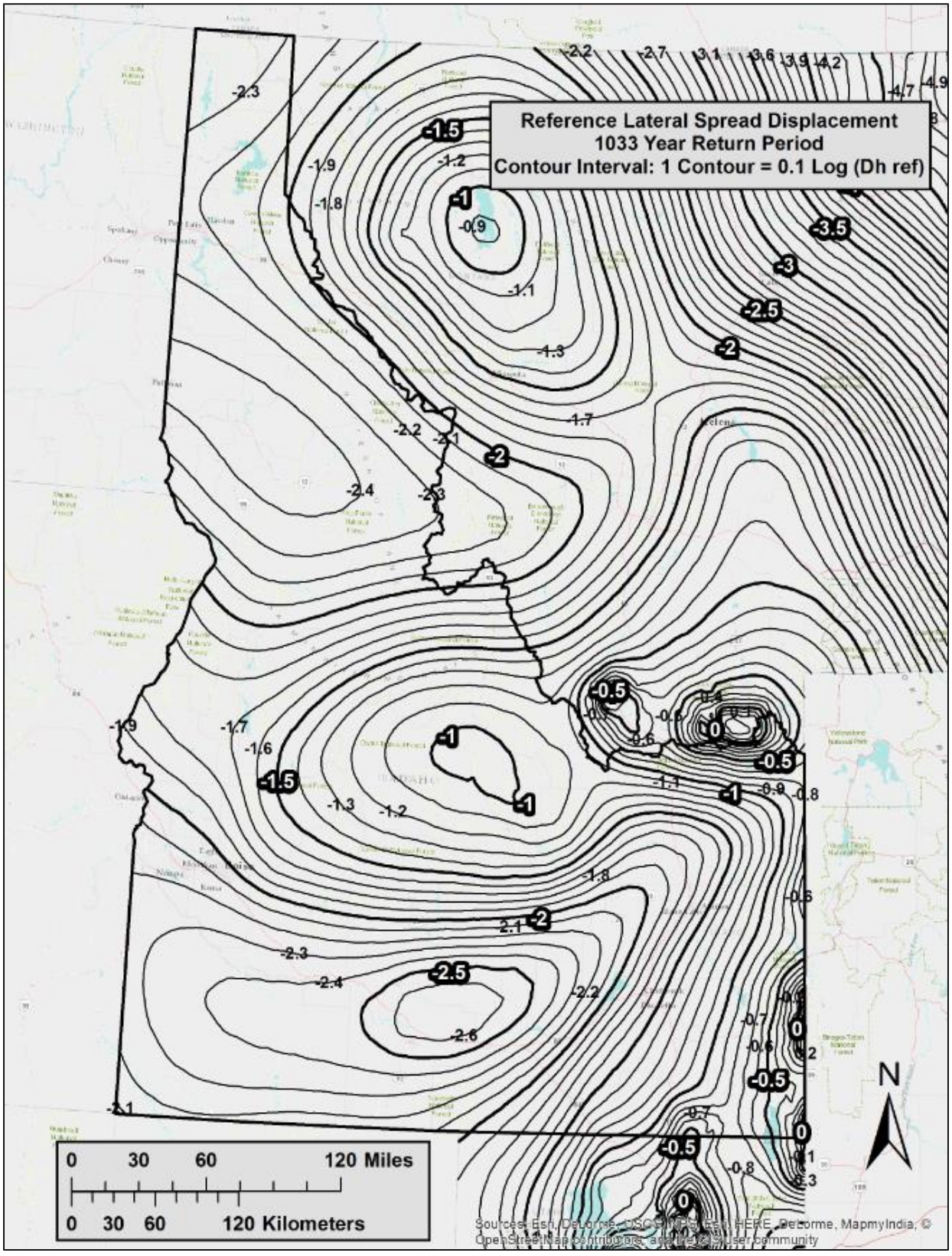

Figure C-8 Lateral Spread Parameter (D_H^{ref}) Map for Idaho (T_r = 1,033)

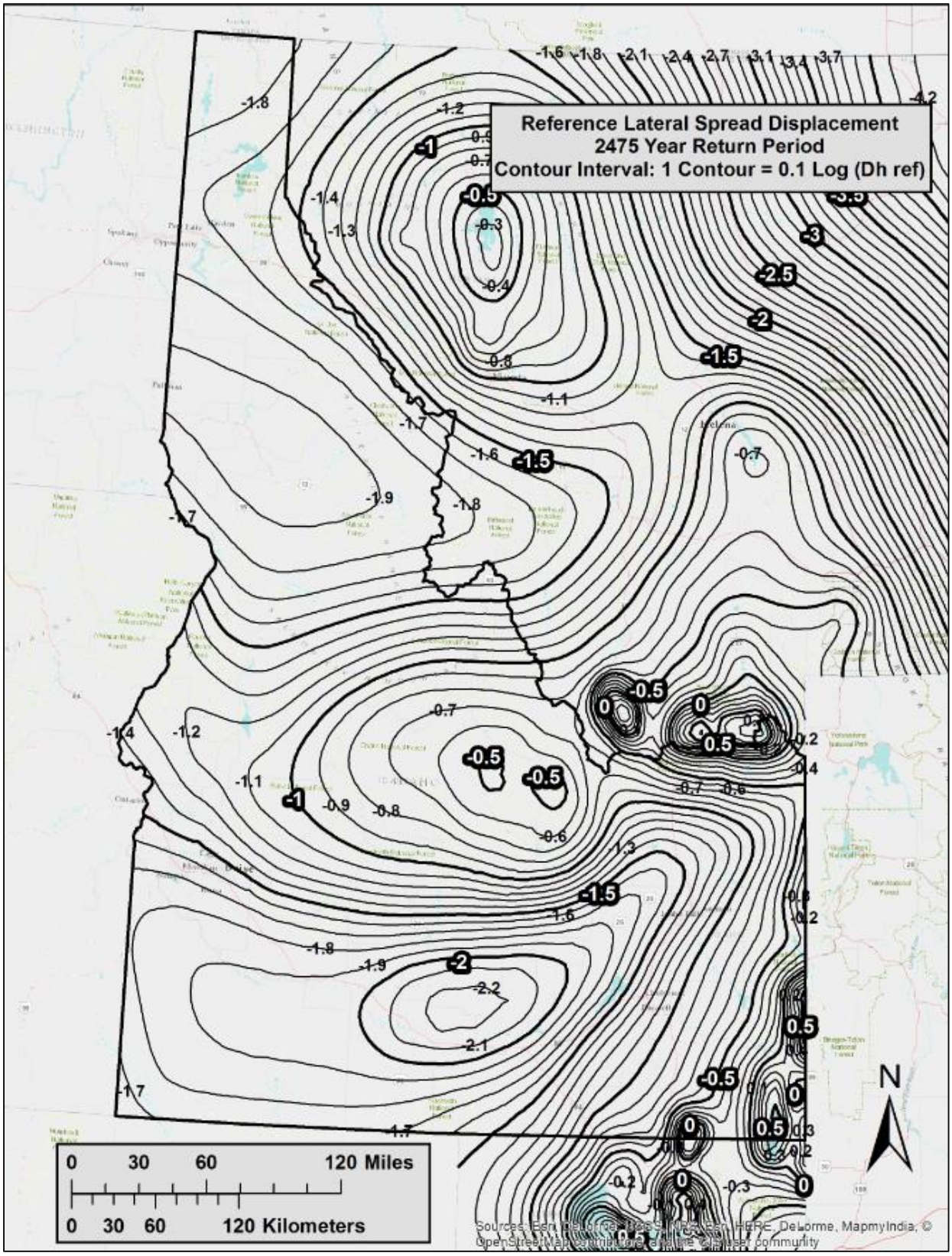

Figure C-9 Lateral Spread Parameter (D_H^{ref}) Map for Idaho (T_r = 2,475)

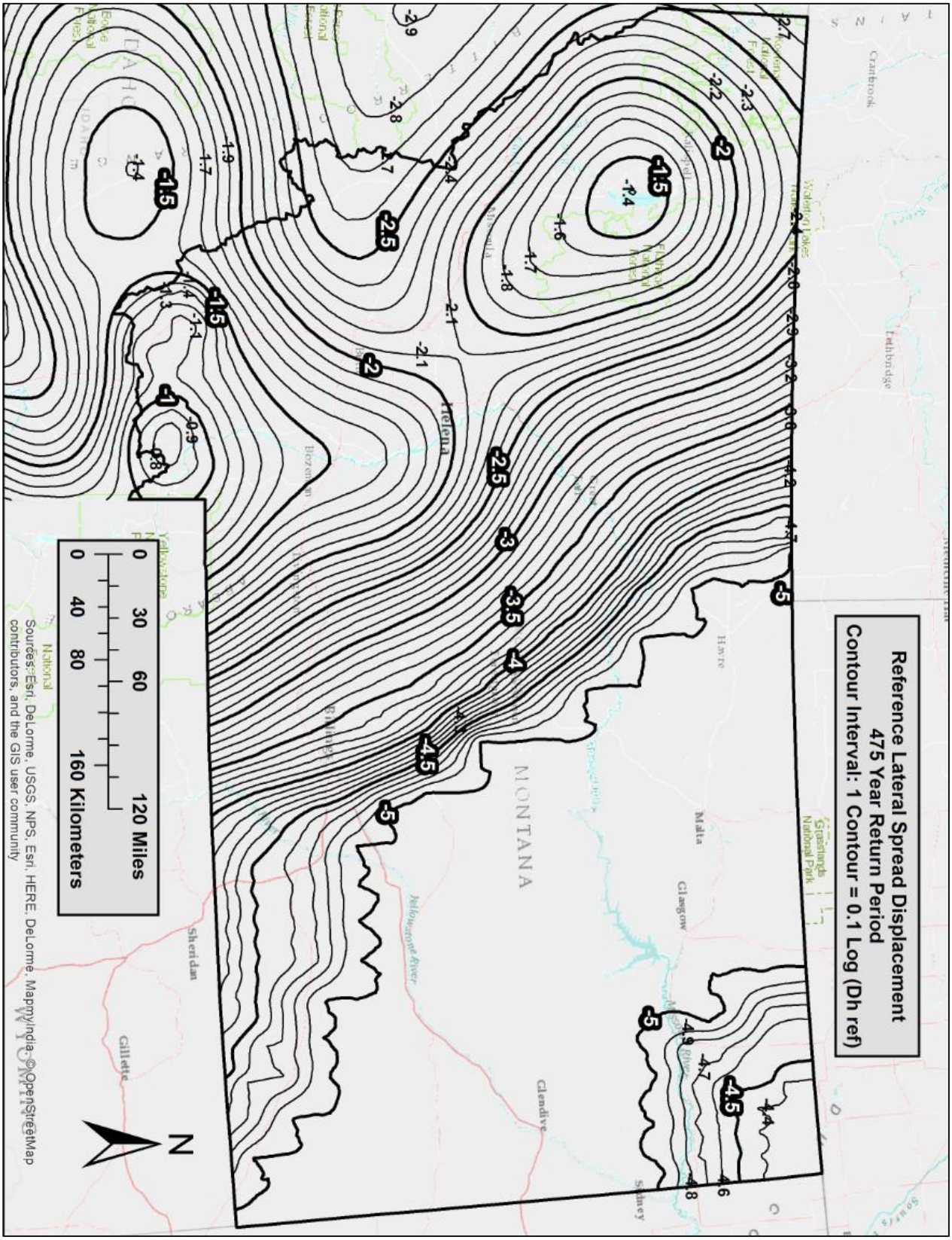

Figure C-10 Lateral Spread Parameter (D_H^{ref}) Map for Montana (T_r = 475)

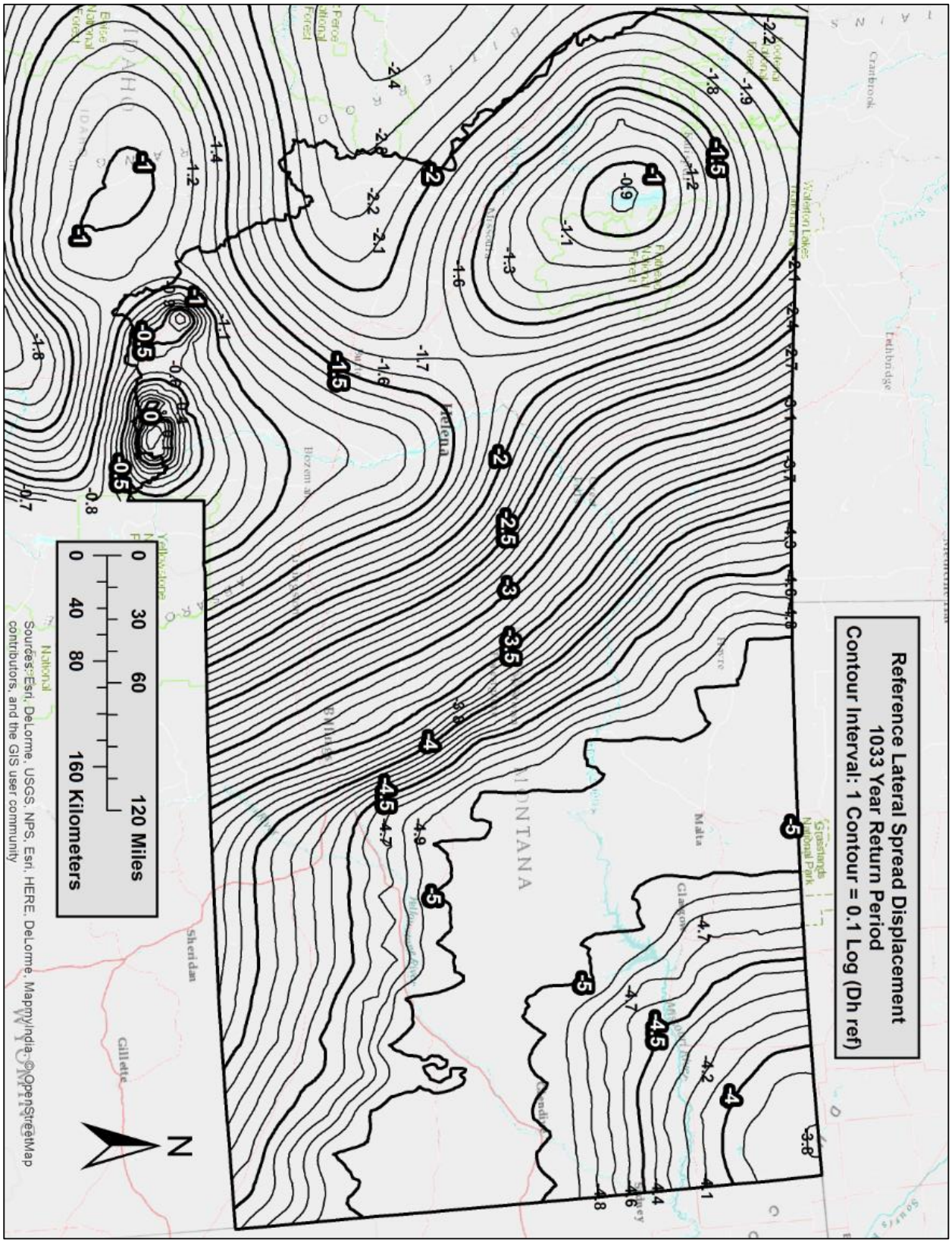

Figure C-11 Lateral Spread Parameter (D_H^{ref}) Map for Montana (T_r = 1,033)

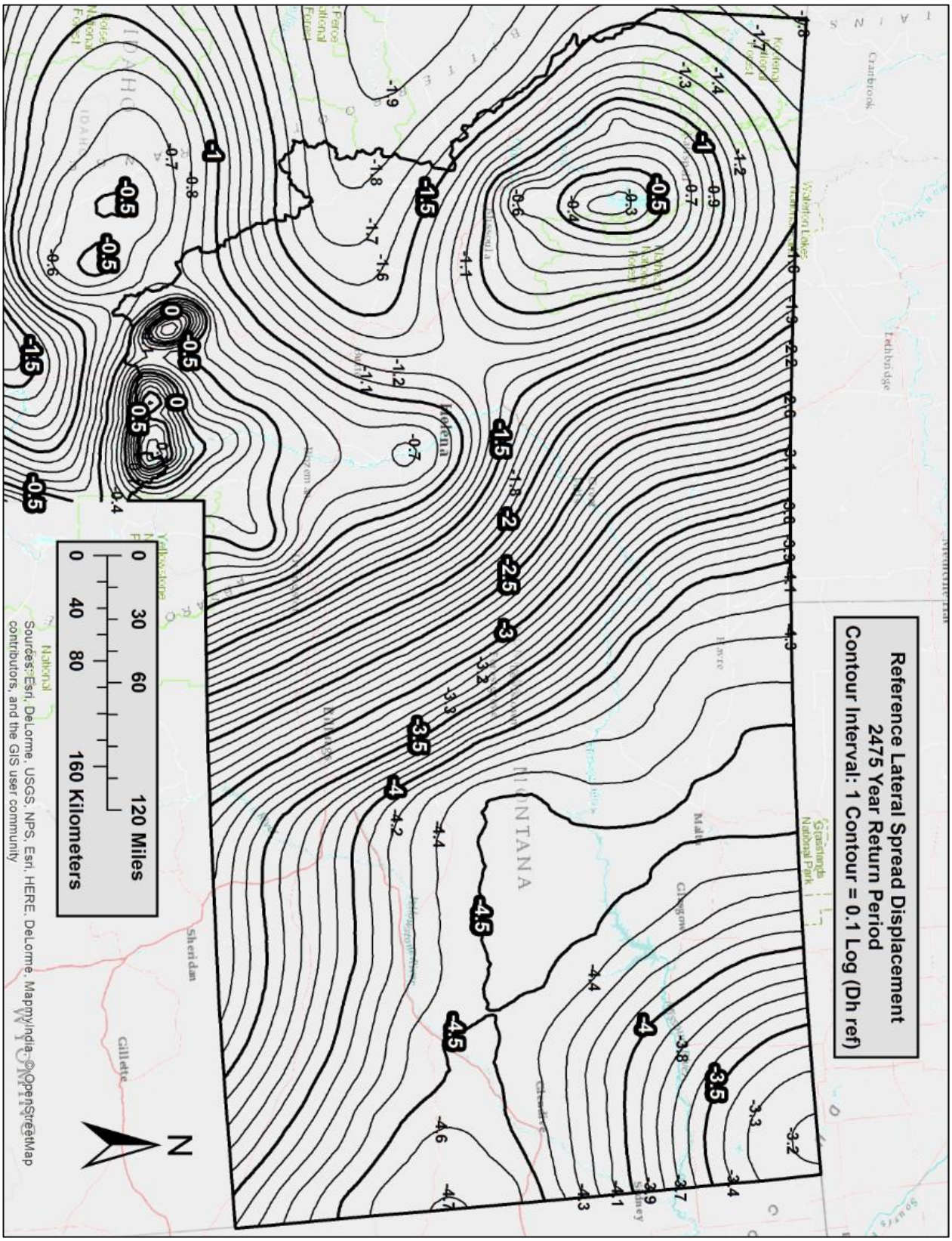

Figure C-12 Lateral Spread Parameter (D_H^{ref}) Map for Montana (T_r = 2,475)

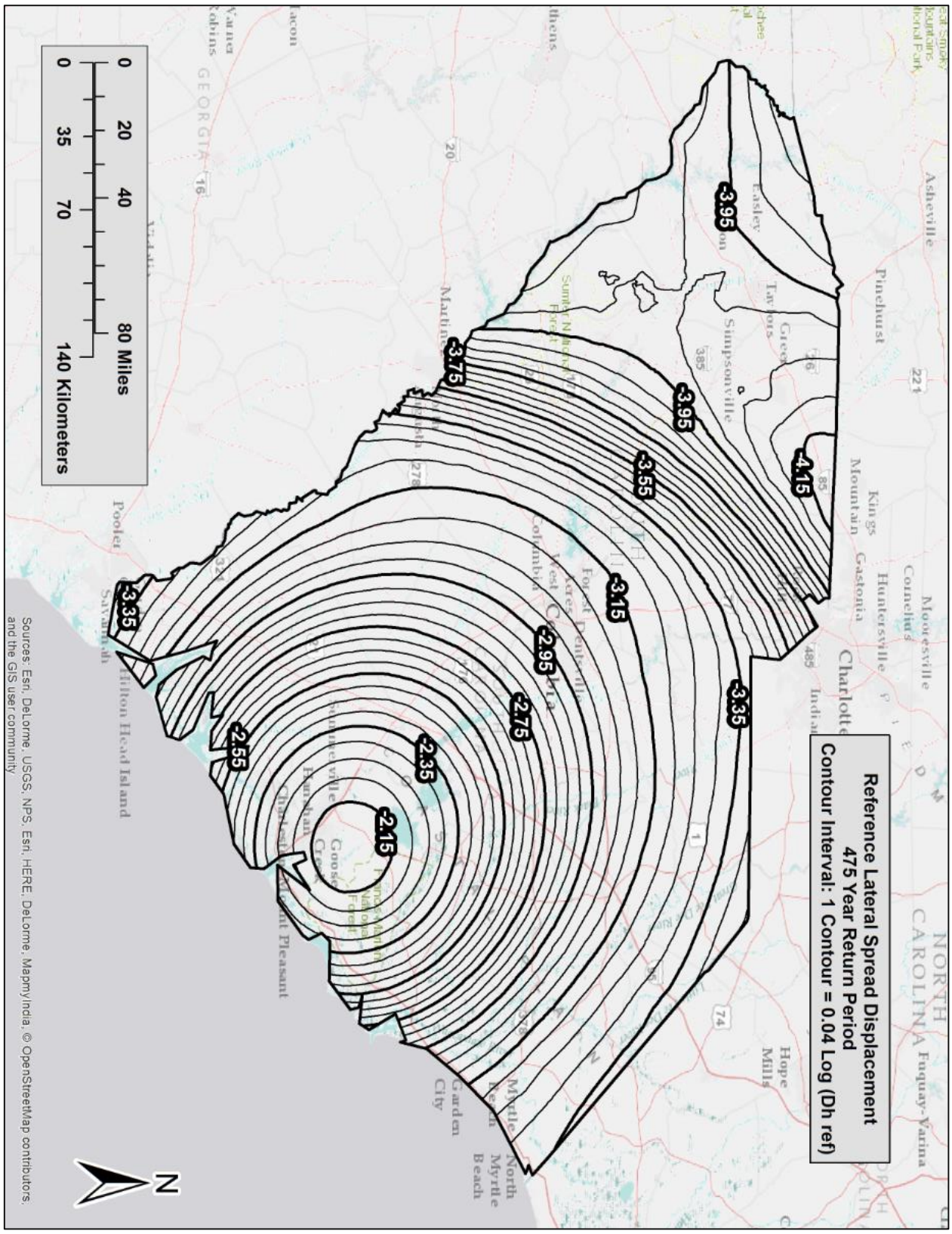

Figure C-13 Lateral Spread Parameter (D_H^{ref}) Map for South Carolina (T_r = 475)

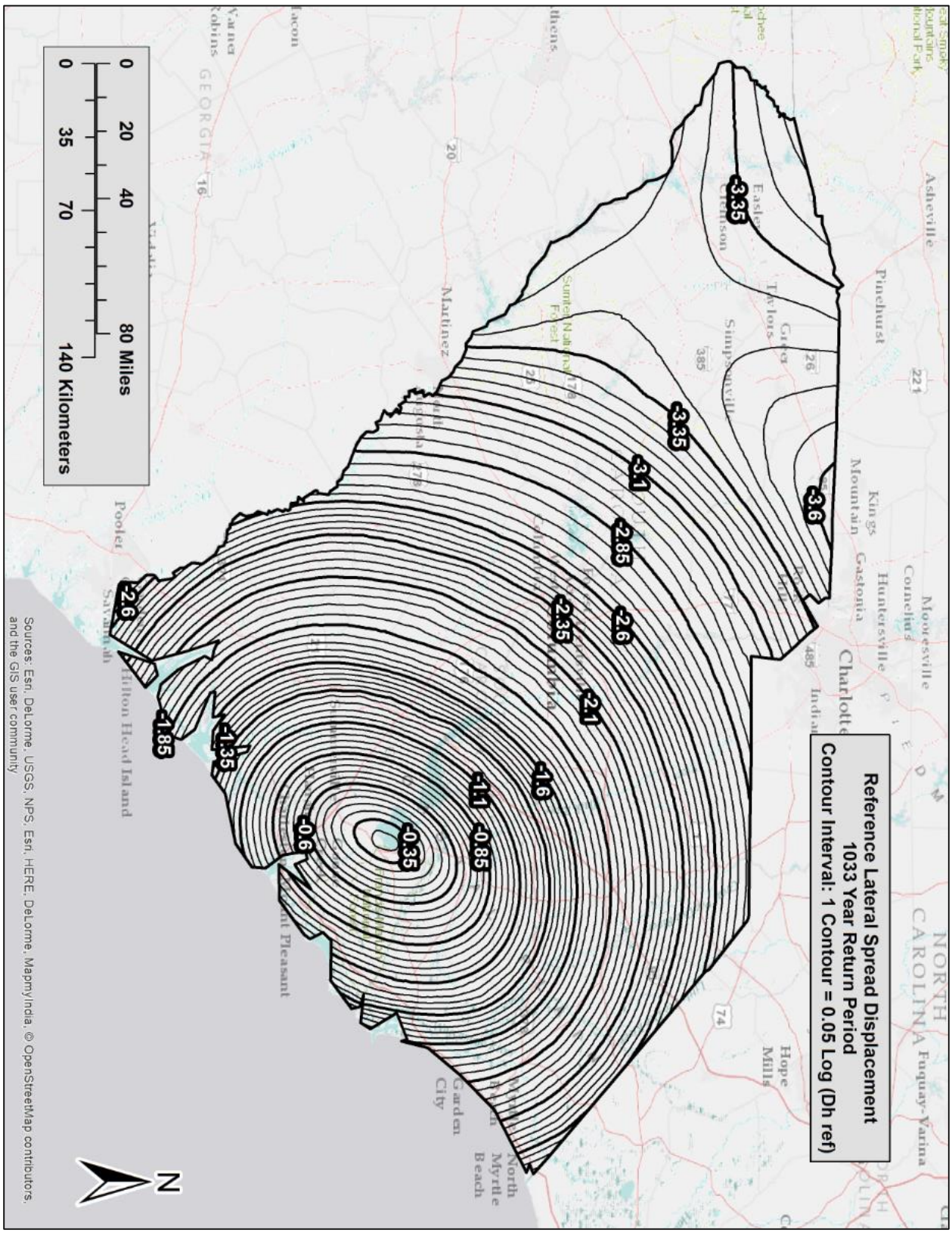

Figure C-14 Lateral Spread Parameter (D_H^{ref}) Map for South Carolina (T_r = 1,033)

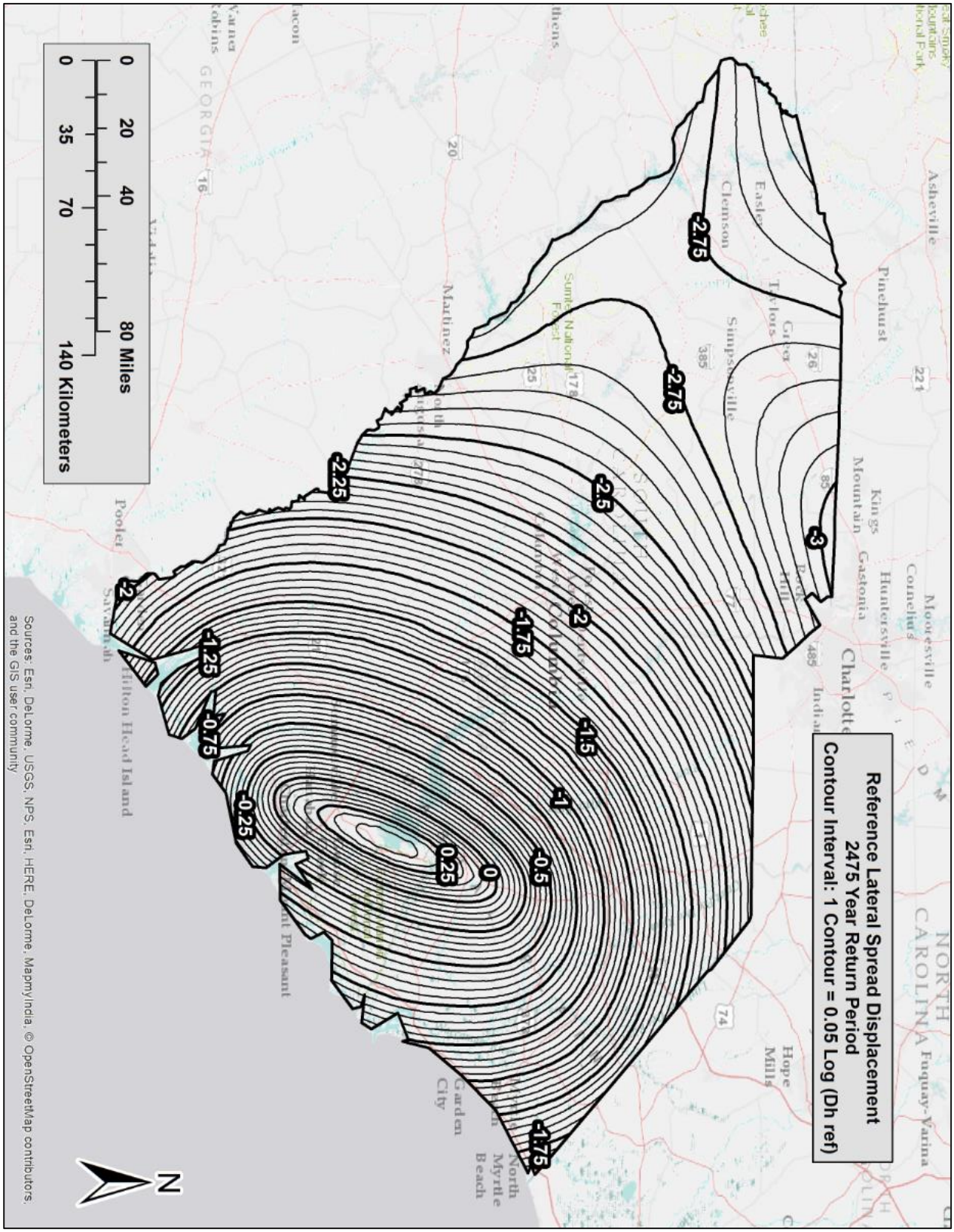

Figure C-15 Lateral Spread Parameter (D_H^{ref}) Map for South Carolina (T_r = 2,475)

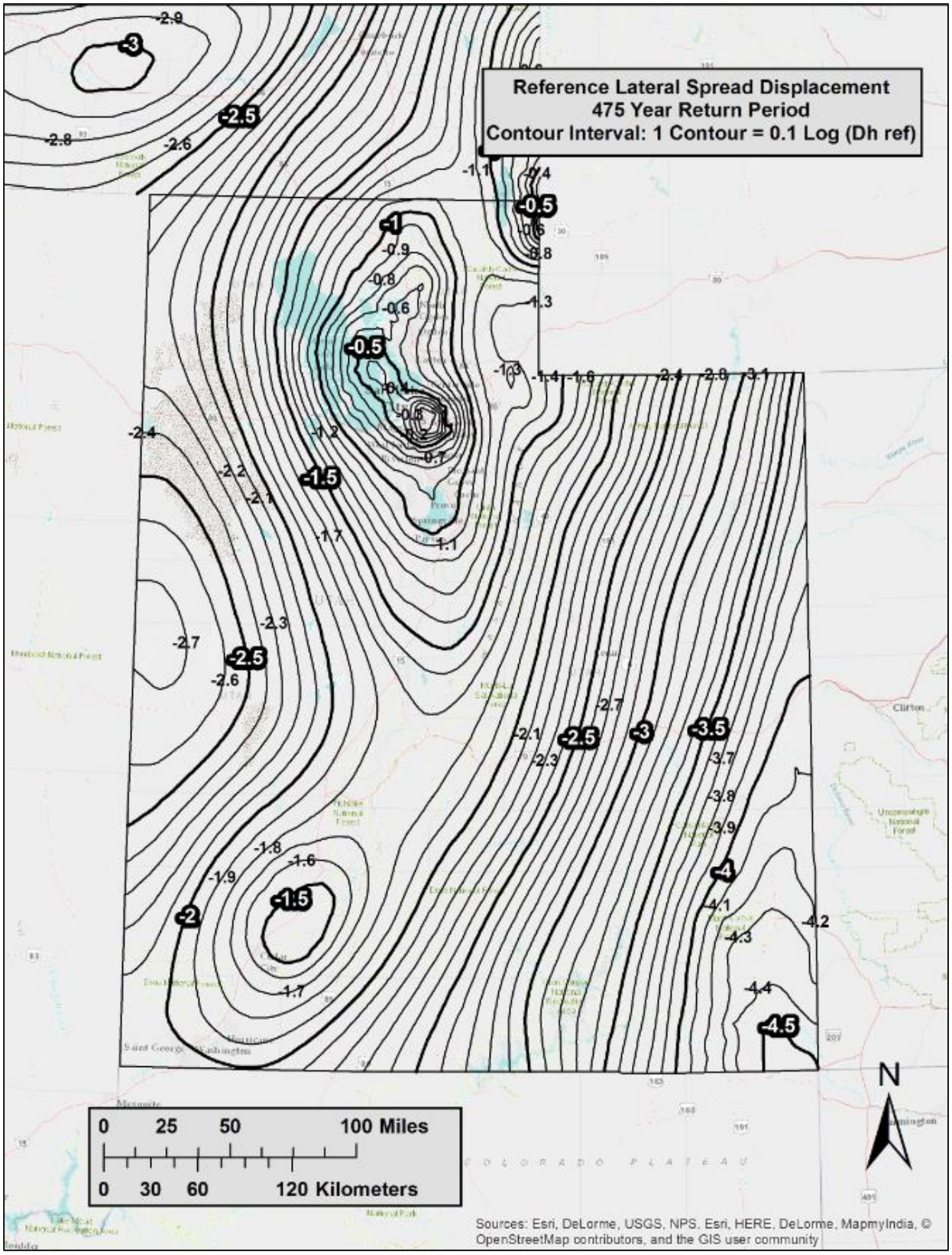

Figure C-16 Lateral Spread Parameter (D_H^{ref}) Map for Utah (T_r = 475)

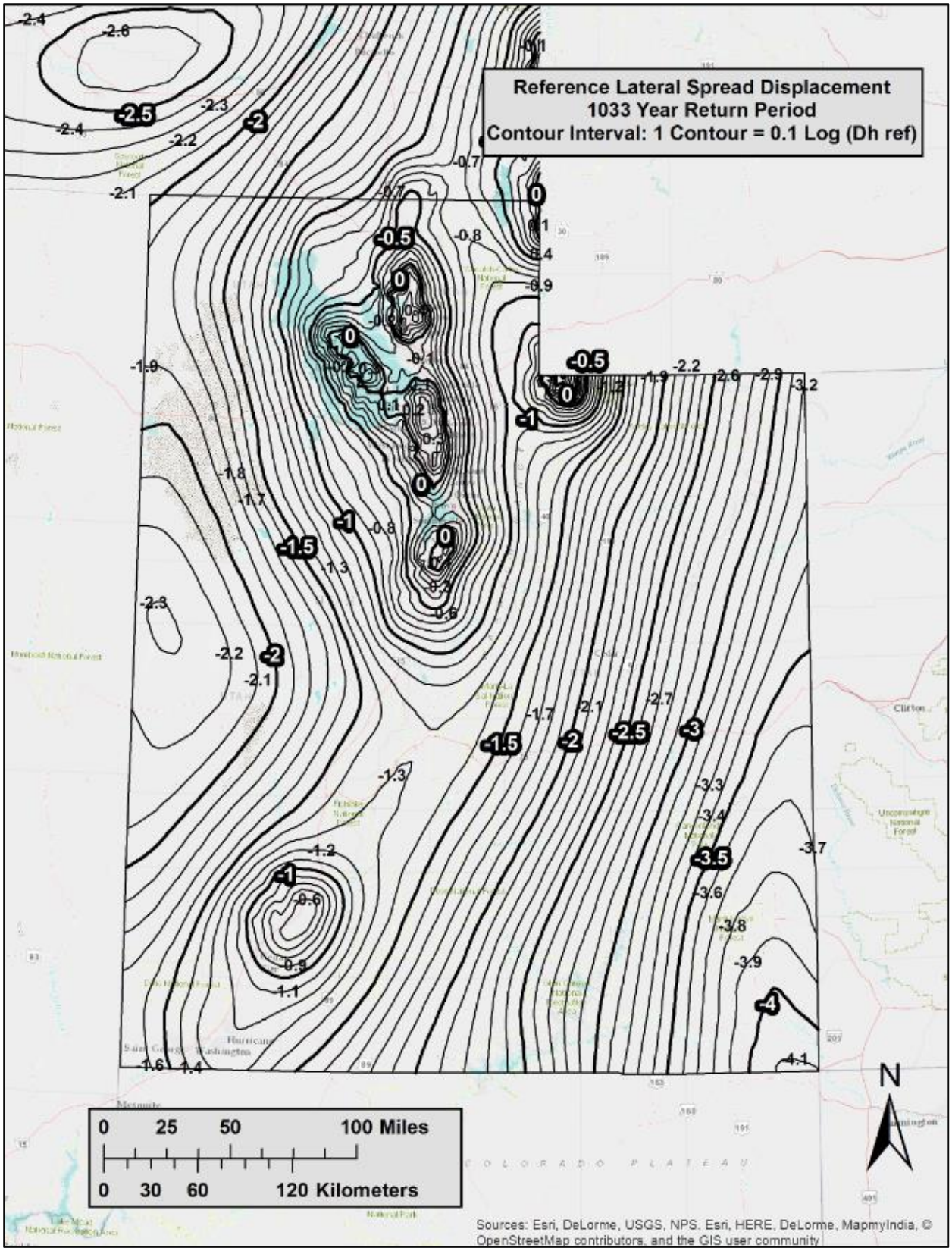

Figure C-17 Lateral Spread Parameter (D_H^{ref}) Map for Utah (T_r = 1,033)

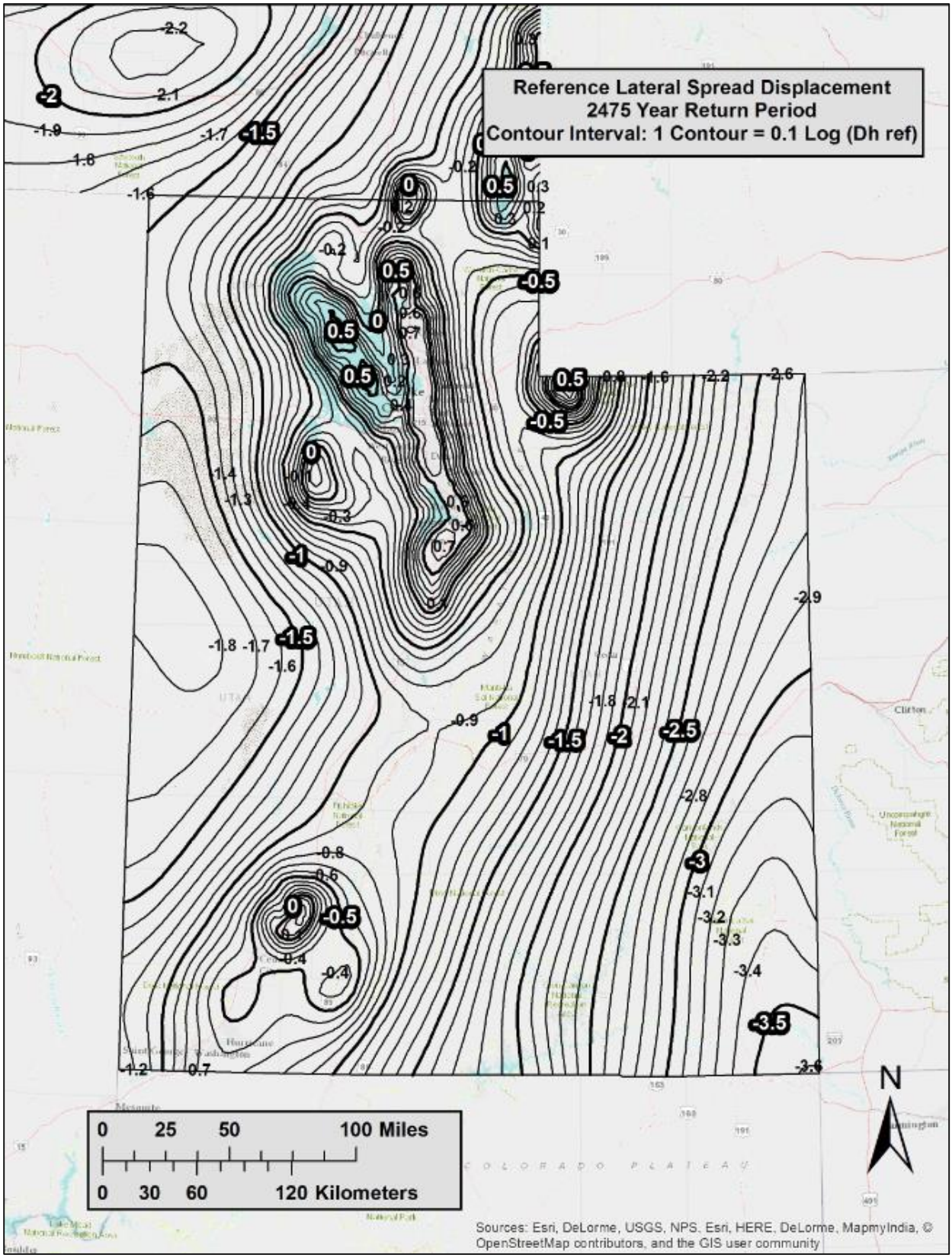

Figure C-18 Lateral Spread Parameter (D_H^{ref}) Map for Utah (T_r = 2,475)

APPENDIX D: Supplementary Deterministic Data

Table D-1 Faults Considered in Deterministic Analysis

					Median Acceleration T_R = 1033			(Median + 1 St. Dev) Acceleration T_R = 1033		
		Seismic Source	**Dist (km)**	**Mag**	***PGA***	***F_{pga}***	***a_{max}***	***PGA***	***F_{pga}***	***a_{max}***
San Francisco										
	1	Northern San Andreas	10.77	8.05	0.3175	1.183	0.3754	0.5426	1.0	0.5426
	2	San Gregorio Connected	16.64	7.5	0.2139	1.372	0.2935	0.3660	1.134	0.4150
	3	Hayward-Rodgers Creek	18.23	7.33	0.1918	1.416	0.2717	0.3282	1.172	0.3846
	4	Mount Diablo Thrust	36.08	6.7	0.1050	1.590	0.1670	0.1811	1.438	0.2604
	5	Calaveras	34.28	7.03	0.0981	1.6	0.1570	0.1682	1.464	0.2462
Salt Lake City										
	1	Wasatch Fault, SLC Section	1.02	7	0.5911	1.0	0.5911	1.0050	1.0	1.0050
	2	West Valley Fault Zone	2.19	6.48	0.5694	1.0	0.5694	0.9842	1.0	0.9842
	3	Morgan Fault	25.04	6.52	0.0989	1.6	0.1583	0.1713	1.457	0.2497
	4	Great Salt Lake Fault zone, Antelope Section	25.08	6.93	0.1016	1.597	0.1622	0.1742	1.452	0.2529
	5	Oquirrh-Southern, Oquirrh Mountain Fault	30.36	7.17	0.0958	1.6	0.1532	0.1641	1.472	0.2415
Butte										
	1	Rocker Fault	4.92	6.97	0.5390	1.0	0.5390	0.9202	1.0	0.9202
	2	Georgia Gulch Fault	45.91	6.42	0.0435	1.6	0.0696	0.0754	1.6	0.1206
	3	Helena Valley Fault	75.56	6.6	0.0294	1.6	0.0470	0.0507	1.6	0.0812
	4	Canyon Ferry Fault	81.32	6.92	0.0327	1.6	0.0523	0.0561	1.6	0.0898
	5	Blacktail Fault	84.27	6.94	0.0317	1.6	0.0508	0.0545	1.6	0.0872
	6	Madison Fault	86.51	7.45	0.0420	1.6	0.0671	0.0719	1.6	0.1150

Table D-2 Characteristics of Rocker Fault (near Butte) and Calculations to Determine *PGA* and M_w.

*M_w calculated based on Wells and Coppersmith (1994): Length = 43 km

(Use "all" slip type, because it's a normal fault and the # of normal events is small)

*PGA calculated based on NGA equations (Linda Al Atik, PEER 2009)

BA08, CB08, and CY08 used with equal weighting

M_w =	6.97		
Dip =	70	degrees	(Another fault near Butte, has a dip of 70-75 degrees)
Depth to bottom of rupture =	16	km	(Assumed)
R_x =	4.92	km	(measured using Google Earth)
Z_TOR =	0	km	(Assumed)
Width =	17.03	km	
R_jb =	0	km	(Assuming the site is on the hanging wall side)
R_rup =	1.68	km	
V_s30 =	760	m/s	
U=	0		
F_RV=	0		
F_NM =	1		
F_HW =	1		
F_measured =	0		
Z_1 =	DEFAULT		
Z_2.5=	DEFAULT		
F_AS=	0		
HW Taper =	1		
--> PGA (50%) =	0.5390	g	(From NGA spreadsheet)
--> PGA (84%) =	0.9202	g	(From NGA spreadsheet)